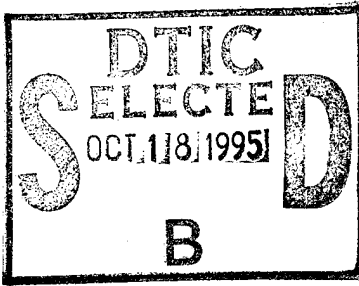
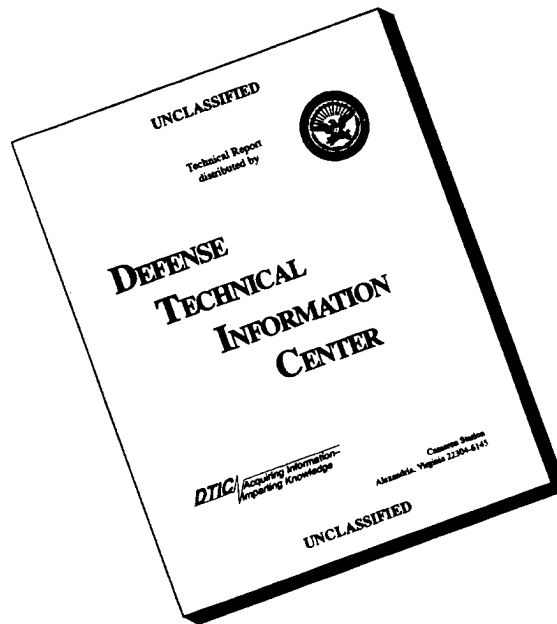


REPORT DOCUMENTATION PAGE			Form Approved OMB No. 0704-0188	
Public reporting burden for this collection of information is estimated to average 1 hour per response, including the time for reviewing instructions, searching existing data sources, gathering and maintaining the data needed, and completing and reviewing the collection of information. Send comments regarding this burden estimate or any other aspect of this collection of information, including suggestions for reducing this burden, to Washington Headquarters Services, Directorate for Information Operations and Reports, 1215 Jefferson Davis Highway, Suite 1204, Arlington, VA 22202-4302, and to the Office of Management and Budget, Paperwork Reduction Project (0704-0188), Washington, DC 20503.				
1. AGENCY USE ONLY (Leave blank)		2. REPORT DATE 10 Sep 95		3. REPORT TYPE AND DATES COVERED
4. TITLE AND SUBTITLE Vertical Distribution of Oxides of Nitrogen In The Semi-Urban Planetary Boundary Layer: Mixing Ratios, Transport, and Sources				5. FUNDING NUMBERS
6. AUTHOR(S) Thomas Clark Moore				
7. PERFORMING ORGANIZATION NAME(S) AND ADDRESS(ES) AFIT Students Attending: North Carolina University				8. PERFORMING ORGANIZATION REPORT NUMBER 95-101
9. SPONSORING/MONITORING AGENCY NAME(S) AND ADDRESS(ES) DEPARTMENT OF THE AIR FORCE AFIT/CI 2950 P STREET, BLDG 125 WRIGHT-PATTERSON AFB OH 45433-7765				10. SPONSORING/MONITORING AGENCY REPORT NUMBER
11. SUPPLEMENTARY NOTES				
12a. DISTRIBUTION/AVAILABILITY STATEMENT Approved for Public Release IAW AFR 190-1 Distribution Unlimited BRIAN D. GAUTHIER, MSgt, USAF Chief of Administration				12b. DISTRIBUTION CODE
13. ABSTRACT (Maximum 200 words)				
				
<p>19951017 156</p> <p>DTIC QUALITY INSPECTED 5</p>				
14. SUBJECT TERMS				15. NUMBER OF PAGES 194
				16. PRICE CODE
17. SECURITY CLASSIFICATION OF REPORT		18. SECURITY CLASSIFICATION OF THIS PAGE		19. SECURITY CLASSIFICATION OF ABSTRACT
				20. LIMITATION OF ABSTRACT

DISCLAIMER NOTICE



THIS DOCUMENT IS BEST QUALITY AVAILABLE. THE COPY FURNISHED TO DTIC CONTAINED A SIGNIFICANT NUMBER OF PAGES WHICH DO NOT REPRODUCE LEGIBLY.

ABSTRACT

MOORE, THOMAS CLARK. Vertical Distribution of Oxides of Nitrogen in the Semi-Urban Planetary Boundary Layer: Mixing Ratios, Transport and Sources. (Under the direction of Viney P. Aneja.)

The role of the family of reactive oxides of nitrogen, NO_Y [composed primarily in the lower troposphere of nitric oxide (NO) + nitrogen dioxide (NO_2) + peroxyacetyl nitrate (PAN) + nitric acid (HNO_3) + particulate nitrate (NO_3^-)], in the photochemical production of and correlation with tropospheric ozone is thought to be well known. Thus a knowledge of the distribution, transport and sources of tropospheric NO and NO_Y is critical to the understanding of the effectiveness of ozone precursor control strategies, and to the development of accurate regional and global atmospheric models, particularly over rural areas. In this study, measurements of the mixing ratios of NO and NO_Y were made over a semi-urban area of central North Carolina at the surface (10 meters) and on a tower at a height of 250 meters (820 feet) and 433 meters (1420 feet) above ground level (AGL) from December 1994 to February 1995. These measurements were compared with synoptic weather data, daily upper air soundings from Greensboro, NC, and upper air soundings from North Carolina State University (NCSU) in a effort to characterize NO and NO_Y in the planetary boundary layer in terms of their vertical distribution, diurnal profile, and related transport/production mechanisms. In particular, the primary goal of this research was investigation of the relationship between the observed vertical

distribution of mixing ratios of NO and NO_y and specific morning transport mechanisms within the boundary layer (i.e., downward mixing).

The results suggest a pronounced decreasing vertical gradient in both NO and NO_y mixing ratios, with a distinct diurnal cycle and nocturnal minimum. The observed data also compare favorably with a proposed one dimensional model of vertical NO distribution that predicts an exponentially decreasing NO mixing ratio with height. Furthermore, the results of the comparisons with meteorological data are conclusive in their agreement that during this study, NO and NO_y were mixed *upward from* the surface during the morning and midday hours by vertical boundary layer processes, and were also mixed upward during other times of the day or night by synoptic meteorological features (and their associated vertical motions).

The overall implication from this research is that mixing ratios of NO and NO_y at the elevated heights did not exist in sufficient concentrations above the inversion layer in the nocturnal boundary layer to be mixed downward by vertical boundary layer transport mechanisms and affect surface measurements. Thus the association of observed increases in surface NO and NO_y mixing ratios solely with downward mixing processes is not justified in all cases, and other sources and processes for these increases must be considered, particularly over rural areas.

Accession For	
NTIS GRA&I	<input checked="checked" type="checkbox"/>
DTIC TAB	<input type="checkbox"/>
Unannounced	<input type="checkbox"/>
Justification	
By	
Distribution/	
Availability Codes	
Dist	Avail and/or Special
A-1	

**VERTICAL DISTRIBUTION OF OXIDES OF NITROGEN
IN THE SEMI-URBAN PLANETARY BOUNDARY LAYER:
MIXING RATIOS, TRANSPORT, AND SOURCES**

by

THOMAS CLARK MOORE

A thesis submitted to the Graduate Faculty of
North Carolina State University
in partial fulfillment of the
requirements for the Degree of
Master of Science

DEPARTMENT OF MARINE, EARTH, AND ATMOSPHERIC SCIENCES


Raleigh

1995

APPROVED BY:


WAYNE P. ROBARGE


DAVID A. DICKEY


VINEY P. ANÉJA
Chair of Advisory Committee

DEDICATION

This thesis is dedicated to my wife, Lynn, for the love, understanding, and support she has provided during the past two hectic years; hopefully this will serve as a partial repayment for her putting up with long hours, short tempers, and more discussion and/or complaints about meteorology and atmospheric chemistry than she ever wanted to hear in one lifetime!

BIOGRAPHY

Thomas Clark (T.C.) Moore was born January 5, 1966, in Charlotte, NC as the second of three children to Sarah and Tom Moore. After growing up in Belmont, NC, and graduating from South Point High School in 1984, he received an Air Force ROTC scholarship and began studying at North Carolina State University. He graduated with a BS in meteorology in May of 1988, was commissioned as a Second Lieutenant in the United States Air Force, and assigned to active duty at Scott AFB, IL, in January of 1989. During his assignment there he served as a weather forecaster for the Military Airlift Command (MAC) Weather Support Unit (WSU); as a weather briefer to the Commander-In-Chief, Military Airlift Command (CINCMAC); and as a Tanker Airlift Control Center (TACC) Staff Weather Officer. He left Illinois in May, 1993 and traveled to Montgomery AFB, AL, to attend Squadron Officer's School while en route to his next assignment. He arrived in Raleigh, NC, in August, 1993 to begin his current two year tour as an MS graduate student in the Atmospheric Sciences program at North Carolina State University.

He is currently married to Lynn Grady Moore, a graduate student in the College of Textiles at North Carolina State University. Upon completion of their studies in the summer of 1995, they will move to San Antonio, TX, where he will begin his next assignment as an Air Quality Meteorologist at Brooks AFB, while she will prepare for the birth of their first child in October.

ACKNOWLEDGEMENTS

I would first like to acknowledge my family (my mother and father, and my two sisters) for providing me with the love, support, and guidance I have received over the years. The values instilled in me while growing up are, without a doubt, part of the reasons I have accomplished all that I have, and are what helped me through some of the darker days that every graduate student experiences.

For financial support, I must acknowledge the U. S. Air Force Institute of Technology, Civilian Institutions (AFIT/CI) program, without which this student might never have returned to graduate school. In particular, I would like to thank Captain Thomas Neu at AFIT/CIRW for his help and guidance in keeping the Air Force happy while I was attending a civilian graduate school. I would also like to acknowledge the support of the United States Environmental Protection Agency (USEPA), which funded part of this research through a cooperative agreement (CR822-58-01) as part of the Characterization of Emissions of Nitrogen Oxides from Soils of the Southeast U.S. Project. Further invaluable funding support was provided by the North Carolina Department of Environmental, Health and Natural Resources (NCDEHNR) under Contract Nos. J-4004 and J-3056.

A variety of people were instrumental in the completion of my research for various reasons, and to whom I extend my thanks: Mike Smith, a technician at NCDEHNR who provided many man hours of technical guidance concerning the instruments used in this research; Irene Joiner, Danny Hampton, Ed Hubbard and Charles Strickland, who

worked in conjunction with the Auburn Tower Partnership to graciously schedule my tower access; and of course my fellow students in the NCSU Air Quality research group, for whom I am indebted for research discussion and advice. In particular, I would like to thank Lee Sullivan and Paul Roelle for their cheerful help in freezing temperatures and 40 mph winds at 1500 feet on the tower; and Regi Oommen for his expertise in tracking a little red balloon launched at 0700 EST in freezing temperatures and somewhat lighter winds.

Finally, I would like to recognize my committee members for the support, advice and direction they provided: Dr. Dickey, for showing me how the science of statistics can help it all make sense (and when it can't!); Dr. Robarge, for showing me what different science disciplines have to offer to each other, and how to make them work together; and of course, Dr. Aneja, for helping to put a jumble of confused ideas together into meaningful research. In addition, I would like to thank my father-in-law, Dr. Perry Grady, for his in-depth perspectives on the graduate school program and general advice for tackling a thesis.

TABLE OF CONTENTS

LIST OF TABLES	ix
LIST OF FIGURES.....	x
1. INTRODUCTION.....	1
1.1 Tropospheric Reactive Nitrogen and the Production of Tropospheric Ozone.....	1
1.2 Importance of Measurements of Reactive Oxides of Nitrogen.....	5
1.3 Downward Mixing of Reactive Oxides of Nitrogen.....	5
1.4 Research Description.....	9
2. PLANETARY BOUNDARY LAYER DEFINITIONS.....	11
2.1 Terms.....	11
2.2 Processes.....	16
3. MATERIALS AND METHODS.....	19
3.1 Experimental Site	19
3.2 Instrumentation	21
3.2.1 NO and NO _y Mixing Ratios.....	21
3.2.1.1 Calibration.....	23
3.2.1.2 Error Calculation.....	24
3.2.1.3 Instrument Minimum Detection Limit Calculation.....	24
3.2.2 Wind Vane/Anemometer	25
3.2.3 Data Loggers	26
3.3 Equipment Placement and Time Period of Research.....	26
3.3.1 Tower Measurements	26
3.3.2 Surface Measurements	27
3.4 Meteorological Analysis	28
3.4.1 Wind Direction.....	28
3.4.2 Synoptic Meteorological Features.....	29
3.4.3 Boundary Layer Height Determination	30
3.4.3.1 Greensboro, NC National Weather Service Upper Air Soundings.....	32
3.4.3.2 Local Upper Air Soundings	34
3.5 Typical Measurement Sequence.....	35
3.6 Statistical Analysis.....	36

4. RESULTS AND DISCUSSION	40
4.1 Overview	40
4.2 NO and NO _y Mixing Ratios: Vertical Gradients and Diurnal Profiles	41
4.2.1 NO Mixing Ratios	41
4.2.2 NO Mixing Ratio Vertical Gradient Model	45
4.2.3 NO _y Mixing Ratios	49
4.3 Correlation of Observed Mixing Ratios with Synoptic Features	51
4.3.1 NO Mixing Ratios	53
4.3.2 NO _y Mixing Ratios	66
4.4 Boundary Layer Formation and Vertical Transport Processes	78
4.4.1 Formation of the Nocturnal Boundary Layer	78
4.4.1.1 Strong Nocturnal Boundary Layer Formation	79
4.4.1.1.1 12 Dec 94	80
4.4.1.1.2 17 Jan 95	82
4.4.1.1.3 18 Jan 95	84
4.4.1.1.4 7 feb 95	86
4.4.1.2 Moderate Nocturnal Boundary Layer Formation	88
4.4.1.2.1 13 Jan 95	89
4.4.1.2.2 3 Feb 95	91
4.4.1.2.3 20 Feb 95	93
4.4.1.3 Nocturnal Boundary Layer Formation Discussion	95
4.4.2 Growth of the Mixed Layer	96
4.4.2.1 8 Dec 94	97
4.4.2.2 9 Dec 94	101
4.4.2.3 13 Dec 94	106
4.4.2.4 18 Jan 95	110
4.4.2.5 25-26 Jan 95	113
4.4.2.6 9 Feb 95	117
4.4.2.7 Mixed Layer Formation Discussion	121
4.4.3 Surface Comparison	121
4.4.4 Boundary Layer Formation and Vertical Transport Processes Summary	123
4.5 Atmospheric Chemistry and Horizontal Transport	124
4.5.1 NO Mixing Ratios	125
4.5.1.1 Atmospheric Chemistry	125
4.5.1.2 Horizontal Transport	125
4.5.2 NO _y Mixing Ratios	128
4.5.2.1 Atmospheric Chemistry	128
4.5.2.2 Horizontal Transport	130

5. SUMMARY	132
5.1 Conclusions	132
5.2 Recommendations for Future Research	137
6. LIST OF REFERENCES	140
7. APPENDICES	148
7.1 Appendix 1. National Weather Service Daily Surface Weather Maps (Valid 0700 EST): December 7-16, 1994; January 12-25, 1995; February 2-23, 1995	149
7.2 Appendix 2. Raw Data	173
7.2.1 250 and 433 meters	174
7.2.1.1 NO Mixing Ratios	174
7.2.1.2 NO _y Mixing Ratios	183
7.2.2 Surface (10 meters); NO Mixing Ratios Only	191

LIST OF TABLES

Page

INTRODUCTION

Table 1.1 Chemical Reactions of Major Reactive Nitrogen Species in the Atmosphere.....	3
--	---

RESULTS AND DISCUSSION

Table 4.1 Mean, Standard Deviation and (Median) of Observed NO and NO _y Mixing Ratios: Surface, 250 Meters and 433 Meters (Dec 94 -Feb 95)	42
Table 4.2 Comparison of the Predicted Mean NO Mixing Ratios to the Mean Observed NO Mixing Ratios at 250 and 433 Meters, 0600-0700 EST (One Dimensional Transport Model).....	48

LIST OF FIGURES

	Page
 INTRODUCTION	
Figure 1.1 Observed and Predicted Variation of the NO _x Mixing Ratio over a Rural Area	7
Figure 1.2 Composite Diurnal Profiles of NO, NO ₂ , and O ₃ : Summer 1992, Candor, NC	7
 DEFINITIONS	
Figure 2.1 Theoretical Nocturnal Boundary Layer	18
Figure 2.2 Downward Mixing (Fumigation) Upon Breakup of the Nocturnal Inversion	18
 MATERIALS AND METHODS	
Figure 3.1 Map of the Experimental Area, Showing Major Population Centers within 200 km and Major Highways	20
Figure 3.2 Estimated 1990 North Carolina Total NO _x Emissions by County in Pounds Per Day	20
Figure 3.3 Typical SBL Vertical Profiles of Absolute Temperature, Potential Temperature, and Wind Speed	31
Figure 3.4 Typical Mixed Layer Vertical Profiles of Potential Temperature and Water Vapor Content During Mid Morning and Noon.....	31
 RESULTS AND DISCUSSION	
Figure 4.1 Composite Diurnal Profile of NO Mixing Ratios, 10 Meters AGL (Jan-Feb 95).....	43
Figure 4.2 Composite Diurnal Profile of NO Mixing Ratios, 250 Meters AGL (Feb 95).....	43

Figure 4.3	Composite Diurnal Profile of NO Mixing Ratios, 433 Meters AGL (Dec 94-Jan 95)	44
Figure 4.4	Composite Diurnal Profiles of NO Mixing Ratios, 3 Heights (Dec 94-Feb 95).....	44
Figure 4.5	Composite Diurnal Profile of NO _y Mixing Ratios, 250 Meters AGL (Feb 95).....	50
Figure 4.6	Composite Diurnal Profile of NO _y Mixing Ratios, 433 Meters AGL (Dec 94-Jan 95).....	50
Figure 4.7	Composite Diurnal Profiles of NO _y Mixing Ratios, 2 Heights (Dec 94-Feb 95).....	52
Figure 4.8	Diurnal Variation of NO and NO _y Mixing Ratios, 250 Meters AGL (2-7 Feb 95).....	52
Figure 4.9a	Diurnal Variation NO Mixing Ratio Overlaid with Synoptic Meteorology, 433 Meters AGL (7-10 Dec 94)	56
Figure 4.9b	Diurnal Variation NO Mixing Ratio Overlaid with Synoptic Meteorology, 433 Meters AGL (11-14 Dec 94)	57
Figure 4.9c	Diurnal Variation NO Mixing Ratio Overlaid with Synoptic Meteorology, 433 Meters AGL (12-15 Jan 95).....	58
Figure 4.9d	Diurnal Variation NO Mixing Ratio Overlaid with Synoptic Meteorology, 433 Meters AGL (15-18 Jan 95).....	59
Figure 4.9e	Diurnal Variation NO Mixing Ratio Overlaid with Synoptic Meteorology, 433 Meters AGL (23-25 Jan 95).....	60
Figure 4.9f	Diurnal Variation NO Mixing Ratio Overlaid with Synoptic Meteorology, 250 Meters AGL (2-4 Feb 95).....	61
Figure 4.9g	Diurnal Variation NO Mixing Ratio Overlaid with Synoptic Meteorology, 250 Meters AGL (5-7 Feb 95).....	62
Figure 4.9h	Diurnal Variation NO Mixing Ratio Overlaid with Synoptic Meteorology, 250 Meters AGL (8-11 Feb 95).....	63
Figure 4.9i	Diurnal Variation NO Mixing Ratio Overlaid with Synoptic Meteorology, 250 Meters AGL (13-17 Feb 95).....	64

Figure 4.9j	Diurnal Variation NO _y Mixing Ratio Overlaid with Synoptic Meteorology, 250 Meters AGL (20-21 Feb 95).....	65
Figure 4.10a	Diurnal Variation NO _y Mixing Ratio Overlaid with Synoptic Meteorology, 433 Meters AGL (12-14 Jan 95).....	68
Figure 4.10b	Diurnal Variation NO _y Mixing Ratio Overlaid with Synoptic Meteorology, 433 Meters AGL (15-18 Jan 95).....	69
Figure 4.10c	Diurnal Variation NO _y Mixing Ratio Overlaid with Synoptic Meteorology, 433 Meters AGL (19-21 Jan 95).....	70
Figure 4.10d	Diurnal Variation NO _y Mixing Ratio Overlaid with Synoptic Meteorology, 433 Meters AGL (22-25 Jan 95).....	71
Figure 4.10e	Diurnal Variation NO _y Mixing Ratio Overlaid with Synoptic Meteorology, 250 Meters AGL (2-4 Feb 95).....	72
Figure 4.10f	Diurnal Variation NO _y Mixing Ratio Overlaid with Synoptic Meteorology, 250 Meters AGL (5-7 Feb 95).....	73
Figure 4.10g	Diurnal Variation NO _y Mixing Ratio Overlaid with Synoptic Meteorology, 250 Meters AGL (7-11 Feb 95).....	74
Figure 4.10h	Diurnal Variation NO _y Mixing Ratio Overlaid with Synoptic Meteorology, 250 Meters AGL (12-17 Feb 95).....	75
Figure 4.10i	Diurnal Variation NO _y Mixing Ratio Overlaid with Synoptic Meteorology, 250 Meters AGL (17-20 Feb 95).....	76
Figure 4.10j	Diurnal Variation NO _y Mixing Ratio Overlaid with Synoptic Meteorology, 250 Meters AGL (21-23 Feb 95).....	77
Figure 4.11	Greensboro, NC NWS Upper Air Sounding - 12 Dec 94 (0600 EST).....	81
Figure 4.12	Greensboro, NC NWS Upper Air Sounding - 17 Jan 95 (0600 EST).....	83
Figure 4.13	Greensboro, NC NWS Upper Air Sounding - 18 Jan 95 (0600 EST).....	85
Figure 4.14	Greensboro, NC NWS Upper Air Sounding - 7 Feb 95 (0600 EST).....	87
Figure 4.15	Greensboro, NC NWS Upper Air Sounding - 13 Jan 95 (0600 EST).....	90
Figure 4.16	Greensboro, NC NWS Upper Air Sounding - 3 Feb 95 (0600 EST).....	92

Figure 4.17	Greensboro, NC NWS Upper Air Sounding - 20 Feb 95 (0600 EST)	94
Figure 4.18a	Greensboro, NC NWS Upper Air Sounding - 8 Dec 94 (0600 EST)	98
Figure 4.18b	NCSU Upper Air Sounding - 8 Dec 94 (0730 EST)	99
Figure 4.18c	Diurnal Variation NO Mixing Ratio, 433 Meters AGL (8 Dec 95)	100
Figure 4.19a	Greensboro, NC NWS Upper Air Sounding - 9 Dec 94 (0600 EST)	102
Figure 4.19b	NCSU Upper Air Sounding - 9 Dec 94 (0845 EST)	103
Figure 4.19c	NCSU Upper Air Sounding - 9 Dec 94 (1030 EST)	104
Figure 4.19d	Diurnal Variation NO Mixing Ratio, 433 Meters AGL (9 Dec 94)	105
Figure 4.20a	Greensboro, NC NWS Upper Air Sounding - 13 Dec 94 (0600 EST)	107
Figure 4.20b	NCSU Upper Air Sounding - 13 Dec 94 (0815 EST)	108
Figure 4.20c	NCSU Upper Air Sounding - 13 Dec 94 (0915 EST)	109
Figure 4.21a	NCSU Upper Air Sounding - 18 Jan 95 (1030 EST)	111
Figure 4.21b	Diurnal Variation NO and NO _y Mixing Ratios, 433 Meters AGL (18 Jan 95)	112
Figure 4.22a	NCSU Upper Air Sounding - 26 Jan 95 (0915 EST)	114
Figure 4.22b	NCSU Upper Air Sounding - 26 Jan 95(1015 EST)	115
Figure 4.22c	Diurnal Variation NO and NO _y Mixing Ratios, 433 Meters AGL (25 Jan 95)	116
Figure 4.23a	Greensboro, NC NWS Upper Air Sounding - 9 Feb 95 (0600 EST)	118
Figure 4.23b	NCSU Upper Air Sounding - 9 Feb 95 (0800 EST)	119
Figure 4.23c	Diurnal Variation NO and NO _y Mixing Ratios, 250 Meters AGL (9 Feb 95)	120
Figure 4.24a	Composite Diurnal Profile of NO Mixing Ratios, Surface and 250 Meters AGL (Feb 95)	122

Figure 4.24b	Diurnal Variation of NO Mixing Ratios, Surface and 250 Meters AGL (10 Feb 95)	122
Figure 4.25	Mean Daytime NO Mixing Ratios vs Wind Direction (Tens of Degrees, Quadrants), 250 and 433 Meters (Dec 94-Feb 95)	127
Figure 4.26	Mean NO _y Mixing Ratios vs Wind Direction (Tens of Degrees, Quadrants) 250 and 433 Meters (Dec 94-Feb 95)	127

1. Introduction

1.1 Tropospheric Reactive Nitrogen and the Production of Tropospheric Ozone

The family of reactive nitrogen species, composed primarily in the lower troposphere of nitric oxide (NO) + nitrogen dioxide (NO₂) + peroxyacetyl nitrate (PAN) + nitric acid (HNO₃) + particulate nitrate (NO₃⁻) [Fahey, et al. 1986; Trainer et al. 1991; Parrish et al., 1993], and referred to here as NO_y, plays a major role in the chemistry of the troposphere. Through an oxidation reaction with peroxy and hydroperoxy radicals (which are themselves the result of oxidation of hydrocarbons), the primary reactive nitrogen species, NO, is converted to NO₂; hydroxyl radicals then oxidize NO₂ into HNO₃, which is removed from the atmosphere by both wet and dry deposition [Levine and Schwartz, 1981; Logan et al., 1981] as a major constituent of acidic deposition [Galloway and Likens, 1981]. Peroxyacetyl radicals can also combine with NO₂ to form PAN [Warneck, 1988], which in elevated concentrations is harmful to human health and can damage crops and forests [Taylor, 1969; *Office of Technology Assessment, U.S. Congress*, 1989, and references therein]. These reactions control to some degree the balance of radicals in the troposphere by acting as sinks for the radicals and thus decreasing the total radical concentration in the atmosphere. These radicals are responsible for the production of such atmospheric oxidants as ozone, hydrogen peroxide, and organic hydroperoxides. The levels of these oxidants, therefore, are strongly coupled to the levels of the NO_y family in the troposphere (Parrish, et al. 1993). In particular, the source species for the NO_y family, NO and NO₂ (together, NO + NO₂ = NO_x; the

remaining members of NO_Y are known as the oxidized species, or NO_Z) play a predominant role as precursors in the production of ozone (O_3) through the photooxidation of carbon monoxide, methane, and other reactive hydrocarbons [Fishman et al., 1979; Logan et al., 1981]. Ozone is a primary component of photochemical smog, and is harmful to humans [Folinsbee et al., 1988] as well as vegetation [Reich and Amundson, 1985; Heck et al., 1982, 1983, 1984]. Our current understanding on transport mechanisms within the troposphere suggests that up to 20 % of tropospheric O_3 is a result of downward mixing from the stratosphere under appropriate conditions [Mohnen et al., 1977; Johnson and Viezee, 1981; Kelly, et al. 1982, Hough and Derwent, 1990]. The remaining 80% of the O_3 in the troposphere is thought to be photochemically produced in-situ through a series of oxidation reactions that involve NO_x , hydrocarbons, and sunlight. This series of reactions results in the photodissociation of NO_2 , and is the only definitely established process for production of ozone in the troposphere [Chameides and Walker, 1973; Fishman et al., 1979; Logan et al., 1981; Hov, 1983; Fishman et al., 1985; Liu et al., 1987; Warneck, 1988].

Reactions 1, 2, and 3 in Table 1.1 outline the atmospheric chemistry processes that result in the production of ozone in the troposphere. Model studies have indicated that the amount of ozone produced per NO_x oxidized depends nonlinearly on the NO_x mixing ratio, with the ozone production efficiency decreasing with increasing NO_x mixing ratio levels (The *mixing ratio* is a dimensionless unit used to specify the abundance of an atmospheric constituent within a parcel of air. Specifically, it is a comparison of the volume of the constituent to the volume of the air containing the constituent, and is given

Table 1.1. Chemical Reactions of Major Reactive Nitrogen Species in the Atmosphere.

<u>Photostationary State:</u>	<u>Rate Constant*</u>
(R1) $\text{NO}_2 + h\nu (\lambda \leq 420 \text{ nm}) \rightarrow \text{NO} + \text{O}(^3\text{P})$	3.5×10^{-3}
(R2) $\text{O}_2 + \text{O}(^3\text{P}) \xrightarrow{\text{M}} \text{O}_3$	6.2×10^{-34}
(R3) $\text{NO} + \text{O}_3 \rightarrow \text{NO}_2 + \text{O}_2$	$2.3 \times 10^{-12} \exp(-1450/T)$
<u>Peroxy Radical Disruption of Photostationary State:</u>	
(R4) $\text{NO} + \text{HO}_2 \rightarrow \text{NO}_2 + \text{OH}$	$4.3 \times 10^{-12} \exp(+200/T)$
(R5) $\text{NO} + \text{RO}_2 \rightarrow \text{NO}_2 + \text{RO}$	8.0×10^{-12}
<u>Formation and Destruction of Nitrous and Nitric Acid:</u>	
(R6) $\text{NO} + \text{OH} \rightarrow \text{HONO}$	5×10^{-12}
(R7) $\text{HONO} + h\nu \rightarrow \text{NO} + \text{OH}$	8.4×10^{-4}
(R7) $\text{NO}_2 + \text{OH} \rightarrow \text{HNO}_3$	1.3×10^{-11}
(R8) $\text{HNO}_3 + h\nu \rightarrow \text{OH} + \text{NO}_2$	1×10^{-7}
<u>Formation and Thermal Decomposition of PAN, and Loss of PAN with NO:</u>	
(R8) $\text{CH}_3\text{CO}_3 + \text{NO}_2 \rightarrow \text{CH}_3\text{CO}_3\text{NO}_2$	6×10^{-12}
$\text{CH}_3\text{CO}_3\text{NO}_2 \rightarrow \text{CH}_3\text{CO}_3 + \text{NO}_2$	$1.12 \times 10^{-16} \exp(-13330/T) \text{ s}^{-1}$
(R9) $\text{CH}_3\text{CO}_3 + \text{NO} \rightarrow \text{CH}_3 + \text{CO}_2 + \text{NO}_2$	1.4×10^{-11}

* Reaction rate units are s^{-1} for unimolecular processes, $\text{cm}^3 \text{ molecules}^{-1} \text{ s}^{-1}$ for bimolecular processes, and $\text{cm}^6 \text{ molecules}^{-2} \text{ s}^{-1}$ for termolecular processes; T is degrees Kelvin.

SOURCE: Logan et al., 1981; Singh, 1987; Warneck et al., 1988.

in units such as *parts per billion by volume* (ppbv). For example, if 1 ml of NO is measured in 1 billion ml of air, then this NO is reported to have a mixing ratio of 1 ppbv). However, the degree of nonlinearity has been found to be strongly dependent on the non-methane hydrocarbon (NMHC) to NO_x ratio [Liu et al., 1987; Lin et al., 1988].

The concentration of O₃ in the troposphere has continued to increase globally in response to a corresponding increase in precursor concentrations, due in large part to human activity [Hough and Derwent, 1990; Finlayson- Pitts and Pitts, 1993]. Relatively high concentrations of ozone continue to be a major environmental and health concern in the United States [National Research Council, 1992] despite 20 years of considerable regulatory and pollution control efforts. It has also been shown that many rural areas are just as susceptible to elevated ozone concentrations as urban areas, and more importantly, that most of this ozone is being produced photochemically from ozone precursors emitted within the region [Research Triangle Institute, 1975; Vukovich et al., 1977, 1985; Cleveland et al., 1977; Spicer, 1977; Wolff and Lioy, 1980; Fehsenfeld et al., 1983; Kelly et al., 1984; Liu et al., 1987, Chameides et al., 1992; Trainer et al., 1993]. As part of its recommendations to reverse these trends, the National Research Council [1992] stated a need for more systematic measurements of the spatial, vertical and temporal variation of NO and NO_x mixing ratios in the troposphere, across both urban and rural areas, to determine the extent to which precursor emissions must be controlled and to verify the effectiveness of the control measures undertaken.

1.2 Importance of Measurements of Reactive Oxides of Nitrogen

A knowledge of the vertical distribution, transport, and sources of the reactive oxides of nitrogen (in particular NO and NO₂) within the planetary boundary layer is critical to the analysis and development of global and regional atmospheric models; in particular those that aim to correctly interpret the ozone production potential of various environmental conditions, such as the Regional Oxidant Model (ROM) and Urban Airshed Model (UAM) currently in use by the US Environmental Protection Agency (EPA). While a growing body of surface measurements of NO, NO_x, and NO_y mixing ratios exists, no research exists that provides an indication of the distribution and/or variation of NO, NO_x, or NO_y mixing ratios as measured from stationary platforms at various heights within the typical day and nighttime planetary boundary layer.

1.3 Downward Mixing of Reactive Oxides of Nitrogen

The origin of tropospheric ozone in rural areas (away from anthropogenic precursor sources) is attributed to a number of sources including natural precursor emissions, horizontal advections, vertical mixing, deposition, and chemical production. Particularly in the area of sources of precursors, much consideration has been given to the process known as "downward mixing", or fumigation from a plume of pollutants during breakup of the nocturnal inversion layer. The downward mixing of pollutants from the plume can produce an increase in ground level mixing ratios of these pollutants, and result

in “peaks” in the measured profiles of pollutants. The general mechanisms by which downward mixing occur are understood in a qualitative sense, and are detailed in the definitions section given below. In particular, downward mixing has been related to increases in surface ozone mixing ratios [Neu et al., 1994] and also to increases in ground level mixing ratios of ozone precursors such as NO_x over rural areas [Aneja et al., 1994]. Trainer et al. [1987,1991] postulate that increases in NO_x mixing ratios at the surface over a rural area in Pennsylvania are attributable to the horizontal transport of NO_x within the nocturnal boundary layer and subsequent downward mixing to the surface during the morning hours. To simulate this phenomenon with a one dimensional model, the authors assumed a continuous NO_x emission rate for the height range 200 to 800 m in 1987 or from 110 to 160 m in 1991. However, the authors do state that the exact height of the emission layer is not critical, provided it is above the inversion layer; but that the width of the assumed layer determines the duration and magnitude of the early morning peak of NO_x . Figure 1.1 shows the variation of the observed NO_x mixing ratios over a rural area compared to the predicted variation of the NO_x mixing ratios as calculated by this model.

However, careful scrutiny of previous research verifies the possibility that sources other than downward mixing may be responsible in part for morning increases in surface mixing ratios of NO_x . Aneja et al. [1994], observed a distinct rise in the NO mixing ratio from the nocturnal minimum that began at 0600 Daylight Savings Time (DST) and peaked at around 0900 DST; NO_2 showed a continuous rise during the night to a maximum at 0600 DST (Figure 1.2). These measurements were made in a location far from any major cities or highways in rural North Carolina during the summer

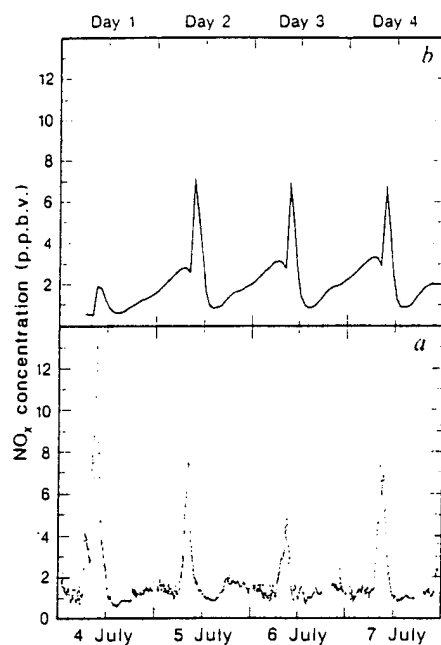
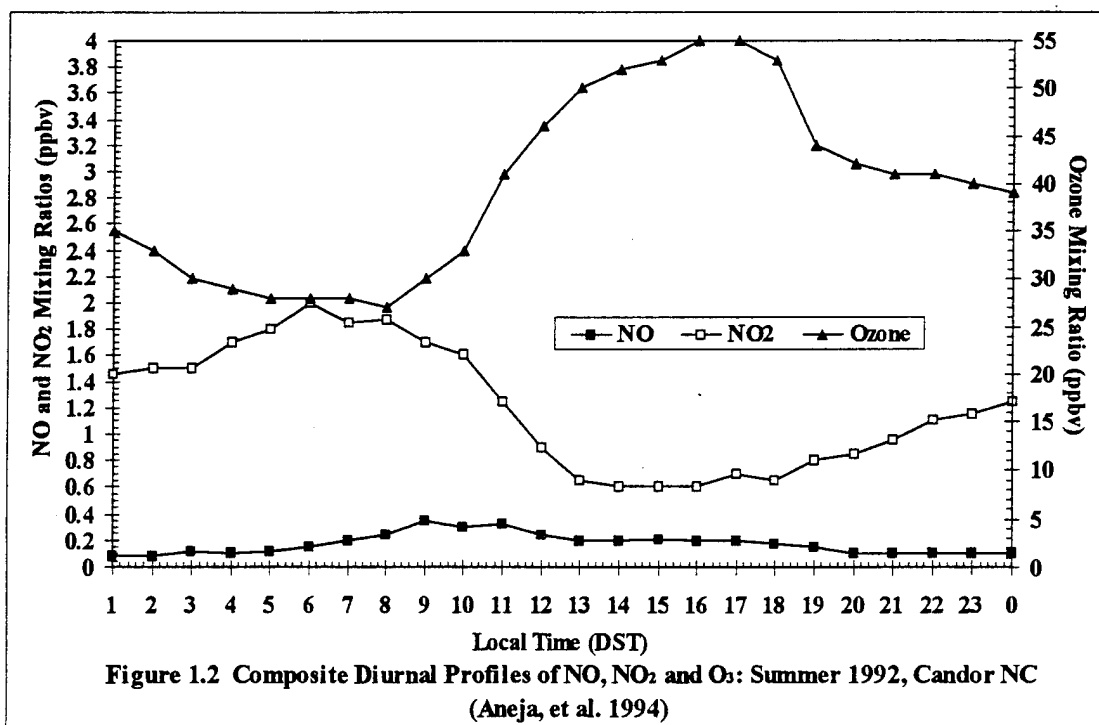


Figure 1.1 Observed (a) and Predicted (b) Variation of the NO_x Mixing Ratio over a Rural Area (Trainer, et al. 1987)



of 1992 and should not be influenced by rush hour traffic. Aneja et al. (1994) suggested three possible sources for the increase in morning NO mixing ratios; the first of which was downward mixing. However, reinspection of the data shows that, given a sunrise occurring between 0600 and 0630 DST during this period, the NO₂ mixing ratio peaks at or just before sunrise, and the NO mixing ratio begins to increase well before the expected breakup of the nocturnal inversion. The time of the breakup of the inversion layer can be estimated from the change in measured O₃ mixing ratios. Ozone is considered a tracer species that is stored in the residual layer and subsequently mixed downward at the breakup of the nocturnal inversion to refresh surface concentrations [Neu et al., 1994]. The ozone mixing ratios observed in this study responded accordingly, with a rise from the nocturnal minimum beginning between 0800 DST and 0900 DST (or about the time of the projected breakup of the inversion). If the NO_x species were transported down via the same process as the O₃, then the NO_x and O₃ profiles would match more closely. The data in Figure 1.2 suggests that downward mixing is not a predominant source of NO and NO₂ at the surface. Aneja et al. (1994) proposed an alternative hypothesis for the increases of NO and NO₂ in which NO emitted from the soil during the night is converted to NO₂ via the reaction with residual O₃, and then the subsequent photolysis of NO₂ at sunrise produces NO (Table 1.1 outlines these reaction processes). Finally, asserting that downward mixing is responsible for all observed increases in surface NO_x mixing ratios is questionable due to its implicit assumption that there is always a NO_x emission layer above the nocturnal boundary layer, without consideration of the direction of the winds at this height, the location of the NO_x sources, or the structure of the boundary layer itself.

In effect, there has to be a constant "river" of NO_x overhead in the nocturnal boundary layer that can be "tapped" by the downward mixing process for transport to the surface.

1.4 Research Description

The primary goal of this research was investigation of the possible relationship between the observed vertical distribution of mixing ratios of NO and NO_Y and specific morning transport mechanisms within the boundary layer (i.e., downward mixing). To this end, mixing ratios of NO and NO_Y were continuously measured on two stationary platforms on a transmitter tower over a semi-urban area of central North Carolina at heights of 250 meters (820 feet) and 433 meters (1420 feet) above ground level (AGL). Concurrent measurements of NO and NO_Y were taken at an ambient height of 10 meters AGL over an agricultural field less than 2 kilometers (1.2 miles) from the base of the transmitter tower. The observed values of NO and NO_Y mixing ratios were then compared with a vertical transport model, synoptic meteorological parameters, and planetary boundary layer structure to characterize their possible sources, atmospheric chemistry, and most importantly, transport processes within the boundary layer. Results will be presented which support the argument that NO and NO_Y did not exist in sufficient quantities above the nocturnal inversion layer to be mixed downward by morning transport processes and affect surface mixing ratios. Instead, the data suggest that NO and NO_Y can be mixed *upward* from the surface during the morning and midday hours by vertical boundary layer processes, and can also be mixed upward during other times of the day or

night by synoptic meteorological features (and their associated vertical motions). The measurements of NO_Y mixing ratios during this study can also be used as a surrogate for NO_X mixing ratios and serve to illustrate transport mechanisms of NO_X during the early morning hours (0600-0900 local time). The major NO_Y constituents PAN and HNO_3 are at a diurnal minimum during the early morning hours [Warneck, 1988], and thus NO_Y consisted largely of NO and NO_2 (or NO_X) during this time.

2. Planetary Boundary Layer Definitions

The troposphere is the lowest layer or region of the earth's atmosphere (mean height is approximately 10 km), and is important because the earth's weather occurs in this layer. The troposphere can be broken into two major regions, the planetary boundary layer (PBL) and the free atmosphere (FA). Furthermore, the PBL is broken into several subregions where particular transport phenomenology is located. For purposes of this manuscript, the general structure and accompanying definitions of the atmosphere and descriptions of the atmospheric processes given by Stull [1988], and also as outlined by Cooper and Eichinger [1994], are presented below for clarity and convenience. Figures 2.1 and 2.2 [Stull, 1988] illustrate the following discussion of terms and processes within the troposphere and are found at the end of this section.

2.1 Terms (Figure 2.1)

Planetary Boundary Layer (PBL): The PBL is defined as the atmosphere between the surface and the free atmosphere (FA). It is directly affected by the properties of the Earth's surface and surface forcings, such as frictional drag, evapotranspiration, heat transfer, pollutant emission, and topography. At the top of the PBL there is typically an inversion layer known as the entrainment zone (EZ).

Free Atmosphere (FA): The FA is the layer above the boundary layer. Profiles in the FA show constant gradients of increasing potential temperature (θ) and decreasing specific humidity (q). Potential temperature is that temperature an air parcel at a certain height (and pressure) would have if it were reduced dry adiabatically (i.e., at constant entropy for dry air) to a standard pressure of 1000 mb. It is considered an indicator of the stability of the atmosphere at that height. Specific humidity is a ratio of the number of grams of water vapor in a gram of air holding that water vapor. FA conditions are considered “geostrophic” where planetary processes such as the Coriolis forces dominate.

Entrainment Zone (EZ): The EZ is a stable capping layer that limits thermal convection, retarding the upward extent of turbulent transport. It can be thought of as an interface where air from one layer is being entrained or mixed into the layer below it. At night or during stable conditions, this capping stable layer is sometimes strong enough to be classified as a temperature inversion (absolute temperature increasing with height) and is thus referred to as the capping inversion layer (CIL).

Mixed Layer (ML): When forcing such as solar heating allows for formation of unstable atmospheric conditions, the mixed layer (ML) is formed. The height of this layer is from the surface layer (SL, defined below) to generally 1-2 km in temperate mid-latitude regions. This layer is the critical layer for surface-generated mass transport, and is defined as the region above the SL where turbulence is convectively driven.. The solar heating of the surface generates convective eddies that govern the ML height and extent of mixing.

The ML is capped by the EZ. Because of the efficiency of the mixing, profiles of potential temperature and humidity tend to be constant with height (a layer with constant potential temperature is known as isothermal). Though technically the daytime planetary boundary layer is composed of three distinct regions (the SL, the ML, and the EZ), in many cases the ML itself is used as a synonym for the daytime PBL.

Stable Boundary Layer (SBL): When conditions allow for formation of stable atmospheric conditions, such as at night under clear skies and light winds, or during certain conditions during the day (when the underlying surface is colder than the air), a stable boundary layer (SBL) can form. Technically speaking, a statically stable layer of air forms with increasing potential temperature near the surface as a result of radiational cooling of the earth's surface. The height of the SBL can range from 60 to 500 meters, with an average height of 100 to 300 meters. The stable air in the SBL acts to suppress continuous turbulence and thus vertical motion, and can therefore produce strong vertical gradients of temperature, water vapor, and pollutants. The strength of the SBL is related to the amount of radiational cooling of the earth's surface, and therefore is related to the presence or absence of clear skies and light winds during the nighttime.

Nocturnal Boundary Layer (NBL): The SBL is also known as the nocturnal boundary layer (NBL) at night, and may also be loosely referred to as the "nocturnal inversion" due to the increase in potential temperature. If the stability of the atmosphere is strong enough, a temperature inversion may form. Plumes of pollutants emitted into the NBL

from tall smoke stacks disperse relatively little in the vertical direction, but disperse more rapidly or “fan out” horizontally (a phenomenon known as fanning). The NBL has a poorly defined (in a physical sense) top that smoothly blends into the layer above it (see residual layer below), and is technically defined as the height where turbulent intensity is a small fraction of its surface value.

A common feature of the NBL near this poorly defined interface with the layer above it is the occurrence of a low level jet (LLJ), or region of low level wind maxima that usually occurs at or just above the nocturnal inversion. The LLJ can transport pollutants in the residual layer hundreds of kilometers downward from their sources. Formal criteria for identification of the LLJ vary; for purposes of this manuscript a loose definition is employed which requires only that wind speed increase from the surface to a maximum at or near the inversion and then decrease for at least 250 meters above this maximum. While the statically stable air of the NBL tends to suppress turbulence, the developing nocturnal jet enhances wind shears that tend to generate turbulence that can occur in relatively short bursts and cause mixing throughout the NBL. As a consequence of this turbulence, deposition of atmospheric constituents such as aerosols or trace gas species can occur as the turbulence brings them in contact with the earth’s surface. This process can lead to a decrease in the mixing ratios of these species in the NBL.

Residual Layer (RL): When conditions that allow for the formation of the SBL exist, a residual layer (RL) forms above the SBL and below the CIL, and generally has a height of 1-1.5 km. The RL is neutrally stratified, and its concentrations of passive scalars, such as

aerosols, are the result of earlier ML decay. Because of the neutral stratification, turbulence is nearly of equal intensity in all directions; passive scalars that are the result of the earlier ML decay are still well mixed, and any pollutant that is introduced into the RL (e.g. stack emission) will tend to disperse at equal rates in the vertical and the lateral directions, creating a cone shaped plume. This plume may disperse to the point that the bottom of the plume hits the top of the NBL (and where the inversion inhibits further downward mixing), however the top of the plume may continue to rise into the neutral air (a process known as lofting). Plumes in the RL can theoretically be transported large horizontal distances. Because of the physical separation of the RL from the Earth's surface, deposition of atmospheric constituents is minimal; and this, combined with the lack of photochemical activity at night leads to the conservation (or storage) of some species (in the absence of reaction with other species) during the night time. The interface between the SBL and RL is weak, however, and diagnostic tools used to isolate the height of these layers and their interface are subjective.

Surface Layer (SL): The bottom of the troposphere is called the surface layer (SL), and has been defined as the region directly above the earth's surface where the variation of turbulent fluxes and stress are less than 10% of their magnitude. It is present in both the mixing layer and the nocturnal boundary layer generally at height of less than 50 meters, and does not usually play as large a role as the NBL or the RL in isolating atmospheric constituents.

2.2 Processes (Figure 2.2)

Breakup of the Nocturnal Inversion: As noted above, nocturnal weather conditions such as clear skies and light winds can lead to the development of the RL and the NBL. Just after sunrise, however, a new ML begins to form from the heating of the earth's surface by the sun and the resulting formation of convective turbulence (eddies or thermals). As the eddies grow larger and higher, they slowly erode the stable boundary layer and then the nocturnal inversion. Once into the RL, the height of the ML grows rapidly in the neutrally stable air. The time it takes for the breakup of the nocturnal boundary layer depends on many factors: stability of the layer, amount of heating, height of inversion, etc., and observed and calculated times vary, but generally it takes from 2 to 3 hours after sunrise for heating to completely breakup the nocturnal inversion [Godowitch et al., 1985; Stull, 1988; Raynor and Watson, 1991; Batchvarova and Gryning, 1991; Hastie, et al., 1993].

Downward Mixing: As noted earlier, plumes emitted from stacks into the top of the NBL or at any height in the RL are rarely dispersed or mixed to the surface during the night due to the lack of vertical turbulence (the strength of the NBL determines how well the emitted pollutants are protected from deposition at the earth's surface and therefore determines the magnitude of the mixing ratios of the pollutant). Instead, these plumes may be transported horizontally hundreds of kilometers from their source, possibly as part of the LLJ. However, after sunrise and the breakup of the nocturnal inversion, the top of

the convective eddies of the newly forming ML can reach the height of the plume, and the pollutants will be entrained into the eddies and mixed both upward and (more importantly) downward to the earth's surface. Given the time for breakup of the nocturnal inversion discussed above, pollutants would not begin to be mixed down to the earth's surface until 2-3 hours after sunrise, at which time surface mixing ratios would peak and then decrease soon thereafter (due to dilution by the increasing volume of the rapidly growing ML).

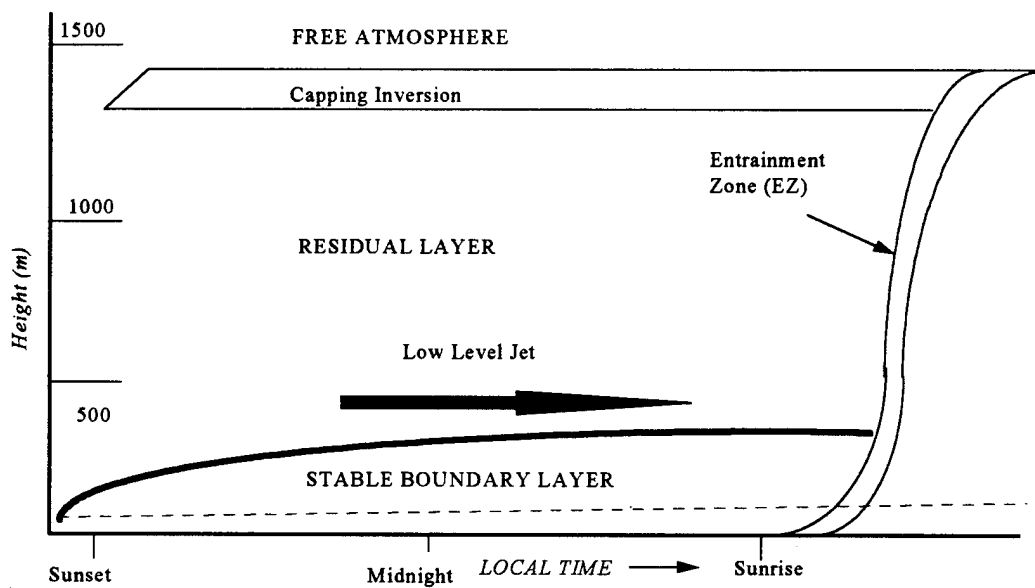


Figure 2.1 Theoretical Nocturnal Boundary Layer (Stull, 1988)

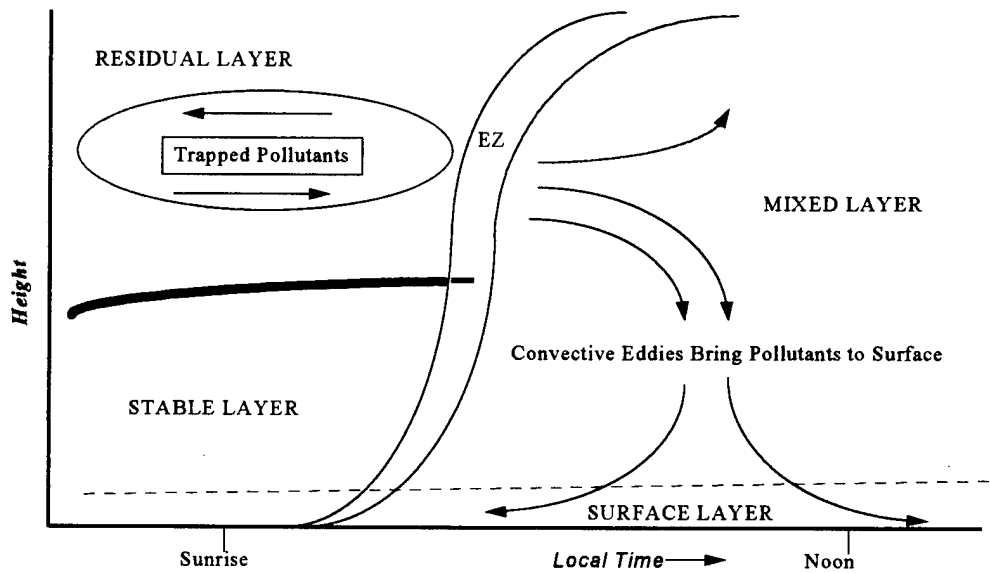


Figure 2.2 Downward Mixing (Fumigation) Upon Breakup of the Nocturnal Inversion

3. *Materials and Methods*

3.1 Experimental Site

Measurements of NO and NO_y mixing ratios were made at 250 and 433 meters on the Auburn Transmitter Tower, a multi-communications tower located near the town of Auburn, North Carolina (N Latitude 35° 40' 35"; W Longitude 78° 32' 09'), approximately 19 kilometers (12 miles) east-southeast of downtown Raleigh, NC (location indicated by the star in Figure 3.1). The tower is located along the Wake County - Johnson County line, which serves as the dividing line between the more urban areas of the west, a region that includes Raleigh, Durham, Chapel Hill, and Cary, and the more agricultural, rural areas of the Upper Coastal Plain of North Carolina to the east. Major population centers within a 200 km radius of the tower as well as the close proximity of major highways, most notably US Highway 70 (US-70), Interstate 40 (I-40), and Interstate 95 (I-95), are identified in Figure 3.1.

From a base elevation of 96 meters (315 feet) above mean sea level (MSL), the tower rises over 600 meters (2000 feet) above a mixture of cleared farmlands and small forest plots composed of a mixture of deciduous and conifer trees. Situated between the low, rolling hills of the Uwharrie mountains (elevation 180 to 275 meters (600 to 900 feet)), approximately 100 km (62 miles) to the west, and the flat topography of the coastal plain to the east, the geography of the experiment site near the tower is fairly uniform, with small changes in elevation of 30 meters (100 feet) or less. Given the uniform

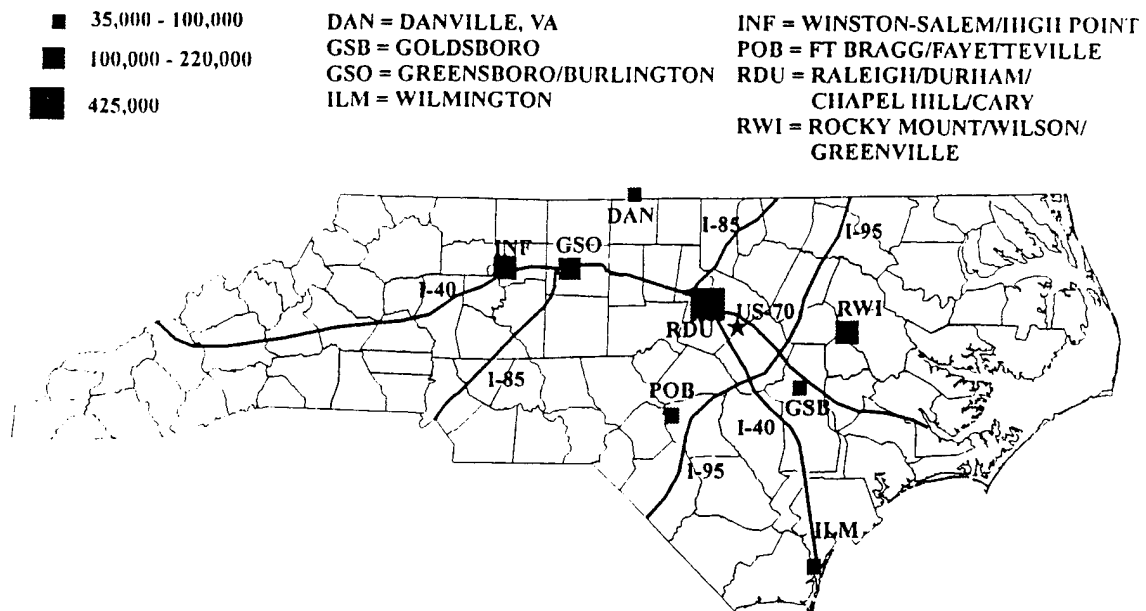


Figure 3.1 Map of Experimental Area, Showing Major Population Centers Within 200 km and Major Highways (research tower location is indicated by the star)

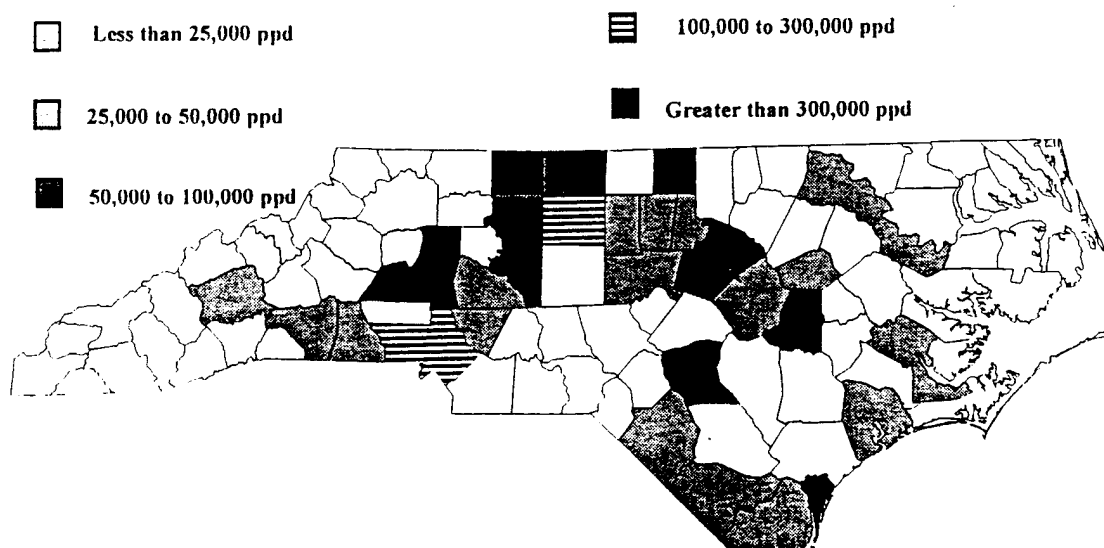


Figure 3.2 Estimated 1990 North Carolina Total NO_x Emissions by County in Pounds Per Day (ppd) (location of research tower is indicated by the star)
SOURCE: North Carolina Department of Environmental, Health, and Natural Resources (NCDEHNR)

topography, there are no recurring micro or mesoscale meteorological phenomena of note, allowing for the possible development of strong nocturnal stable boundary layer (under the prerequisite synoptic meteorological conditions) and its subsequent break down by morning radiant heating.

As the tower is located approximately 1 km (0.6 mile) southwest of US-70 and approximately 3 km (1.8 miles) east of I-40, automobile exhaust is the primary local source for NO_x in this region; however, there are several large NO_x point sources (such as power plants) within a 200 km radius. A county by county breakdown of total NO_x emissions in North Carolina is given in Figure 3.2.

Surface (10 meter) mixing ratios of NO, as well as wind speed and direction, were measured over an agricultural field less than 3 km (2 miles) east of the base of the transmitter tower, as part of a concurrent research study dealing with soil emissions of NO [Sullivan, 1995]. The measurements were made in a location approximately 305 meters (1000 ft) due south from US-70 and 5 km (3.1 miles) east of I-40.

3.2 Instrumentation

3.2.1 NO and NO_y Mixing Ratios

Analysis of the NO mixing ratios at all heights was carried out by using a TECO 42S (Thermal Environmental Instruments Inc.) chemiluminescence high sensitivity NO-

NO_x analyzer. This analyzer achieves high sensitivity by utilizing the reaction between NO in the airstream and an O₃ reagent produced by the instrument itself; chemiluminescence arises from a fraction of the reaction product, NO₂, which is produced in the ²B₁ excited electronic state and subsequently decays by photon emission. The photon flux is linearly proportional to the NO mixing ratio in the airstream [Ridley and Howlett, 1974], and a cooled photomultiplier tube is used to detect the emission of the photon and determine the mixing ratio of NO. The detection limit for this instrument is cited at 0.05 parts per billion volume (ppbv) NO [Thermal Environmental Instruments, Inc. 1992], however individual determination of the instrument's detection limit was calculated for each instrument and run, as outlined below.

While the TECO 42S is produced as an NO-NO_x analyzer, it has been noted that its heated (325° C) molybdenum, used to convert NO₂ to NO for subsequent measurement, also responds nearly quantitatively to the other primary members of the tropospheric NO_y family (PAN, HNO₃, and particulate NO₃⁻) [Winer et al., 1974; Finlayson-Pitts and Pitts, 1986, and references therein]. Thus this instrument is in fact an NO-NO_y analyzer (and hereafter will be referred to as such), and measurements taken with this instrument during this research will be referred to as NO and NO_y mixing ratios. However, since the air stream entering the instrument is filtered through a 5 micron Teflon filter, nearly all particulate nitrate (NO₃⁻) was filtered out before reaching the molybdenum converter, and thus the recorded NO_y mixing ratios are expected to be negatively biased. This bias is variable with respect to the humidity of the troposphere and the subsequent equilibrium ratio between HNO₃ and NO₃⁻. As noted before, however, these NO_y mixing

ratios can be considered as a surrogate for NO_x measurements during the early and mid morning hours due to the minimum values of the major NO_y constituents PAN and HNO_3 observed at this time.

3.2.1.1 Calibration

The TECO 42S instruments were zeroed and calibrated according to protocol by using a TECO 146 gas dilution/titration instrument, a standard containing 614 ppbv NO in N_2 (Scott Specialty Gases, Inc., Plumsteadville, PA), and compressed zero air (National Welders, Raleigh, NC). A multipoint zero and calibration was performed in the NCSU Air Quality laboratory and internal instrument settings were noted prior to the installation of each instrument on the tower. Although conditions on the platform did not allow for daily zero and span checks, it was insured during weekly operational checks that the instruments were operating at the same internal settings those noted during zero and calibration in the laboratory.

For the NO- NO_y instrument used at the surface, the same procedure was used, with the exception that a zero and span procedure was accomplished at the beginning of each day.

3.2.1.2 Error Calculation

After each intensive (which ranged in duration from one to three weeks), the TECO 42S was brought down from the tower and checked for drift against the NO standard. The measured deviation was less than 3% and a correction factor was not applied to the raw data. In addition, discussion with engineers at TECO Instruments indicated that the difference in the standard atmospheric pressure between the calibration at the surface and placement of the instrument at 1500 feet should result in no more than a 4% loss of chemiluminescence detection of NO [Richard Kuran, personal communication].

3.2.1.3 Instrument Minimum Detection Limit Calculation

Due to a concurrent experimental study into soil NO emissions, two different TECO 42S NO-NO_y analyzers were used on the tower (one during December, and one during January and February; see measurement time period section), and a minimum detection limit was calculated for each instrument. This was done by taking a series of readings ($n > 200$) of the lowest recorded signals (which occurred for NO during the night) and assigning the value of three times the standard deviation of these background readings as the instrument minimum detection limit [Taylor, 1987]. The instrument used in January and February performed better than TECO specifications, with a calculated detection limit of approximately 0.04 ppbv; however the instrument used during the December intensive (433 m) performed erratically, possibly due to interference with the

data recording device, and the calculated minimum detection limit was approximately 0.23 ppbv. The compiled NO data for 433 meters (December and January) is therefore shown with a 0.23 ppbv minimum detection cutoff, while the data from 250 meters (February) is shown with a 0.04 ppbv cutoff.

For the NO-NO_y analyzer located at the surface (10 meters), the calculated minimum detection limit was 0.10 ppbv NO.

3.2.2 Wind Vane/Anemometer

Instantaneous surface wind speed and direction were recorded at the surface every 15 minutes with a Fascinating Electronics, Inc. wind vane and anemometer attached to the 10 m mast. Data from this equipment was routed through the Fascinating Electronics Experimenter to its software on the Toshiba laptop for display and recording. These instrument have a rated wind speed detection limit of 1.1 mph and minimum wind direction resolution of 1° [Fascinating Electronics, 1992]. The wind vane was oriented on site with the use of a hand held compass; the wind anemometer is preset and is not capable of being calibrated.

3.2.3 Data Loggers

Each TECO 42S was set to output data in 1 minute rolling averages every 10 seconds (each average is thus composed of 6 observations). These output data were then

collected in 15 minute binned averages by two different data loggers. For the December intensive, the output data was were collected through a Personal Computer Memory Card International Association (PCMCIA) card interface on a Toshiba Model 4700 CS laptop computer loaded with Labview for Windows software (Version 2.5.2, 1992; National Instruments Corp.). For the January and February intensives, the data were recorded by a Campbell Scientific Instruments Model 21 XL Datalogger. The data logging recording devices were calibrated during instrument calibration, and response curves were noted. These response curves were used to correct the raw data.

3.3 Equipment Placement and Time Period of Research

3.3.1 Tower Measurements

The NO-NO_y analyzer, along with a pump and one of the two data loggers, were placed in a weather proof steel chamber located on platforms at the previously mentioned heights; heat from the pump kept the environmental temperature (as measured by the data logger case temperature) within instrument operating range (10-30° C) a majority of the time (environmental temperatures fell below the operating range on a few occasions with no observable effect on measurements). The sample was pulled at 1.5 liters per minute (lpm) through a length of partially shielded 1/8 inch inside diameter perfluoroalkoxy (PFA) Teflon tubing that was attached to a metal bar which extended horizontally 1-2 m from the transmitter tower structure. Research by Kelly, et al. [1980] indicates that Teflon tubing

up to 3 m in length had negligible effect on NO, NO₂ and HNO₃ measurement through line loss. In this study, it was necessary to use longer lengths of tubing (approximately 12 m (40 ft) at 433 m and 6 meters (20 ft) at 250 m) that produced a residence time of 7 - 15 seconds. This longer residence time in the PFA tubing may have resulted in a slight negative bias in the NO_y measurement due to possible deposition of NO₂ and probable deposition of HNO₃ along the lines. Line loss of NO due to reaction with ozone is considered minimal because of the preferential reaction of ozone with other available tropospheric radicals such as the peroxy organic radical (RO₂) and hydroxyl radical (HO₂).

Measurements of NO and NO_y on the tower were made across three months during the winter of 1994-95; specifically, at the height of 433 m AGL December 7-16, 1994 and January 12-25, 1995; and at 250 m AGL February 2-23, 1995. Data from these periods are not continuous; approximately 25% of the elevated height measurements were lost due to malfunctions in the recording devices.

3.3.2 Surface Measurements

The surface (10 meter) mixing ratios of NO were measured adjacent to the agricultural field at various times as part of the previously mentioned soil emissions research between January 18 and February 16, 1995 via a portable 10 meter (33 feet) mast. A 18 meter (60 ft) sample line of perfluoroalkoxy (PFA) Teflon was used to carry the sample to a shock mounted (Armaflex based insulation) TECO 42S NO- NO_y analyzer located in a temperature controlled mobile laboratory (modified Ford Aerostar van). This

length of PFA tubing produced a residence time of approximately 20 seconds; again line loss of NO due to reaction with ozone is considered minimal because of the preferential reaction of ozone with other available radicals such as the peroxy organic radical (RO₂) and hydroxyl radical (HO₂). The Toshiba Model 4700 CS laptop computer loaded with National Instruments Labview software acted as the datalogger.

3.4 Meteorological Analysis

3.4.1 Wind Direction

No measure of meteorological parameters such as temperature, wind speed and direction, and humidity could be made on the tower platforms at 250 and 433 m due to mechanical problems with the meteorological equipment in place. However it was possible to make use of the surface wind direction measurements made on the 10 m mast (as described above) as well as the Raleigh-Durham (RDU) airport National Weather Service (NWS) hourly and special weather observations. RDU is the closest reporting station to the tower, located about 17 miles to the northwest. To validate use of the RDU hourly wind direction observations, a comparison was made between the 10 m mast wind direction observations and RDU observations at the same time; the mean (\pm one standard deviation) difference in the wind direction between the RDU NWS and 10 m mast observations was about 15.4 ± 15.4 degrees. The median difference was 10 degrees, and approximately 75% of the calculated differences were less than 20 degrees. A

comparison was also made with the Greensboro, NC (GSO) airport NWS upper air soundings in order to compare differences in winds at the surface and winds at the 250 and 433 m heights (GSO is located about 85 miles northwest of the tower). The results gave a difference in wind direction of 26.4 ± 38.5 degrees at 250 m and 26.4 ± 28.8 degrees at 433 m. The median differences were 14.5 and 15.5 degrees, respectively, and between 70 and 80% of the calculated differences were less than 25 degrees. These results suggest that while exact comparisons of NO and NO_y mixing ratios with wind directions are not possible, a comparison can provide a valid correlation of mixing ratios to rough divisions of wind directions, such as by 90 degree compass quadrants.

3.4.2 Synoptic Meteorological Features

The term 'synoptic' is used here to define meteorological phenomena that have a time scale of 1-5 days, a length scale of 100-1000 miles, and in this case, those phenomena that involve upward vertical motion (such as low pressure systems, fronts, and troughs). The existence of synoptic features (for comparison with observed NO and NO_y mixing ratios) was identified through the study of NWS daily surface weather maps for each intensive (appendix 1), and verified for the time of local area passage (in relation to the research tower) by comparison with RDU NWS hourly and special surface weather observations. Changes in such parameters as wind speed and direction, temperature, pressure, and cloud cover in the RDU observations were used as indicators of frontal or trough passage.

3.4.3 Boundary Layer Height Determination

The height of the stable boundary layer just before sunrise and the height of the mixed layer during the early morning hours can be determined subjectively through an analysis of upper air soundings, which are vertical profiles of meteorological parameters such as temperature (both potential and absolute), water vapor content, and wind direction and speed. Using Figure 3.3 and the definitions found in section two as guides, the stable boundary layer can be identified from upper air soundings as the region where both the absolute and potential temperature profiles are increasing, water vapor content is either steady or greatly varying with height, and wind speeds are low but increasing with height. Identification of the top of the stable boundary is possible by noting where the vertical absolute temperature profile begins to decrease and the vertical potential temperature profile begins to approach a constant value that changes little with height (both of which are indicative of the RL). In some cases the wind speed profile will reach a maximum (the low level jet) at the top of the SBL, and water vapor profiles will show a decrease above the NBL due to the dryer air of the RL. Using Figure 3.4 and the definitions found in section two as guides, the mixed layer can be identified after sunrise as a layer in which potential temperature and water vapor content remain constant with height (indicative of the effectiveness of the mixing within the layer). Small scale temperature inversions can be identified as layers with increasing potential temperature and decreasing in water vapor content; an inversion such as this at the top of the ML can be identified as the EZ.

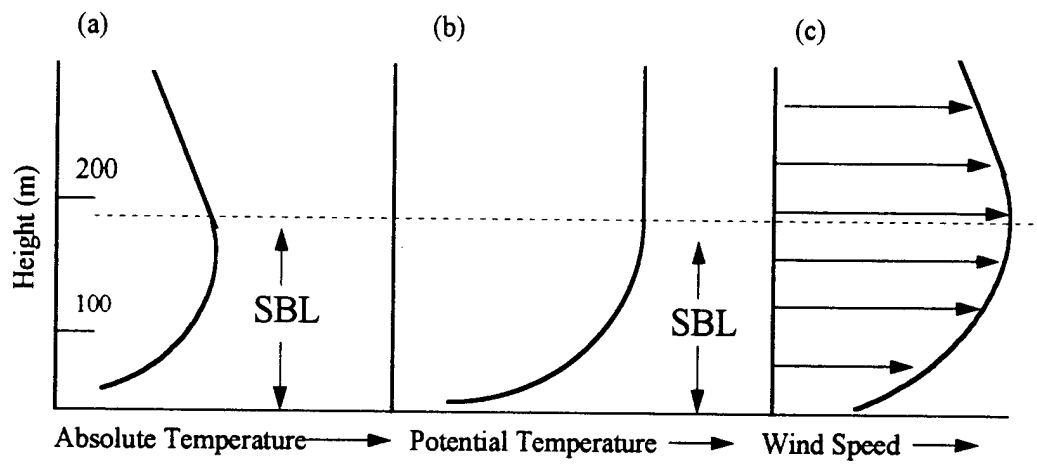


Figure 3.3 Typical SBL vertical profiles of a) absolute temperature
b) potential temperature c) wind speed SOURCE: Stull, 1988

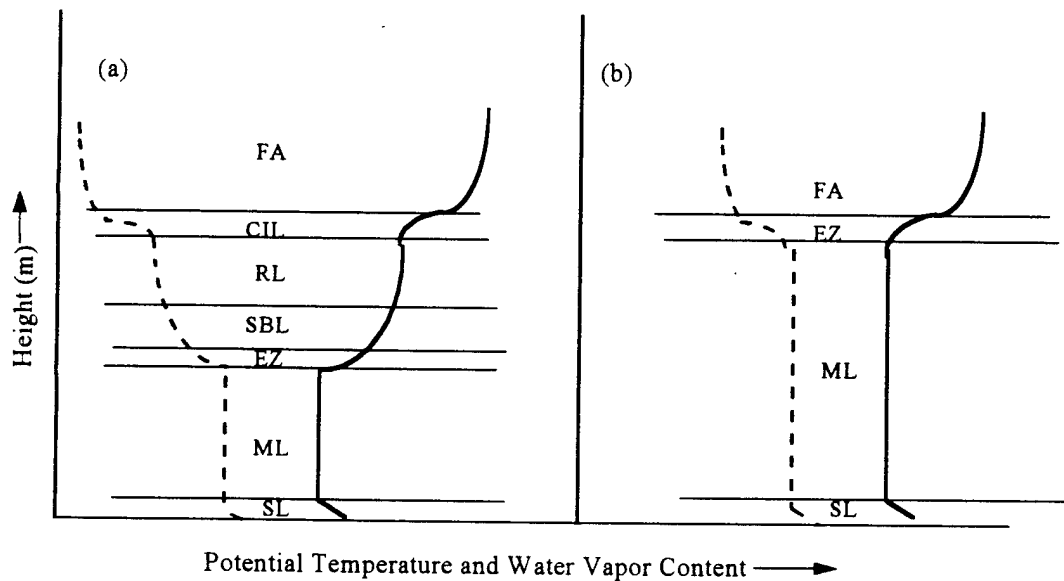


Figure 3.4 Typical mixed layer vertical profiles of potential temperature (—) and water vapor content (---) during a) mid-morning and b) noon SOURCE: Stull, 1988

Determination of the boundary layer heights during each intensive was made through analysis of upper air soundings produced at the GSO NWS office and also locally at North Carolina State University (NCSU) or at the agricultural field near the research tower, as described below. Water vapor content of the troposphere is represented in the upper air soundings by the dew point temperature vertical profile. The dew point temperature is the temperature to which an air parcel must be cooled (at constant pressure) in order for saturation to occur. When the absolute temperature is equal to the dew point temperature, the air parcel is holding the maximum amount of water vapor physically possible (and the relative humidity is 100 %). Therefore, a layer of the troposphere with dew point temperatures close to the absolute temperatures is a moist layer, while a layer with a large difference between the dew point temperatures and the absolute temperatures is a dry layer.

3.4.3.1 Greensboro, NC National Weather Service Upper Air Soundings

Determination of the vertical structure of the nocturnal boundary layer was made through careful analysis of the upper air soundings produced at the NWS office in Greensboro, NC (GSO) [N Latitude 36.1°, W Longitude 79.9°; 270 meters above mean sea level (MSL)], about 85 miles northwest of the tower (see Figure 3.1). The soundings are produced twice daily from the launch of a pilot balloon (PIBAL) equipped with a VIZ B Artsonde rawinsonde, which is an instrument that can detect and transmit atmospheric data such as temperature, wind speed and direction and water vapor content to a receiver

on the ground. The launches are made at 1100 and 2300Z (Zulu or Greenwich Meridian Time) or 0600 and 1800 local time (Eastern Standard Time, or EST). In particular the 0600 EST sounding was used to determine the structure of the nocturnal atmosphere as close to but before sunrise as possible (during the measurement period the time of sunrise ranged from 0655 to 0720 EST). To ensure that boundary layer conditions were similar at both the tower and the GSO office (and thus allow for comparison of data observed), two items were checked: 1) Comparisons were made between hourly weather observations at the Raleigh-Durham Airport (RDU) and the GSO surface observations at the time and site of the rawinsonde launch; and 2) Daily surface weather maps valid at 0700 EST (appendix 1) were studied for synoptic/mesoscale weather or atmospheric conditions that might entail differences in the boundary layer structure between GSO and the tower. If there was a difference (at the time of launch) of more than 30 degrees in surface wind direction measurement or more than 10 knots in wind speed measurement associated with synoptic weather differences, that day was not used for boundary layer structure comparison.

3.4.3.2 Local Upper Air Soundings

Further analysis was conducted on upper air soundings produced from a limited number of locally launched PIBALs equipped with AIR (Atmospheric Instruments Research) Products instrument sondes. These sondes can detect and transmit atmospheric temperature and water vapor content data (but not wind data), and were

launched from the mobile laboratory set up in the agricultural field approximately 2 miles east of tower during the month of December, and from the top of Jordan Hall (33 meters AGL) on the NCSU campus, about 20 km (12 miles) northwest of the tower, during the months of January and February. An AIR Products automated Atmospheric Data Acquisition System (ADAS) receiver routed height, temperature, and water vapor data transmitted by the sonde to a Toshiba Model 3100 laptop for data acquisition. In a few cases, range, direction and azimuth of the launched balloon were also manually tracked and recorded via theodolite to provide for wind speed and direction calculation. The initial data recorded by the ADAS were calibrated before launch with temperature and humidity data recorded by meteorological instruments located on the roof of Jordan Hall or by handheld instruments at the field site. The theodolite was sighted and calibrated with a landmark of known direction. These PIBAL launches also confirmed the validity of the GSO upper air sounding for comparison to tower observations (under similar synoptic weather conditions).

3.5 Typical Measurement Sequence

A typical measurement sequence began with the approval of access to the transmitter tower (due to changing weather conditions, approval was required for each trip up the tower). Then at the NCSU laboratory, a multi-point calibration of the NO-NO_y instrument and its accompanying data logger that were to go on the tower platform was accomplished, noting instrument settings and response curves. The instruments were

then turned off and loaded along with a pump, filters, and power cords into a station wagon for the twenty minute transport to the tower. Upon arrival at the tower, everything was loaded onto a two man elevator for the 8 1/2 to 15 minute ride to the appropriate platform.

Once on the platform, the weatherproof chamber door was removed and the instrument, filters, pump and data logger were placed inside and connections made. After insuring the instrument was operating correctly and at the same internal settings as those recorded in the lab, and that the data logger was recording valid data, the chamber door was secured shut. Once or twice a week the system was checked for operational status, and then the whole system was brought down after an intensive of one to three weeks to check measurement drift and recalibration.

At concurrent times during these measurement periods, the mobile laboratory was set up in place in the agricultural field, and measurements of surface (10 meter) NO began each day at 0600 EST, after a daily zero and span check of the instrument, using the same NO standards as with the tower instrument.

During an intensive, PIBAL balloons were released and tracked from the mobile laboratory in the agricultural field near the tower or from the roof of Jordan Hall on the NCSU campus at various times during the morning hours. This was accomplished by attaching the ADAS antennae to a post on the roof or on the mobile van, while the ADAS itself was hardwired into the Toshiba laptop via serial port cables. Procomm software (Version 2.0, 1986; Datastorm Technologies, Inc.) was used to receive and file the incoming data. The sondes were attached to PIBALs inflated with a commercial grade

helium and then allowed to equilibrate with the outdoor meteorological conditions. The data received by the ADAS was then calibrated with the handheld meteorological instruments (mobile lab) or with the rooftop mounted meteorological instruments (Jordan site). Finally, the theodolite was mounted, leveled and sighted, and the balloon released. The balloon was tracked visually for as long as possible, and was tracked by the ADAS until it reached a height of about 3000 meters.

3.6 Statistical Analysis

The NO and NO_y mixing ratio data for particular heights or time periods are presented in terms of the mean \pm one standard deviation (median in parentheses) for each sample. Since the measured NO mixing ratio sample is truncated or “censored” due to the detection limit of the instruments, the data for NO mixing ratios are calculated as a range between the minimum and maximum possible means, standard deviations, and medians. These minimum and maximum means, standard deviations, and medians represent the theoretical range each censored sample could have if the censored data were known. The minimum range for a censored sample is calculated by assigning a value of zero for all measurements of the sample below the instrument detection limit; the maximum range for a censored sample is calculated by assigning a value of the instrument detection limit for all measurements of the sample below this detection limit. For example, given a sample measured by an instrument with a detection limit of 0.04 ppbv, a minimum mean for that sample is calculated by assigning all observations in that sample below the detection limit

with a value of 0.00; this mean is a physical lower limit to the possible range of uncensored sample means. The maximum mean for that censored sample is then calculated by assigning all observations below the detection limit with a value of 0.04 ppbv; this mean is a physical upper limit to the possible range of uncensored sample means. The true uncensored sample mean would fall somewhere in between; however due to the exceedingly low detection limits of the instruments, the calculated ranges for each sample are quite small, and therefore the minimum and maximum means were tested for statistically significant differences via the use of the t-test method. This mathematical test gives an indication of whether or not the two sets of data are likely to be from different populations. For a pair of sample means, a t-value can be calculated using the observations within each population and their pooled variance (in this case, the variances are assumed equal, since each maximum and minimum are really from the same population). If the calculated t-value is greater than the critical t-value at a certain level of significance, then the data are likely to be from different populations (have statistically different means) at that significance level. In this analysis, all sample populations discussed were tested for differences in means at the .05 significance level. If the minimum and maximum means calculated for a sample failed the t-test (i.e., showed no statistical difference), then only the lower mean value is reported; if the t-test reveals a significant difference then the range is reported.

Further statistical analysis of both the NO and the NO_y data is limited to comparison between means from different samples (heights and time periods) and tests of significance via the t-test method (with unequal variances) at the .05 significance level.

Due to the minimum and maximum range of means and variances calculated for the NO mixing ratio samples, four t-tests had to be calculated for each test of difference in NO sample means. These four tests are based on the four possible combinations of means. The comparisons are: a) The minimum mean of sample 1 compared to the minimum mean of sample 2. b) The minimum mean of sample 1 compared to the maximum mean of sample 2. c) The maximum mean of sample 1 compared to the minimum mean of sample 2. d) The maximum mean of sample 1 compared to the maximum mean of sample 2. A difference in means between NO mixing ratio samples is considered statistically significant only when the t-value is larger than the critical t-value in all four tests (if any one test failed to reject equality, then it can not be stated that there is a difference in sample means at the .05 significance level).

Finally, it must be noted that tests of significance such as the t-test are based on a normally distributed population, and become less valid as the population distribution moves away from normal. However, under certain conditions the t-test method is considered valid with any population through the central limit theorem, which states that a population of means derived from a large enough sample will themselves be approximately normally distributed, and therefore satisfy the normality requirement for validity of the t-test. The number of observations (n) required is not a constant, but instead changes with the degree of nonnormality of the original population. However, it is generally agreed that $n > 100$ would be a sufficient number of observations for validity of the central limit theorem [Snedecor and Cochran, 1989]. In this research, the populations were not normally distributed, but the number of observations in each sample tested for differences

in means was much greater than that required by the central limit theorem for validity (n of at least 200 or more for each sample), and therefore the t-tests conducted are considered statistically valid.

4. Results and Discussion

4.1 Overview

The results of this study are presented in four sections. Each section will contribute to validation of the hypothesis that mixing ratios of NO and NO_y did not exist in sufficient quantities in the nocturnal boundary layer to be mixed downward (and affect surface mixing ratios), and instead they were mixed *upward* by vertical synoptic and boundary layer transport mechanisms during this research period. In the first section, the results presented show a well defined decreasing vertical gradient in both NO and NO_y mixing ratios during both the day and night, emphasizing the surface as a source for NO and NO_y. The observed NO mixing ratios are then used to verify the predicted values from a simple one dimensional vertical model of NO transport. Second, increases in NO and NO_y mixing ratios are associated with the passage of synoptic meteorological features and their associated upward vertical motion, again emphasizing the surface as a source for NO and NO_y. Third, the observed values of NO and NO_y mixing ratios are compared with the structure and evolution of the planetary boundary layer (through a series of case studies) in such a manner that it is clear that vertical (upward) mixing of NO and NO_y during the morning hours is responsible for the observed diurnal maximum values of these species. Finally, a brief discussion of possible atmospheric chemistry and horizontal transport processes are included for completeness.

4.2 NO and NO_y Mixing Ratio: Vertical Gradients and Diurnal Profiles

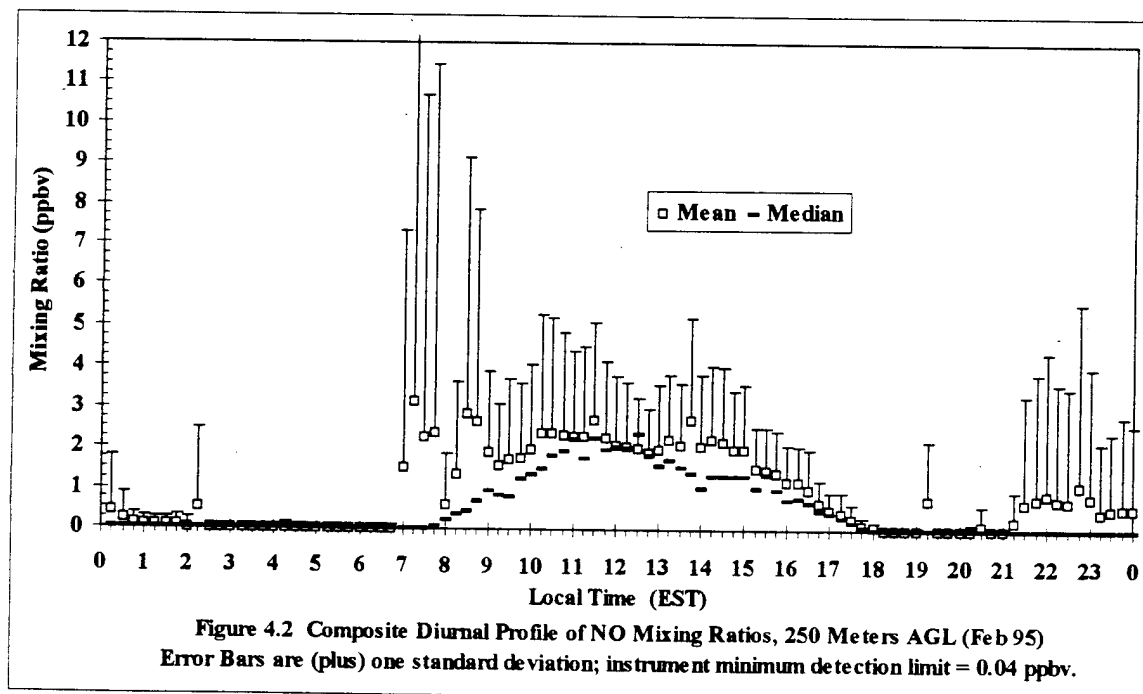
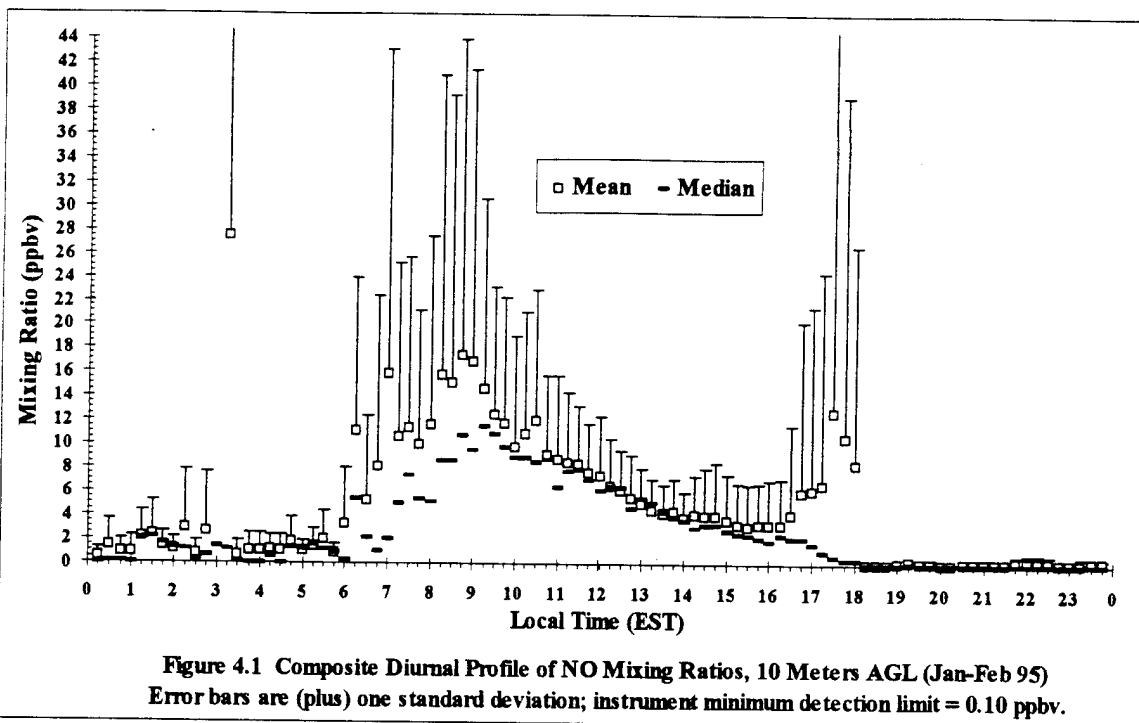
4.2.1 NO Mixing Ratios

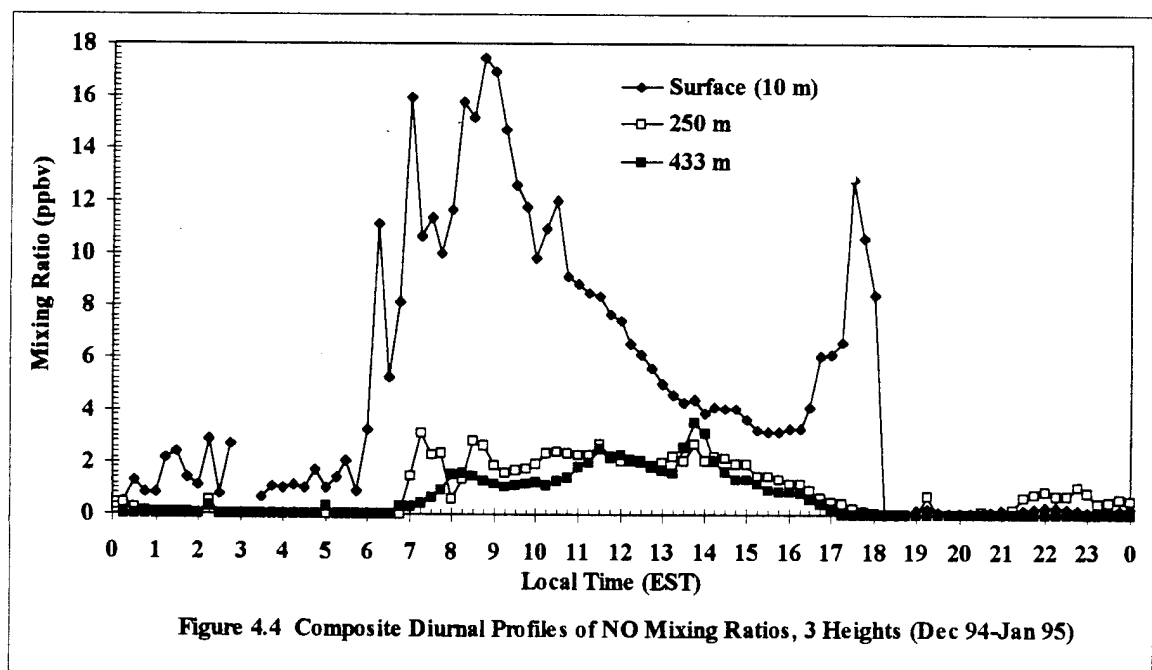
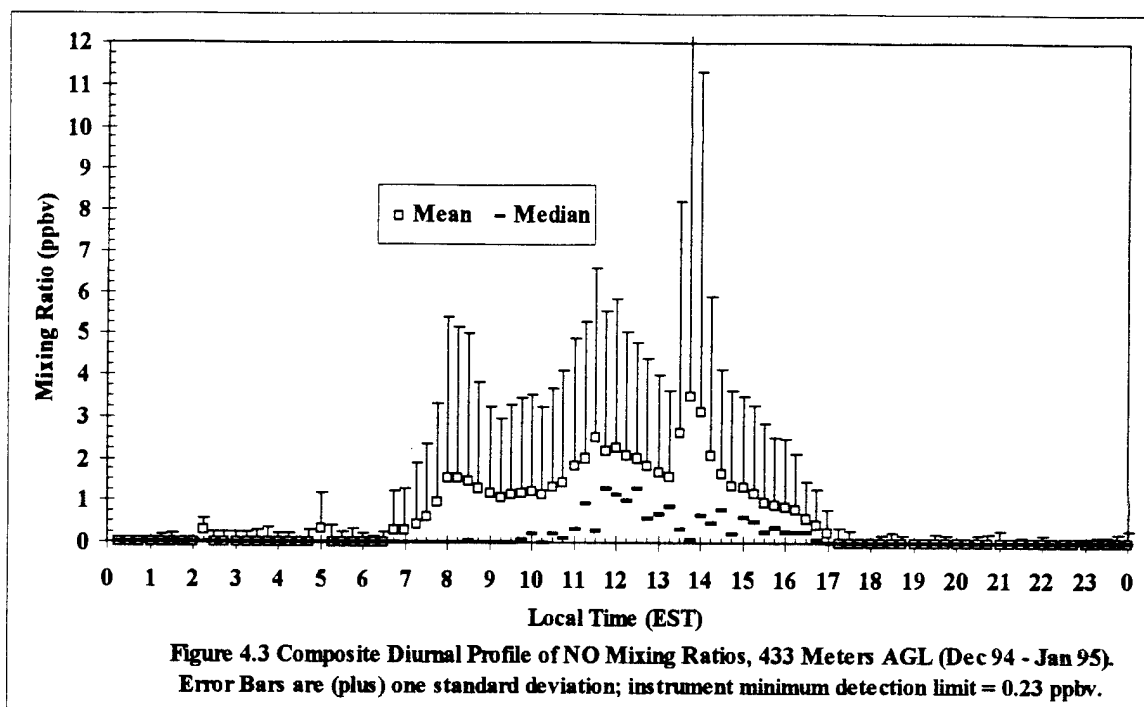
The distribution of the measured NO mixing ratios at all heights is heavily skewed, but displays a strong vertical gradient during both the daytime and the nighttime hours as shown in Table 4.1 (daytime is defined as the hours from 0615 EST to 1800 EST; nighttime is defined as the hours from 1815 EST to 0600 EST). Particularly, there is a significant difference between the mean NO mixing ratio at the surface and the NO mixing ratio at both heights during the day; during the night there is a significant difference between the mean NO mixing ratio at the surface and the mean NO mixing ratio at 433 m. Though the data showed a 17% decrease in mean NO mixing ratios from 250 to 433 m, a test for differences between the daytime NO mixing ratios at 250 m and 433 m failed to reject equality, but only by a very small margin at the .05 significance level. These results suggest very strongly that a decreasing vertical gradient of NO exists during both the day and night.

The mean values in Table 4.1 also suggest a pronounced nocturnal minimum at each height. Given that a high percentage ($\approx 86\%$) of the nighttime readings were below instrument detection limits, and that the mean nocturnal NO mixing ratios are at least an order of magnitude lower than their daytime counterparts, the result is a strong composite diurnal profile for each height, as noted in Figures 4.1, 4.2, and 4.3. The skewed nature of the sample is evident, with large standard deviations for many observations (error bars,

Table 4.1 Mean, Standard Deviation and (Median) of Observed NO and NO_y Mixing Ratios: Surface (10 Meters), 250 Meters, and 433 Meters (Dec 94 - Feb 95)
[Units are ppbv]

<u>NO</u>			
<u>HEIGHT</u>	<u>DAY</u>	<u>NIGHT</u>	<u>DATES</u>
10 m	8.07 ± 13.33 (3.67)	0.32 ± 1.27 (0.00)	20 Jan - 16 Feb 95
250 m	1.56 ± 3.23 (0.69)	0.22 ± 1.46 (0.00)	2-23 Feb 95
433 m	1.30 ± 3.03 (0.00)	0.06 ± 0.23 (0.00) (MIN) to 0.18 ± 0.22 (0.23) (MAX)	7-16 Dec 94 and 12-25 Jan 95
<u>NO_y</u>			
<u>HEIGHT</u>	<u>DAY</u>	<u>NIGHT</u>	<u>DATES</u>
250 m	12.12 ± 7.67 (10.46)	9.48 ± 7.22 (7.93)	2-23 Feb 95
433 m	9.27 ± 6.28 (7.22)	7.31 ± 4.92 (5.74)	7-8 Dec 94 and 12-25 Jan 95





one sided for clarity) and medians that are consistently lower than the averages. This skewness results in part from a relatively few high readings (values of near 100 ppbv at the surface and at 50 ppbv at 250 and 433 m). The NO mixing ratio usually peaked in magnitude around noon and began a slow decline throughout the afternoon hours. There is a sharp drop in the NO mixing ratio at sunset, indicative of the effects of both photochemistry and boundary layer transport processes on NO mixing ratios.

The existence of both the vertical gradient and diurnal profile of NO mixing ratios is highlighted in Figure 4.4, which compares the composite mean diurnal NO mixing ratio profile at each height for the measurement period. The lines connecting the fifteen minute binned average measurements in this figure are for ease of viewing, and are not meant to imply knowledge of continuous mixing ratio values.

4.2.2 NO Mixing Ratio Vertical Gradient Model

A one dimensional model for the vertical transport of NO was developed to predict the early morning (0600-0700 EST) NO mixing ratios observed at 250 and 433 m; this model is similar to one developed by Chameides et al. [1992] for hydrocarbon transport. The basis for the model is a one dimensional continuity equation describing the vertical variation of NO concentration (here concentration and mixing ratio will be held as synonymous):

$$\frac{d}{dt}[\text{NO}] = \frac{d}{dz} K \frac{d}{dz}[\text{NO}] - \{[\text{O}_3]k_{\text{O}_3}(\text{NO}) + [\text{RO}_2]k_{\text{RO}_2}(\text{NO}) + [\text{HO}_2]k_{\text{HO}_2}(\text{NO})\} \quad (4.1)$$

where

t = time

z = height (m)

K = eddy diffusivity coefficient (m^2s^{-1})

$[a]$ = concentration of a (molecules cm^{-3})

$k_a(\text{NO})$ = reactivity of a with NO ($\text{cm}^3\text{molecule}^{-1}\text{s}^{-1}$)

Equation 4.1 is based on the key atmospheric constituents with which NO will preferentially react during the early morning hours. These are ozone (O_3), the peroxy radical (RO_2), and the hydroperoxy radical (HO_2). For a steady state and constant values of K , O_3 , RO_2 , and HO_2 , the solution of the above differential equation yields:

$$[\text{NO}]_z = [\text{NO}]_0 \exp \left[- \left(\sqrt{\frac{k_{\text{O}_3}(\text{NO})[\text{O}_3]}{K}} + \sqrt{\frac{k_{\text{RO}_2}(\text{NO})[\text{RO}_2]}{K}} + \sqrt{\frac{k_{\text{HO}_2}(\text{NO})[\text{HO}_2]}{K}} \right) z \right] \quad (4.2)$$

Equation 4.2 expresses the concentration of NO at height z as a decreasing exponential function of the concentration of NO at the surface (without respect to horizontal advections).

The use of the K term in equation 4.2 leads to some inaccuracy in the prediction of NO mixing ratios due to the limitations involved in the assumptions associated with eddy diffusion. Eddy diffusion theory assumes a similarity between molecular and turbulent energy, and that eddy diffusivity is analogous to molecular kinematic viscosity. Furthermore, it relates the turbulent flux to the gradient of the associated variable; just as transfer of heat occurs down the gradient from high to low temperatures, mass is expected

to be transferred from areas of high to low concentration in the atmosphere. The limitations of this assumption include the fact that turbulence is much more effective than viscosity at causing mixing, thereby producing a large disparity between magnitudes of eddy and molecular viscosities. Molecular viscosity is a function of the fluid, while eddy diffusivity is a function of the flow, and as such can vary by large amounts from one area to another and between flows [Arya, 1988; Stull, 1988]. Therefore, use of a constant K value in equation 4.2 will result in an inaccurate prediction of NO mixing ratios.

However, the use of this model can still provide an acceptable estimate of the concentration of NO at a certain height, given the observed surface concentration of NO at the same time. For this model, the value of K during early morning stable conditions in the winter was estimated to be $5 \text{ m}^2 \text{ s}^{-1}$ (Arya, 1995). The rate constants outlined in Table 1.1 (R3, R4, and R5) were used for the model calculation, assuming an environmental temperature of 10° C . Finally, the concentration of HO_2 was assumed to be $1.5 \times 10^6 \text{ molecules cm}^{-3}$ (Logan, 1981); the concentration of RO_2 was assumed to be 30% of HO_2 and a conservative estimate of 10 ppbv ($2.46 \times 10^{11} \text{ molecules cm}^{-3}$) was chosen for O_3 . The trend in the predicted concentrations (Table 4.2) is consistent with the measured values of NO at 250 and 433 m. In particular, the model predicts an exponentially decreasing NO concentration with height during the early morning hours, and the observations justify this prediction.

Table 4.2. Comparison of the Predicted Mean NO Mixing Ratios to the Observed Mean NO Mixing Ratios at 250 and 433 m, 0600-0700 EST (One Dimensional NO Transport Model, Equation 4.2).

<u>Date</u>	<u>Observed</u>	<u>Predicted</u>	<u>Observed</u>
	<u>(Surface)</u>	<u>(433 m)</u>	<u>(433 m)</u>
24 Jan 95	0.21 ppbv	less than 0.01 ppbv	less than 0.04 ppbv*
25 Jan 95	9.48 ppbv	less than 0.01 ppbv	↓
	<u>(Surface)</u>	<u>(250 m)</u>	<u>(250 m)</u>
4 Feb 95	0.17 ppbv	less than 0.01 ppbv	less than 0.04 ppbv*
7 Feb 95	0.27 ppbv	less than 0.01 ppbv	↓
11 Feb 95	2.40 ppbv	less than 0.01 ppbv	↓
8 Feb 95	10.10 ppbv	less than 0.01 ppbv	↓
14 Feb 95	24.62 ppbv	0.01 ppbv	↓
3 Feb 95	47.82 ppbv**	0.02 ppbv	↓

* Instrument minimum detection limit

** Highest surface mean NO mixing ratio, 0600-0700 EST

4.2.3 NO_y Mixing Ratios

While the distribution of NO_y mixing ratios at 250 and 433 m during the period of measurement was skewed, the lowest readings were still above the instrument minimum detection limit (the lowest values recorded were around 1 ppbv and ranged to a maximum high of 50 ppbv), so that the distribution is approximately lognormal. The skewness of the original population at both heights is evident in the standard deviations (error bars) of the mean diurnal variation and the medians (which are consistently lower than the means) shown in Figures 4.5 and 4.6.

The mean values shown in Table 4.1 suggest that a vertical gradient between 250 and 433 m existed for NO_y mixing ratios (NO_y was not measured at the surface) that is comparable to the observed gradient in the NO mixing ratios. In this case, there was a significant difference of 20-25% between the 250 and 433 m mean NO_y mixing ratios during both the day and night, suggesting a strong decreasing vertical gradient.

As with the NO measurements, the mean NO_y mixing ratio data also show a strong diurnal profile. The figures shown in Table 4.1 indicate that the mean NO_y mixing ratio values decreased between 20 and 25% from the daytime maximum to the nocturnal minimum at both heights. Figures 4.5 and 4.6 show the composite profiles of NO_y at both heights, and a diurnal cycle is clearly indicated. The mean NO_y mixing ratios begin to rise from an overnight minimum between approximately 0700 and 0715 EST, and reach a peak around midday. More importantly, the contrasts between the lowest early morning mean value [7.68 ppbv at 250 m (0300 EST); 4.94 ppbv at 433 m (0545 EST)] and the midday

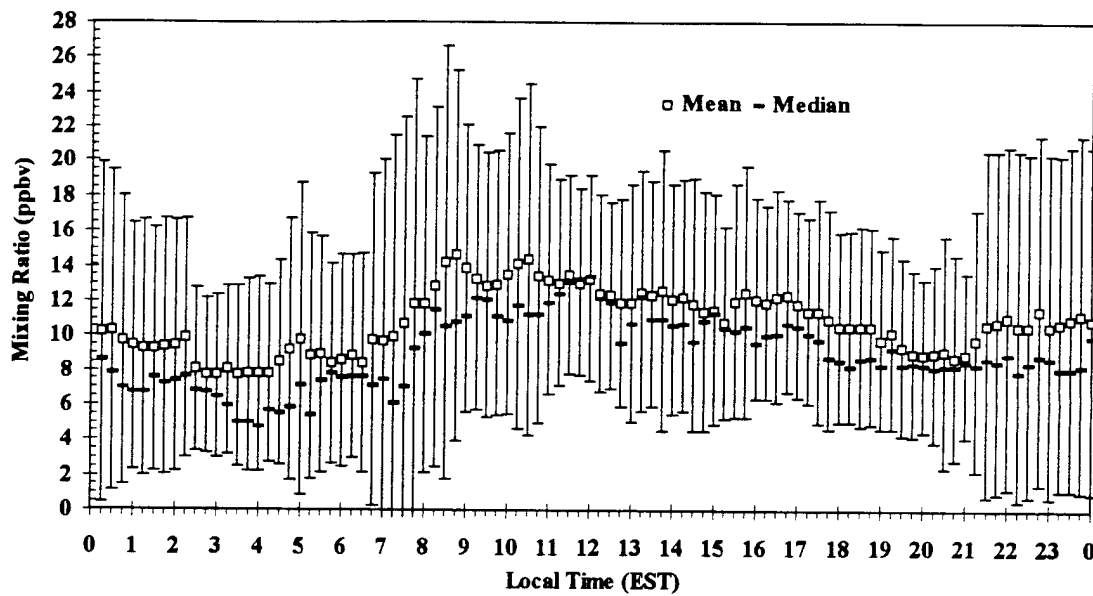


Figure 4.5 Composite Diurnal Profile of NO_y Mixing Ratios, 250 Meters AGL (Feb 95)
Error bars are plus/minus one standard deviation.

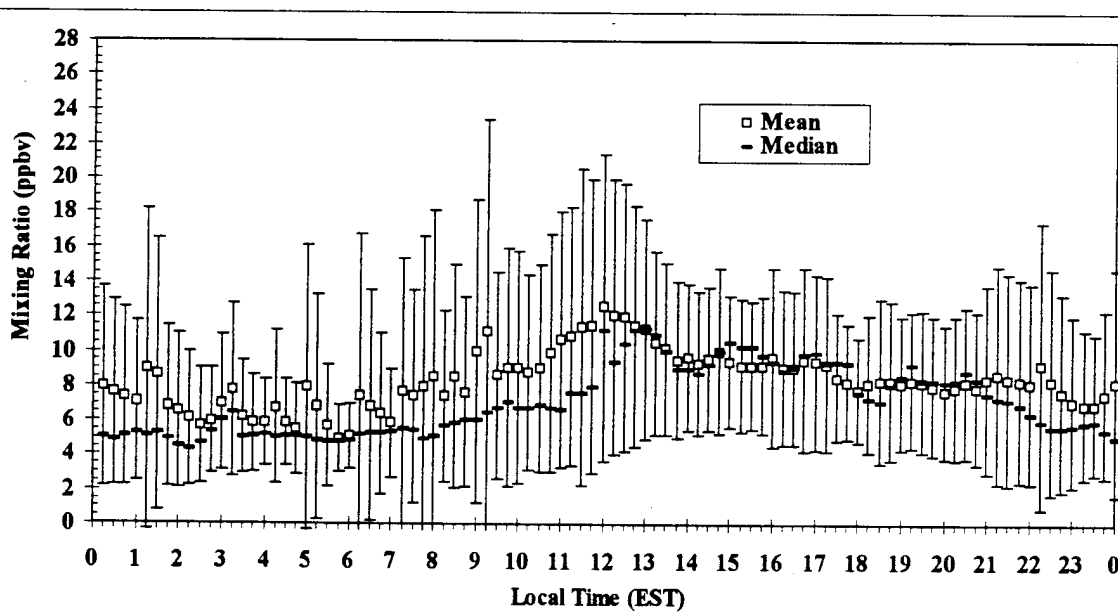


Figure 4.6 Composite Diurnal Profile of NO_y Mixing Ratios, 433 Meters AGL (Dec 94- Jan 95)
Error bars are plus/minus one standard deviation.

mean peak [14.38 ppbv at 250 m (1030 EST); 12.53 ppbv at 433 m (1200 EST) are 2.5 to 4 times the difference between the mean day and night values at the respective heights. This indicates that while some of the NO_Y measured during the day at each height was conserved or formed in the boundary layer during the previous night, an equal or larger portion (45 to 60%) was transported upward to or formed at these heights during the morning hours after sunrise.

As with the NO mixing ratios (Figure 4.4), the existence of both a vertical gradient and diurnal profile in NO_Y mixing ratio can be highlighted with a comparison of the composite mean diurnal NO_Y mixing ratio profile for both heights, as shown in Figure 4.7.

4.3 Correlation of Observed Mixing Ratios with Synoptic Features

A detailed review of combined time sequences of the diurnal profiles of the NO and NO_Y mixing ratios at 250 and 433 m reveals a series of somewhat periodic maxima and minima interspersed with aperiodic peaks; an example for the 250 m height is given in Figure 4.8. Since these maxima usually occur at or around midday, it is hypothesized that this peak is the result of upward transfer of NO and NO_Y from the surface via boundary layer processes (which will be discussed further in the next section) and that the nocturnal minima are the result of the depletion of NO and NO_Y by various chemical reactions. These maxima and minima will be referred to as the "diurnal maximum and minimum" for clarity. Furthermore, it is hypothesized that the aperiodic peaks (different from the diurnal

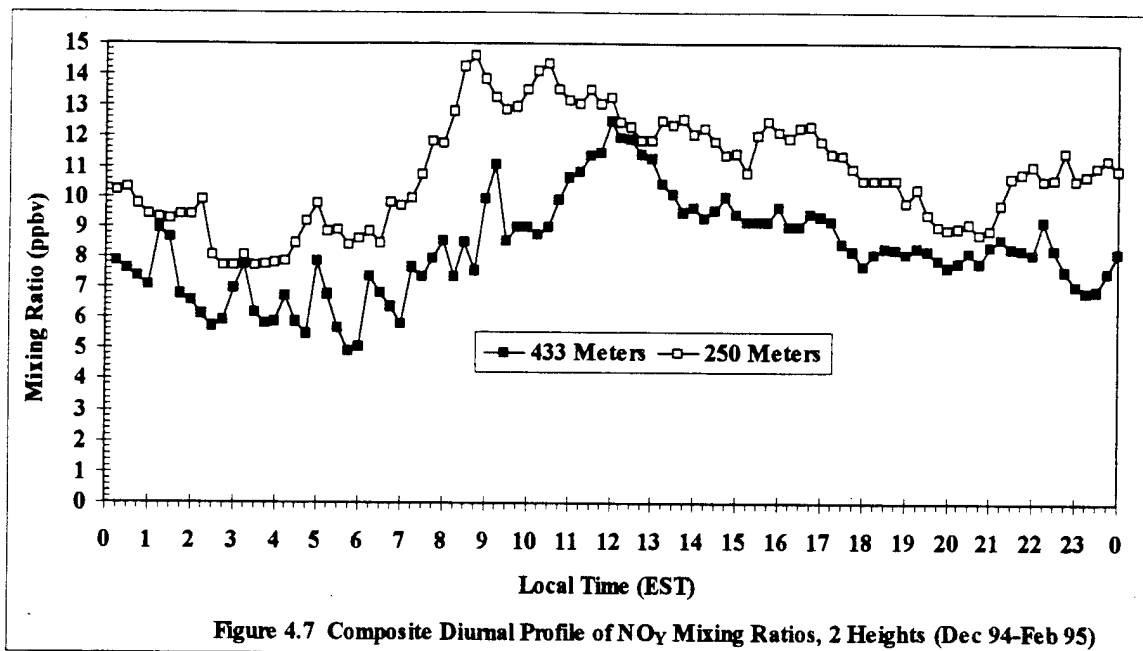


Figure 4.7 Composite Diurnal Profile of NO_y Mixing Ratios, 2 Heights (Dec 94-Feb 95)

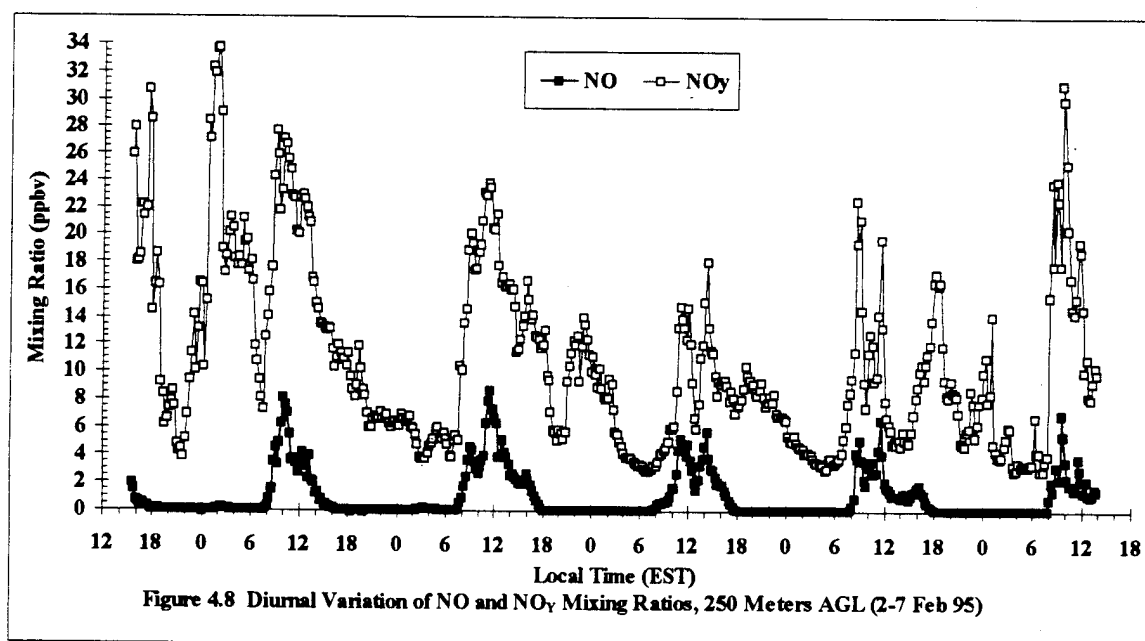


Figure 4.8 Diurnal Variation of NO and NO_y Mixing Ratios, 250 Meters AGL (2-7 Feb 95)

maxima and minima) are the result of synoptic scale meteorological processes that involve upward motion and therefore vertical lifting of NO and NO_y from the surface, further validating the surface as a source of NO and NO_y. A comparison was made of the measured values of NO and NO_y at the 250 and 433 m heights with synoptic meteorological features that passed through central North Carolina during the measurement period, and the results are discussed in the following sections.

4.3.1 NO Mixing Ratios

Figures 4.9a - 4.9j show the relationship between NO mixing ratios and synoptic features through the use of time series graphs of variation of NO mixing ratios throughout the measurement period, overlaid with time of synoptic event passage (these figures are located at the end of this section). The figures illustrate the association between synoptic events and NO spikes or maxima not associated with the diurnal maximum. In general, the nocturnal NO mixing ratios were below instrument detection limits during periods of high pressure (noted as "absence synoptic forcing" in Figures 4.9a - 4.9j). However, during the passage of a front, low pressure or trough, the NO mixing ratios rose above minimum instrument detection limits. These local maxima have varying magnitudes and time scales, but nevertheless are consistent phenomena.

Two particular instances have been chosen to highlight the potential for vertical transport of large amounts of NO via synoptic events and its accompanying vertical motion. On December 10, 1994, the 15 minute mean NO mixing ratio (433 m) increased

from 0.88 ppbv at 1315 EST to 23.46 ppbv at 1330 EST and then to 40.78 ppbv at 1345 EST (Figure 4.9a). A comparison with the surface maps and the RDU observations indicates that the passage of a warm front through the region occurred on that date between 1300 and 1400 EST. The NO mixing ratio had increased to a diurnal maximum of 1.29 ppbv at 1200 EST and was decreasing towards the diurnal minimum when the front came through and brought the large increase in NO mixing ratio. In the second case, on February 16, 1995, the 15 minute mean NO mixing ratio (250 m) increased from 0.24 ppbv at 2100 EST to 14.88 ppbv at 2200 EST (Figure 4.9i). A comparison with surface maps and RDU observations indicate that a cold front moved through the region between 1900 and 2000 EST on that date. The resolution of the synoptic meteorological data does not allow for the calculation of the exact time of frontal passage at the tower, which may explain the apparent time lag in the increase of NO mixing ratios.

During the time period for which valid NO mixing ratio data was recorded at the two tower heights, there were approximately fourteen identifiable synoptic events that passed through the region, and all fourteen produced observable increases in the NO mixing ratios. In addition, there were four peaks in the NO mixing ratio during the nocturnal time periods that do not match up with identifiable synoptic scale events; these may be the result of mesoscale (1-100 miles length scale, 1-10 hours time scale) or smaller meteorological phenomena that provide some vertical lifting but were not identifiable with the given meteorological data. In particular, three of these peaks were observed at the time rain and drizzle were recorded by the RDU NWS, which are indicators of possible vertical motion in the troposphere.

While it is possible that a change in wind direction (which is usually concurrent with a synoptic event passage) is alone responsible for the noted increases in NO concentrations, (due to winds changing from a relatively "clean" direction to a more polluted direction), the data does not bear this hypothesis out. Consistent with all these observations is the fact that the spikes or maxima occur without preference to wind direction, and that in most cases the maxima begins to decrease when there has been no change in the wind direction. This leads to the conclusion that upward vertical motion (and transport from the surface) is responsible for the noted increases in NO mixing ratios during synoptic event passage.

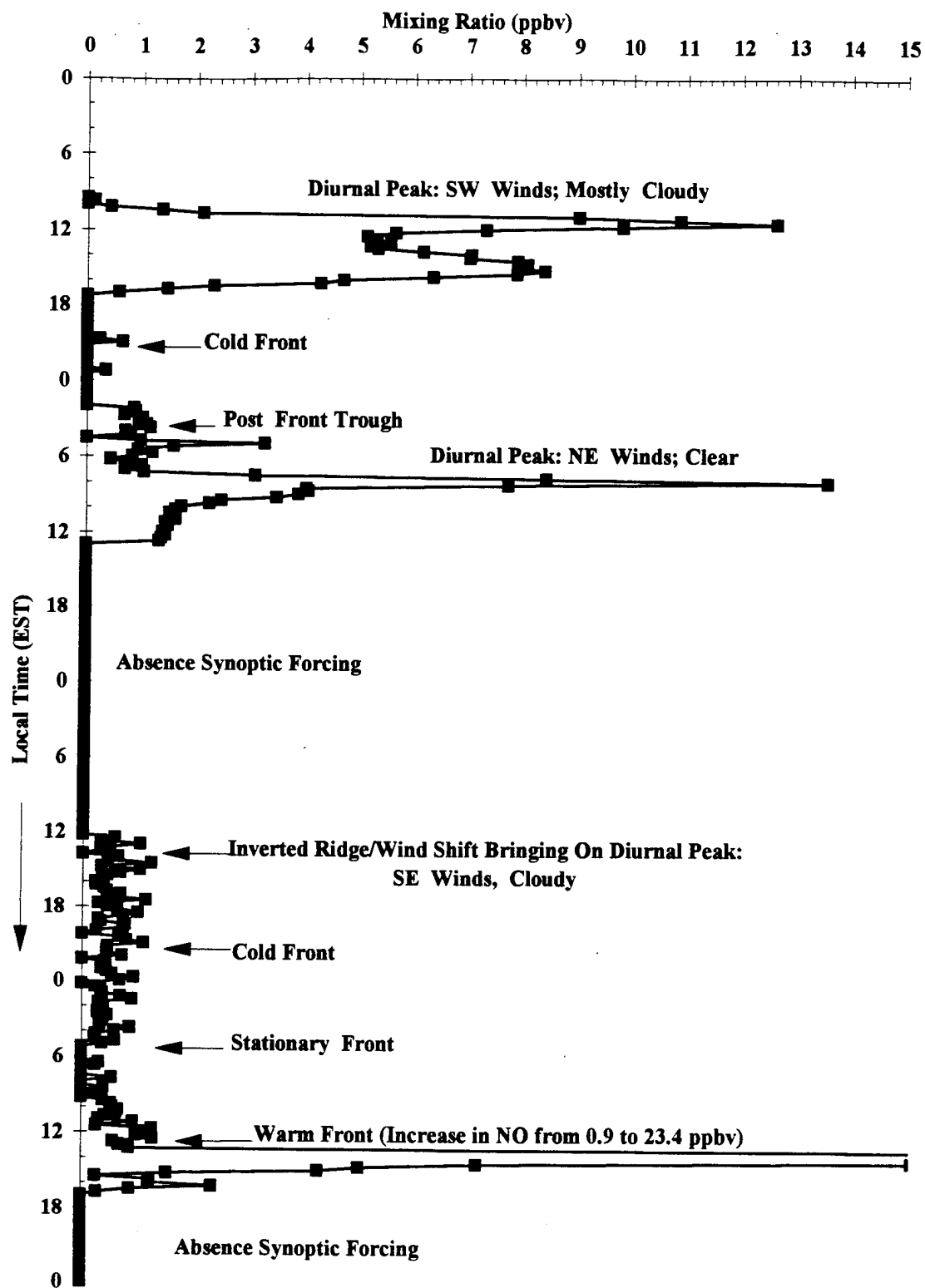


Figure 4.9a Diurnal Variation NO Mixing Ratio Overlaid with Synoptic Meteorology, 433 Meters AGL (7-10 Dec 94)

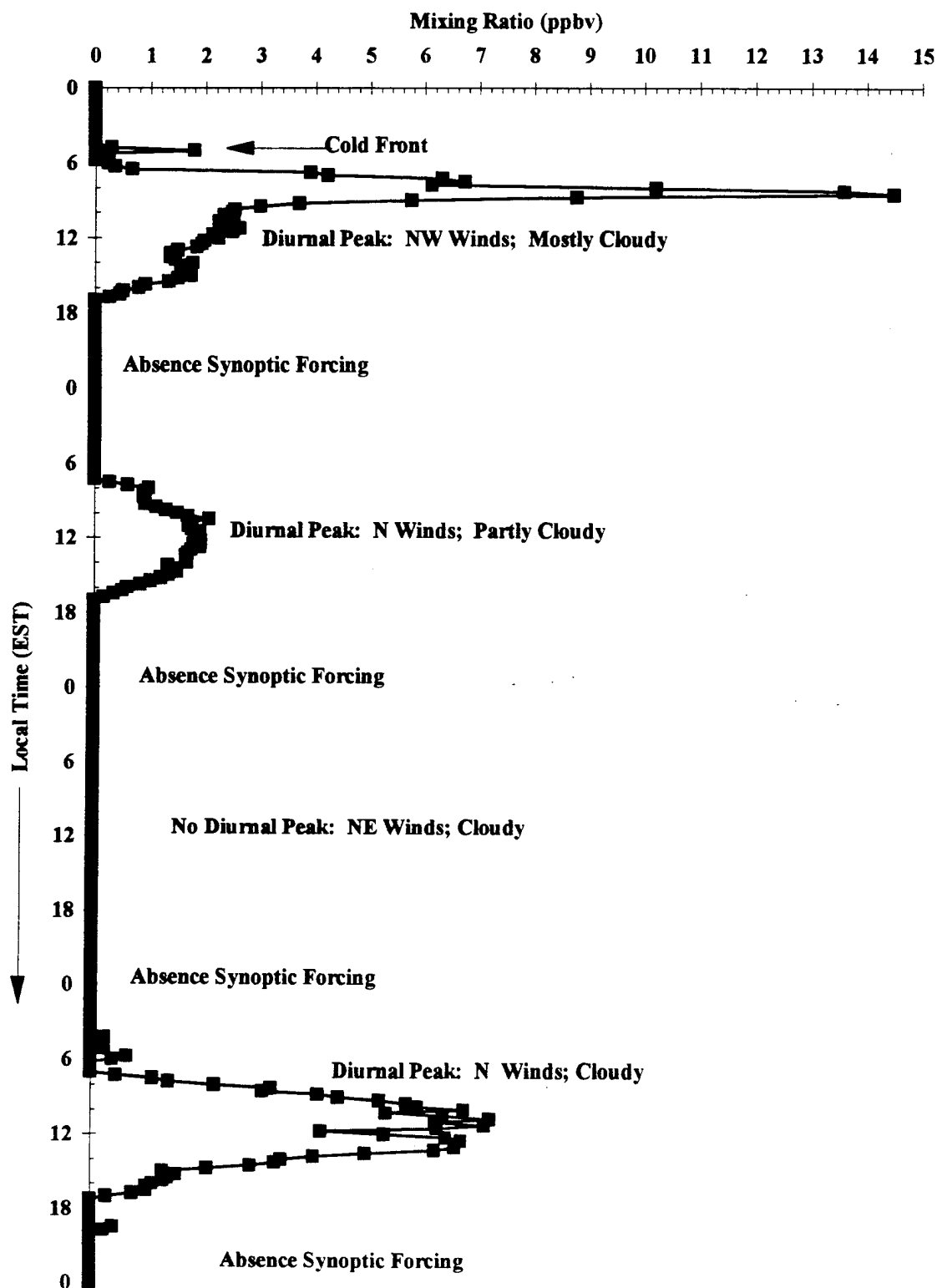


Figure 4.9b Diurnal Variation NO Mixing Ratio Overlaid with Synoptic Meteorology, 433 Meters AGL (11-14 Dec 95)

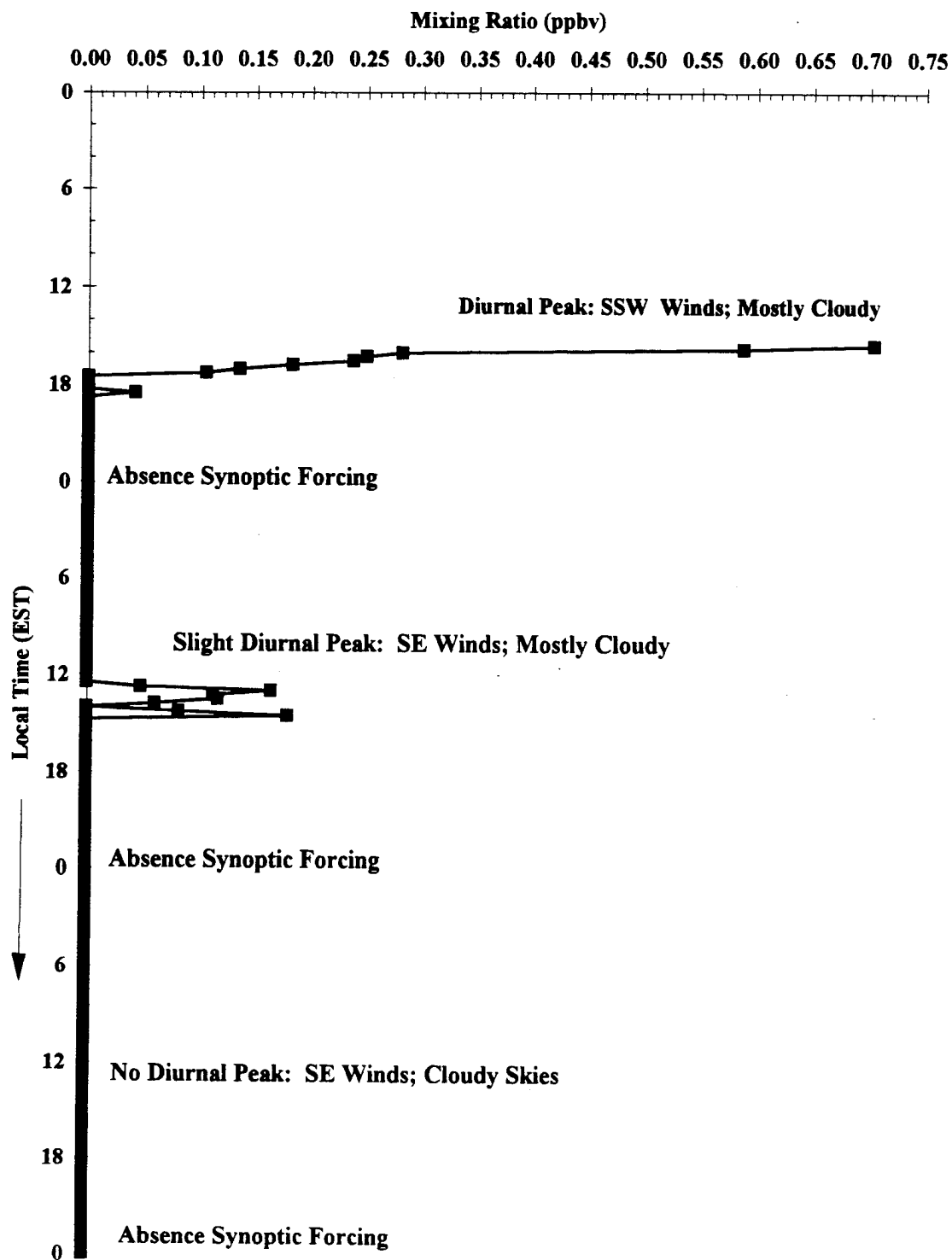


Figure 4.9c Diurnal Variation NO Mixing Ratio Overlaid with Synoptic Meteorology, 433 Meters AGL (12-15 Jan 95)

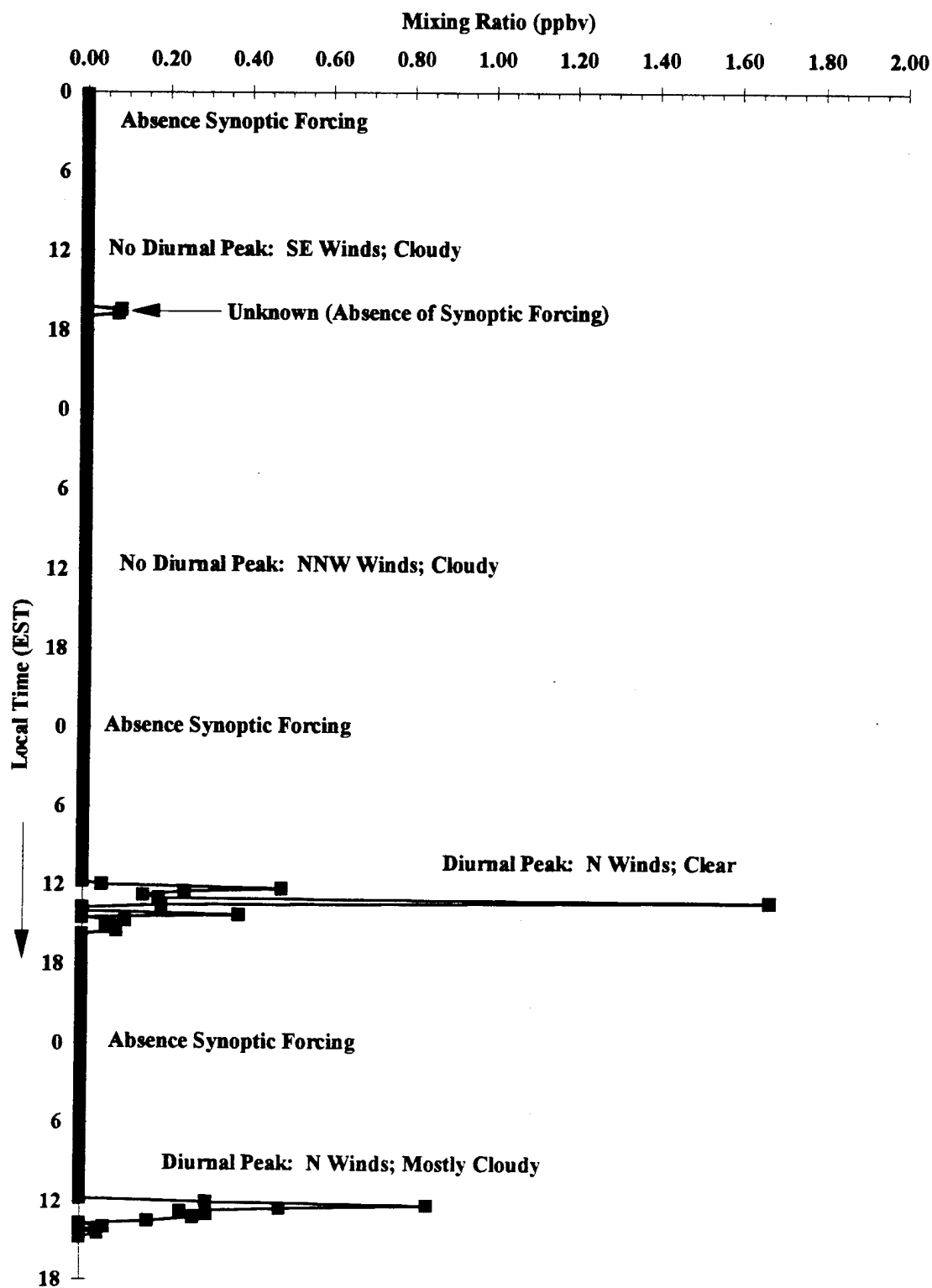


Figure 4.9d Diurnal Variation NO Mixing Ratio Overlaid with Synoptic Meteorology, 433 Meters AGL (15-18 Jan 95)

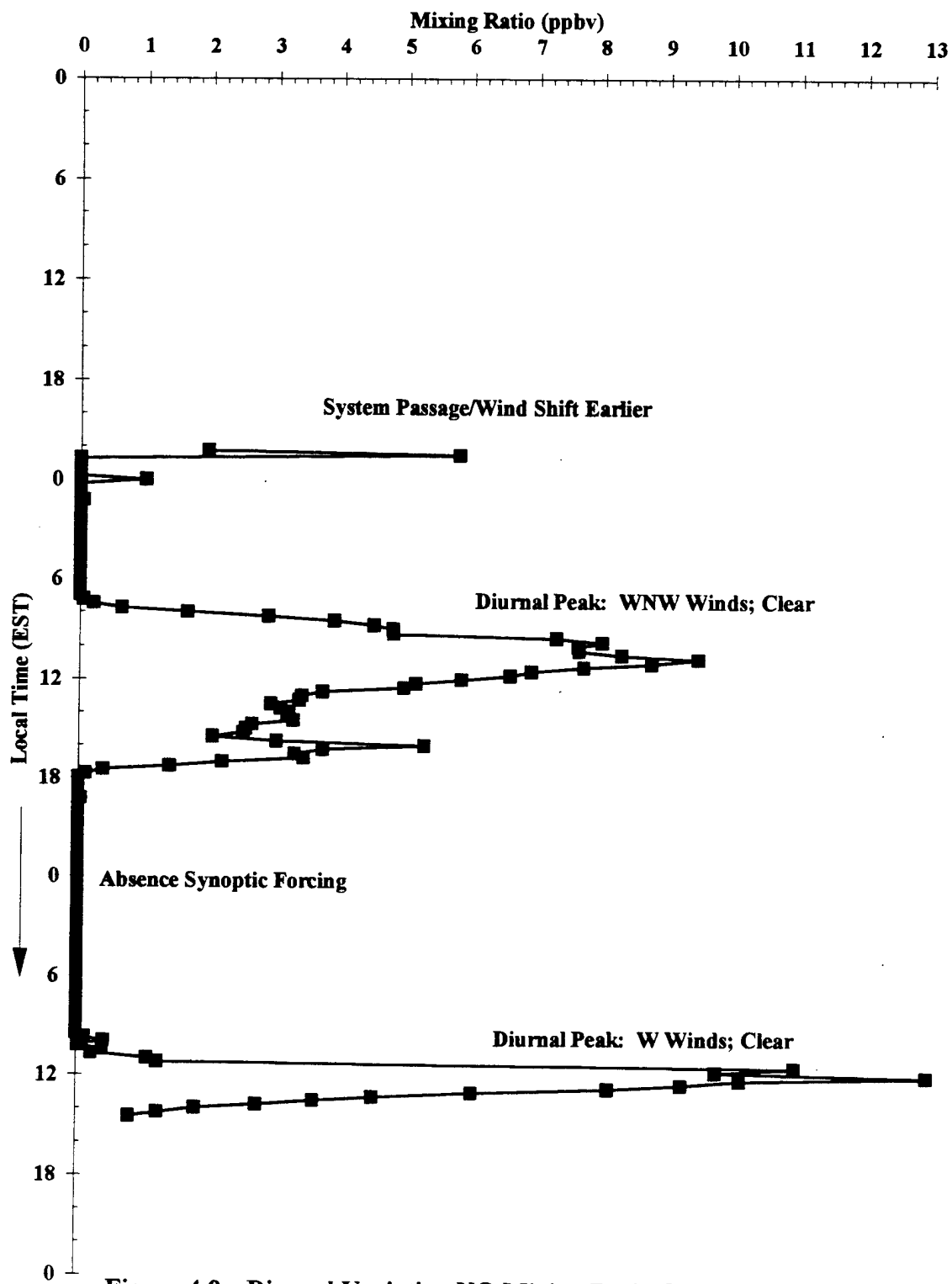


Figure 4.9e Diurnal Variation NO Mixing Ratio Overlaid with Synoptic Meteorology, 433 Meters (23-25 Jan 95)

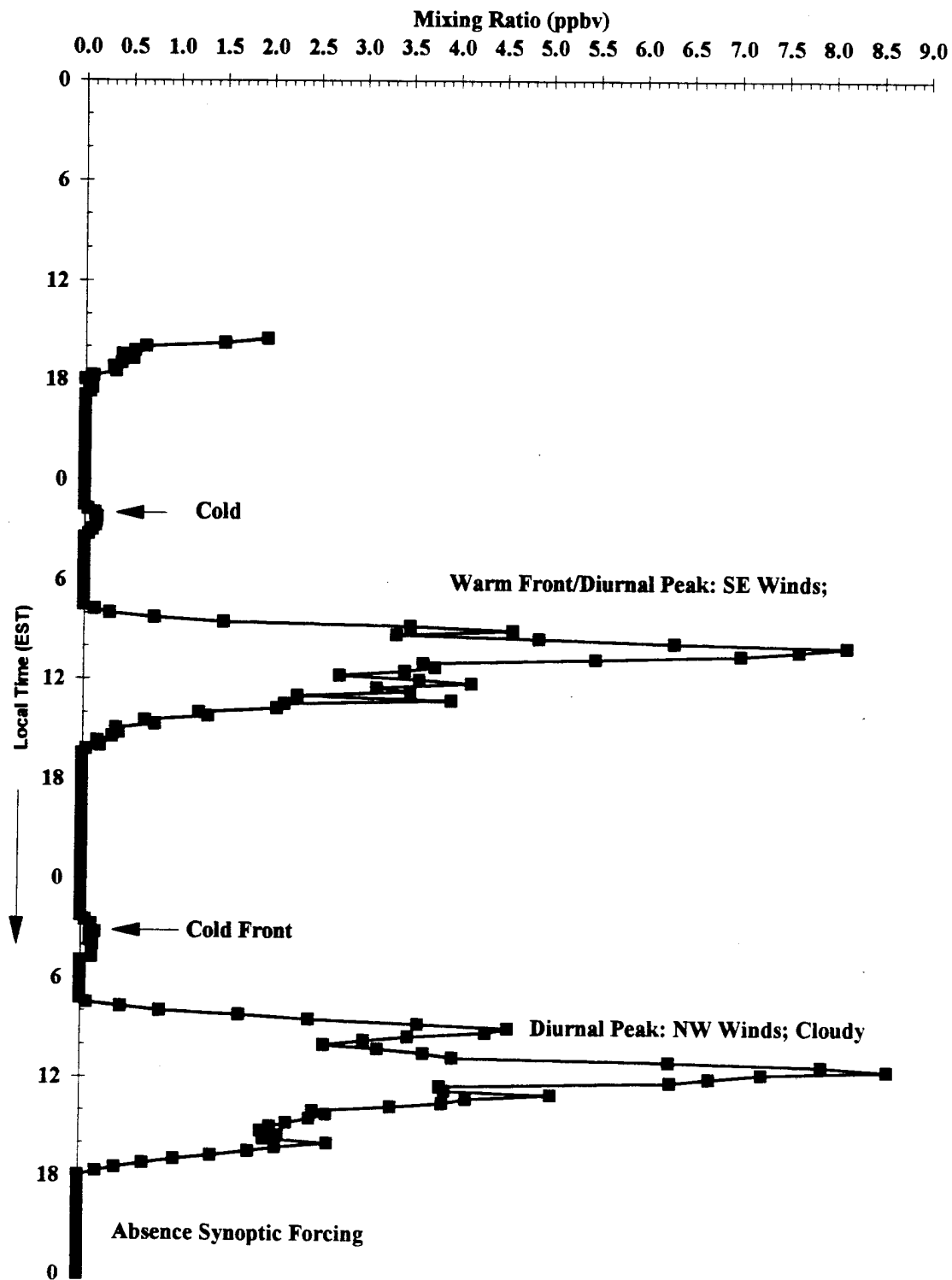


Figure 4.9f Diurnal Variation NO Mixing Ratio Overlaid with Synoptic Meteorology, 250 Meters AGL (2-4 Feb 95)

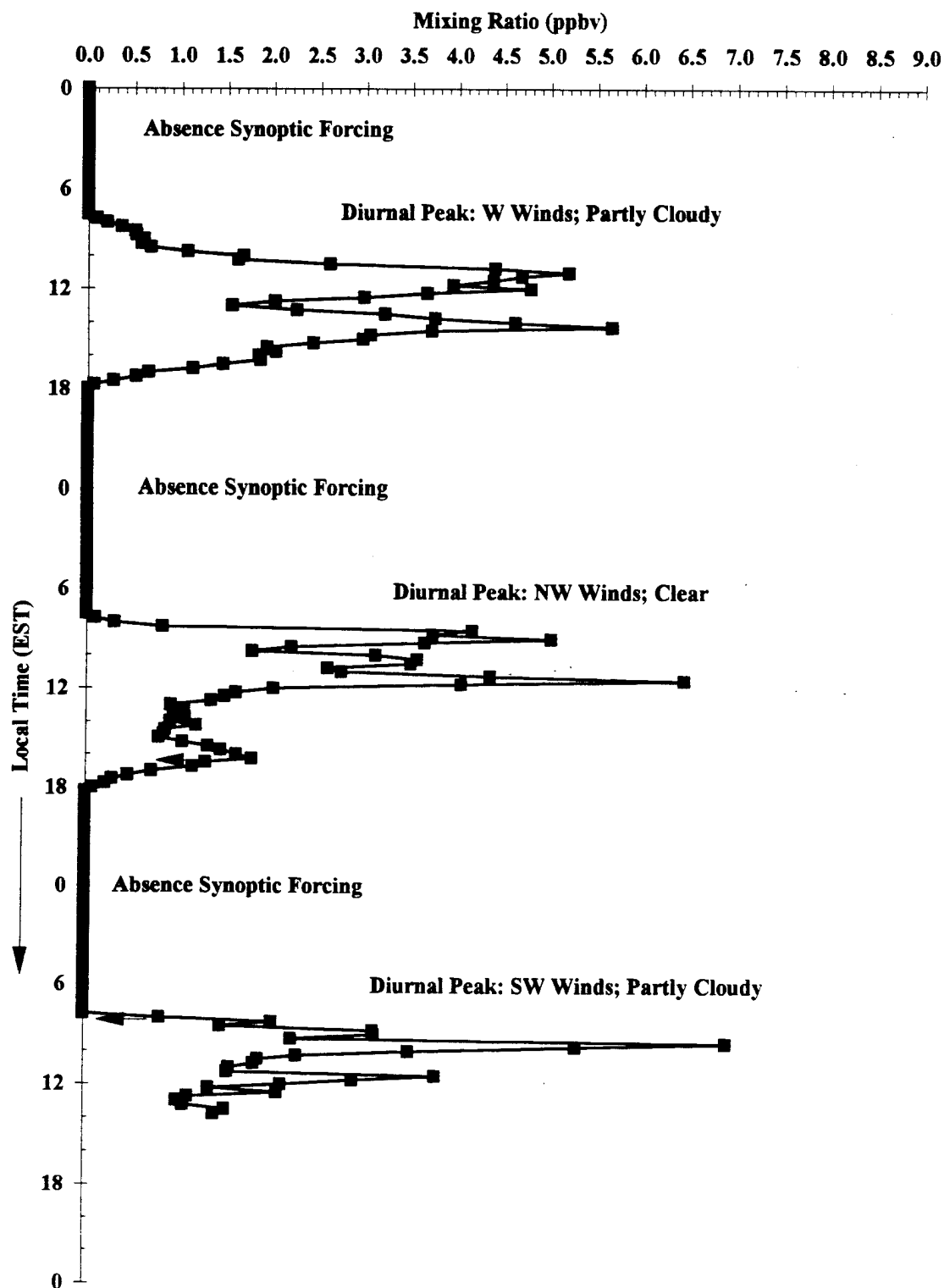


Figure 4.9g Diurnal Variation NO Mixing Ratio Overlaid with Synoptic Meteorology, 250 Meters AGL (5-7 Feb 95)

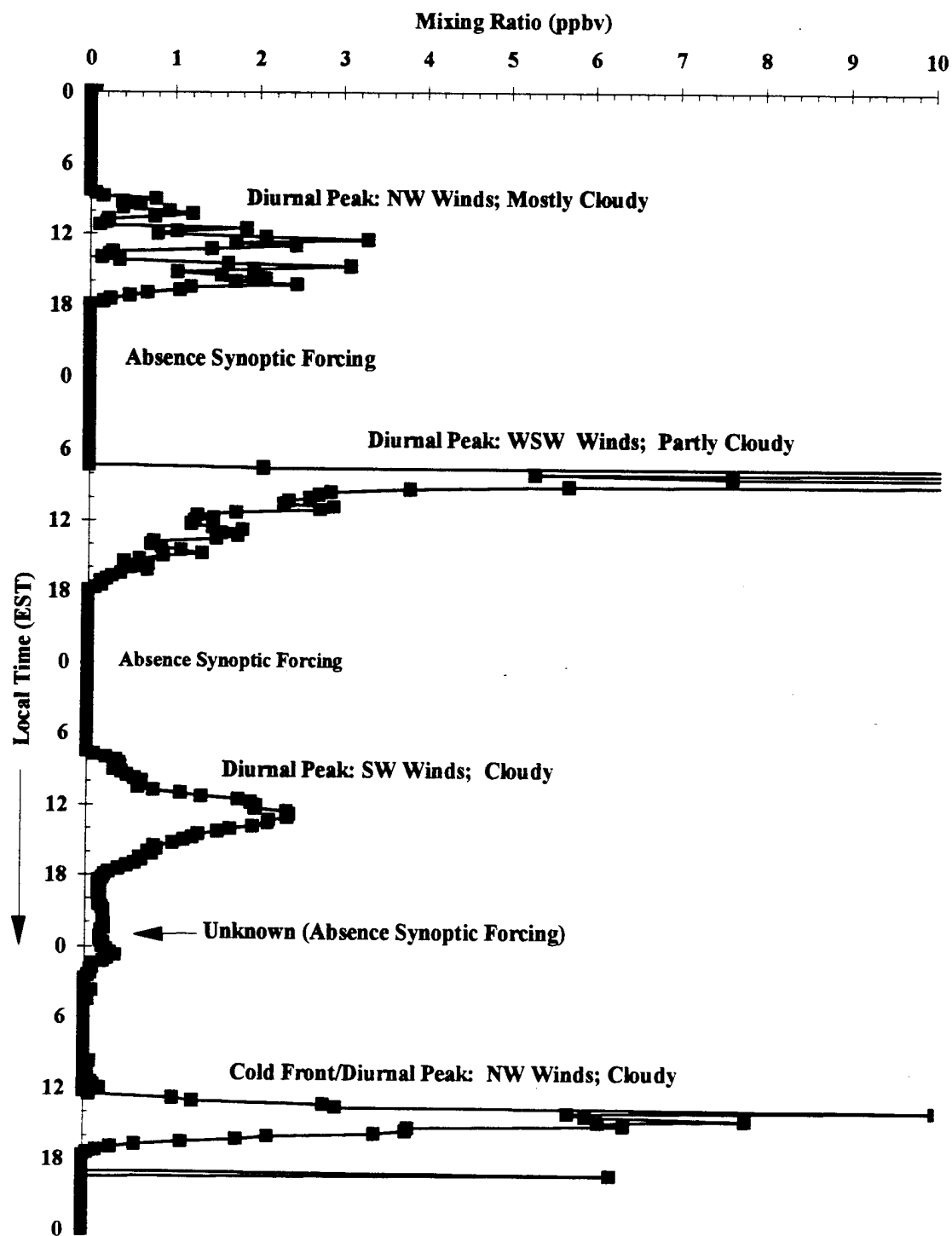


Figure 4.9h Diurnal Variation NO Mixing Ratio Overlaid with Synoptic Meteorology, 250 Meters AGL (8-11 Feb 95)

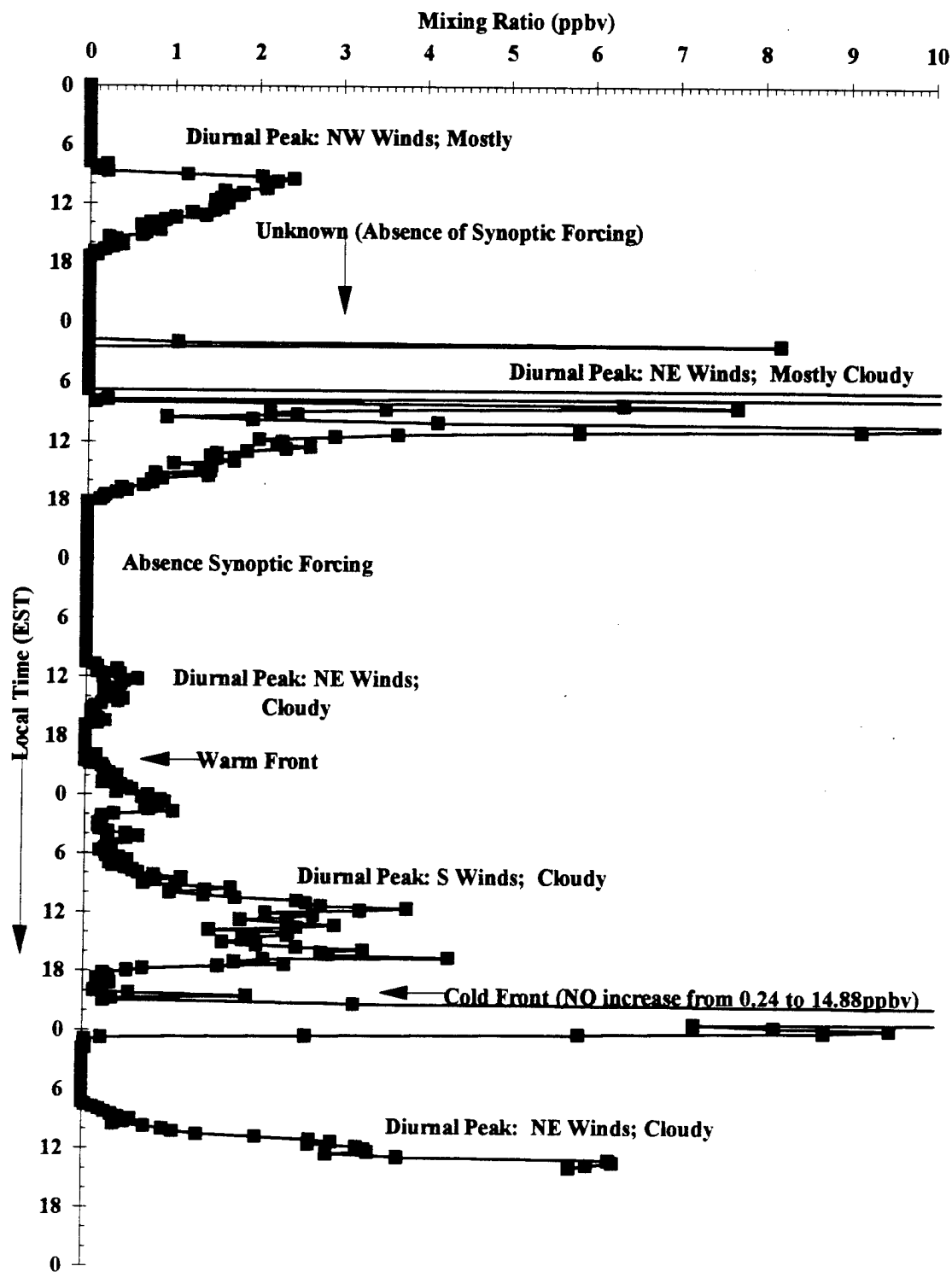


Figure 4.9i Diurnal Variation NO Mixing Ratio Overlaid with Synoptic Meteorology, 250 Meters AGL (13-17 Feb 95)

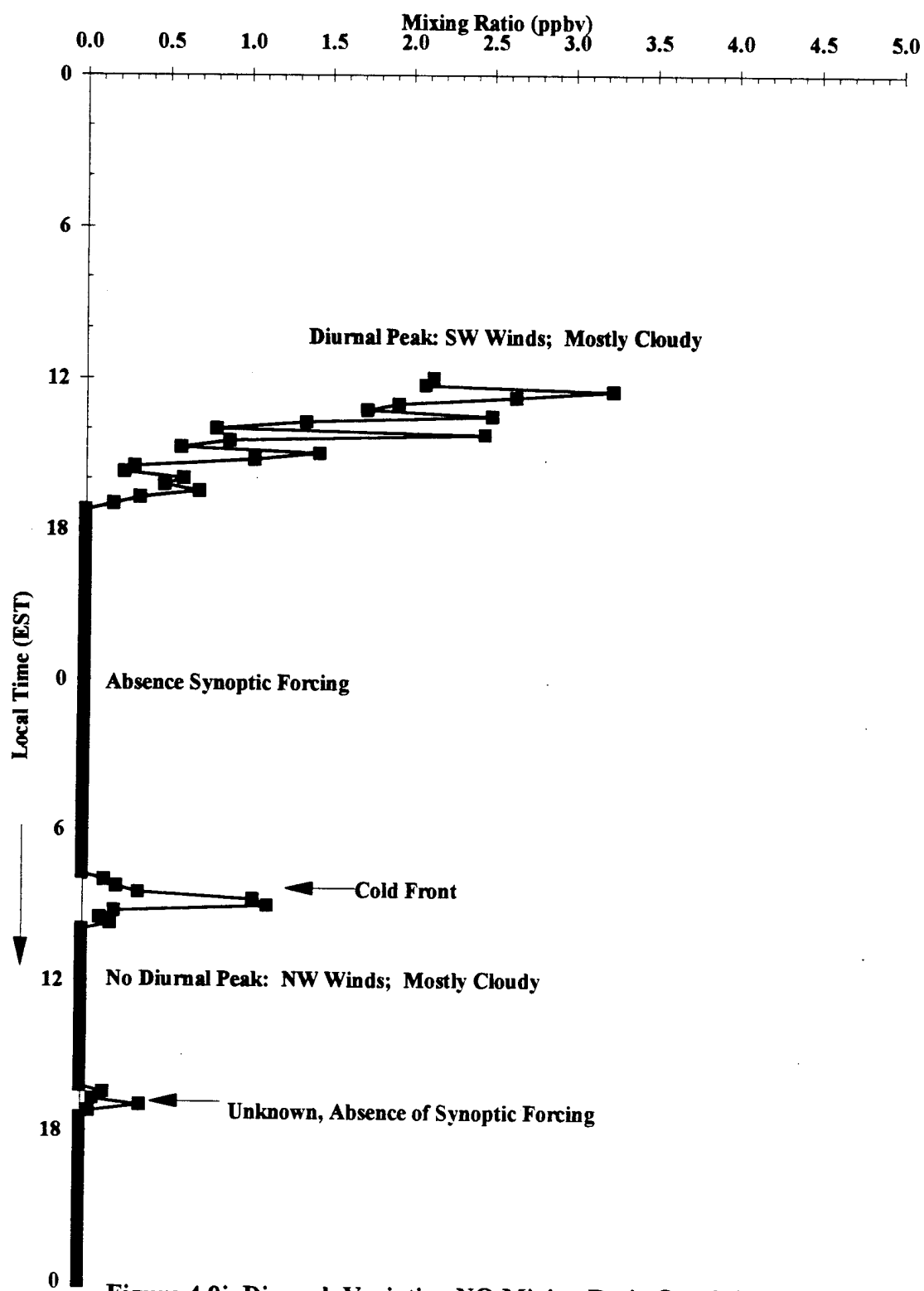


Figure 4.9j Diurnal Variation NO Mixing Ratio Overlaid with Synoptic Meteorology, 250 Meters AGL (20-21 Feb 95)

4.3.2 NO_y Mixing Ratios

The mixing ratios of NO_y did not show as consistent an association with synoptic events (Figures 4.10a-4.10j) as did the NO mixing ratios. For example, on the night of the February 2 and 3, 1995, a cold front passed through the local area of the tower just after midnight. During this time, NO mixing ratios (250 m) rose from below instrument detection limits (0.04 ppbv) to a maximum of 0.14 ppbv at 0200 EST (Figure 4.9f), and the NO_y mixing ratios (250 m) rose from 10.15 ppbv to a maximum of 33.68 ppbv at 0200 EST (Figure 4.10e); in each case the increase was a factor of approximately 3.5. Here it may be surmised that the vertical motion associated with the front transported both species from the surface and was reflected in the increased mixing ratios. However, the very next night (3-4 February, 1995) saw another cold front move through at 0300 EST, and while NO mixing ratios (250 m) rose to about the same level as before (0.15 ppbv at 0315 EST) (Figure 4.9f), the NO_y mixing ratio (250 m) only rose from 3.75 ppbv to 5.98 ppbv by 0500 EST (Figure 4.10e), before beginning to decrease again. The magnitude of this rise is within the usual nocturnal variation of NO_y mixing ratios, and therefore cannot be attributed with certainty to an association with the synoptic event (cold front passage).

In several cases, however, the NO_y mixing ratios did show an increase during the passage of a synoptic meteorological feature, but seemingly with a time lag greater than the NO mixing ratios. On the night of February 16, 1995, a cold front passage between 1900 and 2000 EST led to the previously mentioned increase of NO mixing ratios (250 m) from 0.24 ppbv to 14.88 ppbv in one hour (Figure 4.9i); here the NO_y rose slowly from

17.53 ppbv at 1900 EST to 23.41 ppbv by 2100 EST (Figure 4.10h), and then suddenly increased to 49.88 ppbv by 2200 EST. The lag may be an indicator that the air mass being transported up to the 250 m height was carrying a greater proportion of NO to the oxidized nitrogen species (NO_2), and replaced some of the air from which the instrument was previously sampling. If this were true, then the instrument would report a large increase in the NO mixing ratio, but the NO_Y mixing ratio would remain steady, because the increase in the NO measured as NO_Y would be offset by the decrease in oxidized species (NO_Z) measured as NO_Y .

There were approximately ten identifiable synoptic features that moved through the local area of the tower during the times in which NO_Y mixing ratios were recorded, and seven of them were associated with increases in the NO_Y mixing ratio. The other three events did not seem to have an effect on the NO_Y mixing ratios. In addition, there were numerous instances of increases in NO_Y mixing ratios during the nocturnal hours that could not be associated with synoptic events. These are discussed further under the section on atmospheric chemistry and horizontal transport.

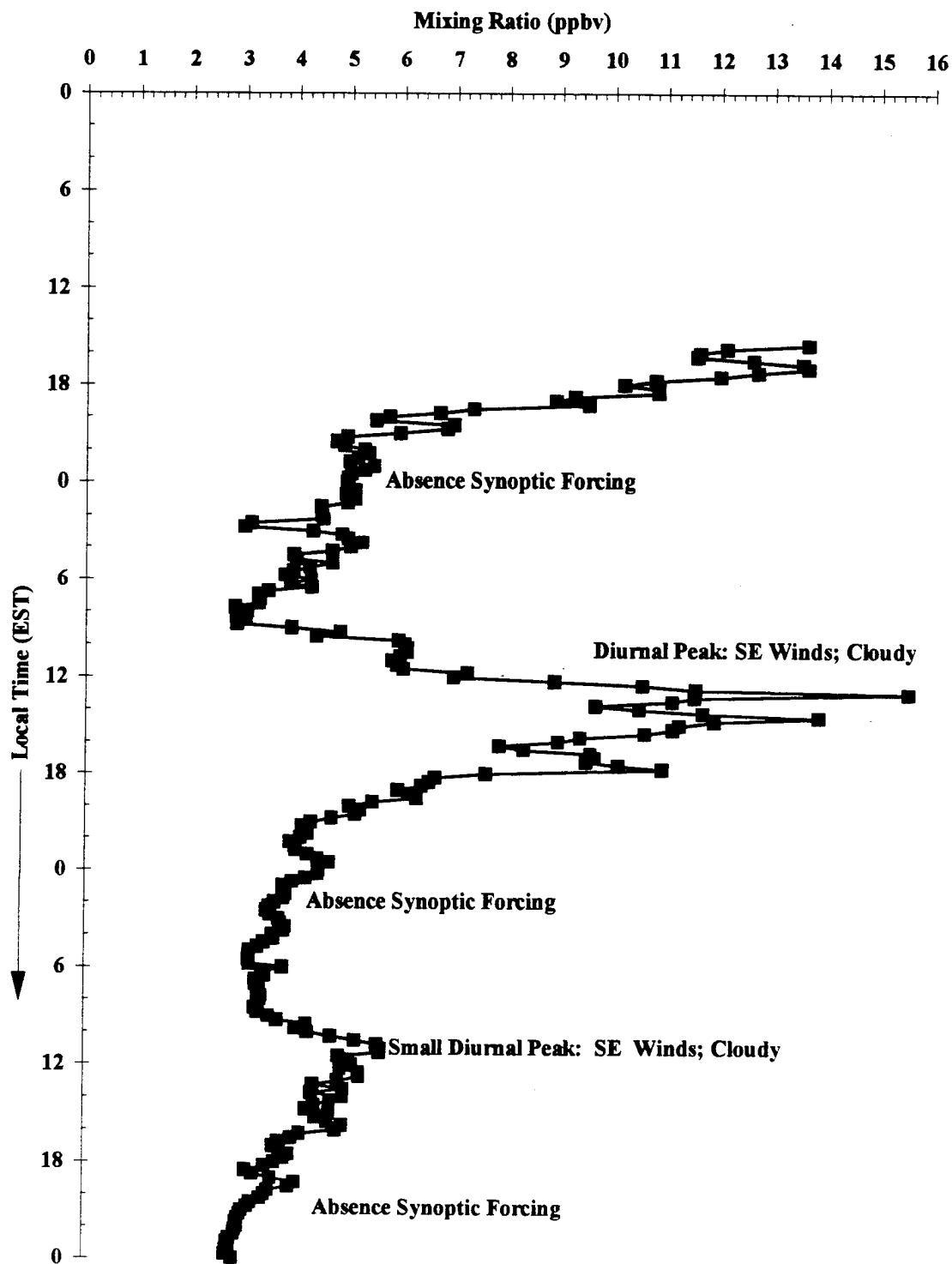


Figure 4.10a Diurnal Variation of NO_y Mixing Ratio Overlaid with Synoptic Meteorology, 433 Meters AGL (12-14 Jan 95)

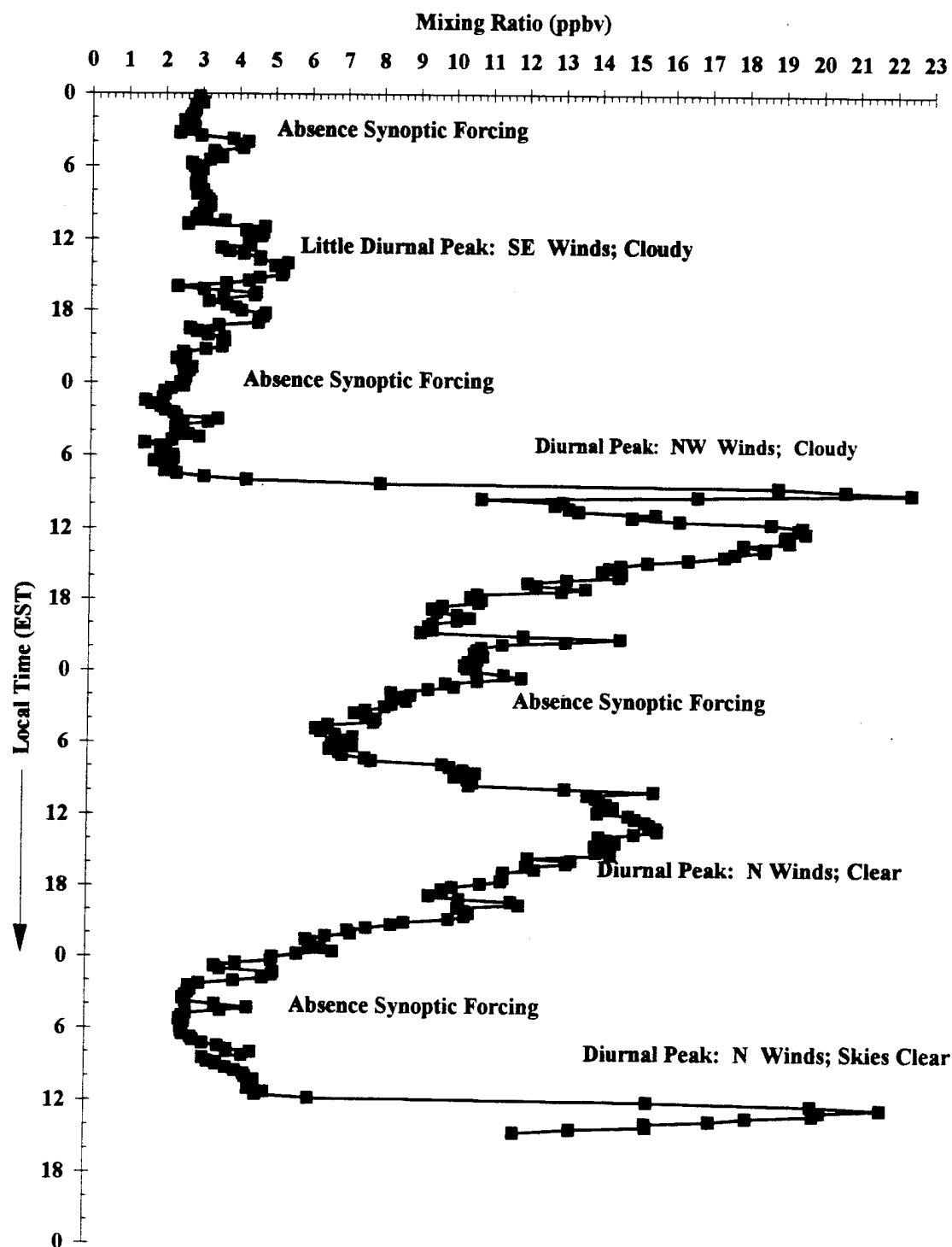


Figure 4.10b Diurnal Variation of NO_y Mixing Ratio Overlaid with Synoptic Meteorology, 433 Meters AGL (15-18 Jan 95)

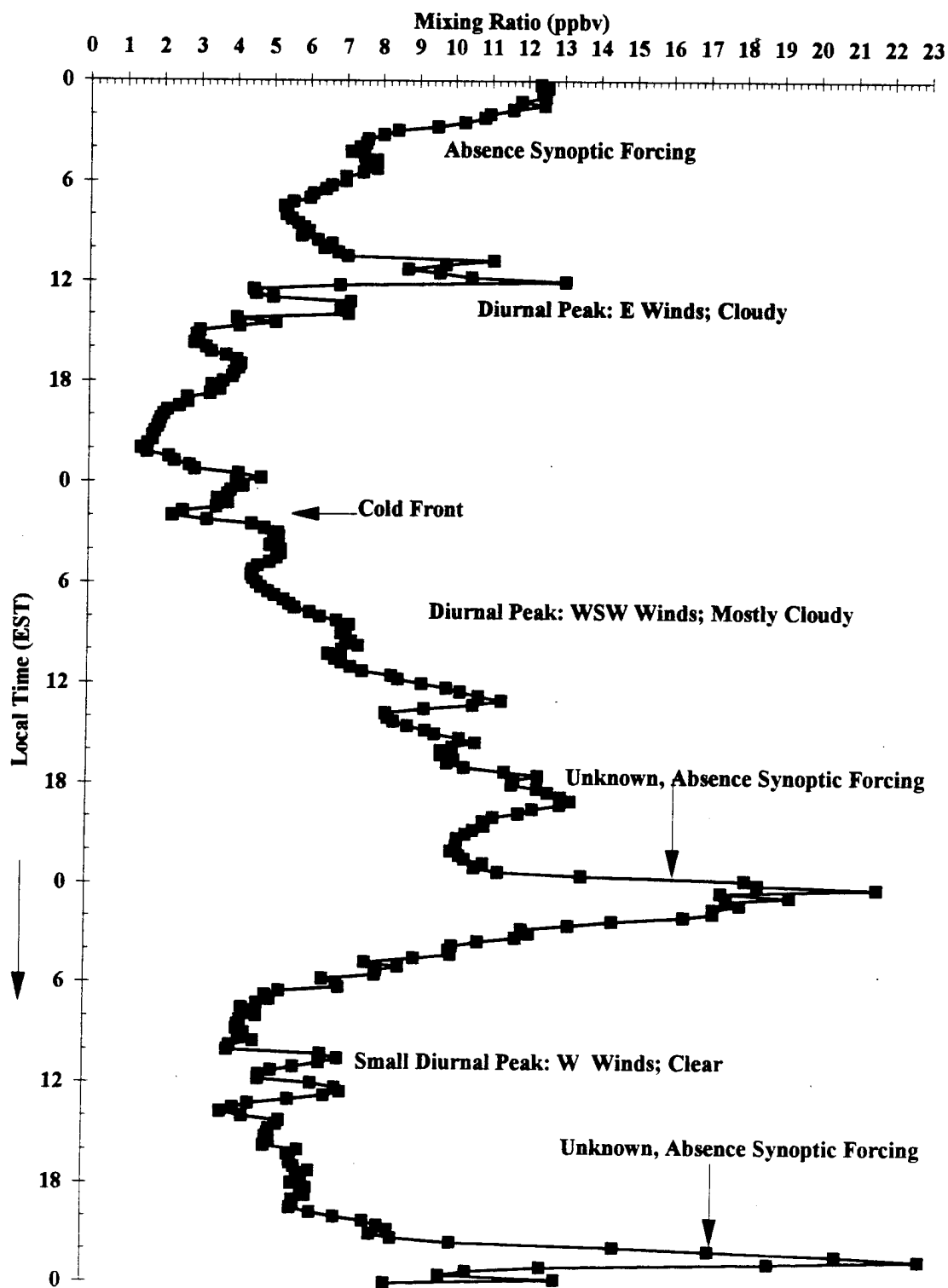


Figure 4.10c Diurnal Variation of NO_y Mixing Ratio Overlaid with Synoptic Meteorology, 433 Meters AGL (19-21 Jan 95)

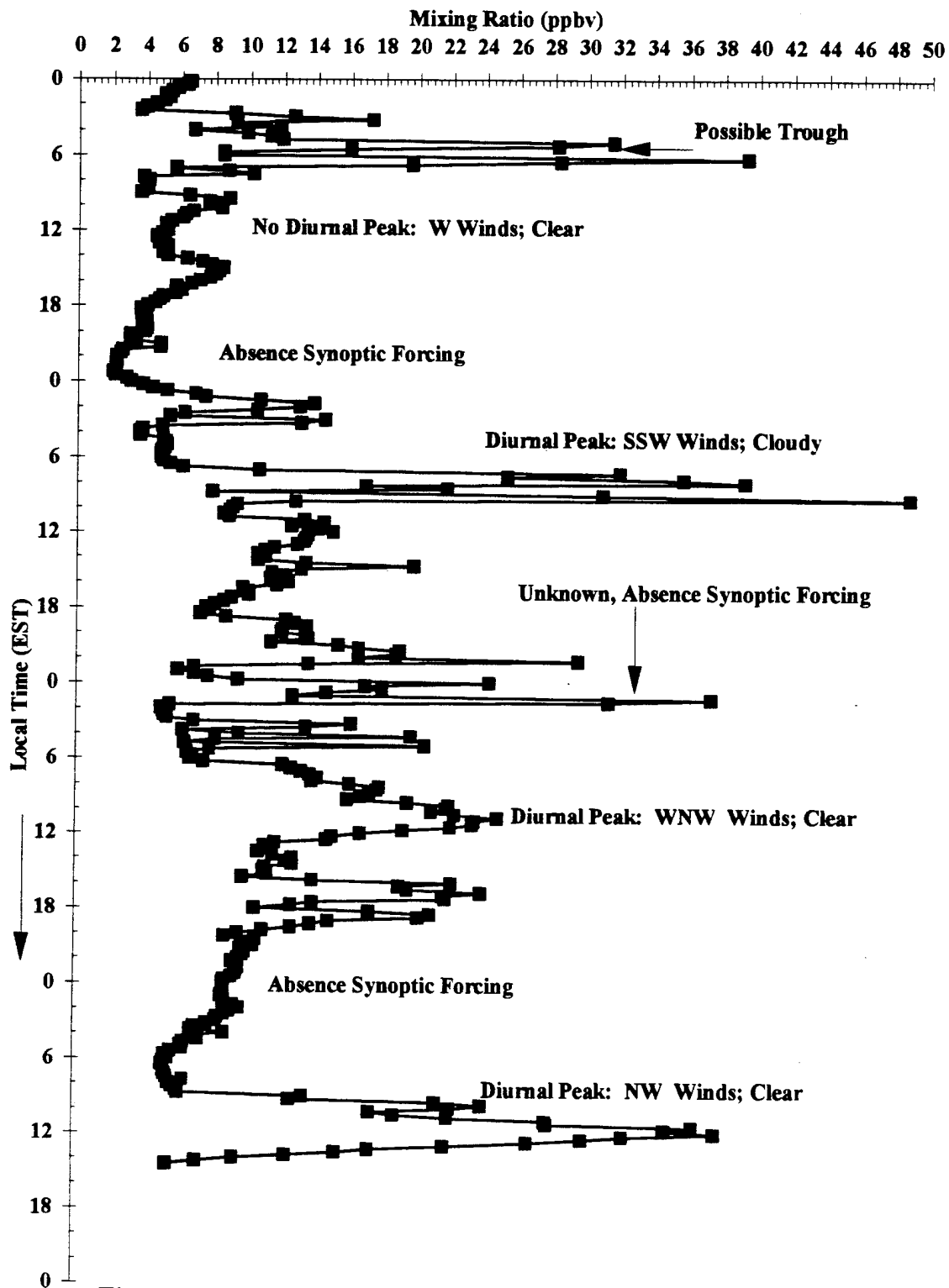


Figure 4.10d Diurnal Variation NO_y Mixing Ratio Overlaid with Synoptic Meteorology, 433 Meters AGL (22-25 Jan 95)

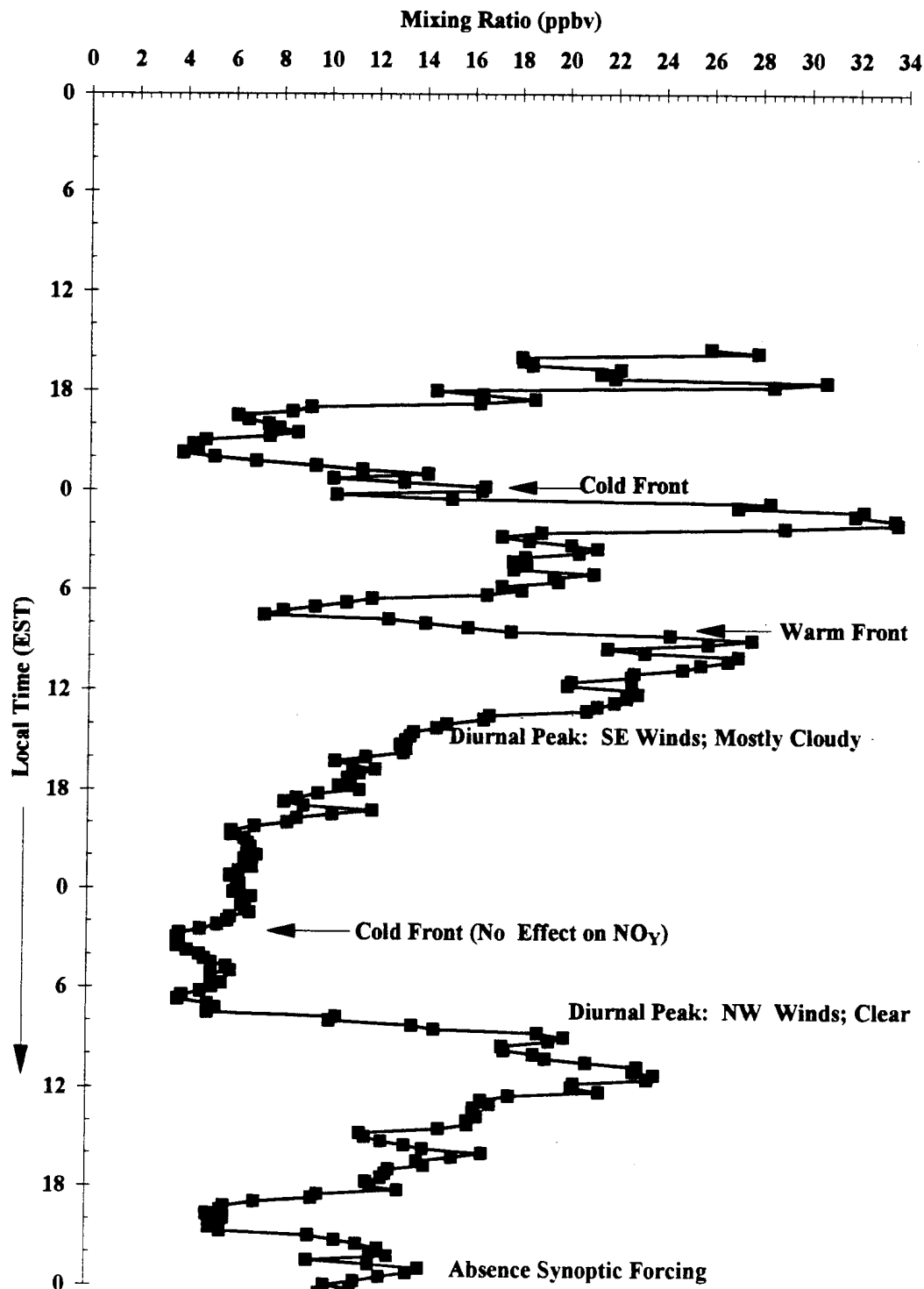


Figure 4.10e Diurnal Variation NO_y Mixing Ratio Overlaid with Synoptic Meteorology, 250 Meters AGL (2-4 Feb 95)

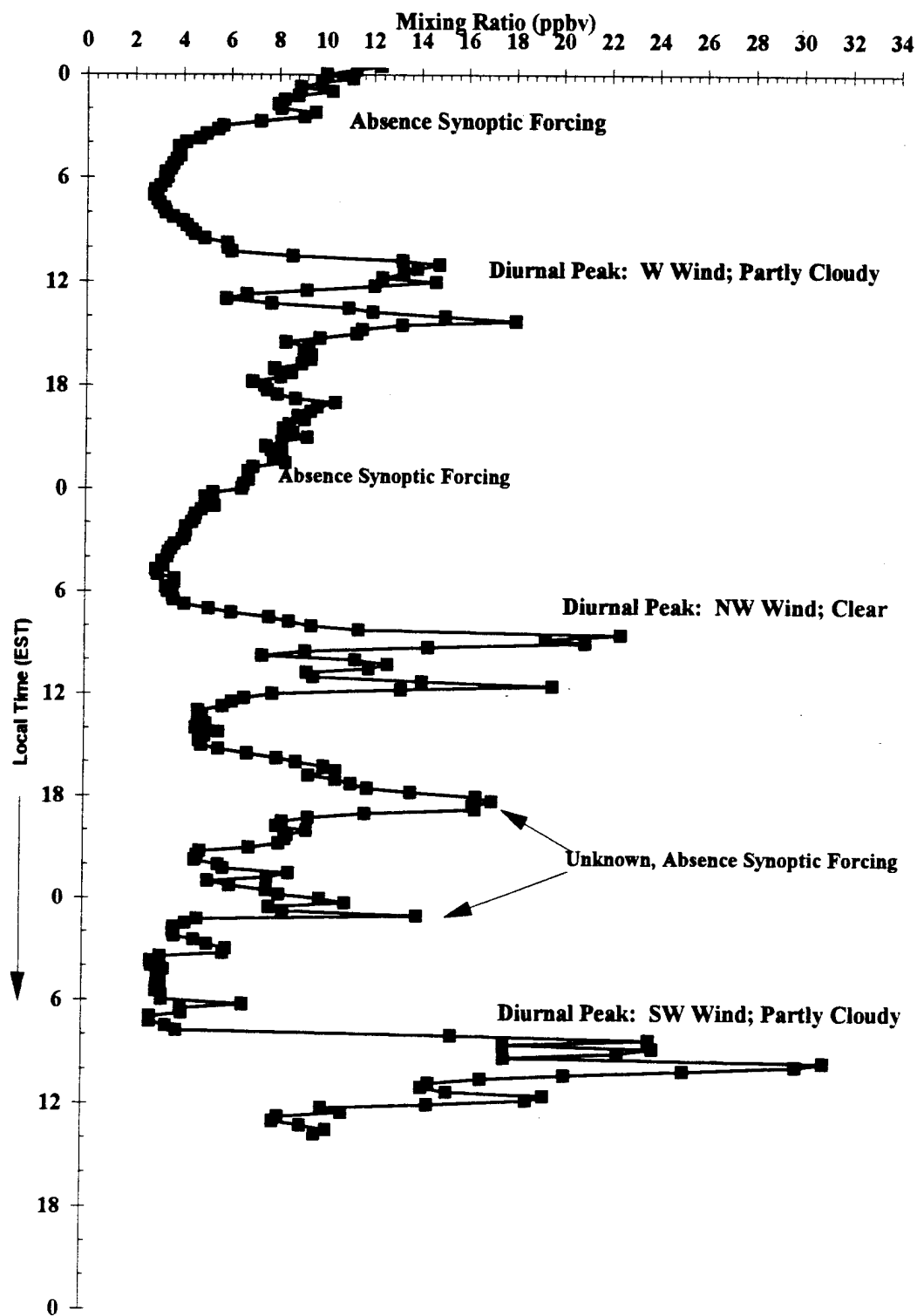


Figure 4.10f Diurnal Variation NO_y Mixing Ratio Overlaid with Synoptic Meteorology, 250 Meters AGL (5-7 Feb 95)

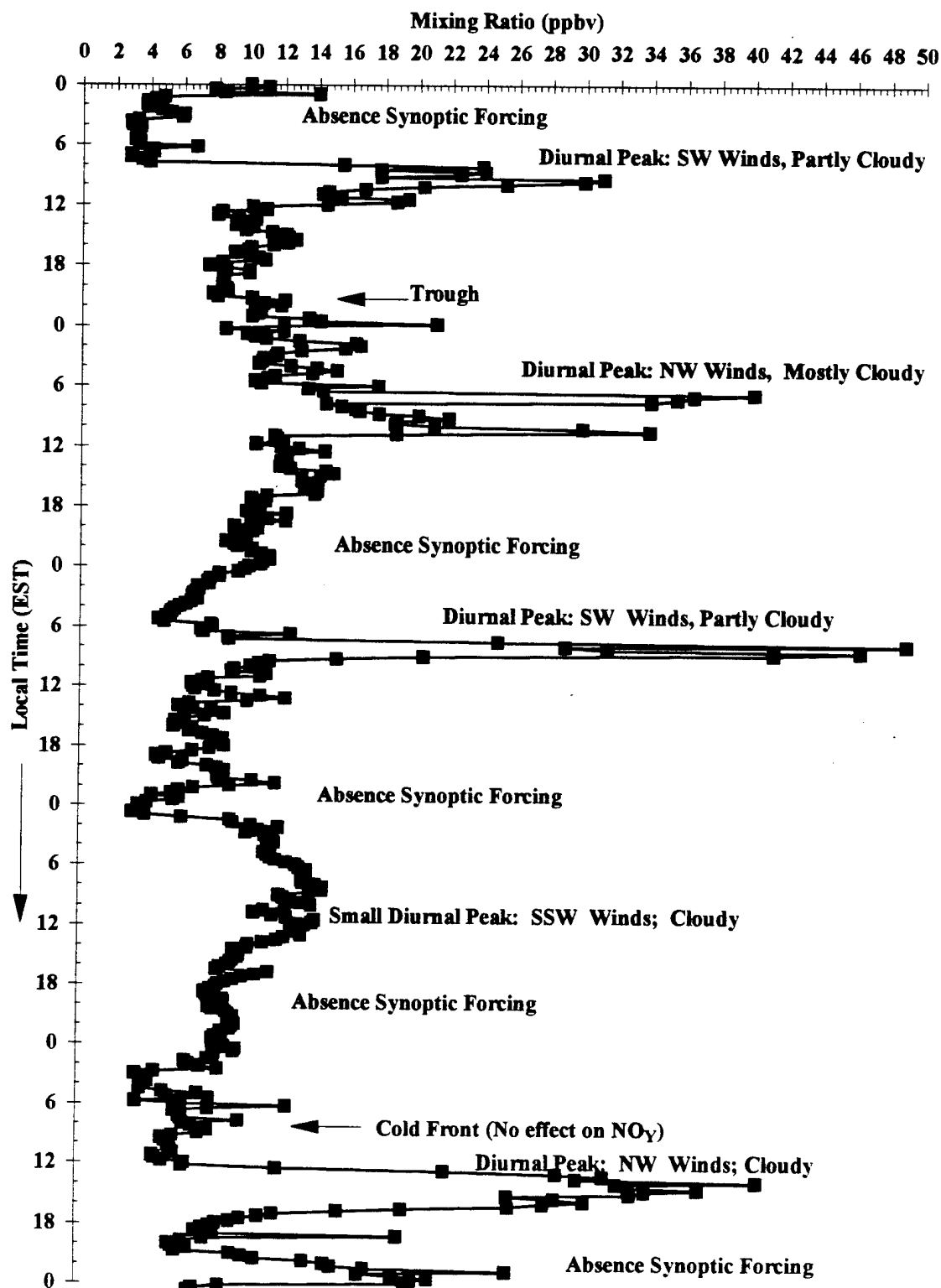


Figure 4.10g Diurnal Variation NO_y Mixing Ratio Overlaid with Synoptic Meteorology, 250 Meters (7-11 Feb 95)

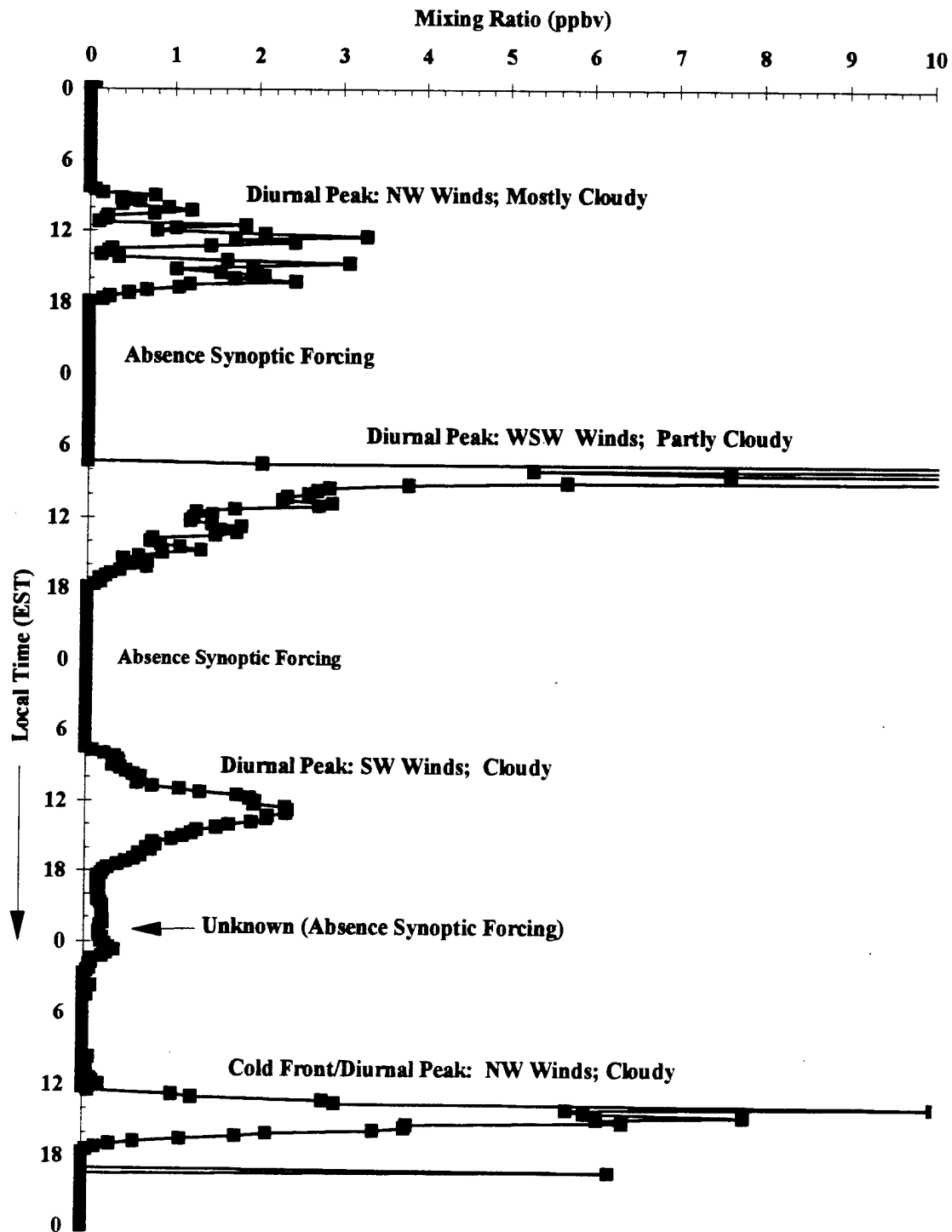


Figure 4.9h Diurnal Variation NO Mixing Ratio Overlaid with Synoptic Meteorology, 250 Meters AGL (8-11 Feb 95)

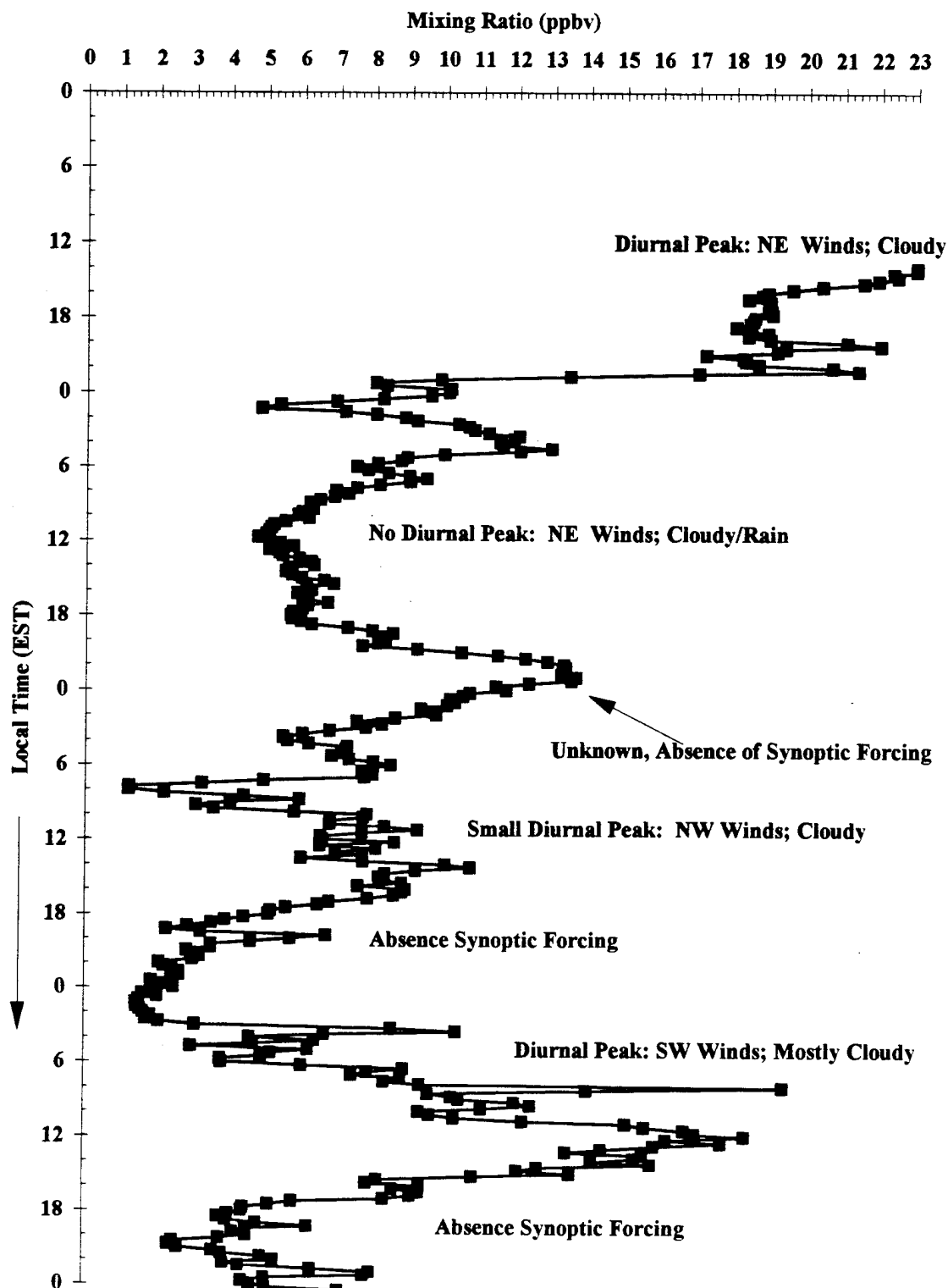


Figure 4.10i Diurnal Variation NO_y Mixing Ratio Overlaid with Synoptic Meteorology, 250 Meters AGL (17-20 Feb 95)

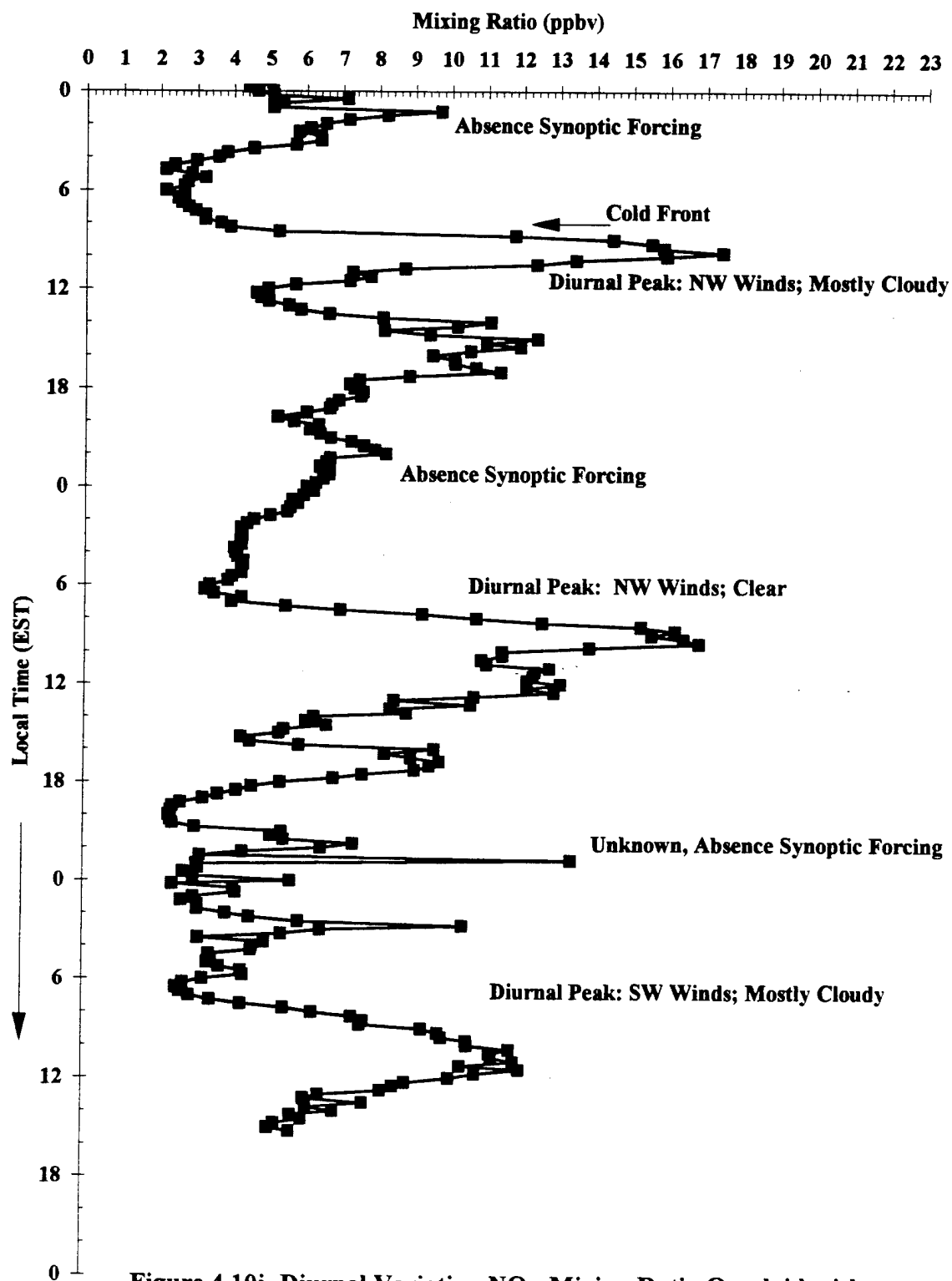


Figure 4.10j Diurnal Variation NO_y Mixing Ratio Overlaid with Synoptic Meteorology, 250 Meters AGL (21-23 Feb 95)

4.4 Boundary Layer Formation and Vertical Transport Processes

The formation of the various layers contained within both the day and nighttime planetary boundary layers and their relationship to diurnal vertical transport processes and the measured mixing ratios of NO and NO_y can be best understood by considering the following two processes: 1) formation of the nocturnal boundary layer (NBL) and possible conservation aloft of NO and NO_y, and 2) growth of the mixed layer (ML) and subsequent "upward mixing" of NO and NO_y. For each of these processes, a series of case studies is presented in which boundary layer structures were determined through an analysis of the upper air data for a specific date, and then the measured values of the NO and NO_y mixing ratios are given for comparison and validation of the hypothesis that the nitrogen species did not exist in high enough mixing ratios to be mixed downward and affect surface measurements, but instead were mixed upward from sources near the surface during the morning hours.

4.4.1 Formation of the Nocturnal Boundary Layer

The presence of the NBL was determined by the analysis of atmospheric conditions as given by meteorological data and upper air soundings collected during each measurement period. For this study, the atmospheric conditions under which formation of the NBL occurs can be divided into two specific categories: Strong NBL Formation and Moderate NBL Formation. Here, the term strong NBL formation refers to conditions

under which a strong NBL would be expected to form, i.e., clear skies and light winds under high pressure. The term moderate NBL formation refers to conditions under which a strong NBL would usually not occur, such as under cloudy skies or gusty wind conditions. The terms are meant to convey information about the conditions under which a strong or moderate NBL may form, and are not meant to imply information about the strength of the NBL itself (which was not measured).

4.4.1.1 Strong Nocturnal Boundary Layer Formation

The daily surface weather maps and the RDU observations for each intensive were first searched for the appropriate meteorological conditions that allow for the formation of a strong nocturnal boundary layer. This search identified only eleven nights out of forty-four as having the prerequisite clear skies and absence of synoptic events necessary for formation of a strong NBL. Of these eleven nights, only six had the light winds necessary for the formation of a strong stable layer. The GSO NWS upper air soundings at 0600 EST for these six nights were then studied for evidence of the height of the stable layer through the temperature, dew point temperature and wind speed profiles; four of these soundings provided the information necessary for defining the stable boundary layer and are discussed in the following sections.

4.4.1.1.1 12 Dec 94

During the night of 11-12 Dec 94, under the influence of high pressure to the north, the RDU NWS recorded clear skies, light winds of 3-8 kts, and temperatures falling from 41 degrees °F at sundown to 26 degrees °F at 0600 EST. Figure 4.11 shows the GSO NWS upper air sounding for this date at 0600 EST, which indicates a surface layer to about 30 m, a stable boundary layer to about 155 m, and a residual layer capped by a possible subsidence inversion that begins at around 500 m. A low level jet existed, with a direction/speed of 060/18 kts at about 300 m. The NO-NO_y analyzer was located at 433 m (within the residual layer), where winds were approximately 88% of the low level maximum speed and were within 5 degrees of the direction of the maximum wind speed. On this night, the instrument recorded NO values below the detection limit of 0.23 ppbv until after sunrise. NO_y mixing ratios were not measured on this date.

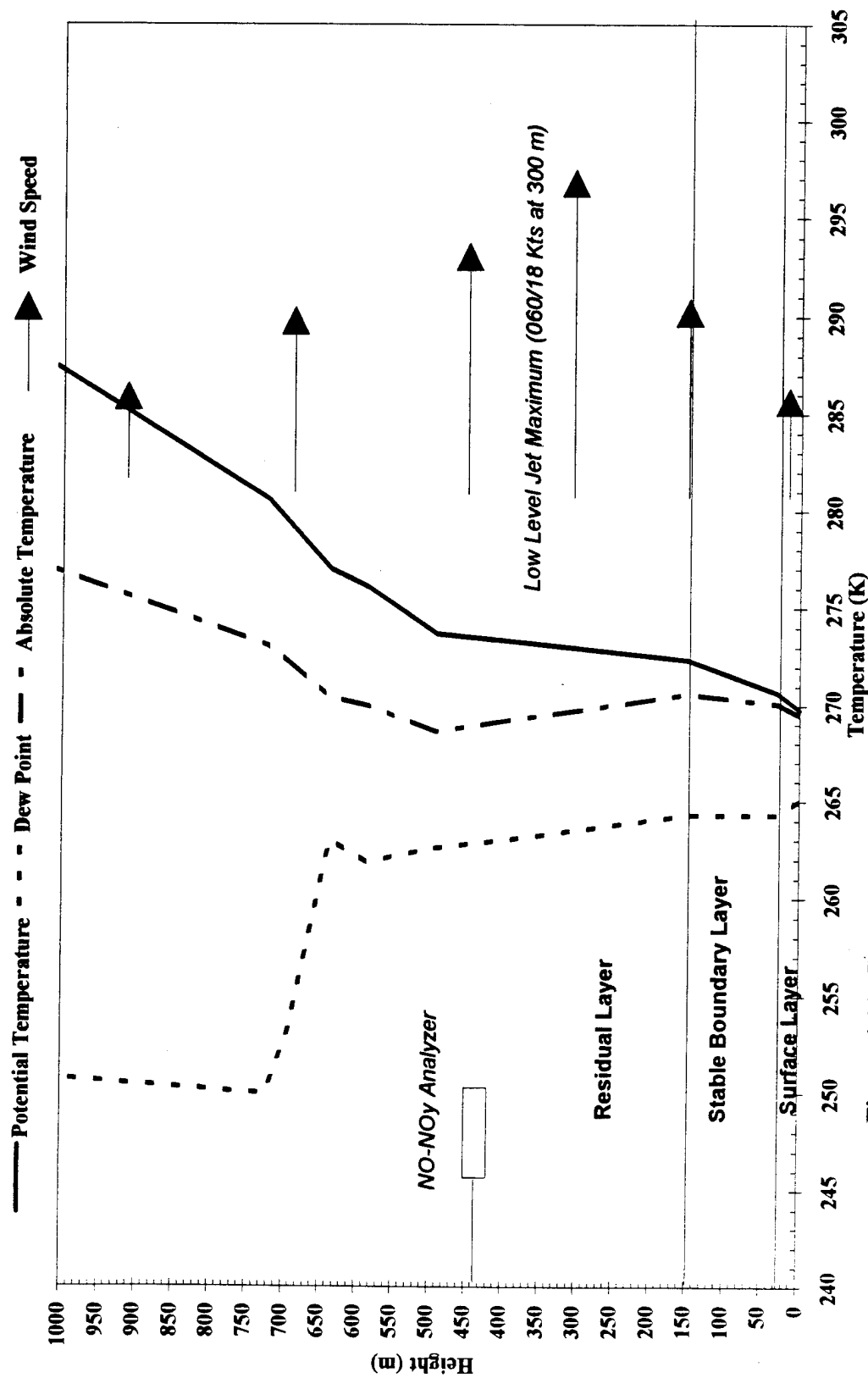


Figure 4.11 Greensboro, NC NWS Upper Air Sounding - 12 Dec 94 (0600 EST)
 (Arrows show relative magnitude of wind speed at that height)

4.4.1.1.2 17 Jan 95

On the night of 17 Jan 95, under the influence of high pressure to the north, the RDU NWS recorded clear skies after midnight, winds of 3-8 kts after 2000 EST, and temperatures falling from 58 degrees °F at sundown to 39 degrees °F at 0600 EST. The GSO upper air sounding at 0600 EST (Figure 4.12) shows surface layer to about 25 m, a stable layer to about 135 m, and a residual layer that extended beyond 1000 m. The wind speed profile does not show a low level maximum. The NO-NO_y analyzer was located at 433 m (within the residual layer); the instrument recorded NO mixing ratios below the instrument detection limits of 0.04 ppbv throughout the night and into the morning. NO_y mixing ratios fell from peak of 11.42 ppbv at midnight to a nocturnal minimum of 6.26 ppbv at 0445 EST; values at 0600 EST were near this nocturnal minimum at 6.69 ppbv.

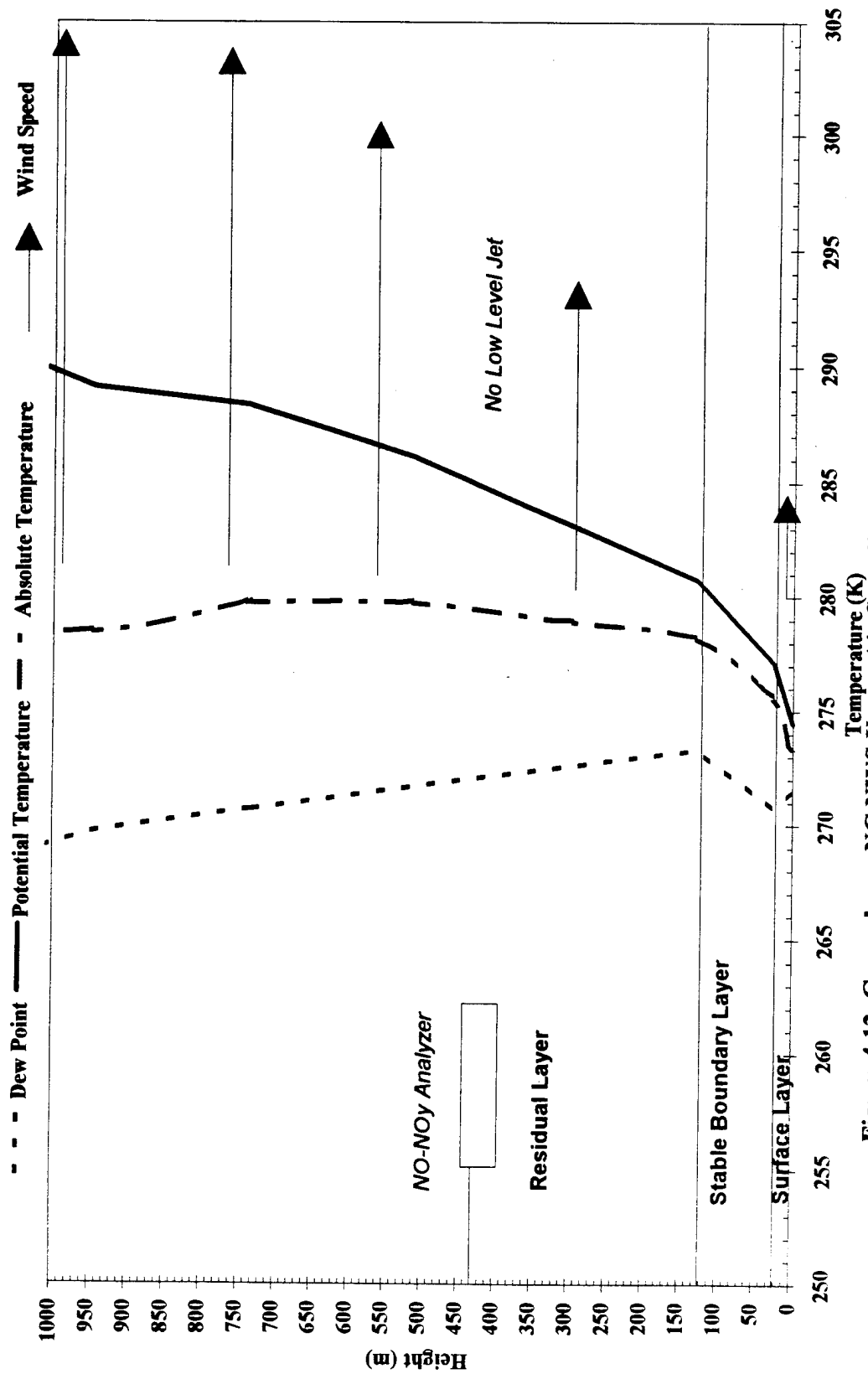


Figure 4.12 Greensboro, NC NWS Upper Air Sounding - 17 Jan 95 (0600 EST)
(Arrows show relative wind speed at that height)

4.4.1.1.3 18 Jan 95

On the night of 18 Jan 95, under continued influence of high pressure to the northeast, the RDU NWS recorded mostly clear skies, light winds from 0 to 5 kts, and temperatures falling from 52 degrees °F at sundown to 37 degrees °F at 0600 EST.

Figure 4.13 shows the GSO upper air sounding for 0600 EST, 18 Jan 95. A surface layer is evident to about 33 m, a stable boundary layer is evident from 33 to about 240 m, and residual layer is evident from the top of the SBL to a capping inversion that begins at approximately 900 m. The wind speed profile does not indicate a low level jet. The NO-NO_y analyzer, located at 433 m, again recorded NO mixing ratios that were below the instrument detection limit (less than 0.04 ppbv) throughout the night and into the morning. NO_y mixing ratios fell steadily throughout the night to a nocturnal minimum of 2.63 ppbv, which occurred at 0600 EST.

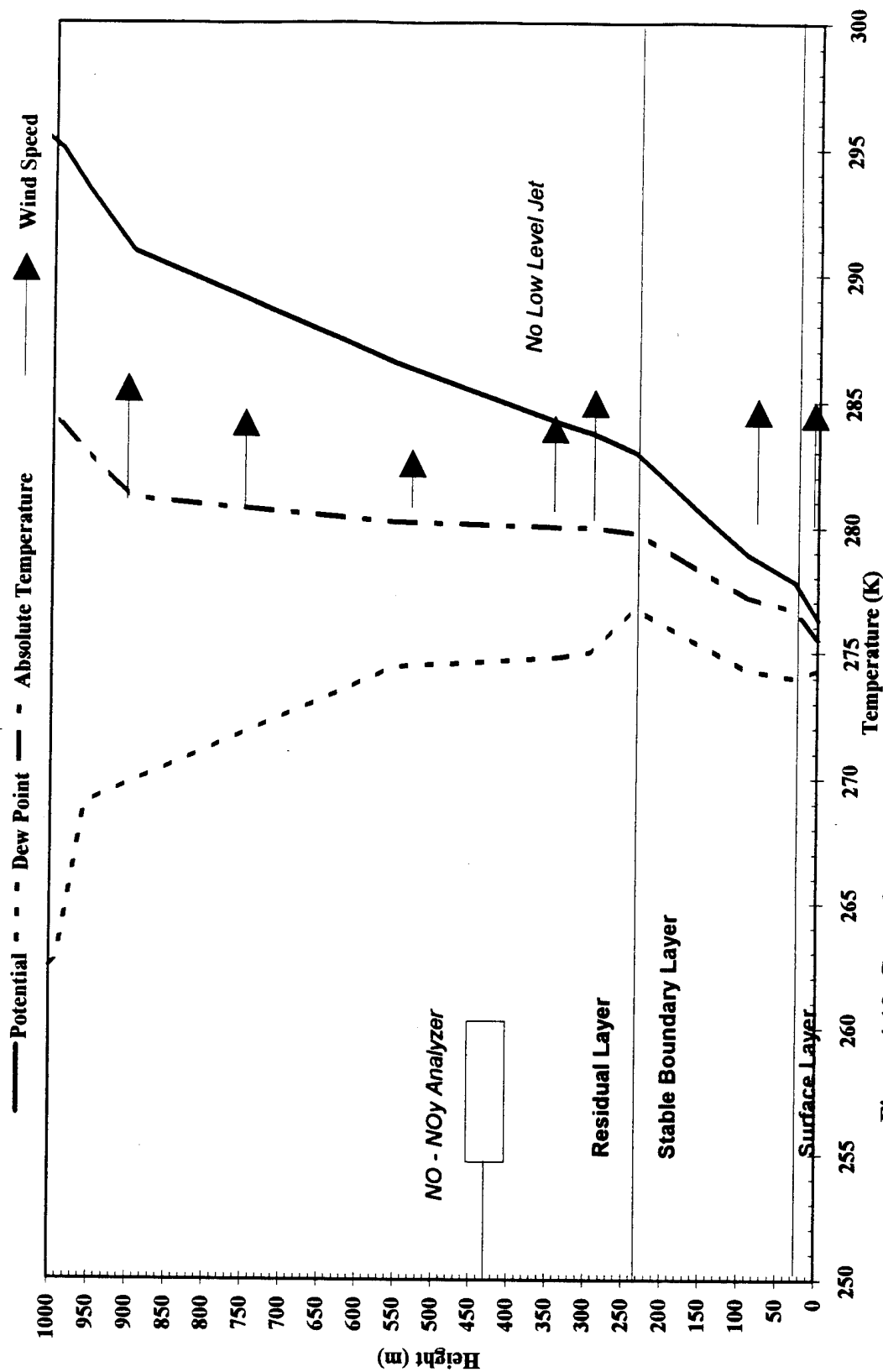


Figure 4.13 Greensboro, NC NWS Upper Air Sounding - 18 Jan 95 (0600 EST)
(Arrows show relative wind speed at that height)

4.4.1.1.4 7 Feb 95

On the night of 7 Feb 95, under the influence of high pressure to the south, the RDU NWS recorded clear skies, winds of 0-7 kts, and temperatures falling from 33 degrees °F at sundown to 13 degrees °F at 0600 EST. Figure 4.14 shows the GSO upper air sounding at 0600 EST, and indicates a combination surface layer and stable layer to about 50 m, with a residual layer above this stable layer capped by an inversion at about 850 m. No low level winds were recorded during this sounding. The NO-NO_y analyzer, located at 250 m (within the residual layer), recorded NO mixing ratios below the instrument detection limit (0.04 ppbv) throughout the night until after sunrise. The NO_y mixing ratios fell from a peak of 14.02 ppbv at 0100 EST to a nocturnal minimum of 2.92 ppbv at 0400 EST; and the value at 0600 EST of 3.34 ppbv was close to the recorded nocturnal minimum.

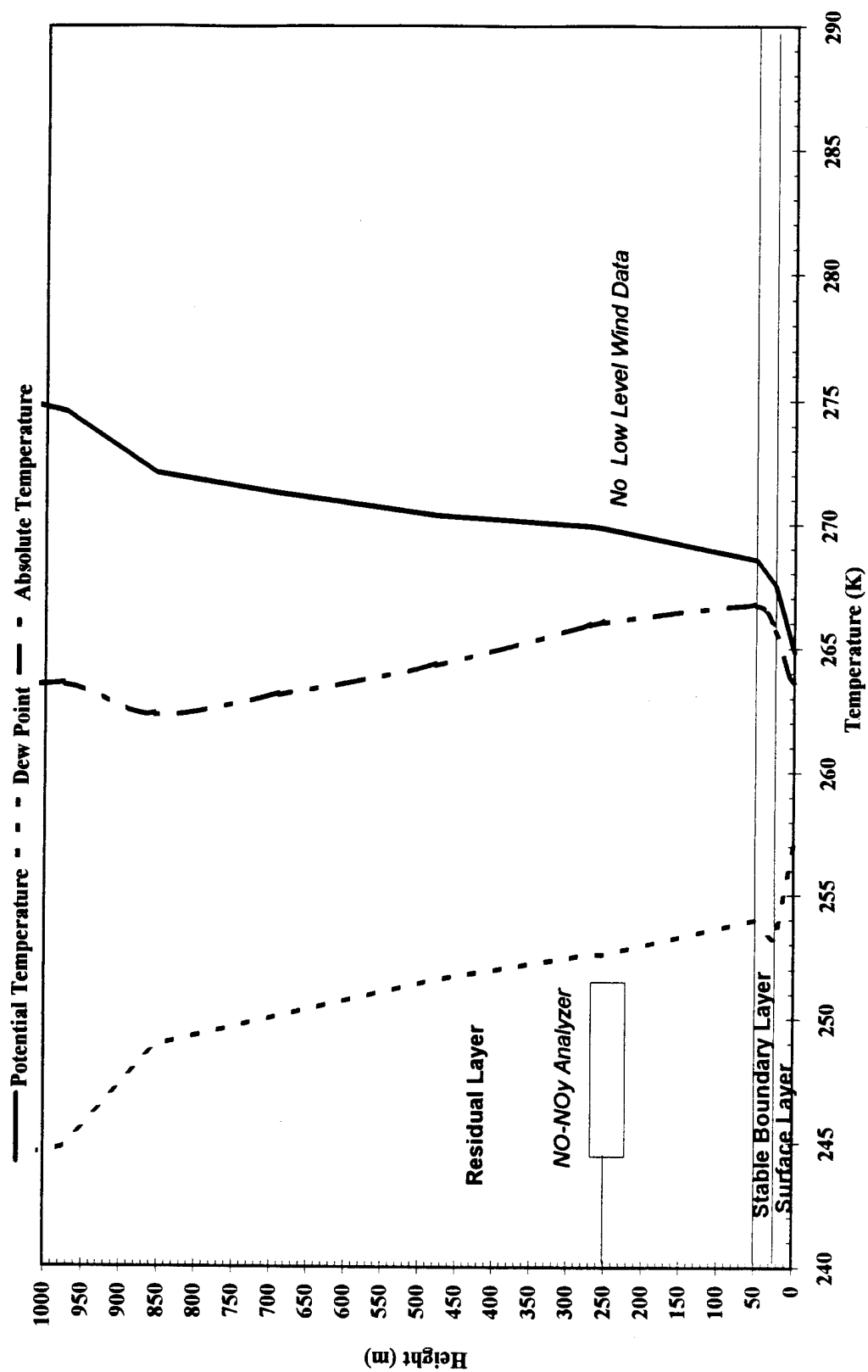


Figure 4.14 Greensboro, NC NWS Upper Air Sounding - 7 Feb 95 (0600 EST)

4.4.1.2 Moderate Nocturnal Boundary Layer Formation

Further review of the GSO upper air soundings for the measurement period indicates that three soundings show the development of a possible moderate stable layer under meteorological conditions (such as cloudy skies or gusty winds) that were not favorable for development of a strong stable layer. These three soundings are discussed in the following sections to provide insight into boundary layer mechanisms and their relation to mixing ratios of NO and NO_y under differing meteorological conditions.

4.4.1.2.1 13 Jan 95

On the night of 13 Jan, under the influence of a high pressure over the northwestern Atlantic Ocean, the RDU NWS recorded mostly cloudy skies, winds of 0-8 kts, and a temperature drop from 64 degrees °F at sundown to 49 degrees °F at 0600 EST. Figure 4.15 shows the GSO upper air sounding at 0600 EST. Evident in this sounding is a surface layer to about 30 m, a stable boundary layer to about 200 m, and a residual layer extending to at least 800 m. Also evident is a strong low level jet located just above the SBL/RL interface, and which reaches a maximum direction/speed of 210/20 kts in the layer from 200 to 500 m. The NO-NO_y analyzer, located at 433 m, did not record any NO mixing ratios above the instrument detection limit (0.04 ppbv) throughout the night and even throughout the rest of the day. NO_y mixing ratios slowly decreased throughout the night to a nocturnal minimum of 2.81 at 0745 EST; the value at 0600 EST was near this minimum at 4.25 ppbv.

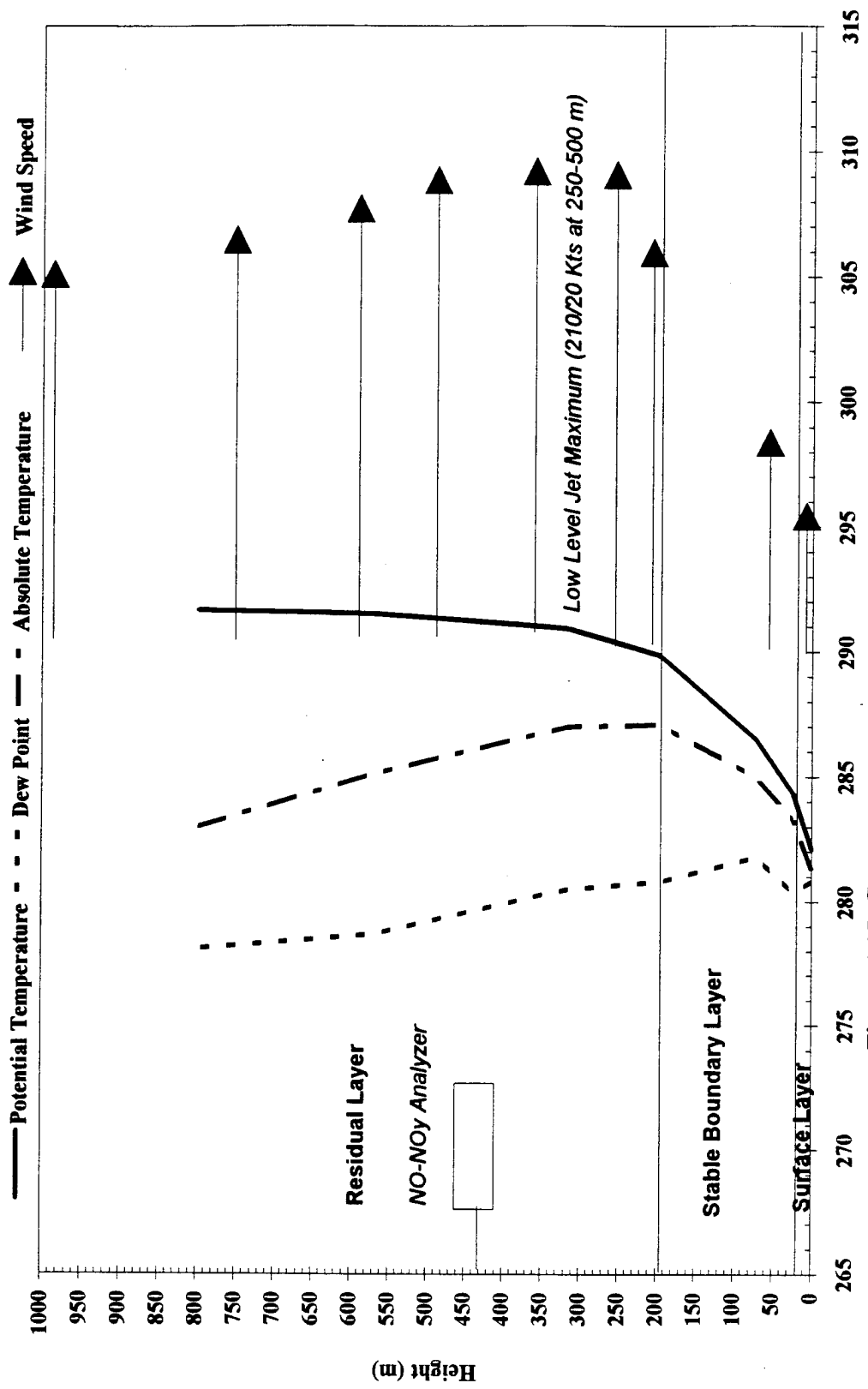


Figure 4.15 Greensboro, NC NWS Upper Air Sounding - 13 Jan 95

(Arrows show relative wind speed at that height)

4.4.1.2.2 3 Feb 95

On the night of 3 Feb 95, the RDU NWS recorded clear skies and winds of 6-10 kts after passage of a weak cold front at midnight, with temperatures dropping from 49 degrees °F at sundown to 33 degrees °F at 0600 EST. The GSO upper air sounding (Figure 4.16) at 0600 EST indicates a surface layer to about 35 m, a stable boundary layer to about 175 m, and a residual layer above the stable layer capped with an inversion beginning at approximately 800 m. A weak low level jet maximum of 040/11 kts occurs between 250 and 300 m. The NO-NO_y analyzer, located in the heart of the low level jet and just above the RL/SBL interface, measured NO mixing ratios below instrument detection limits (0.04 ppbv) throughout the night (except during passage of cold front as discussed in previous section) until after sunrise. NO_y mixing ratios at 0600 EST, while higher than normal at 18.08 ppbv, were nevertheless at a nocturnal minimum, being lower than measurements at 0145 EST (33.55 ppbv) during frontal passage and measurements during the subsequent diurnal peak (27.14 ppbv at 1000 EST).

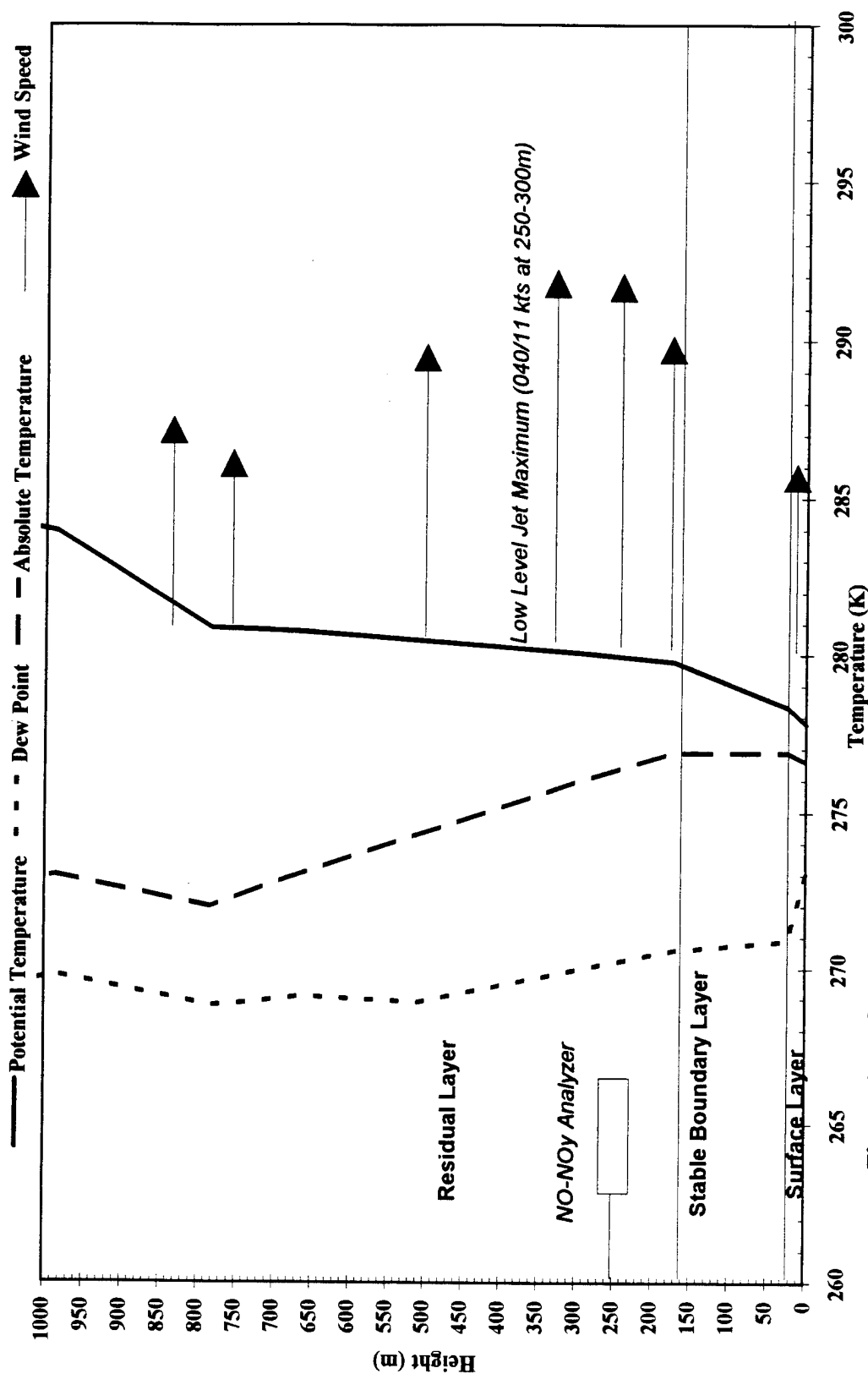


Figure 4.16 Greensboro, NC NWS Upper Air Sounding - 3 Feb 95 (0600 EST)
(Arrows show relative wind speed at that height)

4.4.1.2.3 20 Feb 95

On the night of 20 Feb 95, under the influence of a very weak high over the Carolinas, the RDU NWS recorded cloudy skies, winds of 0-6 kts, and a temperature drop from 56 degrees °F at sundown to 45 degrees °F at 0600 EST. The GSO upper air sounding (Figure 4.17) shows a that a surface layer developed to about 25 m, a stable boundary layer existed to about 190 m, and above that a residual layer rose to above 1000m. Also evident is a low level jet (340/11 kts) from 240-260 m. At 250 m, the NO-NO_y analyzer was once again located in the heart of the low level jet, just above the RL/SBL interface. Unfortunately at this time the data logger was not recording the NO channel correctly, and therefore there is no NO mixing ratio data available. However, the NO_y mixing ratios were recorded, and indicate that these ratios dropped to the lowest levels recorded (1.45 ppbv) during the entire study at around 0130 EST; thereafter the mixing ratios rose somewhat to a value of 3.82 ppbv at 0600 EST.

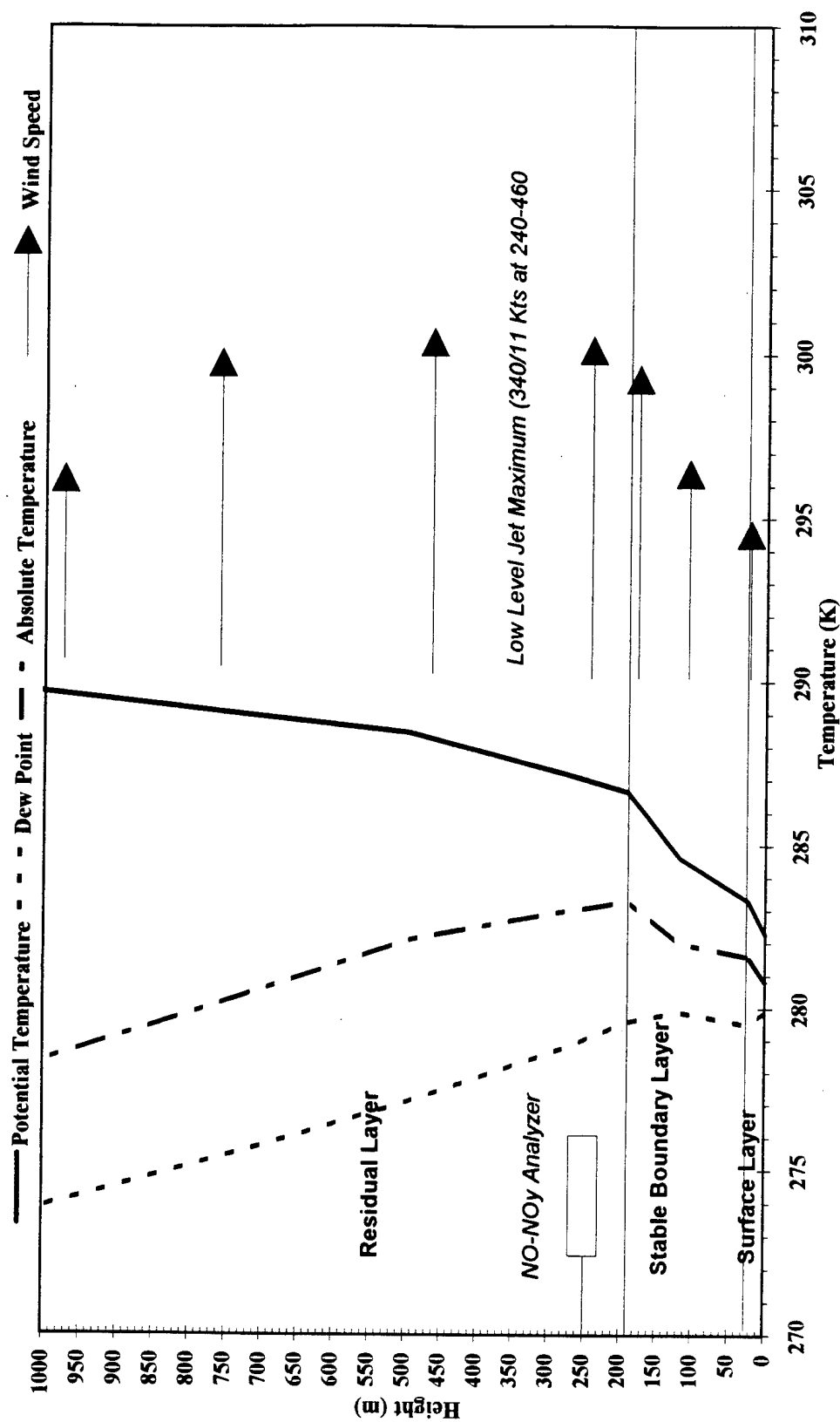


Figure 4.17 Greensboro, NC NWS Upper Air Sounding - 20 Feb 95 (0600 EST)
(Arrow show relative wind speed at that height)

4.4.1.3 Nocturnal Boundary Layer Formation Discussion

As outlined in the definition and experimental background sections, the formation of a nocturnal boundary layer, and in particular, the formation of separate stable and residual layers is a requirement for downward mixing of pollutants after sunrise [Trainer, 1987; Stull, 1988]. Pollutants such as NO and NO_y trapped at or above the interface of the residual and stable layers (and possibly transported by the low level jet usually found at this interface) can be mixed downward to the surface upon breakup of the nocturnal boundary layer in the morning. However, during the course of this research, in the seven cases the NO-NO_y analyzer was located at a height that was at or above the identifiable interface of a SBL and the RL above it, measured NO and NO_y mixing ratios were at or near their nocturnal minimums. Therefore, NO and NO_y did not exist in sufficient quantities in these seven cases to affect surface mixing ratios upon being mixed downward. In addition, outside of the previously mentioned synoptic episodes, NO mixing ratios were, with one exception, *always* below instrument detection limits (0.23 ppbv in December, 0.04 ppbv in January and February) during the early morning hours just before sunrise, no matter what the state of the boundary layer. This includes seventeen mornings at 433 m and seventeen mornings at 250 m. The one exception occurred on 14 Dec 95; NO mixing ratios ranging from zero to 0.66 ppbv were measured from 0415 to 0630 EST. In this case, however, rain and drizzle were recorded throughout the night at the RDU NWS office, indicative of possible small scale vertical lifting (not evident in the large scale resolution of the meteorological data). The NO_y mixing ratios

were, with three exceptions, at or near the nocturnal minimum values during the early morning hours just before sunrise, no matter what the state of the boundary layer; this includes fourteen mornings at 433 m and twenty-one mornings at 250 m. Of the three exceptions, two were measured during periods of rain and drizzle (as recorded by the RDU NWS office) and hence were possibly affected by small scale vertical lifting. The final exception, for which no synoptic or precipitation events can be associated, occurred on 14 Feb 95. In this case, the NO_Y mixing ratios reached a nocturnal minimum at approximately 0330 EST (3.83 ppbv) and then rose quickly to 20.70 ppbv at 0600 EST. The ratios continued to rise, however, reaching a peak of near 50 ppbv between 0715 and 0800 EST.

4.4.2 Growth of the Mixing Layer

Although the mean diurnal profile indicates the average time of increase from the nocturnal minima for the NO and NO_Y mixing ratios at 250 and 433 m is between 0700 and 0800 EST (see Figures 4.1, 4.2, 4.3, 4.5, and 4.6), individual profiles show a wide variation in time of increase to the diurnal peak (Figures 4.8-4.10). As stated before, it is hypothesized that this diurnal peak is related to the growth of the mixed layer and the subsequent "upward mixing" of NO and NO_Y from the surface via the convective eddies that make up the mixed layer. To test this hypothesis, NCSU upper air sounding data from six case studies is presented in order to compare mixed layer heights with the observed diurnal NO and NO_Y mixing ratio increases.

4.4.2.1 8 Dec 94

GSO upper air sounding at 0600 EST (Figure 4.18a) indicates a lack of an identifiable stable boundary layer (skies were mostly cloudy during the night as a cold front passed through; a strong stable boundary layer was not expected to develop). The NCSU upper air sounding from the agricultural field site at 0730 EST (Figure 4.18b) indicates that in the absence of a strong stable boundary layer, the mixed layer rose quickly to nearly 525 m soon after sunrise. The instrument located at 433 m recorded a maximum diurnal NO mixing ratio (13.64 ppbv) soon after the rise of the mixed layer past the height of the instrument at 0800 EST (Figure 4.18c). NO_y mixing ratios were not measured on this date.

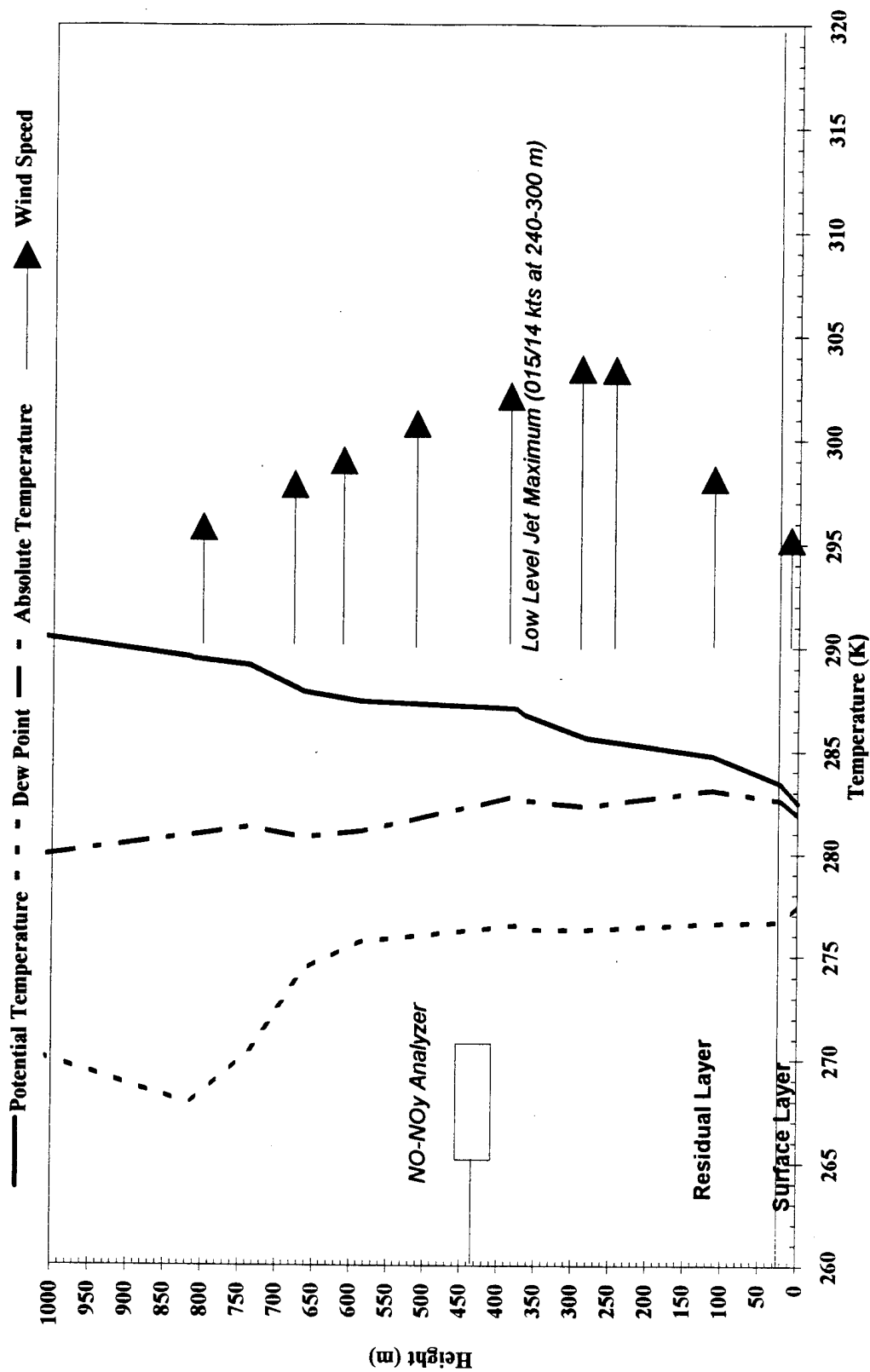


Figure 4.18a Greensboro, NC NWS Upper Air Sounding - 8 Dec 94 (0600 EST)
(Arrows show relative wind speed at that height)

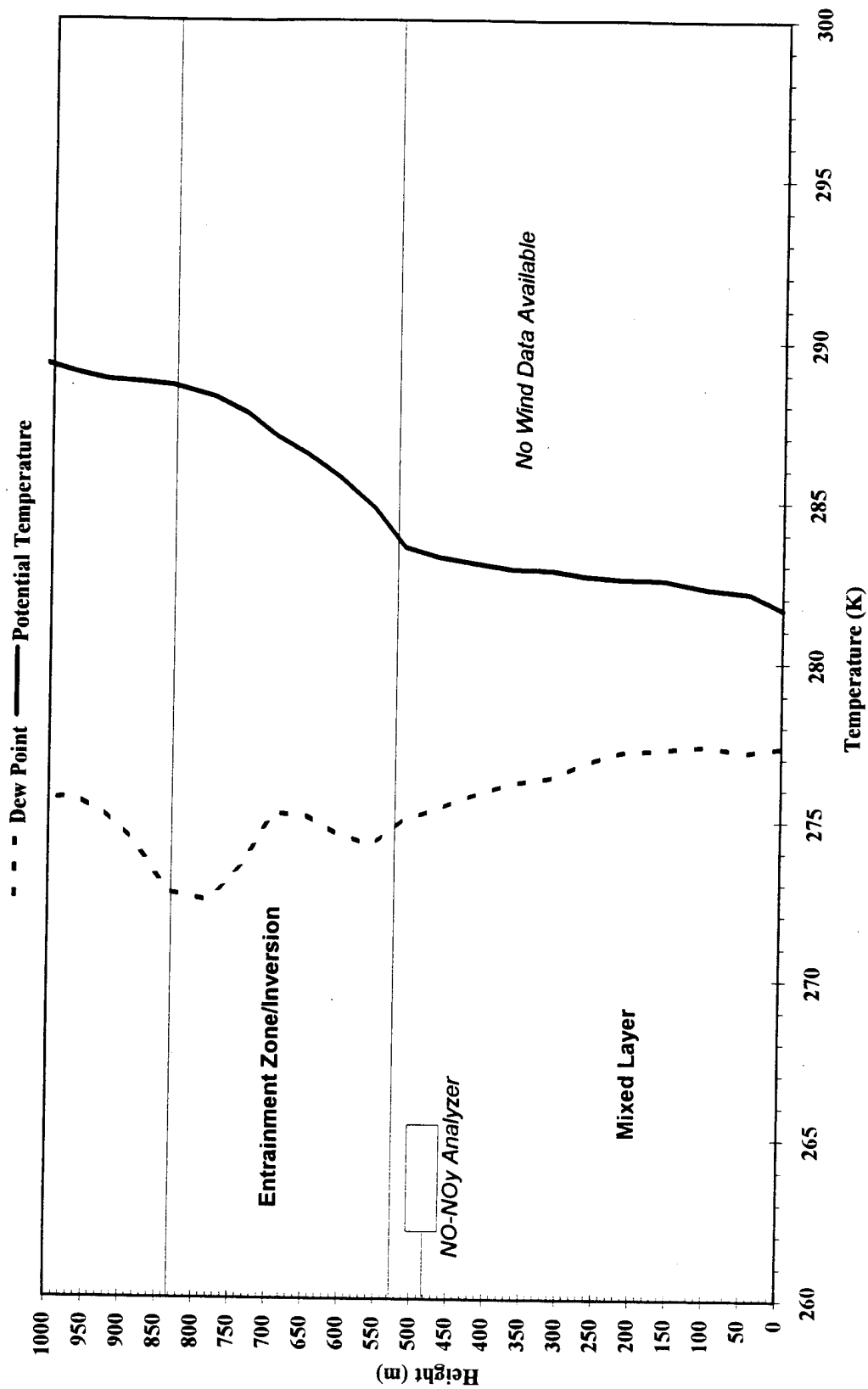


Figure 4.18b NCSU Upper Air Sounding - 8 Dec 94 (0730 EST)

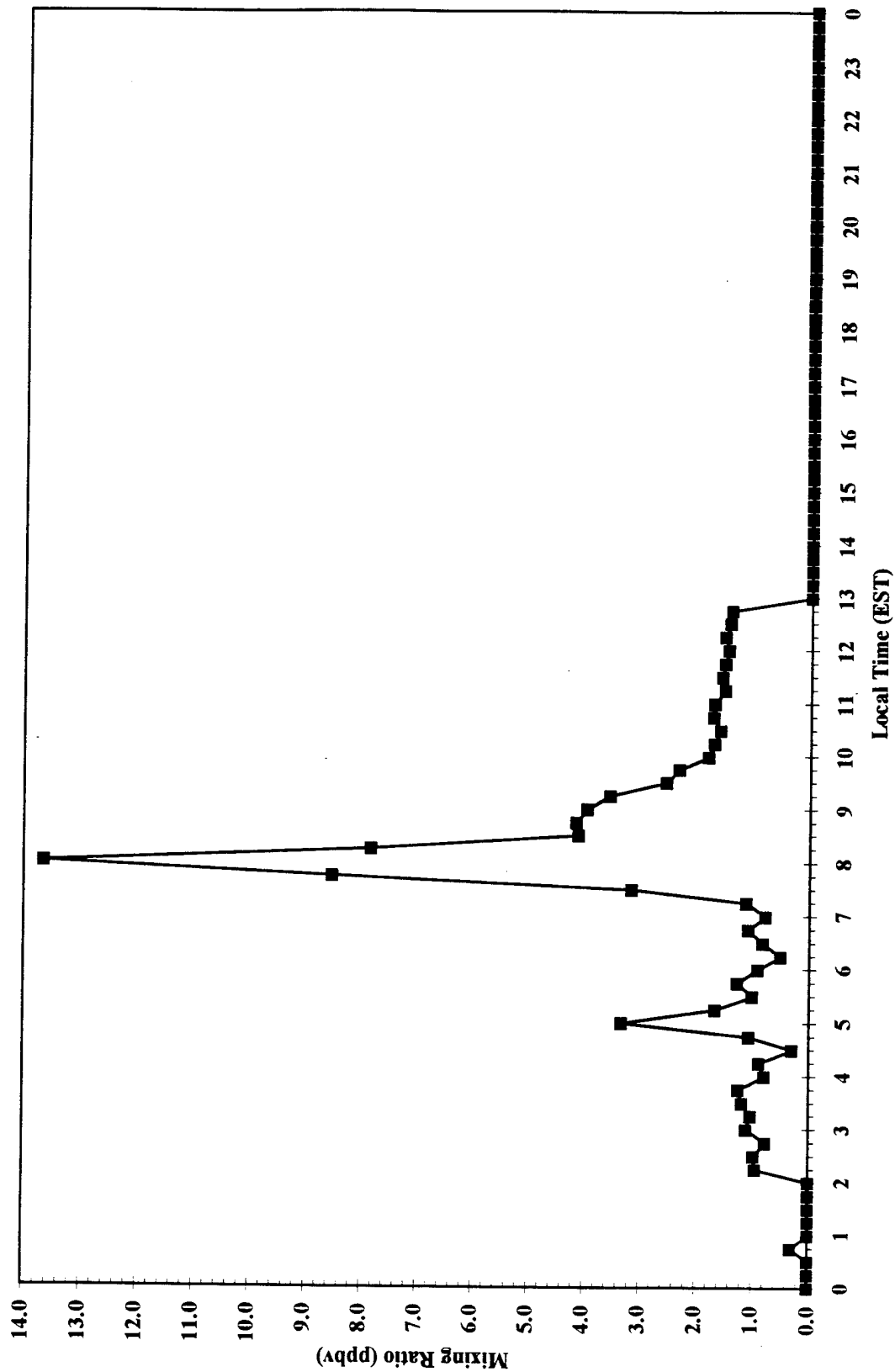


Figure 4.18c Diurnal Variation NO Mixing Ratio, 433 Meters (8 Dec 95)

4.4.2.2 9 Dec 94

The GSO upper air sounding at 0600 EST (Figure 4.19a) indicates a possible moderately stable boundary layer (skies were partly cloudy during the night with winds 3-9 kts) to a height of 80 m, with a weak inversion in the residual layer. The NCSU upper air sounding from the agricultural field site at 0845 EST (Figure 4.19b) indicates that the mixed layer had only reached a height of approximately 150 m at that time. Another NCSU sounding at 1030 EST (Figure 4.19c) shows that the mixed layer had only reached a height of about 230 m. In other words, the mixed layer had not yet reached the height of the NO-NO_y analyzer, located at 433 m, by 1030 EST. The instrument did not measure appreciable amounts of NO up to that point in time; in fact the instrument did not measure NO mixing ratios above the instrument detection limit (0.23 ppbv) until 1230 EST (Figure 4.19d), or about the time the slowly rising mixing layer would have been expected to reach the height of the instrument. NO_y mixing ratios were not recorded on this date.

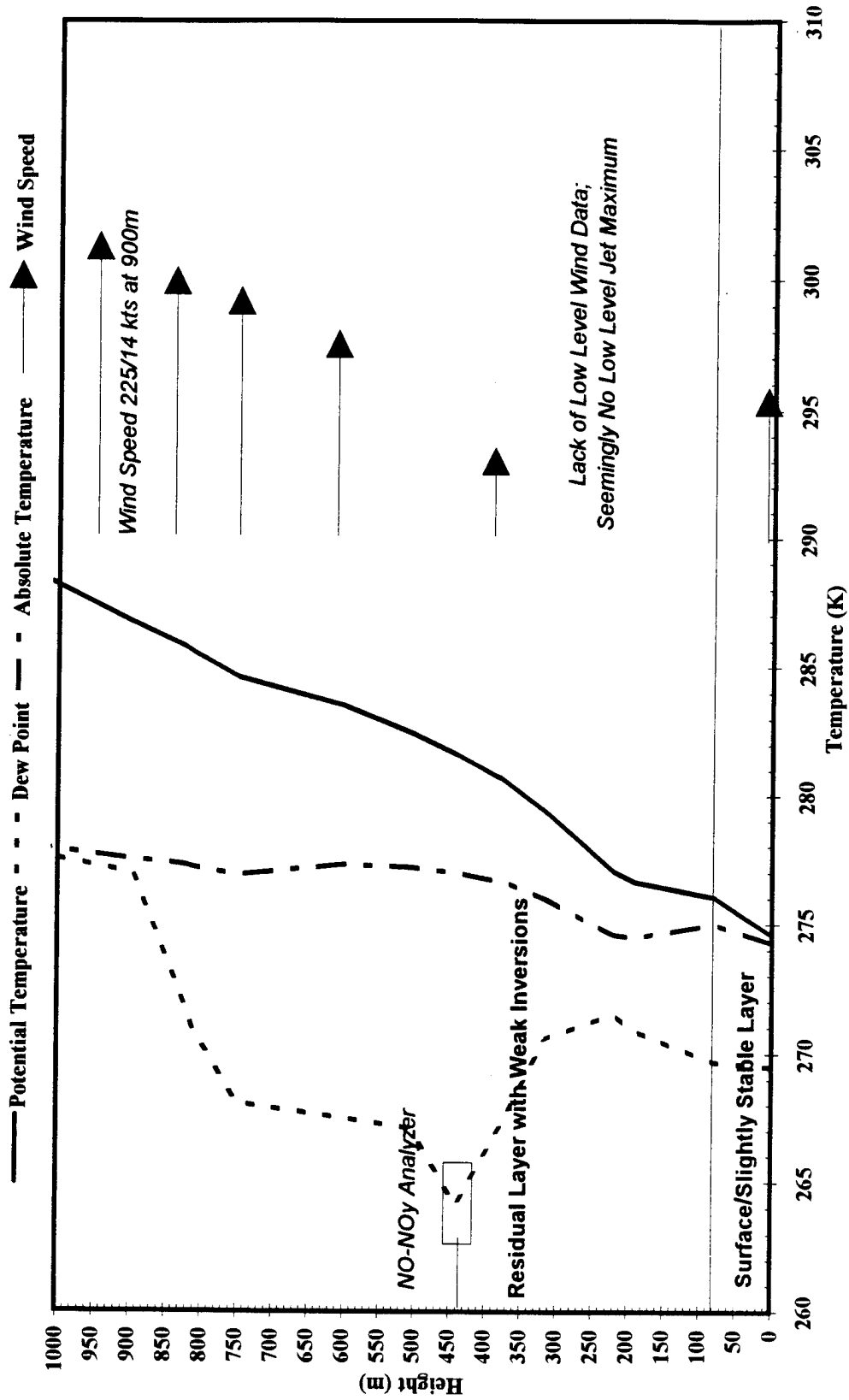


Figure 4.19a Greensboro, NC NWS Upper Air Sounding - 9 Dec 94 (0600 EST)
(Arrows show relative wind speed at that height)

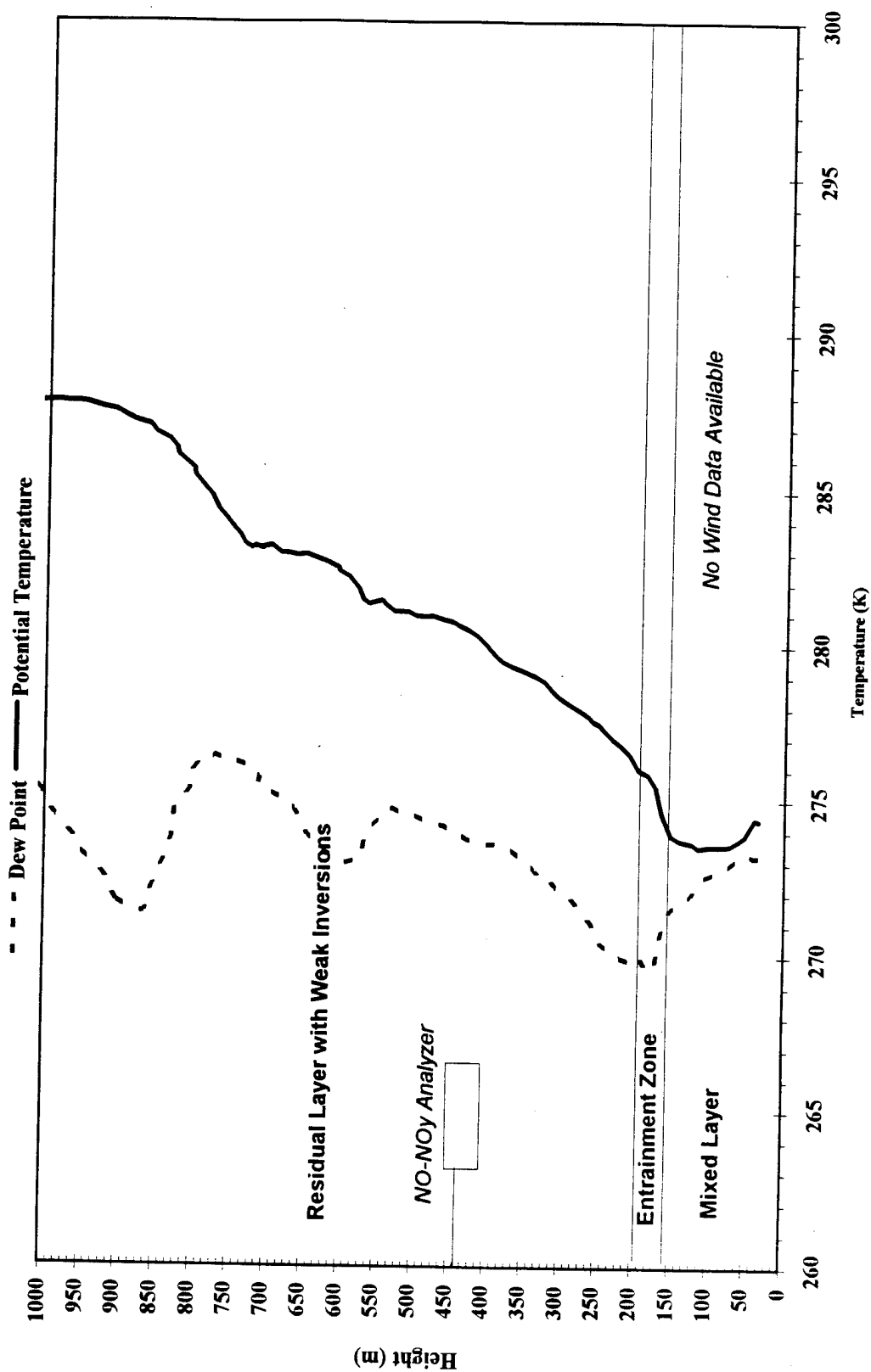


Figure 4.19b NCSU Upper Air Sounding - 9 Dec 94 (0845 EST)

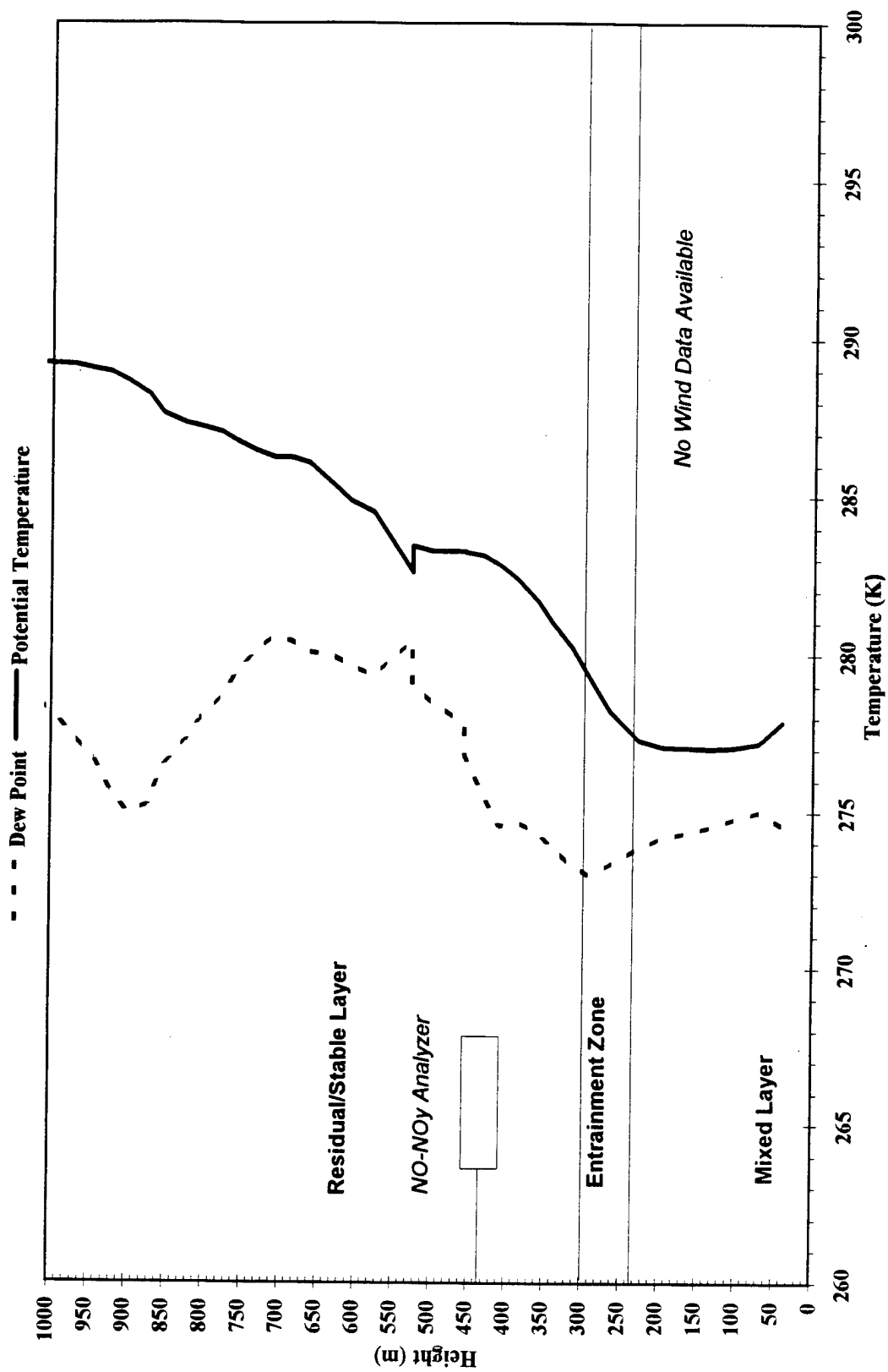


Figure 4.19c NCSU Upper Air Sounding - 9 Dec 94 (1030 EST)

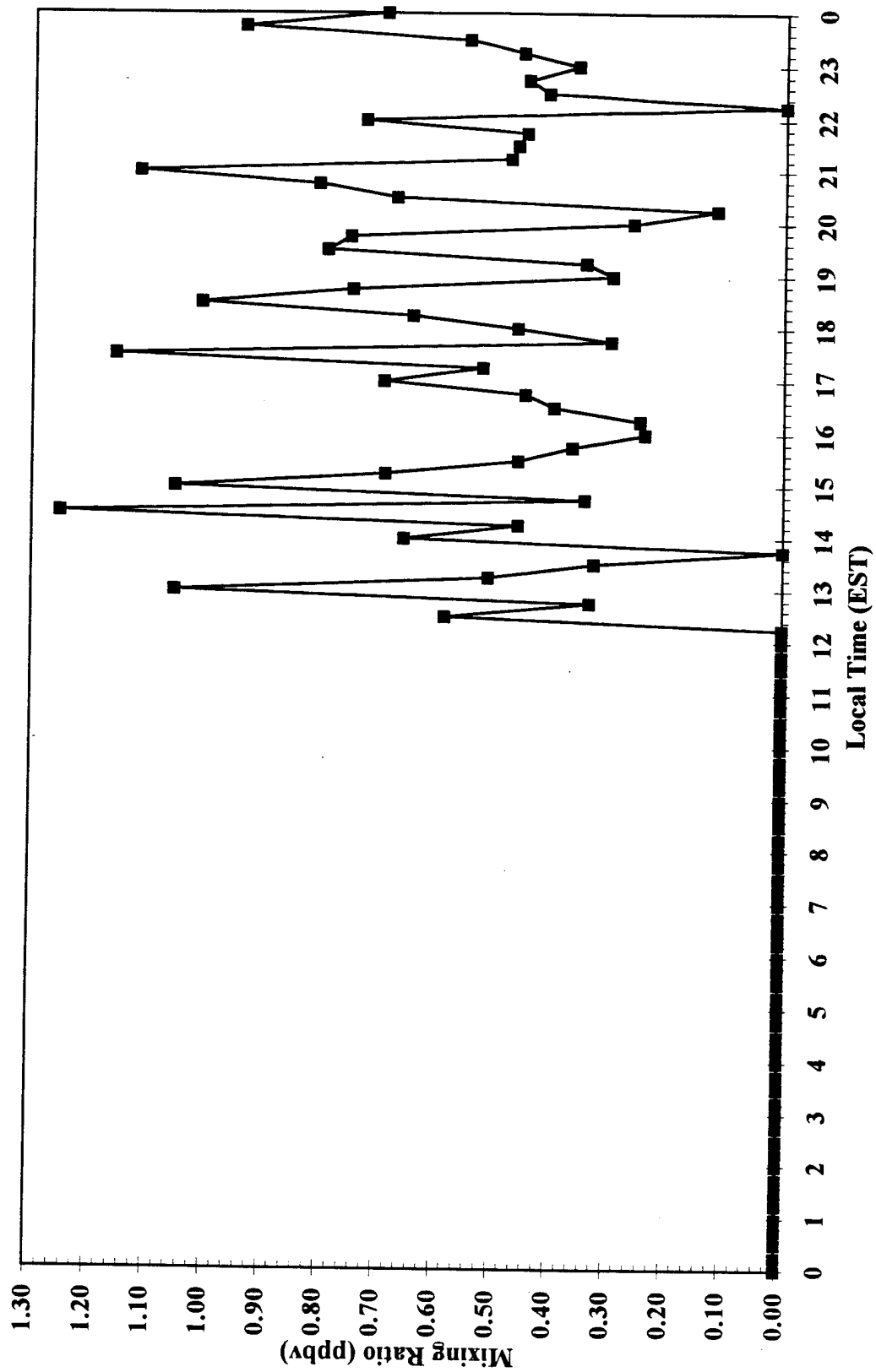


Figure 4.19d Diurnal Variation NO Mixing Ratio, 433 Meters (9 Dec 94)

4.4.2.3 13 Dec 95

GSO upper air sounding (Figure 4.20a) indicates a lack of any definite layers except for a residual layer that contained weak to moderate inversions (skies were mostly cloudy with winds of 5 - 10 kts overnight, and a strong stable boundary layer was expected to develop). The NCSU sounding from the agricultural field site at 0815 EST (Figure 4.20b) shows that the mixed layer had risen to about 310 m by that time. Another NCSU sounding at 0915 EST (Figure 4.20c) shows a mixed layer height of about 340 m, or an increase in the height of the mixed layer of only about 30 m in 60 minutes. The NO mixing ratios measured at 433 m did not rise above the instrument detection limits (0.23 ppbv) at any point during the morning or afternoon of 13 Dec 94; it is possible that due to the heavy overcast and strong cold advection from the northeast (temperatures remained steady in the mid 30s throughout the day), the mixed layer never reached the height of the instrument (and subsequently never transported any NO upward to the instrument for detection). NO_y mixing ratios were not recorded on this date.

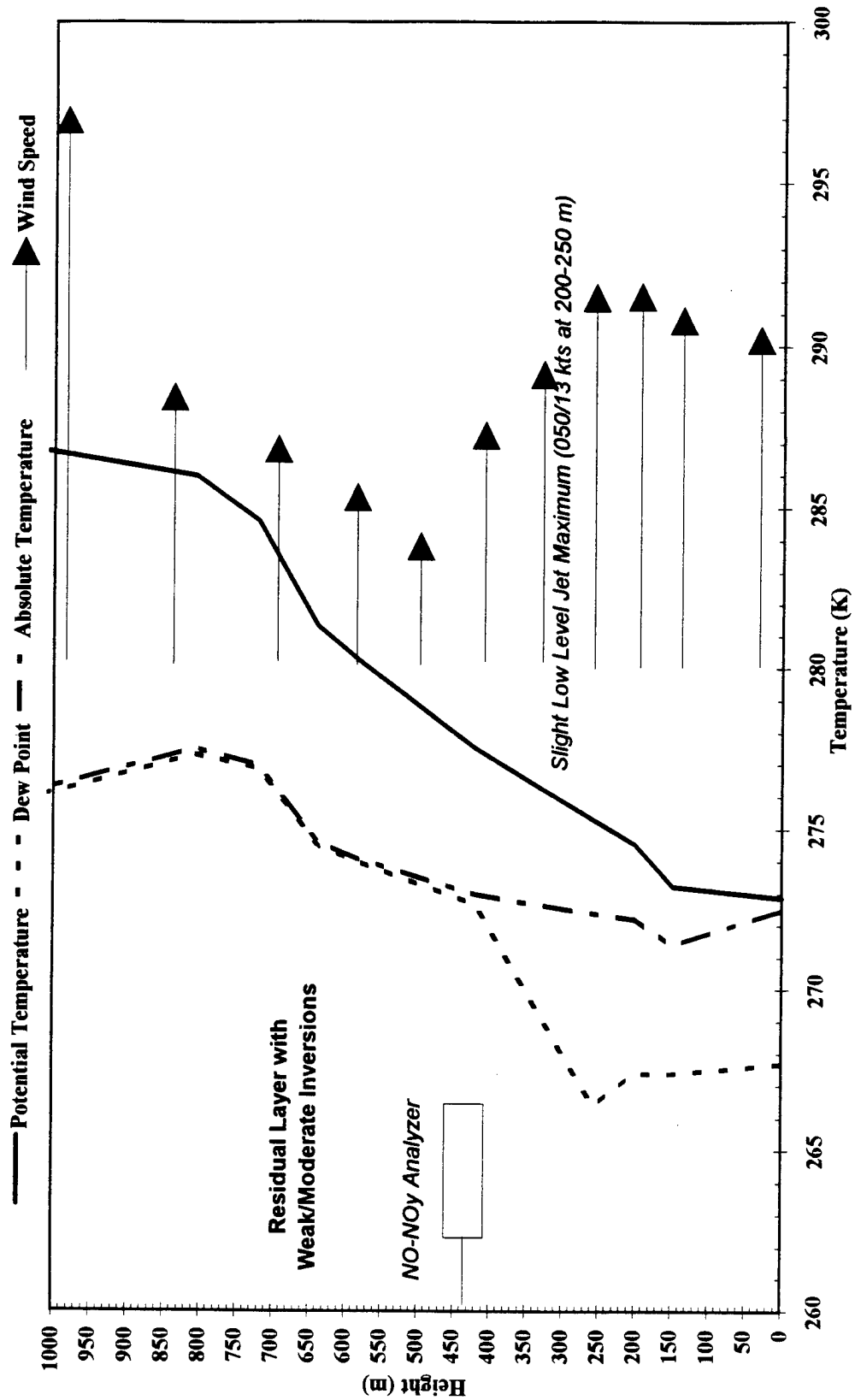


Figure 4.20a Greensboro, NC NWS Upper Air Sounding - 13 Dec 94 (0600 EST)
 (Arrows show relative wind speed at that height)

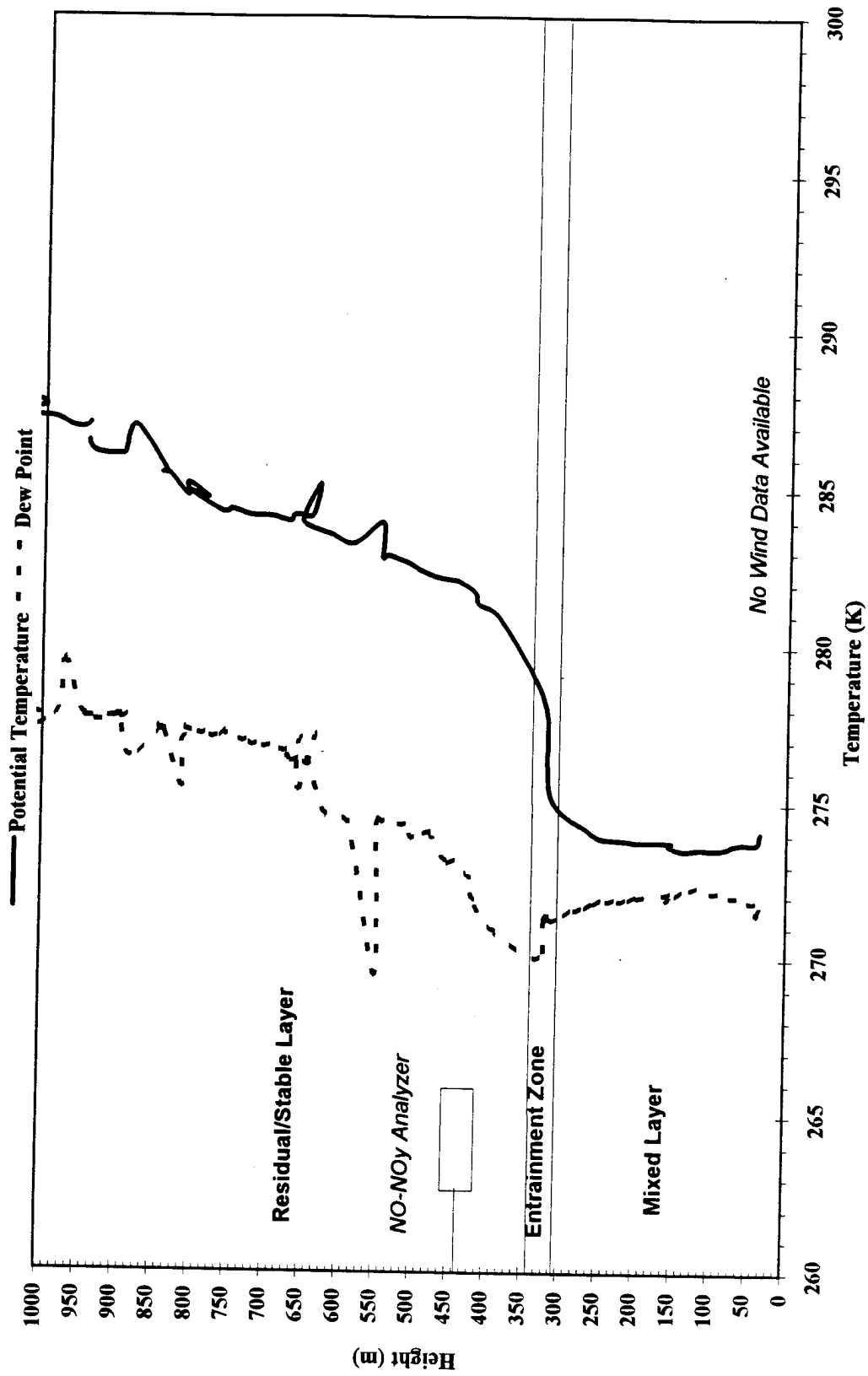


Figure 4.20b NCSU Upper Air Sounding - 13 Dec 94 (0815 EST)

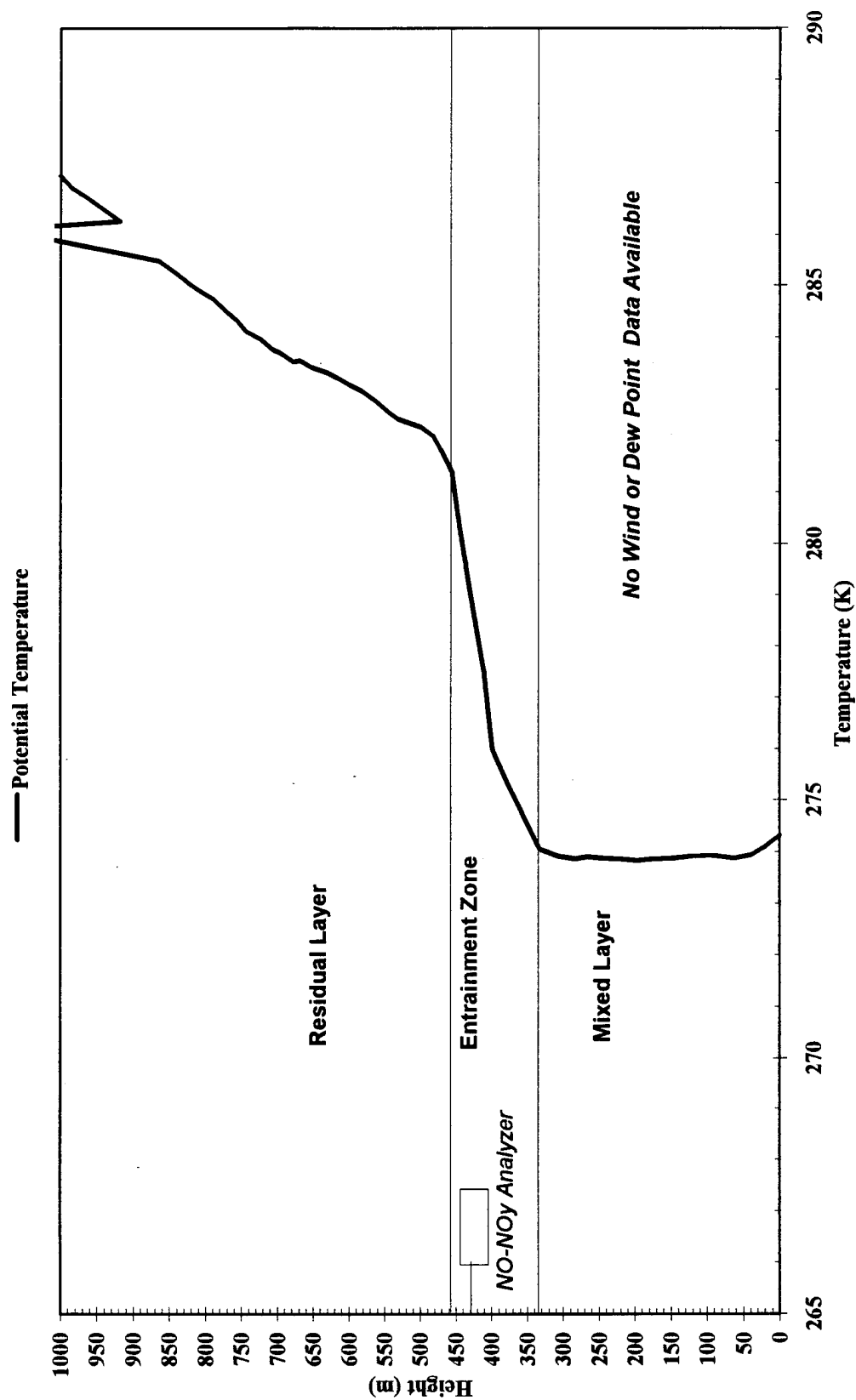


Figure 4.20c NSCU Upper Air Sounding - 13 Dec 95 (0915 EST)

4.4.2.4 18 Jan 95

The GSO upper air sounding at 0600 EST (see Figure 4.13) indicates a stable boundary layer to a height of 240 m (skies were mostly clear with light winds during the night, leading to possible strong SBL development) and a residual layer above the SBL. The NCSU sounding from the Jordan Hall site at 1030 EST (Figure 4.21a) indicates that the mixed layer had only reached a height of about 220 m by that time. Mixing ratios measured at 433 m (Figure 4.21b) showed NO values below instrument detection limits (0.04 ppbv) and NO_y values near nocturnal minimum until 1145 EST. The NO mixing ratios reached a maximum diurnal peak at 1215 EST, and NO_y mixing ratios followed with a peak at 1230 EST (both at about the time the slow moving mixed layer would have reached the 433 m height).

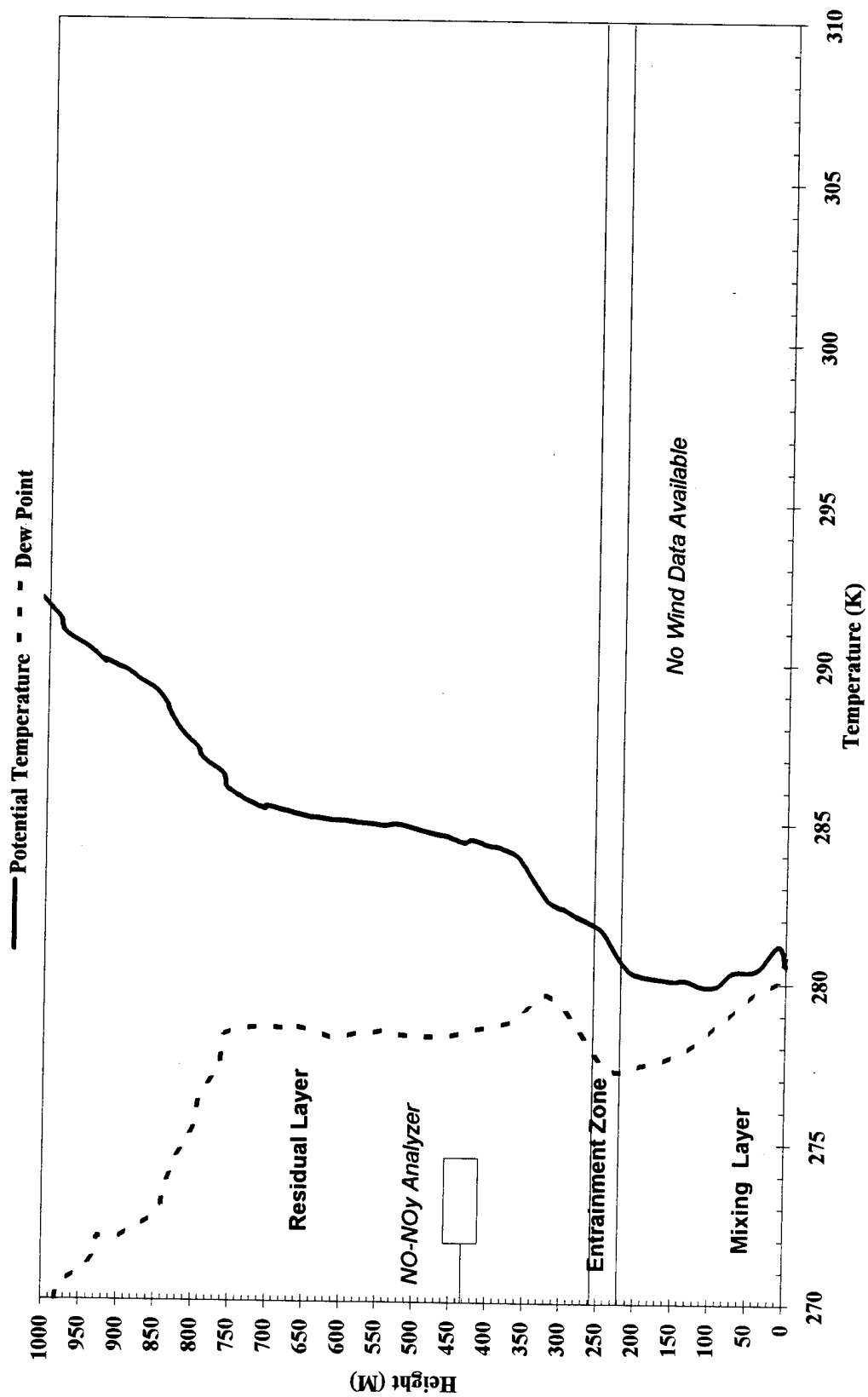


Figure 4.21a NCSU Upper Air Sounding - 18 Jan 95 (1030 EST)

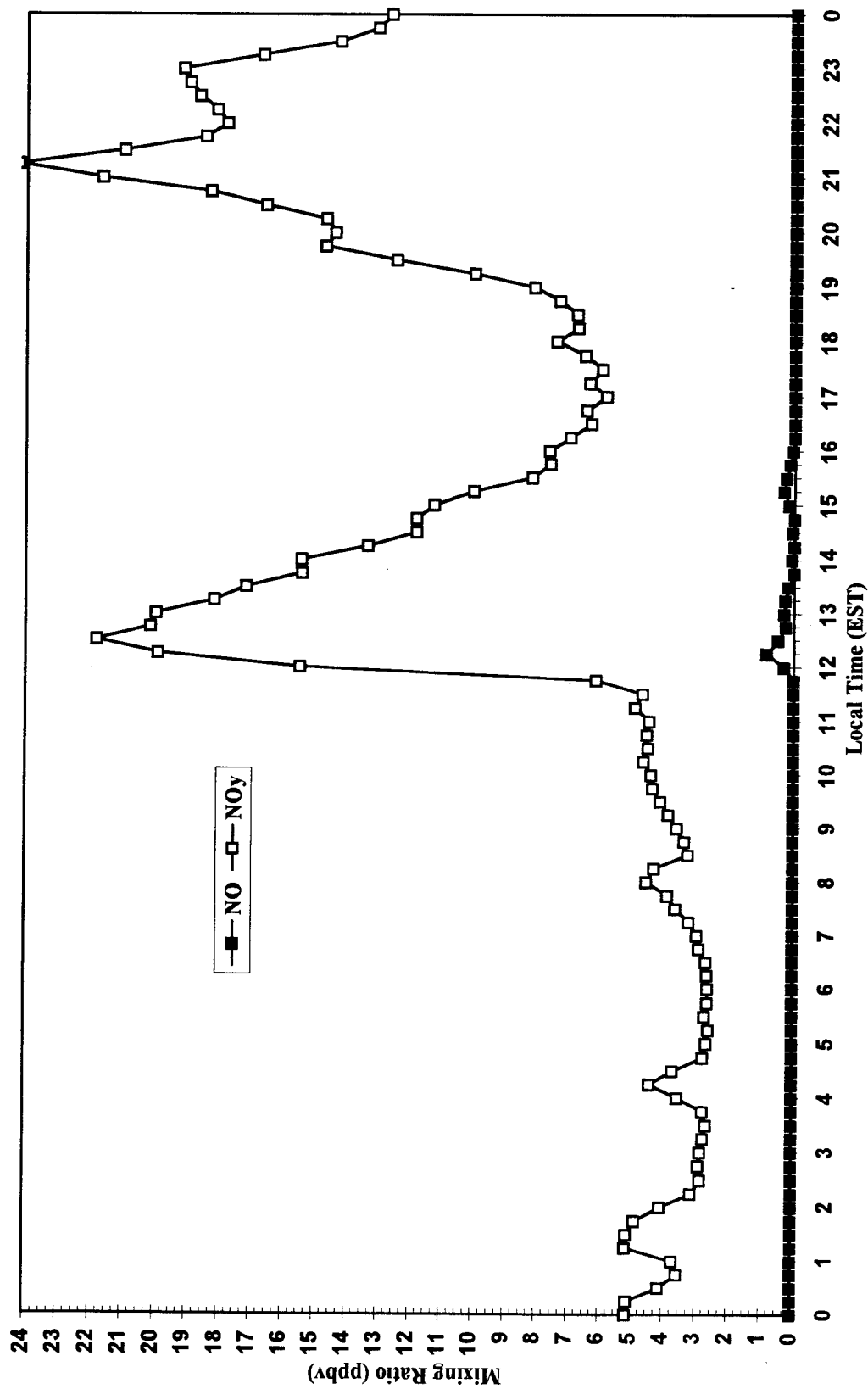


Figure 4.21b Diurnal Variation NO and NO_y Mixing Ratios, 433 Meters (18 Jan 95)

4.4.2.5 25-26 Jan 95

The NCSU upper air sounding from the Jordan Hall site for 26 Jan 95 (Figure 4.22a) indicates that by 0915 EST, the mixed layer had reached a height of about 430 m. A second NCSU sounding at 1015 EST (Figure 4.22b) shows that the mixed layer had reached a height of approximately 550 m at that time (the GSO 0600 EST sounding was not available). Thus the mixed layer passed the height of the instrument (433 m) between 0915 and 1015 EST. While mixing ratios of NO and NO_y were not recorded on 26 Jan, they were recorded on 25 Jan; conditions for both days under the influence of a high pressure to the south were very similar with respect to sky cover, winds, and temperatures. Mixing ratios for NO rose above the instrument detection limit (0.04 ppbv) at 0945 EST and reached a diurnal peak at 1200 EST. The NO_y mixing ratios rose abruptly between 0900 and 0945 EST from their nocturnal minimum, reaching a local maximum; further increases lead to the diurnal maximum at 1200 EST (Figure 4.22c). Thus, in this case the NO and NO_y mixing ratios began to increase from their nocturnal minimums at the time of possible passage of the top of the mixed layer past the instrument.

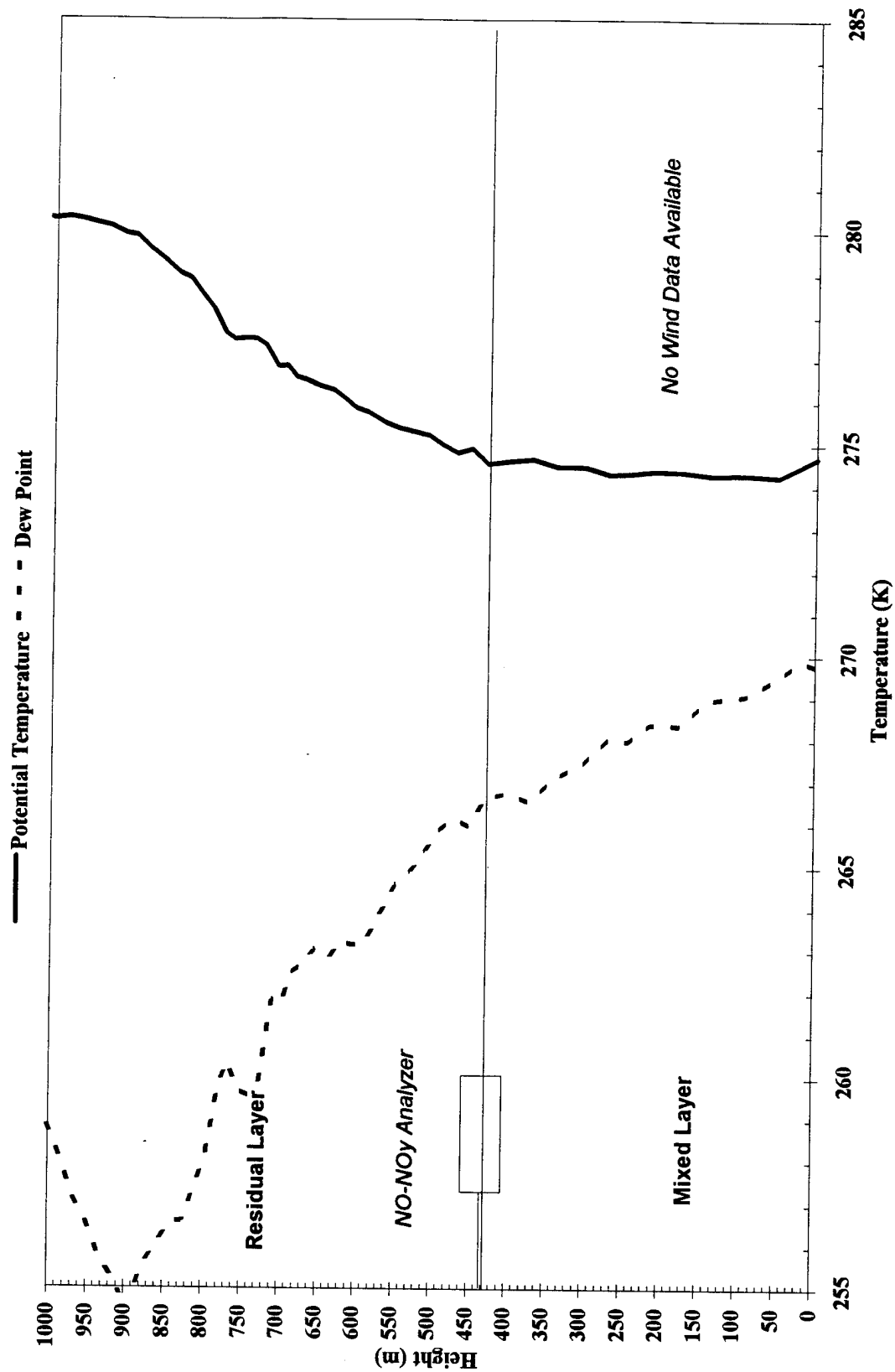


Figure 4.22a NCSU Upper Air Sounding - 26 Jan 95 (0915 EST)

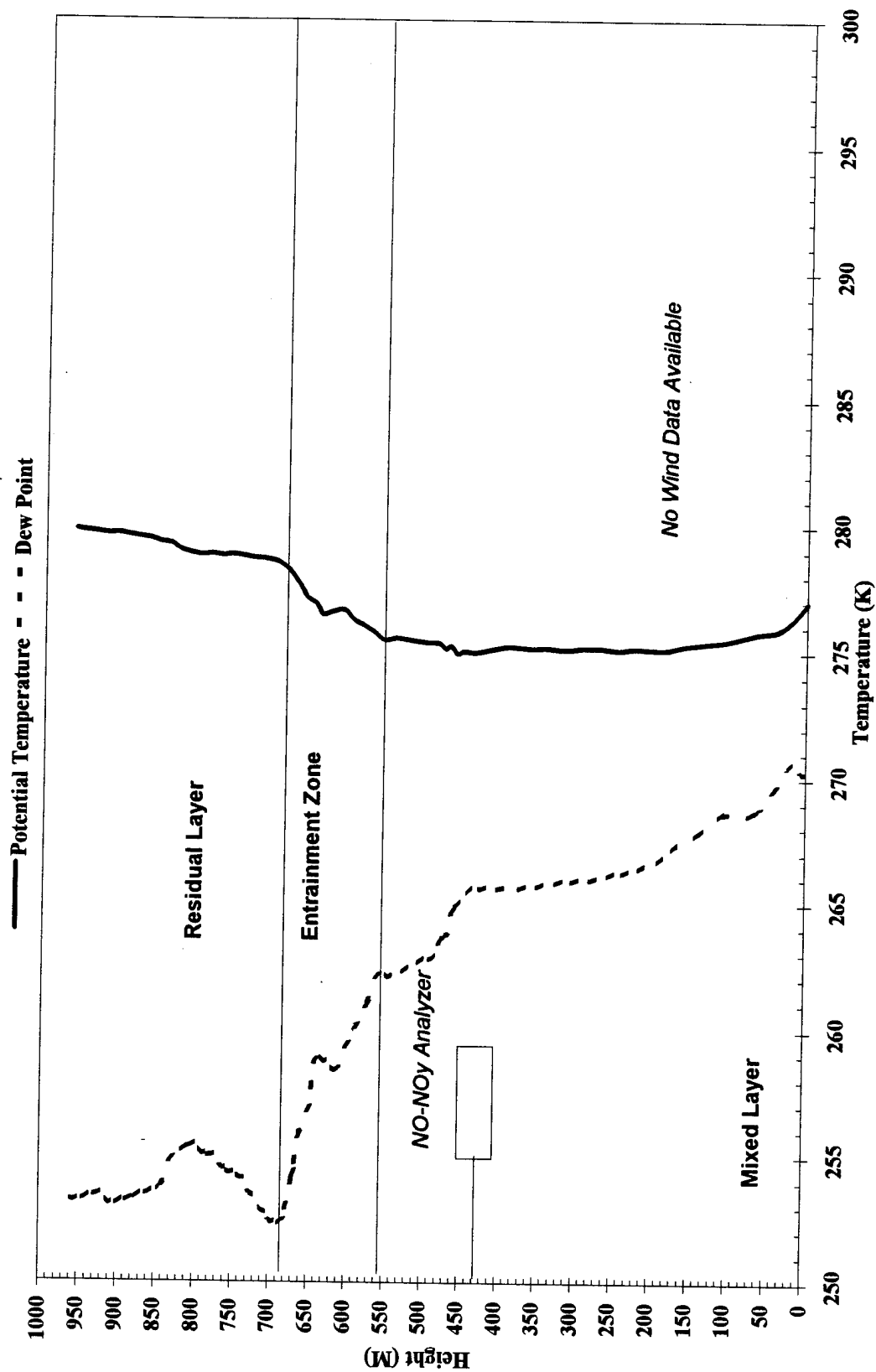


Figure 4.22b NCSU Upper Air Sounding - 26 Jan 95 (1015 EST)

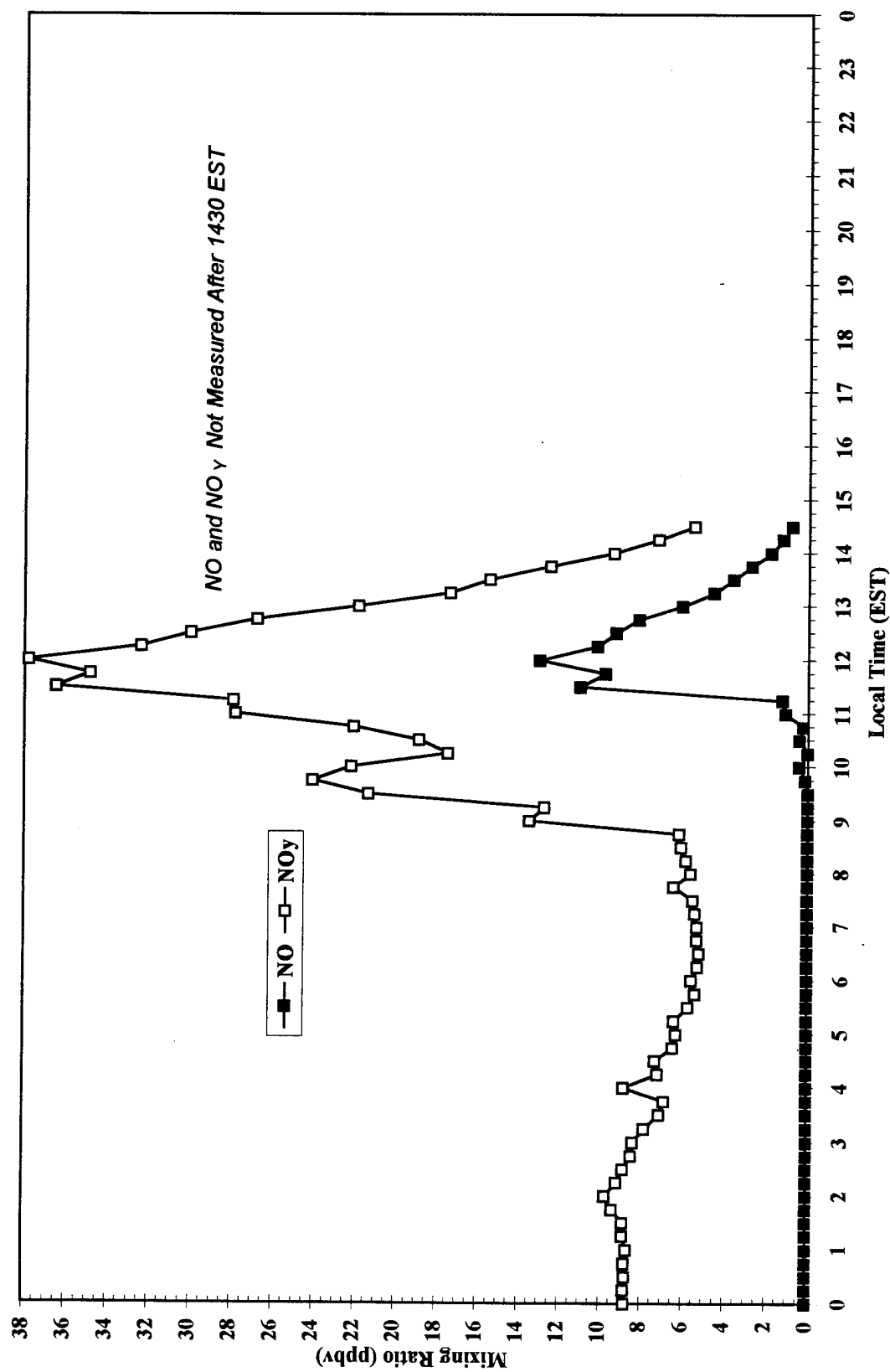


Figure 4.22c Diurnal Variation NO and NO_y Mixing Ratios, 433 Meters (25 Jan 95)

4.4.2.6 9 Feb 95

The GSO upper air sounding for 9 Feb 95 (Figure 4.23a) shows an absence of a definite stable boundary layer (skies were clear overnight but gusty winds and the passage of trough did not favor development of a strong stable layer). The NCSU upper air sounding from the Jordan Hall site at 0800 EST (Figure 4.23b) shows that the mixed layer had reached height of nearly 300 m at that time. NO mixing ratios measured at 250 m rose above the instrument detection limit (0.04 ppbv) at 0730 EST, reaching a diurnal peak at 0745 EST; NO_y mixing ratios also began rising above the nocturnal minimum at 0730 EST, and like NO, reached its diurnal peak at 0745 EST (Figure 4.23c).

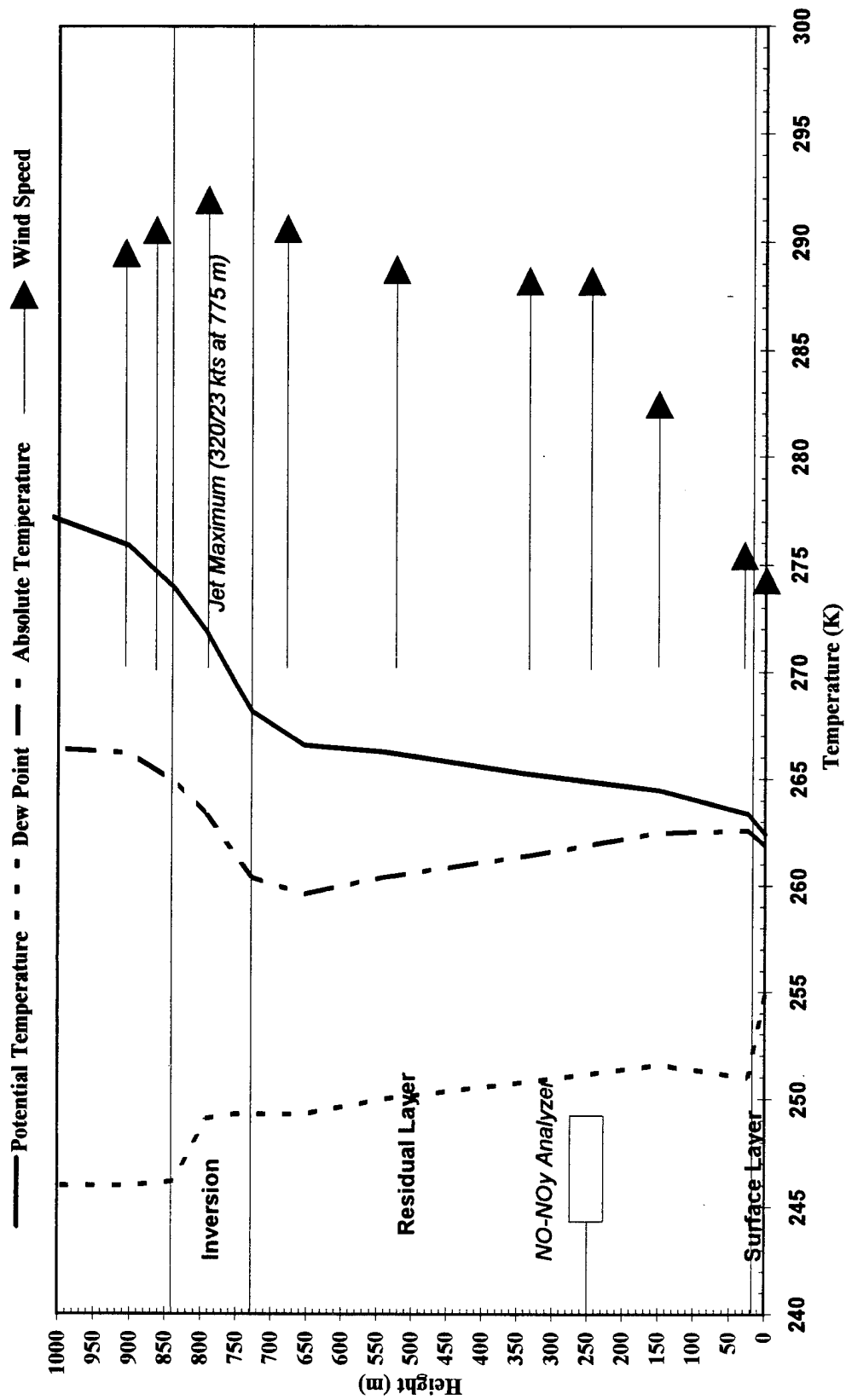


Figure 4.23a Greensboro, NC NWS Upper Air Sounding - 9 Feb 95 (0600 EST)
(Arrows show relative wind speed at that height)

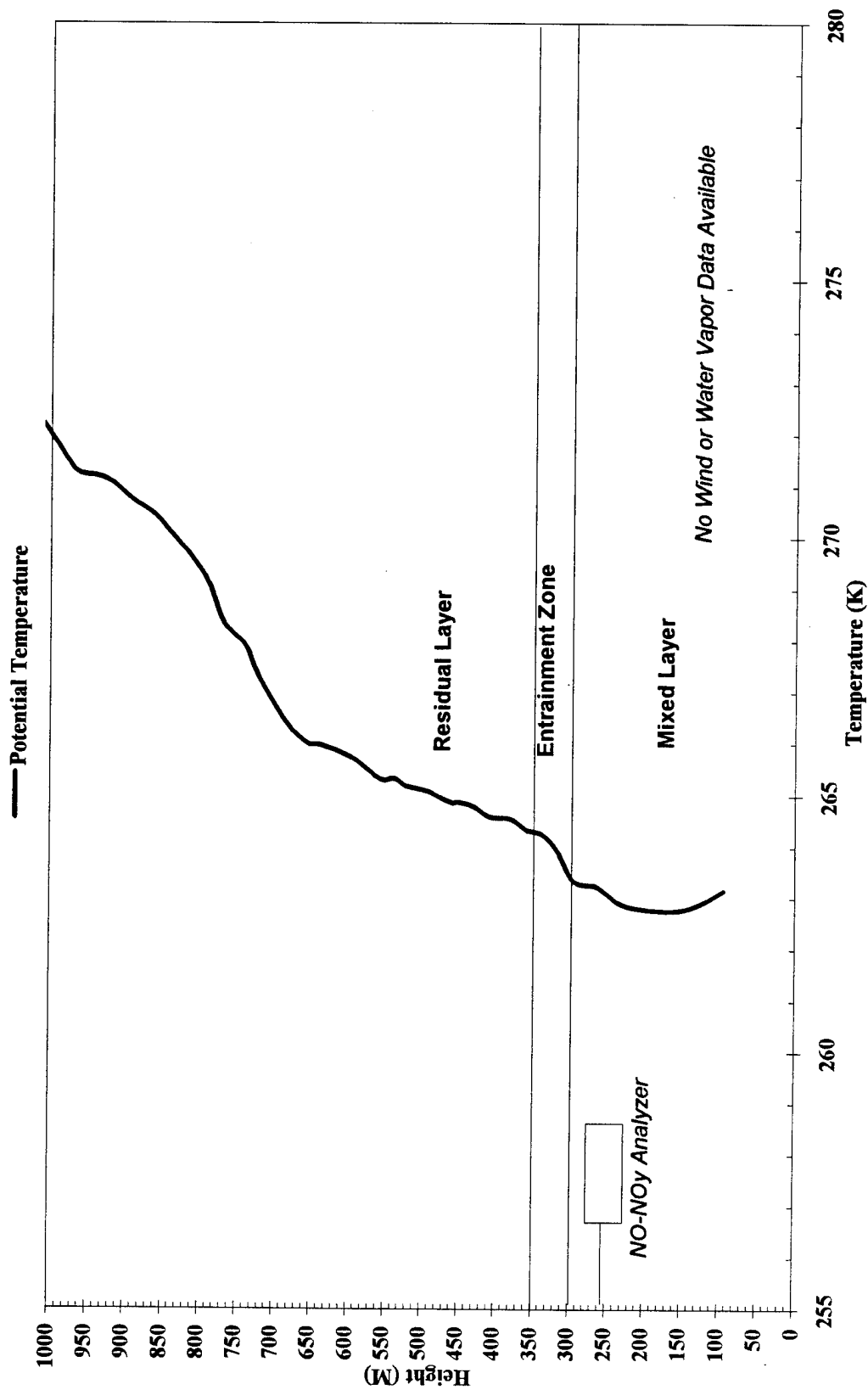


Figure 4.23b NCSU Upper Air Sounding - 9 Feb 95 (0800 EST)

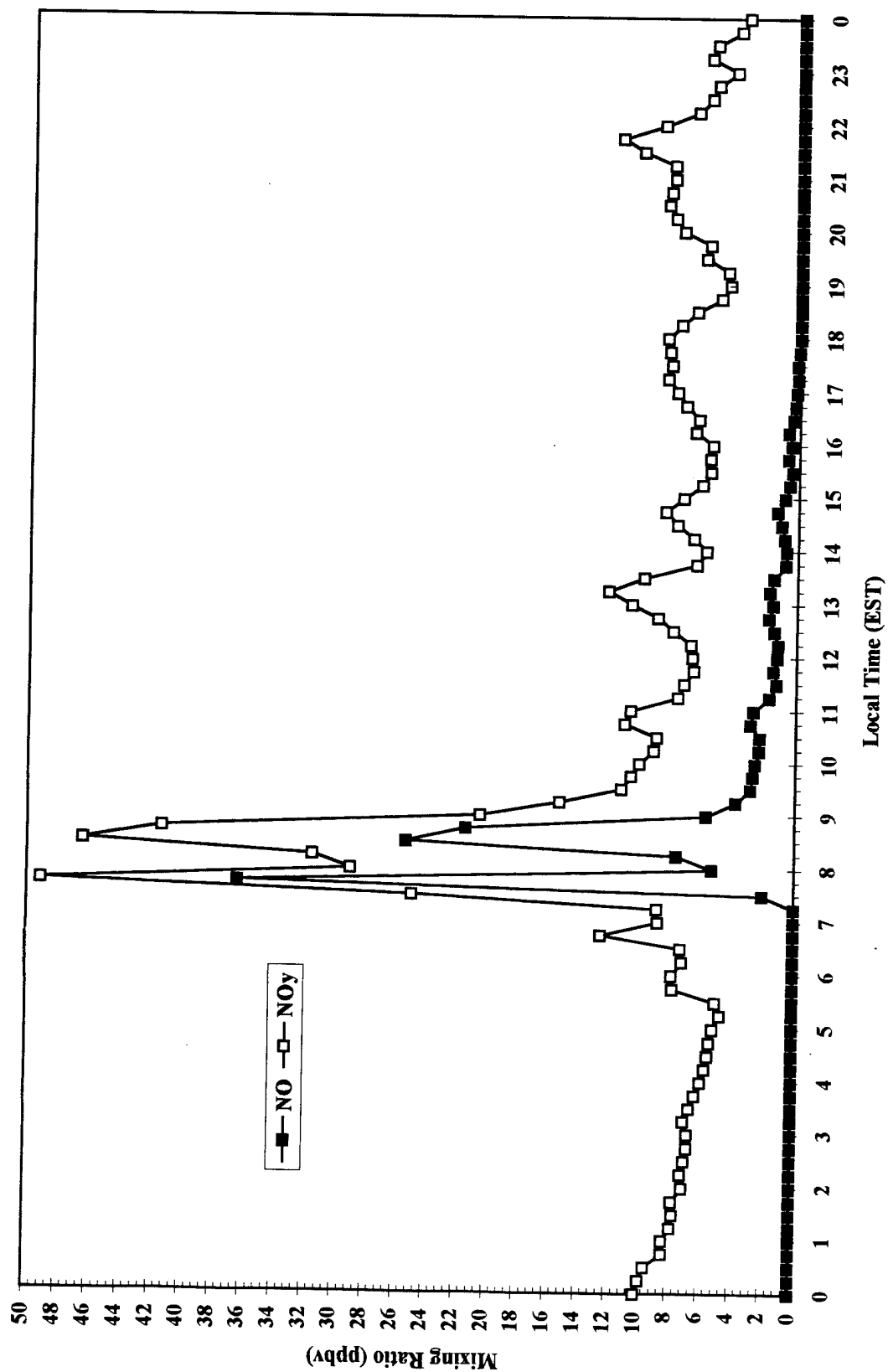


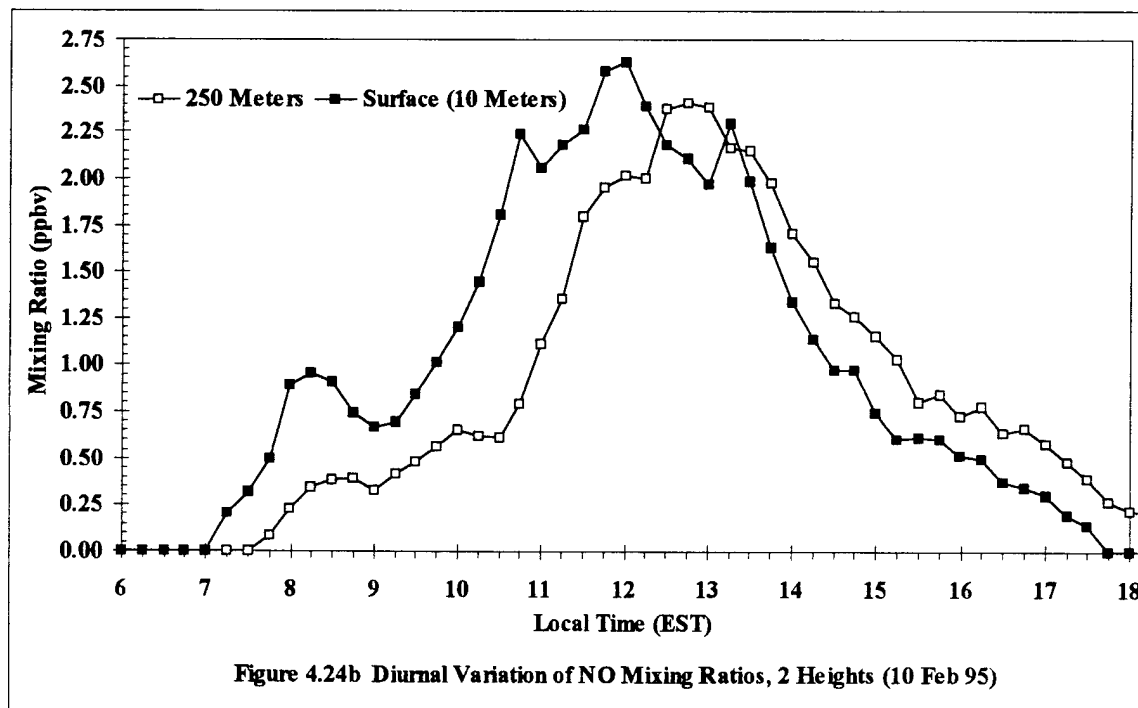
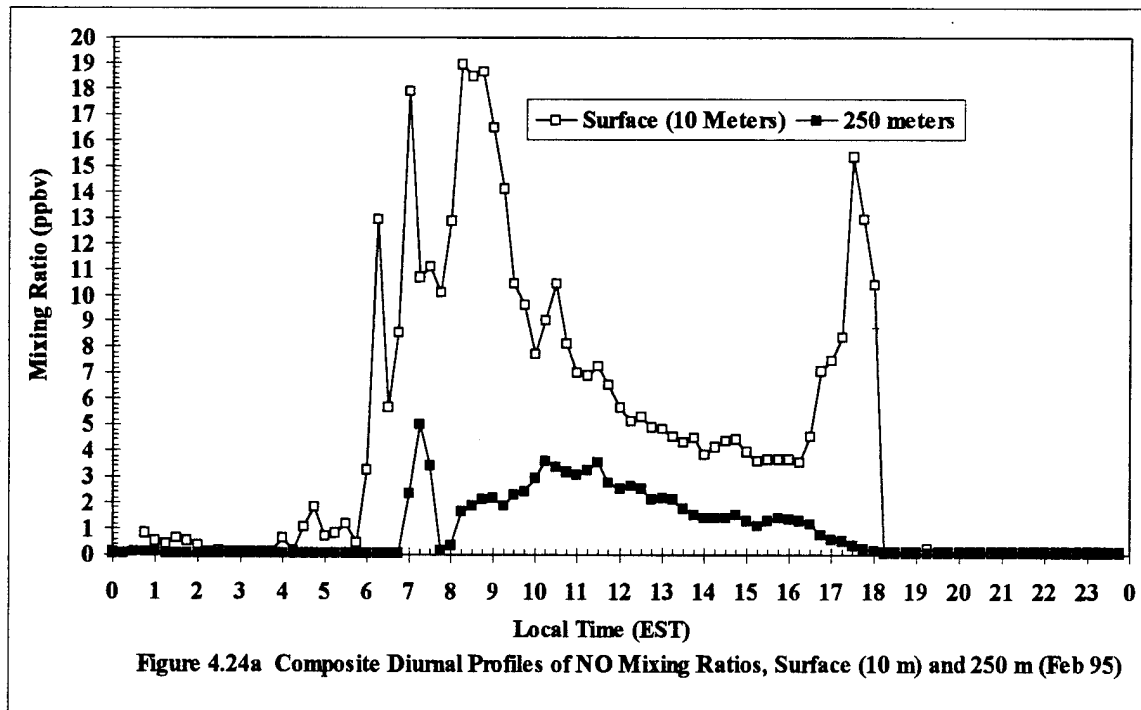
Figure 4.23c Diurnal Variation NO and NO_y Mixing Ratio, 250 Meters (9 Feb 95)

4.4.2.7 Mixed Layer Formation Discussion

In general, these results indicate that the time of the diurnal peak of the mixing ratios of NO and NO_Y measured on the tower is dependent on the rate of growth of the mixed layer during the morning hours. Specifically, mixing ratio values measured at 250 and 433 m are usually at a minimum *before* the mixed layer reaches that height, and do not reach a peak until *after* the mixed layer has reached or surpassed that height. These results lead to the conclusion that in these cases, NO and NO_Y were mixed upward from the surface to the elevated heights, as opposed to being mixed down.

4.4.3 Surface Comparison

Since it is hypothesized that the increase in mixing ratios of NO at 250 and 433 m is due to the mixing upward of NO from the surface, it is necessary to determine if there is enough NO present at the surface to provide for the increase aloft (NO_Y was not measured at the surface). Although the overall increasing gradient of NO towards the surface was discussed in a previous section, some attention is paid here to more specific cases. For example, Figure 4.24a shows a comparison between the mean diurnal variation of the NO mixing ratio at the surface and at 250 m. While the data is somewhat skewed at the surface due to the close proximity of the highway, a pattern is evident in which NO mixing ratios at the surface begin to rise much sooner in the morning than those at 250 m, adding to the premise that NO is mixed upward. By midday, however, the boundary layer has become more well mixed due to the convective eddies, and the two mixing ratios come much closer together in terms of magnitude and profile.



Near sundown and the time of the evening rush hour, the profiles change dramatically: the surface measurements increase abruptly in response to the rush hour emissions before dropping below the instrument detection limit. However the 250 m measurements do not show this abrupt increase but instead immediately begin to drop off below the instrument detection limit by sunset. Evidently as the convective eddies begin to lose some of their turbulent momentum with the loss of the sun's radiant energy, less NO is transported upward to the instrument. To reduce the difference in morning magnitudes attributable to the proximity of traffic at the surface, Figure 4.24b shows a comparison of the diurnal variation of the NO mixing ratios on 10 Feb 95 at the two heights. Since winds were out of the south on this date, values at both heights were much less affected by local traffic emissions, and the magnitudes of the values at both heights are reflective of this fact. Furthermore, both profiles are within good agreement with each other, but still indicate that surface mixing ratios increase before mixing ratios at 250 m during the early morning hours.

4.4.4 Boundary Layer Formation and Vertical Transport Processes Summary

The data presented here shows that NO and NO_y mixing ratios measured at the 250 and 433 m heights follow a general diurnal trend, with a daily minimum occurring during the night for NO mixing ratios and just before sunrise for NO_y mixing ratios. A comparison with the boundary layer structure just before sunrise confirms the supposition that there is not enough NO and NO_y conserved in the residual layer to be mixed

downward upon breakup of the nocturnal inversion. In fact, the daily maximum in NO and NO_y mixing ratios that occurs on an irregular basis between 0700 and 1200 EST is closely related to the growth of the mixed layer. It is hypothesized that this diurnal peak is dependent on the transport of NO and NO_y upward from the surface with the growth of the mixed layer. In effect, as the rate of the growth of the mixed layer varies due to differences in nocturnal boundary layer stability and/or daytime heating, the time at which the NO and NO_y mixing ratios show a daytime peak at the two heights on the tower also varies.

4.5 Atmospheric Chemistry and Horizontal Transport

Apart from the previously discussed comparisons of synoptic and diurnal vertical boundary layer processes, two other factors, in-situ atmospheric chemistry and horizontal transport (or advection), play a part in the variation of mixing ratios of NO and NO_y within the planetary boundary layer. The scope of this study did not provide for in depth analysis of these factors and their association with the measured values of NO and NO_y mixing ratios; however some general statements relating NO and NO_y mixing ratios to these processes are discussed in the following sections for completeness.

4.5.1 NO Mixing Ratios

4.5.1.1 Atmospheric Chemistry

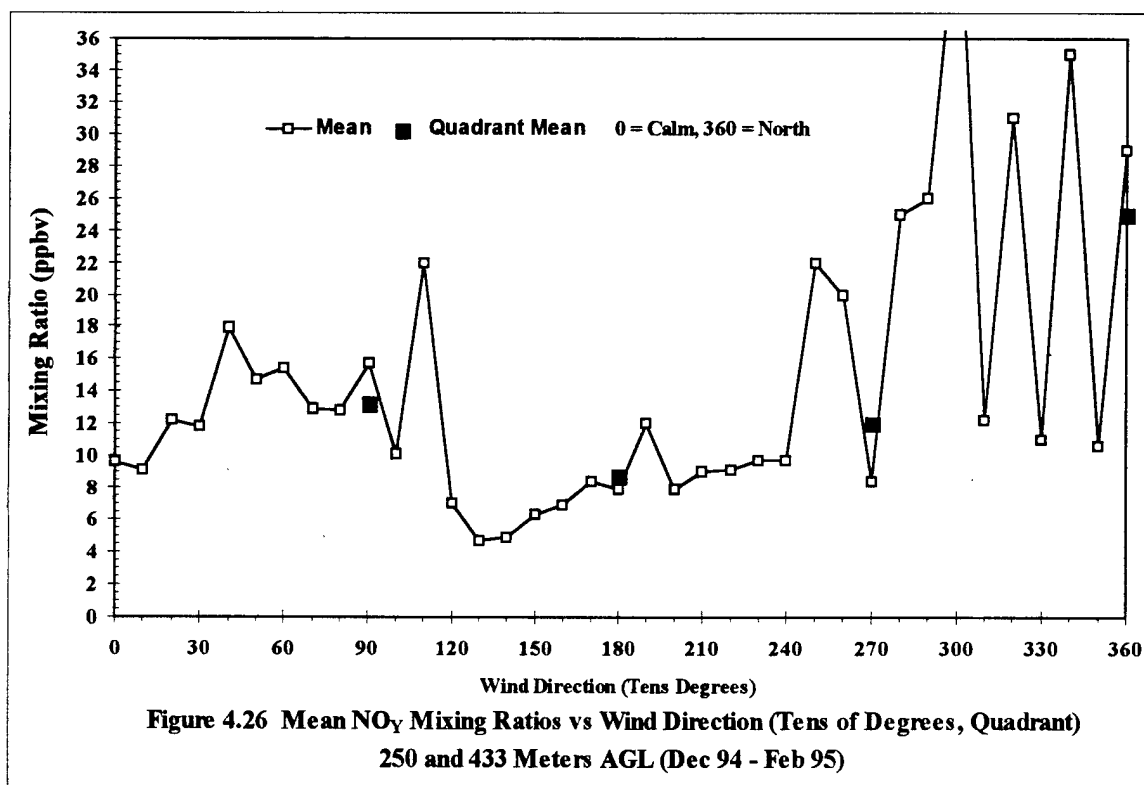
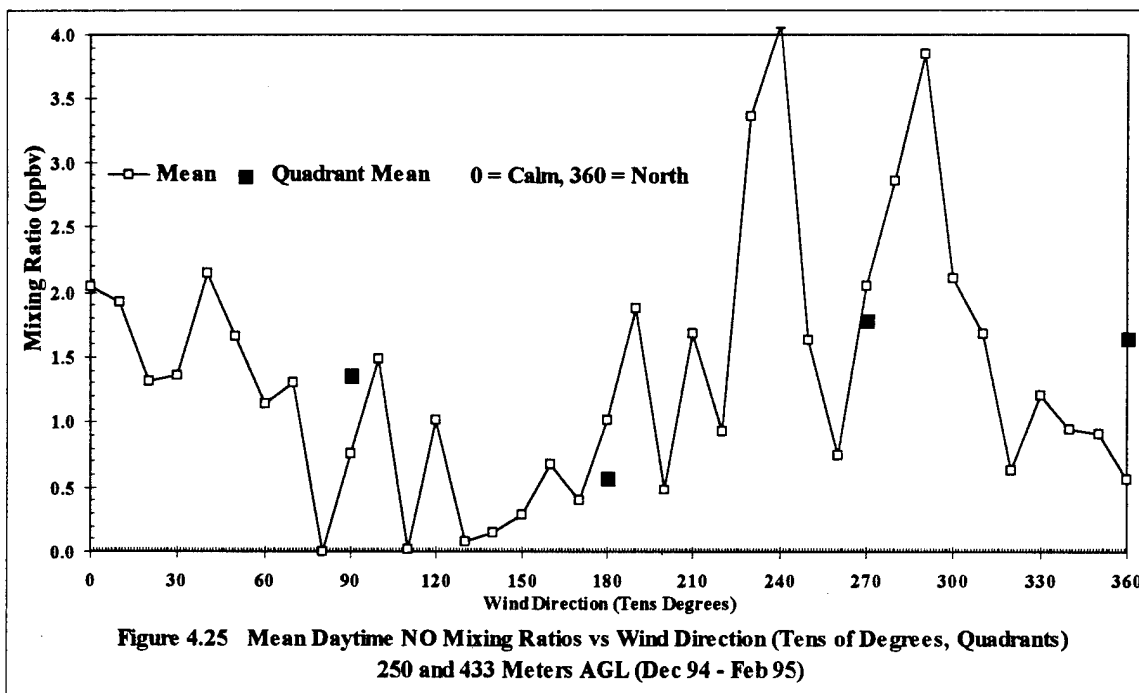
The observed diurnal variation in mixing ratios of NO during this study were consistent with the nocturnal atmospheric chemistry of NO. The titration of NO by residual ozone and by the OH radicals during the nighttime would be expected to lead to low or non-existent mixing ratios of NO [Finlayson-Pitts and Pitts, 1986, and Warneck, 1988]. In contrast, those photochemical processes involving NO and therefore initiated by the rising of the sun, were not identifiable in this study. However, some of the small increases or decreases in NO mixing ratios, noted in certain cases soon after the rise of the boundary layer, may be related to photochemical production or destruction.

4.5.1.2 Horizontal Transport

As with atmospheric chemistry, horizontal transport of NO did not seem to play an identifiable role in controlling the increase or decrease of NO mixing ratios at various heights in the boundary during this study. This is due in part to the fact that NO is a source species, and is at its highest mixing ratio near the source. As it is transported away from the source, it is oxidized to the other members of the NO_Y family, and its mixing ratio levels drop. In this study, the effect of transport of NO upward (via the previously

discussed vertical boundary layer processes) from its local source (the adjacent highways) seems to be overwhelming detection of NO transported by more distant sources at the two heights on the tower.

A comparison of surface wind direction with surface NO mixing ratio measurements is heavily skewed by the close proximity of US-70 so that the correlation is subsequently highest when the winds are off the highway. This is an indicator of the dominance of local horizontal transport of NO at the surface. An example of the longer range horizontal transport of NO is given by the comparison of the 250 and 433 m NO mixing ratio data with surface wind. Prevailing winds during the research period were generally westerly but were distributed throughout the 360 degree compass during the observation period (with no less than 15% of the total observations occurring in any one quadrant). Figure 4.25 shows the mean NO mixing ratios by ten degree wind direction interval as well as by 90 degree quadrant interval. As would be expected from the geography of and the location of point and area sources in North Carolina, the southeast quadrant produces the lowest mean mixing ratio as compared to the other three quadrants; an average of 63% lower for NO mixing ratios. Thus winds from the southeast, which are only several hundred miles removed from the Atlantic Ocean and its relatively cleaner air, and pass over fewer population centers and point sources, have lower mixing ratios of NO. Conversely, it is expected that winds from the northwest, which pass over several highly populated areas and point sources, would show the highest mean mixing ratios. However, comparison with NO mixing ratios does not show a quadrant preference for



highest mean mixing ratio; the northeast, southwest and northwest quadrants all show little difference in mean NO mixing ratios.

4.5.2 NO_y Mixing Ratios

4.5.2.1 Atmospheric Chemistry

In contrast to NO mixing ratios, evidence from this research indicates that the observed NO_y mixing ratios and changes therein can be related to atmospheric chemistry processes as well as boundary layer transport processes.

After peaking near 1200 EST, the mean NO_y values at 250 and 433 m begin to fall off, gradually decreasing towards the overnight minimum just before sunrise (see Figures 4.5 and 4.6). The NO_y values do not show the sharp drop-off around sunset that is characteristic of the NO profile. As indicated previously, there was a wide variation in individual diurnal NO_y profiles, with some days actually seeing increases after sunset (see Figure 4.8). This is not unexpected, given the complicated chemistry that is possible during the night involving members of the NO_y family. In particular, atmospheric chemistry seemed to play an identifiable role in the variation of NO_y mixing ratios at the elevated heights during the early morning hours just after sunrise. Specifically, the data indicates that in some cases just after sunrise, NO_y mixing ratios were already increasing from a nocturnal minimum *before* the mixed layer reached that height. For example, in the previously discussed mixing layer growth case of 18 Jan 95 (Figure 4.21c), NO_y had been

slowly rising from a minimum of 2.63 ppbv measured an hour before sunrise to a value of 4.90 ppbv measured at 1115 EST, just before the abrupt increase to 21.79 ppbv at 1230 EST attributed to the rise of the mixed layer. In the example of 9 Feb 95 (Figure 4.23c), the NO_Y mixing ratios had increased from the nocturnal minimum of 4.67 ppbv detected at 0515 EST to a value of 8.84 ppbv measured at 0730 EST, just before the abrupt increase to 49.10 ppbv at 0745 EST which is attributed to the rise of the mixed layer. The nearly 90% increase in NO_Y mixing ratios before the apparent rise of the boundary layer in these cases is likely due to chemical processes.

In these cases, NO_Y mixing ratios increased without a corresponding increase in NO mixing ratios, and therefore the increase in NO_Y must be due to increases in reactive oxides of nitrogen other than NO, such as NO_2 , PAN, HNO_3 , etc. Since conversion of one detectable NO_Y constituent to another should not lead to a change in total NO_Y mixing ratio (aside from instrument conversion efficiency differences), possible atmospheric chemistry reactions responsible for the increase in NO_Y mixing ratios are limited to processes that produce the above reactive oxides of nitrogen from non-detectable species.

Based on this premise, it is proposed that the increasing relative humidity common during the nocturnal hours leads to destruction of HNO_3 by its conversion to particulate NO_3^- (which is not detected by the NO_Y instrument due to its absorption by the Teflon filter), and thus results in the decrease in the overall measured NO_Y mixing ratios just before sunrise. After sunrise the relative humidity begins to fall as the troposphere is warmed, leading to an equilibrium shift from NO_3^- back to HNO_3 , which is then

converted and measured by the instrument; the result is the increase in NO_Y mixing ratios discussed above. Prior observations of NO_3^- , HNO_3 , and the ratio between the two over semi-rural to urban areas indicate they exist in high enough concentrations and mixing ratios to make this hypothesis viable for the observed increases in this particular study [Warneck, 1988, and reference therein]. Further conclusions concerning the relative magnitude of this process in relation to the observed increase in NO_Y during this study are not possible due to the lack of measured NO_3^- data.

4.5.2.2 Horizontal Transport

NO_Y is composed of source species as well as source species that have been oxidized, and as such can be measured much farther away from its sources than can NO . Therefore, measurement of NO_Y mixing ratios will not be overwhelmed by local highway sources and their vertical transport mechanisms (as with NO mixing ratios). Instead, horizontal transport of different airmasses from different NO_Y source regions to the tower location most likely played a major role in the observed large variation in nighttime NO_Y mixing ratios. While the lack of the wind instruments on the tower prohibits a detailed analysis of this process, the comparison of the surface wind direction data and the NO_Y mixing ratios is valid for general discussion. As with NO mixing ratios, the results (Figure 4.26) from this comparison show a correlation of lower values when the wind is from the southeast quadrant (40% lower than the other quadrants). Unlike NO , however, NO_Y also shows a correlation of higher values when the wind is from the northwest (almost twice as

high as the two remaining quadrants), and is not surprising, given the number of metropolitan areas and NO_x sources located to the northwest of the tower.

5. SUMMARY

5.1 Conclusions

The tropospheric boundary layer distributions of mixing ratios of NO and NO_y (defined as NO + NO₂ + HNO₃ + PAN + NO₃⁻) were measured over a semi-urban area of central North Carolina at the surface and at two heights (250 m and 433 m) on a tower for a period of nearly 45 days starting in December of 1994 and continuing through January and February of 1995. These measurements were then compared to synoptic and upper air meteorological data in order to characterize the diurnal variations of both NO and NO_y mixing ratios in terms of temporal and spatial variations within the various layers that make up the day and nighttime boundary layer. From this characterization conclusions concerning the source of NO and NO_y mixing ratios at both the surface and at elevated heights within the boundary can be made.

The NO mixing ratios showed a strong diurnal profile, with a negative gradient associated with height. In the absence of synoptic meteorological features, the mean nocturnal NO mixing ratios were below instrument detection limits, which ranged from 0.04 to 0.23 ppbv, and the mean daytime NO mixing ratios were at least an order of magnitude greater than the mean nighttime NO mixing ratios. The absence of NO during the night is reflection of nocturnal atmospheric chemistry in which the NO titrated out by residual ozone and OH radicals, and indicates that there was an absence of local sources of NO in the nocturnal boundary layer. A comparison of observed mixing ratios with those

predicted by a one dimensional model of vertical NO transport during the early morning hours showed good agreement; in both cases the NO mixing ratios followed an exponentially decreasing vertical gradient. These results are important when considered against the process of downward mixing of NO, which requires an increasing vertical gradient at some point during the early morning hours. This would only be possible if there was a continued source of NO in the nocturnal boundary layer. NO_y mixing ratios measured at 250 and 433 m also indicated a negative or decreasing vertical gradient, as well as a 22% decrease from the mean daytime values to the mean nighttime values. More importantly, the large increase from the nocturnal minimum (usually just before sunrise) to the diurnal maximum peak indicated that only 40 to 55 % of the daytime increase is due to NO_y conserved or formed in the nocturnal boundary layer overnight; the rest is either transported to or formed at the height within the hours after sunrise. The results observed for both NO and NO_y mixing ratios indicate the importance of the local surface as a source for both constituents.

The passage of of synoptic meteorological features were related to increases in NO and NO_y mixing ratios measured at the 250 and 433 m heights. In particular, the passage of a synoptic feature during the nocturnal hours capable of inducing upward vertical motion in the atmosphere, such as a front or trough, produced an identifiable increase in the NO mixing ratios above the detection limit of the instrument in every observable case. It is hypothesized that the NO mixing ratios at the elevated heights drop to negligible levels during the nocturnal hours due to reaction with residual ozone and hydroxyl radicals (OH), and thus the NO analyzer recorded levels below the detection limit. Upon the

passage of a synoptic feature, however, the upward motion induced by the front or trough transports NO up to the height of the instrument from the surface. This again verifies that the surface is the source for the NO measured on the tower platforms during this research, and that horizontal transport of NO in the nocturnal boundary layer at those heights was non-existent. The relationship of the passage of these synoptic meteorological events with increases in NO_y mixing ratios were less identifiable, possibly due to the more complex nocturnal chemistry and transport processes with which NO_y is associated. However, the NO_y mixing ratios did respond to the synoptic meteorological events in enough instances (70%) to validate that under certain circumstances, NO_y is also transported upward by the vertical motion produced by the passage of synoptic features. Maxima in NO and NO_y mixing ratios showed no dependence on wind direction and tended to decrease in some cases shortly after passage of the synoptic meteorological feature, which negates the idea that the observed increase was due only to horizontal transport of NO and NO_y from the wind direction associated with the front or trough.

The most important information gained from this research, however, is the comparison of observed values to the structure of the nocturnal boundary layer, in particular with regard to the theory of downward mixing as a source of surface peaks in the diurnal profile of NO and NO_y. Throughout the measurement period, diurnal minimum values of these species were recorded (except the previously mentioned synoptic event induced increases) at heights of 250 and 433 m just before sunrise, regardless of the structure of the nocturnal boundary layer. Comparison with upper air soundings at 0600 EST indicate that in at least seven of these cases, the instruments were in the residual

layer, and thus this research indicates that the residual layer can not be assumed to act as a significant reservoir of either NO or NO_Y (or by association, NO_X) for downward mixing. Furthermore, in several instances, the analyzer was located directly in the low level jet just above the interface between the stable layer and the residual layer, but still recorded minimum values of NO and NO_Y. In these cases the low level jet was not transporting a plume of NO and NO_Y that could be transported down or fumigated to the surface upon breakup of the inversion.

Instead, comparison with upper air soundings taken at various times in the morning during the development of the mixed layer indicates that increases in NO and NO_Y mixing ratios (at the 250 and 433 m heights) are the result of the *upward* mixing of these gases from the surface. It is possible that in some of the cases a plume of NO and/or NO_Y may have been present in a layer just below the height of the instrument (and subsequently went undetected by the instrument, given the lack of vertical motion in the nocturnal boundary layer), and which was subsequently mixed upward upon the rise of the mixed layer. However, models such as those postulated by Trainer et al. assume a continuous emission source of NO_X at varying heights ranging from 200-800 m [1987] or from 110-160 m [1991], but stress that the exact height of the source layer is not critical, so long as it is *above* the inversion layer. In at least two of the cases presented here, the NO-NO_Y instrument was located approximately 70 meters above the inversion layer interface (leaving little room for a plume to come between the instrument and the layer interface), and within the low level jet maximum that is commonly accepted (and used for modeling) as the preferential location for such a plume to exist. However, the instrument

still measured a minimum for both NO and NO_Y mixing ratios during this time (and recording a diurnal peak later in the day with the rise of the mixed layer).

Based on this data, there are several assumptions that have to be made in order to accept downward mixing as a source for surface mixing ratio peaks of NO and NO_Y over rural areas. First, since the residual layer is not storing or conserving enough of the species to be downward mixed to account for the observed increases, it has to be assumed that there is always a plume of NO and/or NO_Y located at some level, no matter which direction the wind is coming from (and therefore it has to be assumed that there is no preference for sources such as major metropolitan areas). Second, it has to be assumed that the plume is not always located at the interface between the stable boundary layer and the residual layer and carried by the low level jet. These assumptions are not particularly valid given current understanding of NO and NO_Y plumes and their relationships to sources and nocturnal boundary layer processes. Finally, it was noted that in previous research, the surface peaks in NO and NO_Y mixing ratios occurred both too early and out of phase with the ozone peaks to be attributed to downward mixing processes.

In conclusion, it is felt that the knowledge gained during this study provides a better understanding of the vertical distribution and transport processes related to the mixing ratios of NO and NO_Y (and through NO_Y, the mixing ratios of NO_X). Furthermore, it points towards a rethinking of processes and sources related to rural surface mixing ratios of the oxides of nitrogen, and to that extent, the effectiveness of current NO_X emission and source control policies. Clearly, more comprehensive research

into the role the various constituents of the oxides of nitrogen play in atmospheric chemistry and the production of ozone is necessary.

5.2 Recommendations for Future Research

While the limitations of the tower environment prohibit large scale increases in the scope of research in this area, some additional process and method adjustments in association with measurements on the tower (as well as at the surface) will provide added insight into the transport and source relationship of the oxides of nitrogen.

To begin with, it is possible to increase the accuracy and precision of the measurements by employing a process in which daily zero and span checks of the NO_Y analyzer are completed while the instrument is on the tower. This can be accomplished through the use of a specially designed transportable gas dilution instrument and small portable cylinders of calibration gas and compressed air.

Further recommended instrument modifications include the removal of the NO_Y converter from the instrument and its placement as close to the sample line inlet as possible, to convert NO_Y species to NO before it travels the length of the sample line (and thus avoid bias through line loss of HNO_3 and NO_2). In order to better understand the chemistry of HNO_3 and NO_3^- and their equilibrium ratio during the nocturnal and early morning hours, a comparison could be made between an instrument measuring NO_3^- (via the removal of the Teflon filter) and an instrument with the filter in place (and therefore filtering out NO_3^-).

As this research was conducted in late winter, it is highly recommended that research of this type be conducted in the summer, when the measurements of oxides of nitrogen can be compared to measurements of ozone taken by the state of North Carolina. Other important measurements that would provide insight into the NO-NO₂-O₃ cycle include the measurement of the NO₂ mixing ratios (possibly with a Luminol based system). While the physical limitations of the tower environment may overrule the possibility of these measurements, it is not a certainty - in the case of the research outlined in this manuscript, it was never certain that measurement of NO and NO_y on the tower were possible until it happened. It must be noted that some type of cooling system may be required during the summer to keep the environmental conditions within the instrument's operating range.

In order to better understand the vertical transport processes, three NO-NO_y analyzers should be placed at the base of the tower, at 250 m, and at 433 m, all at the same time if possible, to analyze temporal differences in the vertical gradient and remove some of the traffic interference. Furthermore, a more detailed interrogation of the nocturnal structure and morning evolution of the PBL at the tower location is needed, possibly through the use of an instrument capable of instantaneous measurement of the height of the PBL (such as an acoustic sounder, or SODAR) that is corroborated with balloon launch data, as well as calculation of such turbulence intensity indicators as the Richardson number.

For a better understanding of processes affecting rural mixing ratios of oxides of nitrogen at the surface, a more detailed measurement of truly "rural" surface NO and NO_y

mixing ratios and comparison to the data produced from the aforementioned boundary layer interrogation processes (made at the site of the measurement of rural NO and NO_y mixing ratios) is necessary.

Finally, comparison of data gathered on the tower with back trajectory analysis, with winds interpolated at the tower platform heights (via the NCSU GEMPAK weather data interpolation system), and/or with meteorological data from the tower platform which may someday be available, will all provide insight into horizontal transport processes and their affect on NO and NO_y mixing ratios.

REFERENCES

- Altshuller, A.P. (1986) The role of nitrogen oxides in nonurban ozone formation in the planetary boundary layer over North America, Western Europe and adjacent areas of ocean. *Atmospheric Environment* **20** (2), 245-268.
- Aneja, V.P., Das, M., Kim, D.S., and Hartsell, B.E. (1994) Measurement and analysis of photochemical oxidants and trace gases in the rural troposphere of the southeast United States. *Israel Journal of Chemistry* **34**, 387-401.
- Arya, S.P. (1988) *Introduction to Micrometeorology*. Academic Press, Inc., San Diego, CA.
- Arya, S.P. (1995) North Carolina State University, Raleigh, NC, personal communication.
- Atkinson, R., Winer A. M., and Pitts, J.N., Jr. (1986) Estimation of nighttime N_2O_5 concentrations from ambient NO_2 and NO_3 radical concentrations and its role in nighttime chemistry. *Atmospheric Environment* **20** (2), 331-339.
- Batchvarova, E., and Gryning, S. (1991) Applied model for the growth of the daytime mixed layer. *Boundary Layer Meteorology* **56** (3), 261-274.
- Bollinger, M.J., Hahn, C.J., Parrish, D.D., Murphy, P.C., Albritton, D.L., and Fehsenfeld, F.C. (1984) NO_x measurements in clean continental air and analysis of the contributing meteorology. *Journal of Geophysical Research* **89**, 9623-9631.
- Broll, A., Helas, G., Rumpel, K.J., and Warneck, P. (1984) NO_x background mixing ratios in surface air over Europe and the Atlantic Ocean. Third European Symposium of Physico-Chemical Behavior of Atmospheric Pollutants, Varese, Italy.
- Buhr, M.P., Parrish, D.P., Norton, R.B., Fehsenfeld, F.C., and Sievers, R.E (1990) Contribution of organic nitrates to the total reactive nitrogen budget at a rural eastern U.S. site. *Journal of Geophysical Research* **95** (D7), 9809-9816.
- Chameides, W. L., and Walker J.C.G. (1973) A photochemical theory of tropospheric ozone. *Journal of Geophysical Research* **78**, 8751-8760.
- Chameides, W.L., Fehsenfeld, F.C., Rodgers, M.O., Cardelino, C., Martinez, J., Parrish, D.D., Lonneman, W., Lawson, D.R., Rasmussen, R.A., Zimmerman, P., Greenberg, J., Middleton, P., and Wang, T. (1992) Ozone precursor relationships in the ambient atmosphere. *Journal of Geophysical Research* **94** (D5), 6037-6055.

- Cleveland, W.S., Kleiner, B., McRae, J.E., Warner, J.L., and Pasceri, R.E. (1977) Geographical properties of ozone concentrations in the northeastern United States. *Journal of the Air Pollution Control Association* **27**, 325-328.
- Cooper, D.I., and Eichinger, W.E. (1994) Structure of the atmosphere in an urban planetary boundary layer from lidar and radiosonde observations. *Journal of Geophysical Research* **99** (D11), 22,937-22,948.
- Cox, R.A., (1977) Some measurements of ground level NO, NO₂, and O₃ concentrations at an unpolluted maritime site. *Tellus* **29**, 356-363.
- Decker, C.E., Ripperton, L.A., Worth, J.J., Vukovich, F.M., Bach, W.D., Tommerdahl, J.B., Smith, F., and Wagoner, D.E. (1976) Formation and transport of oxidants along the Gulf Coast and in the northern U.S. Report EPA-450/3-76-033, U.S. Environmental Protection Agency, Research Triangle Park, NC.
- Delany, A.C., Dickerson, R.R., Melchior, F.L., Jr., and Wartburg, A.F. (1982) Modification of commercial NO_x detectors for high sensitivity. *Review of Science Instruments* **53**, 1899-1902.
- Dickerson, R.R., Delany, A.C., and Wartburg, A.F. (1984) Further modification of commercial NO_x detectors for high sensitivity. *Review of Science Instruments* **55**, 1995-1998.
- Doddridge, B.G., Dickerson, R.R., Wardell, R.G., and Civerolo, K.L. (1992) Trace gas concentrations and meteorology in rural Virginia - 2. Reactive nitrogen compounds. *Journal of Geophysical Research* **97** (D18), 20,631-20,646.
- Fahey, D.W., Hubler, G., Parrish, D.D., Williams, E.J., Norton, R.B., Ridley, B.A., Singh, H.B., Liu, S.C., and Fehsenfeld, F.C. (1986) Reactive nitrogen species in the troposphere: Measurements of NO, NO₂, HNO₃, particulate nitrate, peroxyacetyl nitrate (PAN), O₃, and total reactive odd nitrogen (NO_y) at Niwot Ridge, Colorado. *Journal of Geophysical Research* **91**, 9781-9793.
- Fascinating Electronics Inc. (1992) *Reference Manual and Applications Guide, Version 1.0*. Beaverton, OR.
- Fehsenfeld, F.C., Bollinger, M.J., Liu S.C., Parrish, D.D., McFarland, M., Trainer, M., Kley, D., Murphy, P.C., Albritton, D.L., and Lenschow, D.H. (1983) A study of ozone in the Colorado mountains. *Journal of Atmospheric Chemistry* **1**, 87-105.

Fehsenfeld, F.C., Dickerson, R.R., Hübler, G., Luke, W.T., Nunnermacker, L.J., Williams, E.J., Roberts, J.M., Calvert, J.G., Curran, C.M., Delany, A.C., Eubank, C.S., Fahey, D.W., Fried, A., Gandrud, B.W., Langford, A.O., Murphy, P.C., Norton, R.B., Pickering, K.E., and Ridley, B.A. (1987) A ground-based intercomparison of NO, NO_x, and NO_y measurement techniques. *Journal of Geophysical Research* **92** (D12), 14,710-14,722.

Fehsenfeld, F.C., Parrish, D.D., and Fahey, D.W. (1988) The measurement of NO_x in the nonurban troposphere. In *Tropospheric Ozone* (edited by Isaksen, I.S.A.), pp 185-215. D. Reidel Publishing Company, Hingham MA.

Finlayson-Pitts, B.J., and Pitts, J.N. Jr. (1986) *Atmospheric Chemistry: Fundamentals and Experimental Techniques*. John Wiley & Sons, New York, New York.

Finlayson-Pitts, B.J. and Pitts, J.N. Jr. (1993) Atmospheric chemistry of tropospheric ozone formation: scientific and regulatory implications. *Journal of the Air and Waste Management Association* **43** (8), 1091-1100.

Fishman, J., Solomon, S., and Crutzen, P.J. (1979) Observational and theoretical evidence in support of a significant in-situ photochemical source of tropospheric ozone. *Tellus* **31**, 432-446.

Fishman, J., Vukovich F.M., and Browell, E.V. (1985) The photochemistry of synoptic scale ozone synthesis: implications for the global tropospheric ozone budget. *Journal of Atmospheric Chemistry* **3**, 299-320.

Folinsbee, L.J., McDonnell W.E., and Hortsman D.H. (1988) Pulmonary function and symptom response after 6.6 hour exposure to 0.12 ppm ozone with moderate exercise. *Journal of the Air Pollution Control Association* **38**, 28-35.

Galloway, J.N., and Likens, G.E. (1981) Acid precipitation: the importance of nitric acid. *Atmospheric Environment* **15** (6), 1081-1085.

Godowitch, J.M., Ching, J.K.S., and Clarke, J.F. (1985) Evolution of the nocturnal inversion layer at an urban and nonurban location. *Journal of Climate and Applied Meteorology* **24** (8), 791.

Hameed, S., Pinto, J.P., and Stewart, R.W. (1979) Sensitivity of the predicted CO-OH-CH₄ perturbation to tropospheric NO_x concentrations. *Journal of Geophysical Research* **84** (C2), 763-768.

Harrison, R.M., and McCartney, H.A. (1980) Ambient air quality at a coastal site in rural northwest England. *Atmospheric Environment* **14**, 233-244.

Hastie, D.R., Shepson, P.B., Sharma, S., Schiff, H.I. (1993) The influence of the nocturnal boundary layer on secondary trace species in the atmosphere at Dorset, Ontario. *Atmospheric Environment* **27A** (4), 533-541.

Heck, W.W., Taylor, O.C., Adam, R.M., Bingham, G., Miller, J., Preson, E., and Weinstein, L. (1982) Assessment of crop loss from ozone. *Journal of the Air Pollution Control Association* **32**, 353-361.

Heck, W.W., Adams, R.M., Cure, W.W., Heagle, A.S., Heggstad, H.E., Kohut, R.J., Kress, L.W., Rawlings, J.O., and Taylor, O.C. (1983) A reassessment of crop loss from ozone. *Environmental Science and Technology* **17**, 572A-581A.

Heck, W.W., Cure, W.W., Rawlings, J.O., Zaragosa, L.J., Heagle, A.S., Heggstad, H.E., Kohut, R.J., Kress, L.W., and Temple, P. J. (1984) Assessing impacts of ozone on agricultural crops - 1. Overview. *Journal of the Air Pollution Control Association* **34**, 729-735.

Helas, G. and Warneck, P. (1981) Background NO_x mixing ratios in air masses over the North Atlantic Ocean. *Journal of Geophysical Research* **86**, 7283-7290.

Hough, A.M. and Derwent, R.G. (1990) Changes in the global concentration of tropospheric ozone due to human activities. *Nature* **344** (6267), 645-648.

Hov, O. (1983) One dimensional vertical model for ozone and other gases in the atmospheric boundary layer. *Atmospheric Environment* **17** (3), 535-549.

Hurley, P. and Physick, W. (1991) A lagrangian particle model of fumigation by breakdown of the nocturnal inversion. *Atmospheric Environment* **25A** (7), 1313-1325.

Johnson, W.B. and Viezee, W. (1981) Stratospheric ozone in the lower troposphere - 1. Presentation and interpretation of aircraft measurements. *Atmospheric Environment* **15** (7), 1309-1323.

Kelly, T.J., Stedman, D.H., Ritter, J.A., and Harvey, R.B. (1980) Measurement of oxides of nitrogen and nitric acid in clean air. *Journal of Geophysical Research* **85** (C12), 7417-7425.

Kelly, N.A., Wolff, G.T., and Ferman, M.A. (1982) Background pollution measurements in air masses affecting the eastern half of the United States - 1. Air masses arriving from the northwest. *Atmospheric Environment* **16** (5), 1077-1088.

- Kelly, N.A., Wolff, G.T., and Ferman, M.A. (1984) Sources and sinks of ozone in rural areas. *Atmospheric Environment* **18** (7), 1251-1266.
- Kley, D., Drummond, J.W., McFarland, M., and Liu, S.C. (1981) Tropospheric profiles of NO_x. *Journal of Geophysical Research* **86**, 3153-3161.
- Levine, S.Z., and Schwartz, S.E. (1982) In-cloud and below-cloud scavenging of nitric acid vapor. *Atmospheric Environment* **16** (7), 1725-1734.
- Levy, H. (1971) Normal atmosphere: large radical and formaldehyde concentrations predicted. *Science* **173**, 141-143.
- Lin, X., Trainer, M., and Liu, S.C. (1988) On the nonlinearity of the tropospheric ozone production. *Journal of Geophysical Research* **93** (D12), 15,879-15,888.
- Liu, S.C. (1977) Possible effects on tropospheric O₃ and OH due to NO emissions. *Geophysical Research Letters* **4**, 325-328.
- Liu, S.C., Trainer, M., Fehsenfeld, F.C., Parrish, D.D., Williams, E.J., Fahey, D.W., Hübler, G., and Murphy, P.C. (1987) Ozone production in the rural troposphere and the implications for regional and global ozone distribution. *Journal of Geophysical Research* **92** (D4), 4191-4207.
- Logan, J.A. (1983) Nitrogen oxides in the troposphere: global and regional budgets. *Journal of Geophysical Research* **88** (C15), 10,785-10,807.
- Logan, J.A., Prather, M.J., Wofsy, S.C., and McElroy, M.B. (1981) Tropospheric chemistry: a global perspective. *Journal of Geophysical Research* **86** (C8), 7210-7254.
- Martin A., and Barber, F.R. (1981) Sulfur dioxide, oxides of nitrogen, and ozone measured continuously for two years at a rural site. *Atmospheric Environment* **15** (4), 567-578.
- Martinez, J.R. and Singh, H.B., (1979) Survey of the role of NO_x in nonurban ozone formation. Final Report on SRI Project 6780-8, prepared for Monitoring and Analysis Division, Office of Air Quality Planning and Standards, Research Triangle Park, NC 27711.
- Messina, S.R. (1985) Analysis of the relationship between meteorology and air pollution at Dueselbach, West Germany. MS Thesis, Graduate School, University of Maryland, College Park, MD 20742

Mohnen, V.A., Hogan, A., and Coffey, P. (1977) Ozone measurements in rural areas. *Journal of Geophysical Research* **82**, 5889-5895.

National Research Council (1992) *Rethinking the Ozone Problem in Urban and Regional Air Pollution*. National Academy Press, Washington, D.C.

Neu, U., Künzle, T., and Wanner, H. (1994) On the relation between ozone storage in the residual layer and daily variation in the near surface ozone concentration - a case study. *Boundary Layer Meteorology* **69** (3), 221-247.

Office of Technology Assessment, U.S. Congress (1989) *Catching our Breath: Next Steps for Reducing Urban Ozone*. Report OTA-0412, U.S. Government Printing Office, Washington, D.C.

Parrish, D.D., Williams, E.J., Norton, R.B., Fehsenfeld, F.C. (1985) Measurements of odd-nitrogen species and O₃ at Point Arena, California. *EOS, Transactions, American Geophysical Union* **66**, 820.

Parrish, D.D., Williams, E.J., Buhr, M.P., Norton, R.B., Fehsenfeld, F.C., Gandrud, B.W., Ridley, B.A., Shetter, J.D. (1986) Partitioning of odd-nitrogen species at a rural, eastern U.S. site. *EOS, Transactions, American Geophysical Union* **67**, 891.

Parrish, D.D., et al. (1993) The total reactive oxidized nitrogen levels and the partitioning between the individual species at six rural sites in Eastern North America. *Journal of Geophysical Research* **98** (D2), 2927-2939.

Platt, U., Perner, D. (1980) Direct measurements of atmospheric CH₂O, HNO₂, O₃, NO₂, and SO₂ by differential optical absorption in the near UV. *Journal of Geophysical Research* **85**, 7453-7458.

Platt, U., Perner, D., Schroder, J., Kessler, C., and Toenissen, A. (1981) The diurnal variation of NO₃. *Journal of Geophysical Research* **86**, 11965-11970.

Pratt, G.C., Hendrickson, R.C., Chevone, B.I., Christopherson, D.A., O'Brien, M.V., and Krupa, S.V. (1983) Ozone and oxides of nitrogen in the rural midwestern U.S.A. *Atmospheric Environment* **10**, 2013-2023.

Raynor, K.N. and Watson, I.D. (1991) Operational prediction of daytime mixed layer height. *Atmospheric Environment* **25A** (8), 1427-1436.

Reich, P.B. and Amundson, R.G. (1985) Ambient levels of ozone reduce net photosynthesis in trees and crop species. *Science* **230**, 566-570.

Research Triangle Institute (1975) Investigation of rural oxidant levels as related to urban hydrocarbon control strategies. Report EPA-450/3-75-036, U.S. Environmental Protection Agency, Research Triangle Park, NC.

Ridley, B.A. (1991) Recent measurements of oxidized nitrogen compounds in the troposphere. *Atmospheric Environment* **25A** (9), 1905-1926.

Ridley, B.A., and Howlett, L.C. (1974) An instrument for nitric oxide measurements in the stratosphere. *Review of Science Instruments* **45**, 742-746.

Ripperton, L.A., Kornreich, L., and Worth, J.J.B. (1970) Nitrogen dioxide and nitric oxide in non-urban air. *Journal of the Air Pollution Control Association* **20**, 589-592.

Ritter, J.A., Stedman, D.H., and Kelly, T.J. (1979) Ground level measurements of nitric oxide, nitrogen dioxide, and ozone in rural air. In *Nitrogenous Air Pollutants: Chemical and Biological Implications* (edited by Grosjean, D.), pp 325-343. Ann Arbor Science Publishers, Inc., Ann Arbor, MI.

Singh, H.B. (1987) Reactive nitrogen in the troposphere: chemistry and transport of oxides of nitrogen and peroxyacetyl nitrate. *Environmental Science and Technology* **21** (4), 320-326.

Snedecor, G.W. and Cochran, W.G. (1989) *Statistical Methods*. Iowa State University Press, Ames, IA.

Spicer, C.W. (1977) The fate of nitrogen oxides in the atmosphere. In *Advances in Environmental Science and Technology*, Vol. 7 (edited by Pitts, J.N. Jr., and Metcalf, R.L.), pp 163-261. Wiley Interscience, John Wiley.

Stull, R.B. (1988) *An Introduction to Boundary Layer Meteorology*. Kluwer Academic Publishers, Dordrecht, The Netherlands.

Sullivan, L. J. (1995) Biogenic Nitric Oxide Emissions: Trends, Seasonal Analysis and Interpretations. MS Thesis, Graduate School, North Carolina State University, Raleigh, NC 27695.

Taylor, J.K. (1987) *Quality Assurance of Chemical Measurements*. Lewis Publishers, Chelsea, MI.

Taylor, O.C. (1969) The importance of peroxyacetyl nitrate (PAN) as a phytotoxic air pollutant. *Journal of the Air Pollution Control Association* **19**, 347-351.

Thermo Environmental Instruments Company (TECO) (1992) *Instruction Manual Model 42S: Chemiluminescence NO-NO₂-NO_x analyzer*. Designated reference RFNA-1289-074, Franklin MA.

Trainer, M., Williams, E.J., Parrish, D.D., Buhr, M.P., Allwine, E.J., Westberg, H.H., Fehsenfeld, F.C., and Liu, S.C. (1987) Models and observations of the impact of natural hydrocarbons on rural ozone. *Nature* **329**, 705-707.

Trainer, M., Buhr, M.P., Curran, C.M., Fehsenfeld, F.C., Hsie, E.Y., Liu, S.C., Norton, R.B., Parrish, D.D., and Williams, E.J. (1991) Observations and modeling of the reactive nitrogen photochemistry at a rural site. *Journal of Geophysical Research* **96 (D2)**, 3045-3063.

Trainer, M., Parrish, D.D., Buhr, M.P., Norton, R.B., Fehsenfeld, F.C., Anlauf, K.G., Bottenheim, J.W., Tang, Y.Z., Wiebe, H.A., Roberts, J.M., Tanner, R.L., Newman, L., Bowersox, V.C., Meagher, J.F., Olszyna, K.J., Rodgers, M.O., Wang, T., Berresheim, H., Demerjian, K.L., and Roychowdhury, U.K. (1993) Correlation of ozone with NO_y in photochemically aged air. *Journal of Geophysical Research* **98 (D2)**, 2917-2925.

Vukovich, F.M., Bach, W.D., Jr., Crissman, B.W., and King, W.J. (1977) On the relationship between high ozone in the rural surface layer and high pressure systems. *Atmospheric Environment* **11 (10)**, 967-983.

Vukovich, F.M., Fishman, J., and Browell, E.V. (1985) The reservoir of ozone in the boundary layer of the Eastern United States and its potential impact on the global ozone budget. *Journal of Geophysical Research* **90 (D3)**, 5687-5698.

Warneck, P. (1988) *Chemistry of the Natural Atmosphere*. International Geophysics Series Vol. 41, Academic Press, Inc., San Diego, CA.

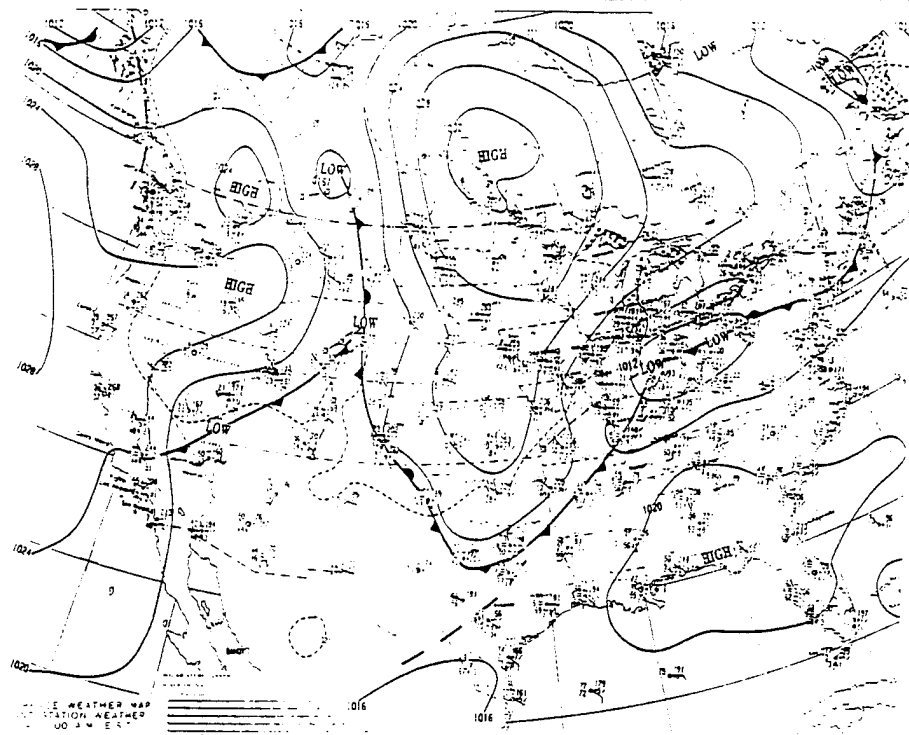
Winer, A.M., Peters, J.W., Smith, J.P., and Pitts, J.N. Jr. (1974) Response of commercial chemiluminescent NO-NO₂ analyzers to other nitrogen containing compounds. *Environmental Science and Technology* **8 (13)**, 1118-1121.

Wolff, G.T. and Lioy, P.J. (1980) Development of an ozone river associated with synoptic scale episodes in the eastern United States. *Environmental Science and Technology* **14**, 1257-1260.

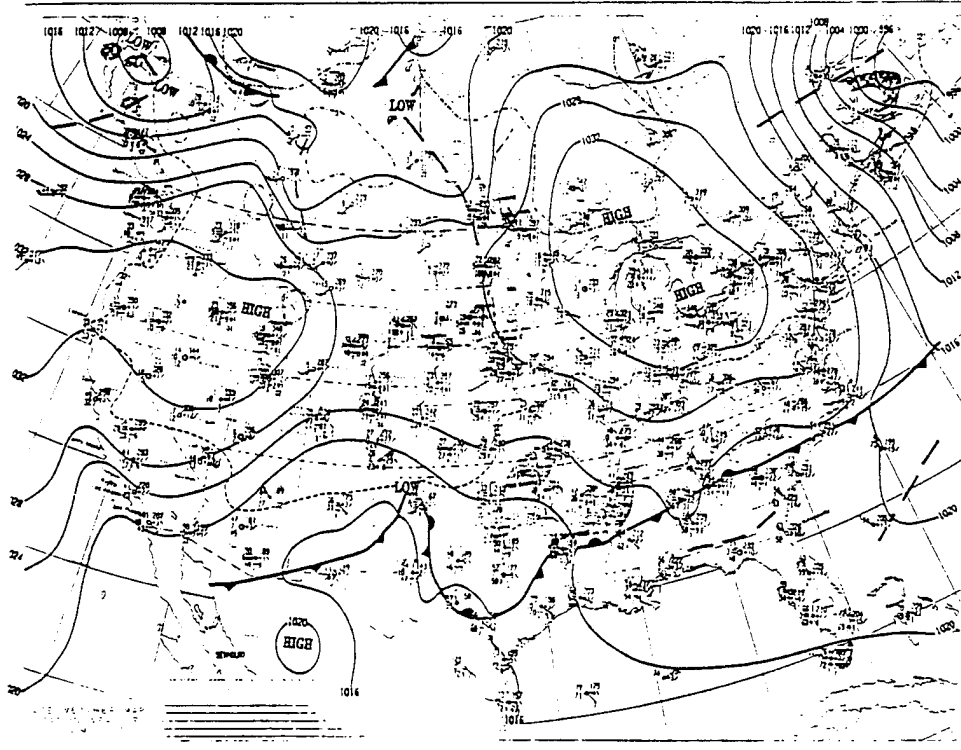
7. APPENDICES

**7.1 Appendix 1: National Weather Service Daily Surface
Weather Maps (Valid 700 EST): December 7-16, 1994; January
12-25, 1995; February 2-23, 1995**

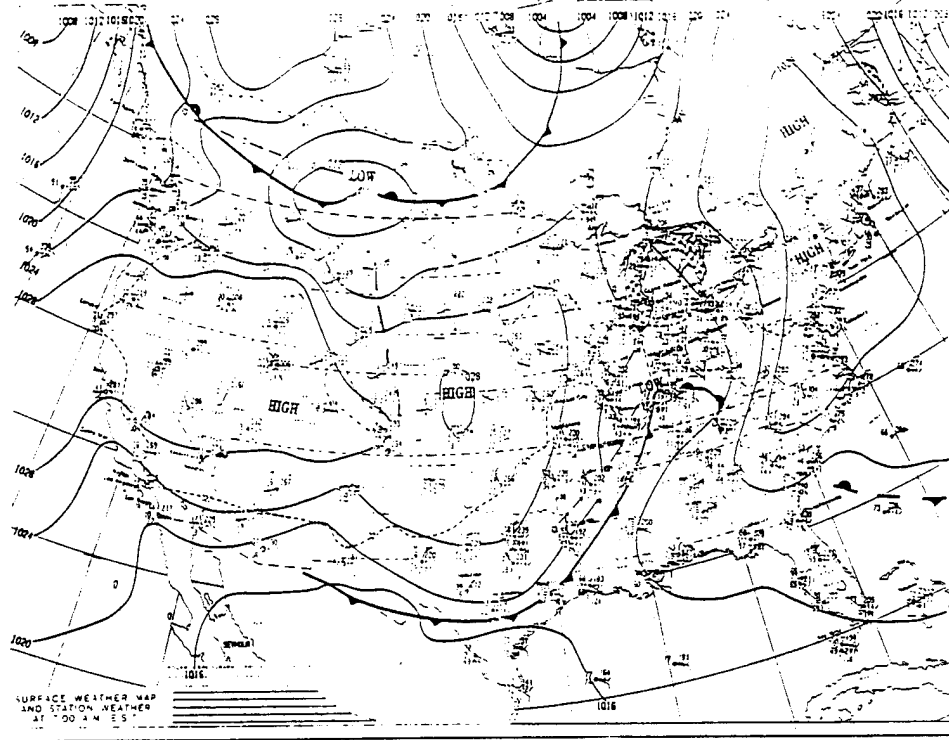
WEDNESDAY, DECEMBER 7, 1994



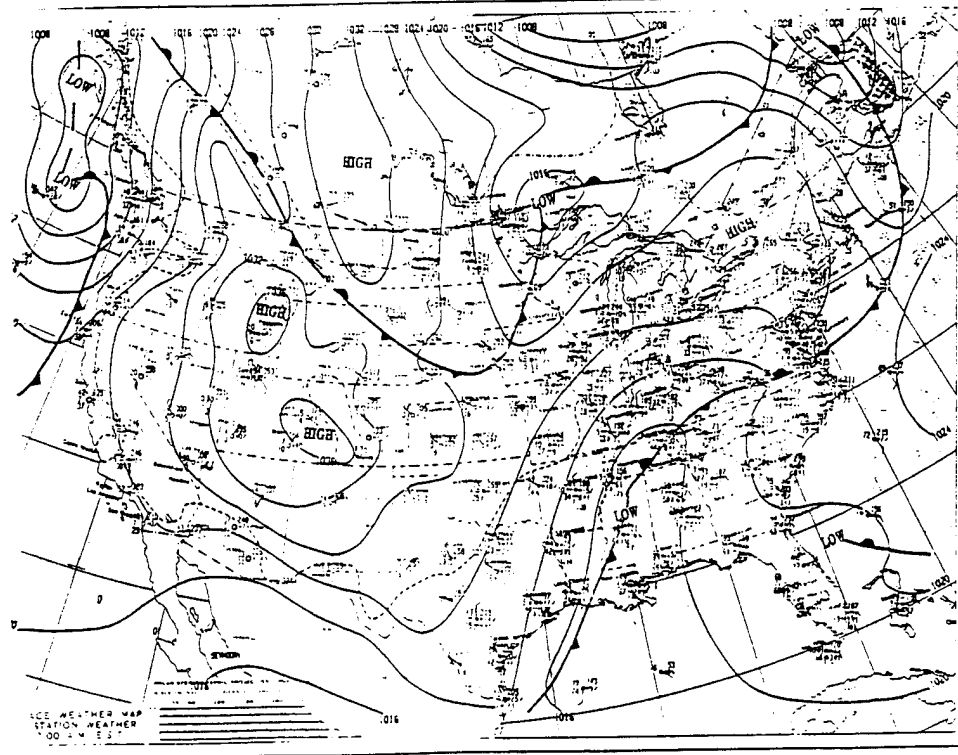
THURSDAY, DECEMBER 8, 1994



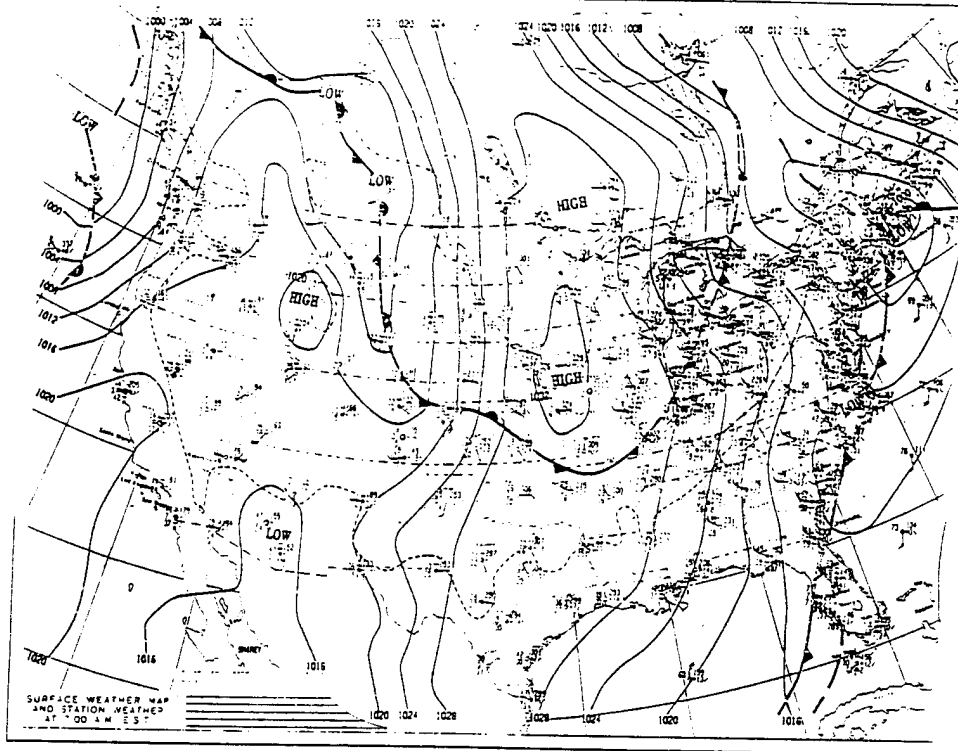
FRIDAY, DECEMBER 9, 1994



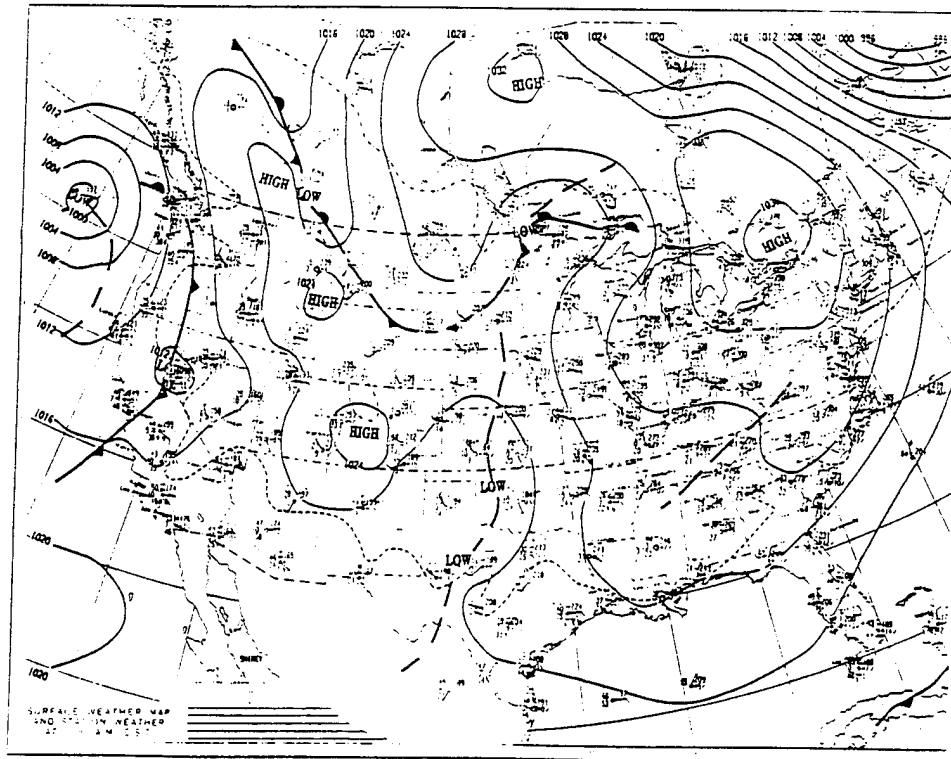
SATURDAY, DECEMBER 10, 1994



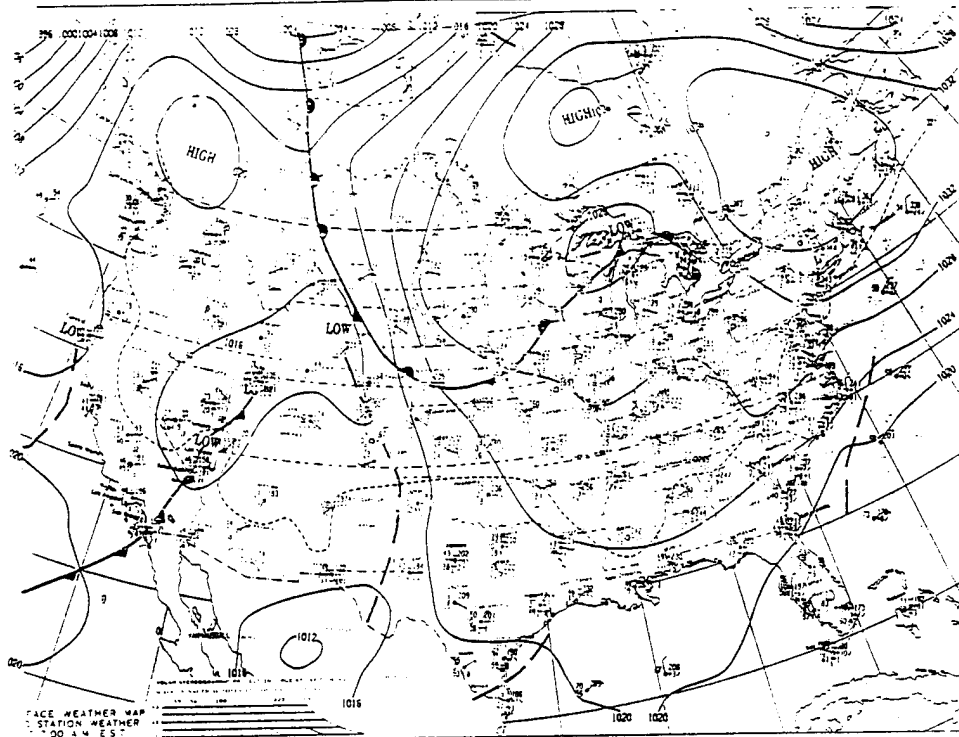
SUNDAY, DECEMBER 11, 1994



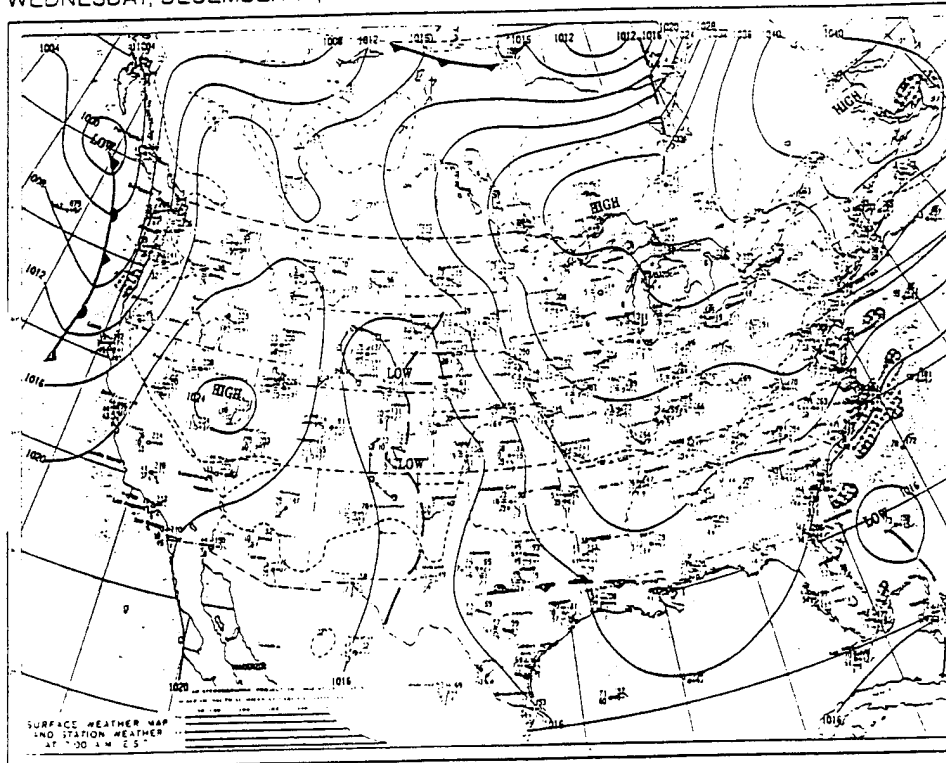
MONDAY, DECEMBER 12, 1994



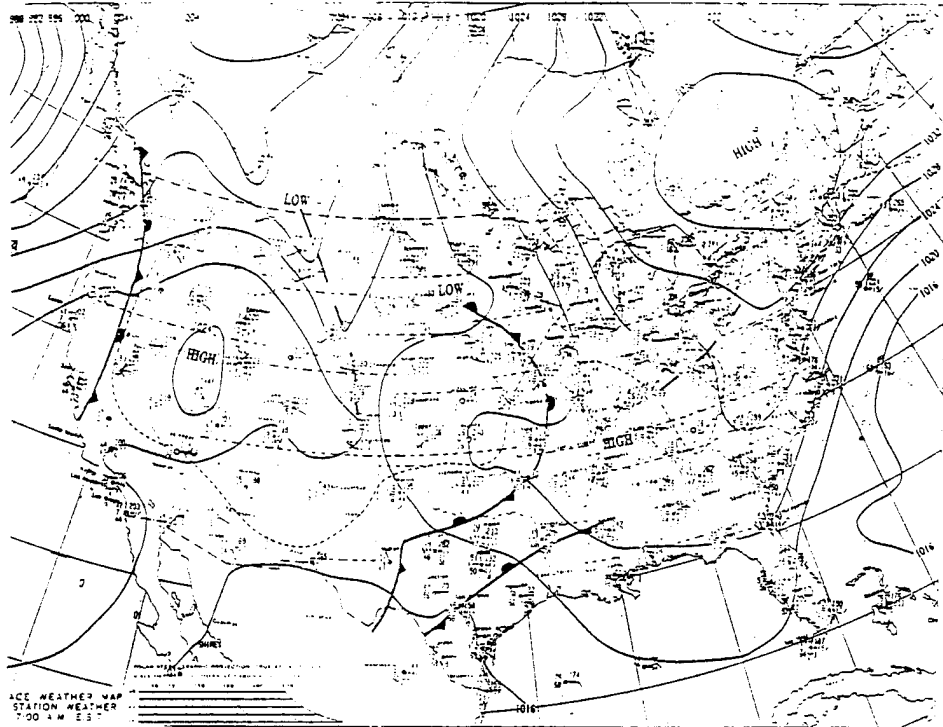
TUESDAY, DECEMBER 13, 1994



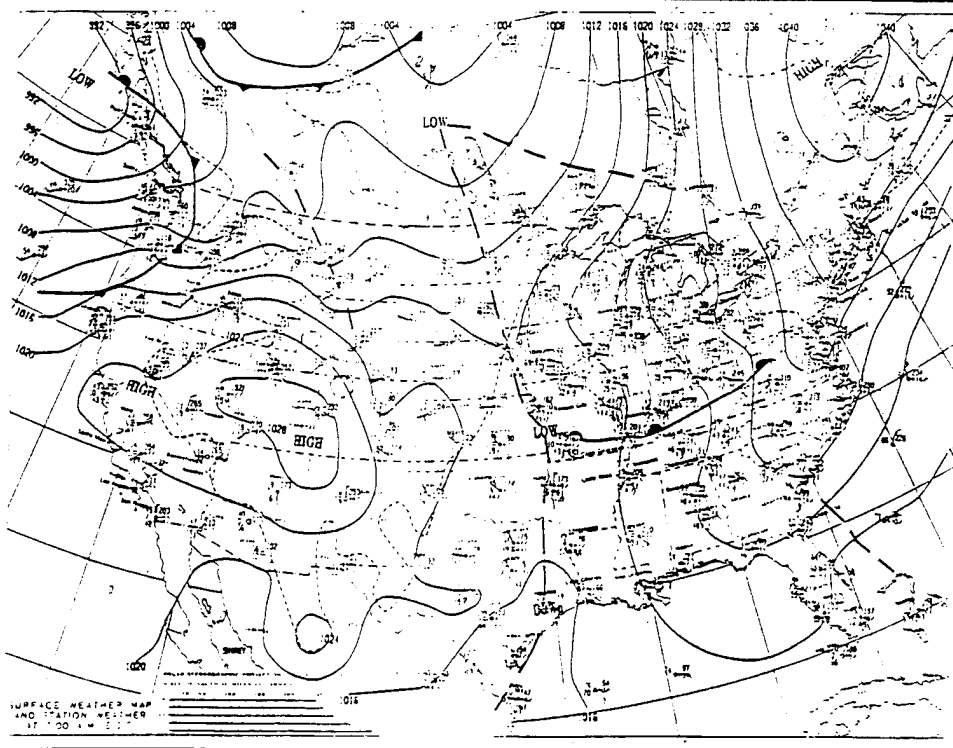
WEDNESDAY, DECEMBER 14, 1994



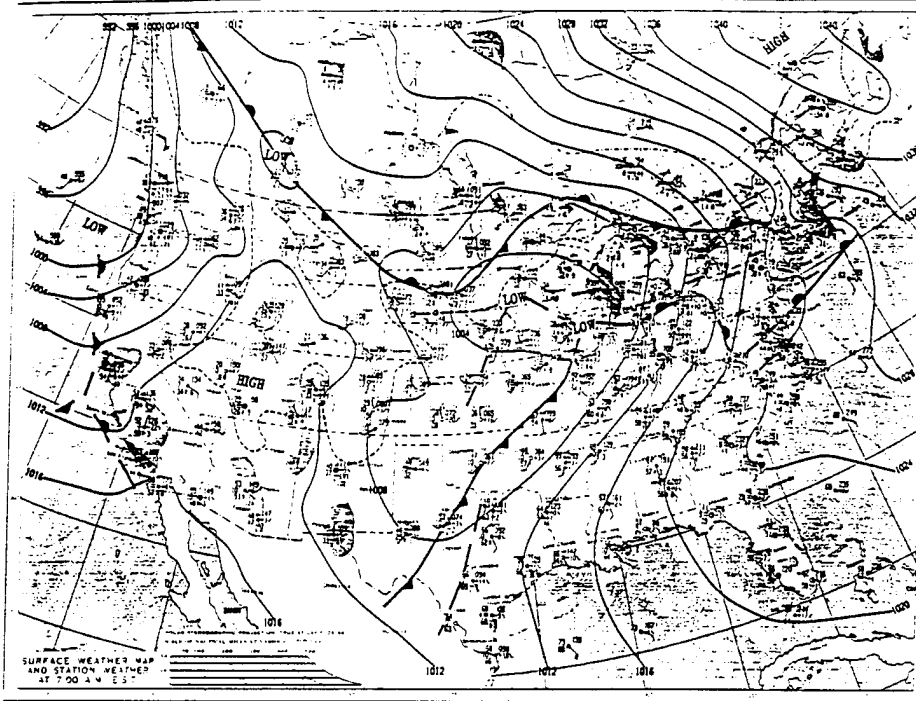
THURSDAY DECEMBER 15 1994



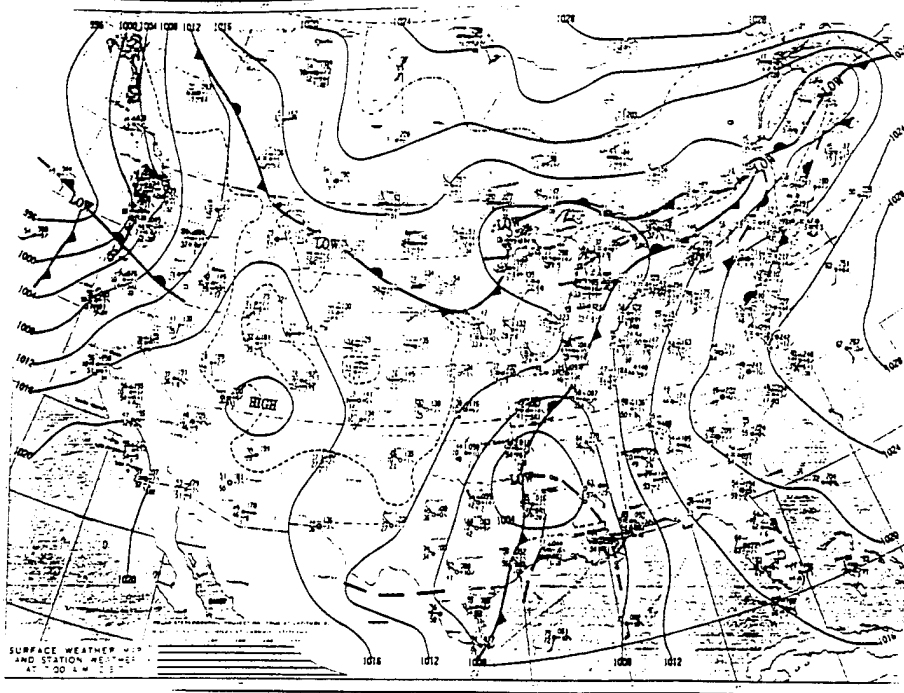
FRIDAY, DECEMBER 16, 1994



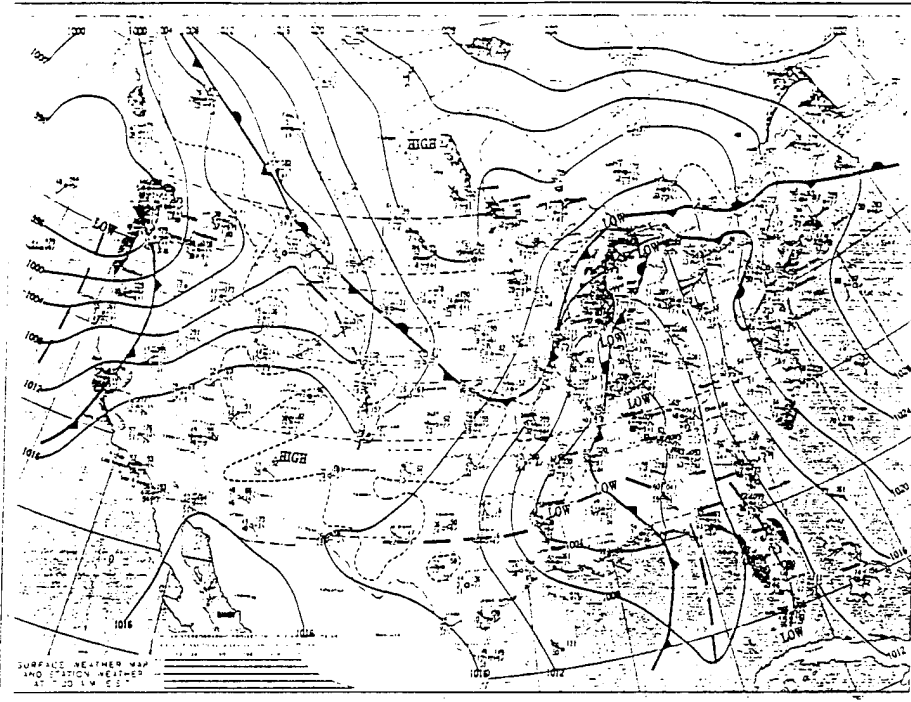
THURSDAY, JANUARY 12, 1995



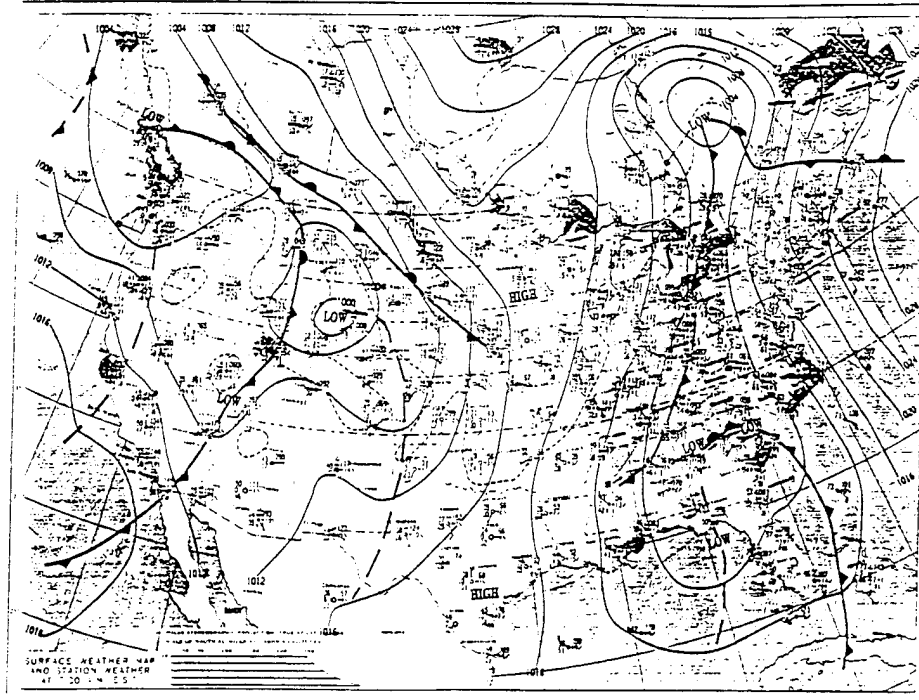
FRIDAY, JANUARY 13, 1995



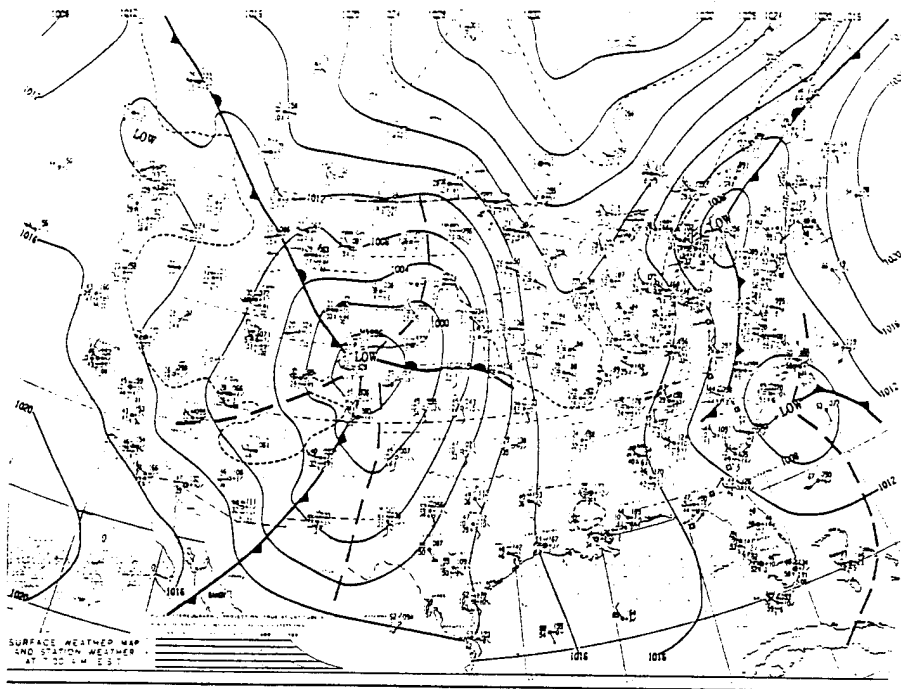
SATURDAY JANUARY 14, 1995



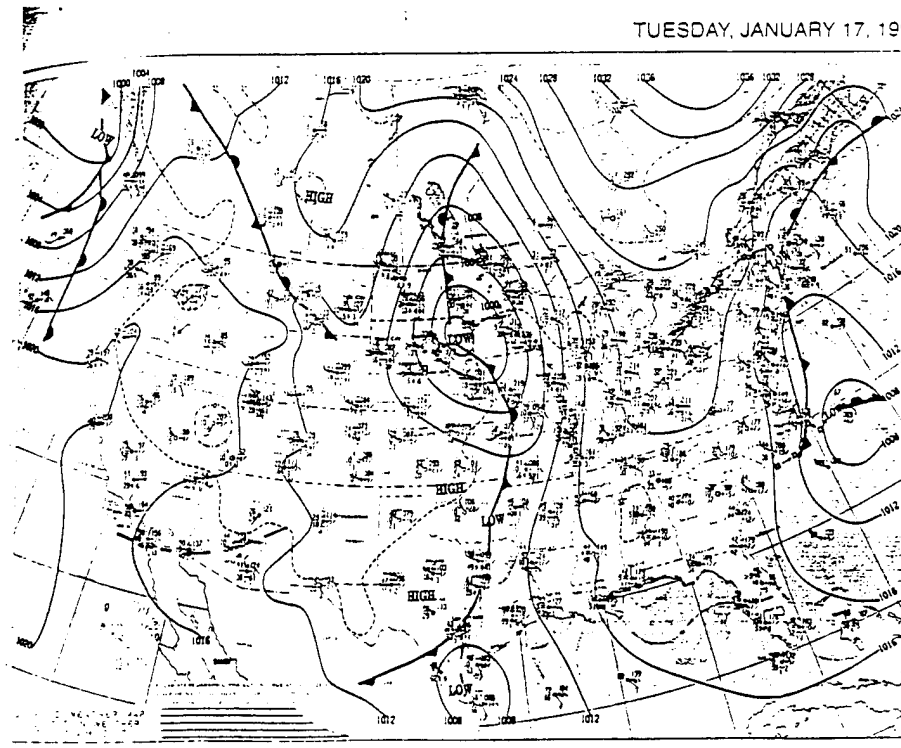
SUNDAY, JANUARY 15, 1995



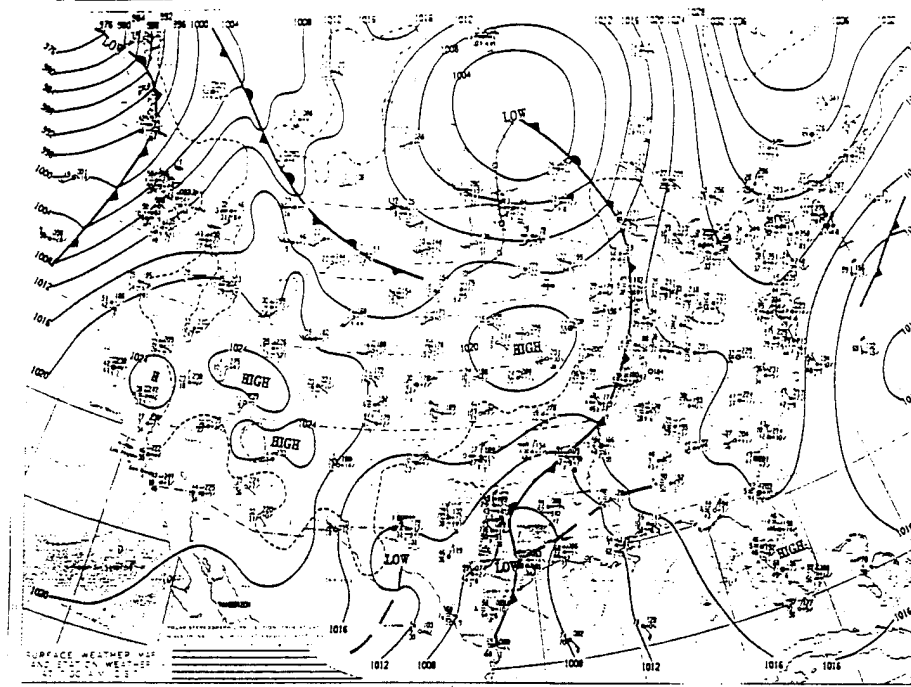
MONDAY, JANUARY 16, 1995



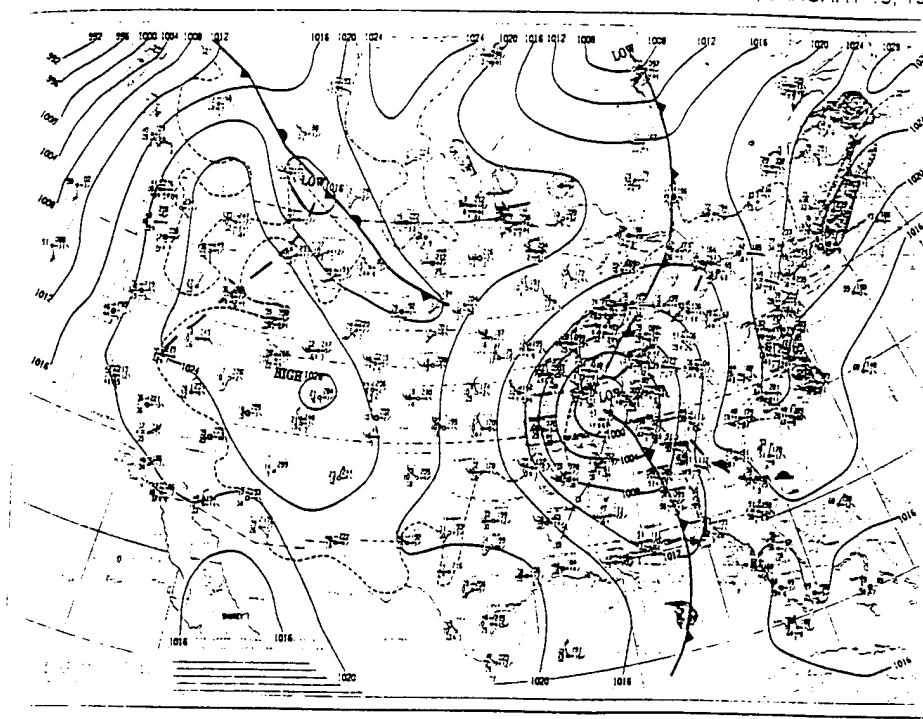
TUESDAY, JANUARY 17, 1995



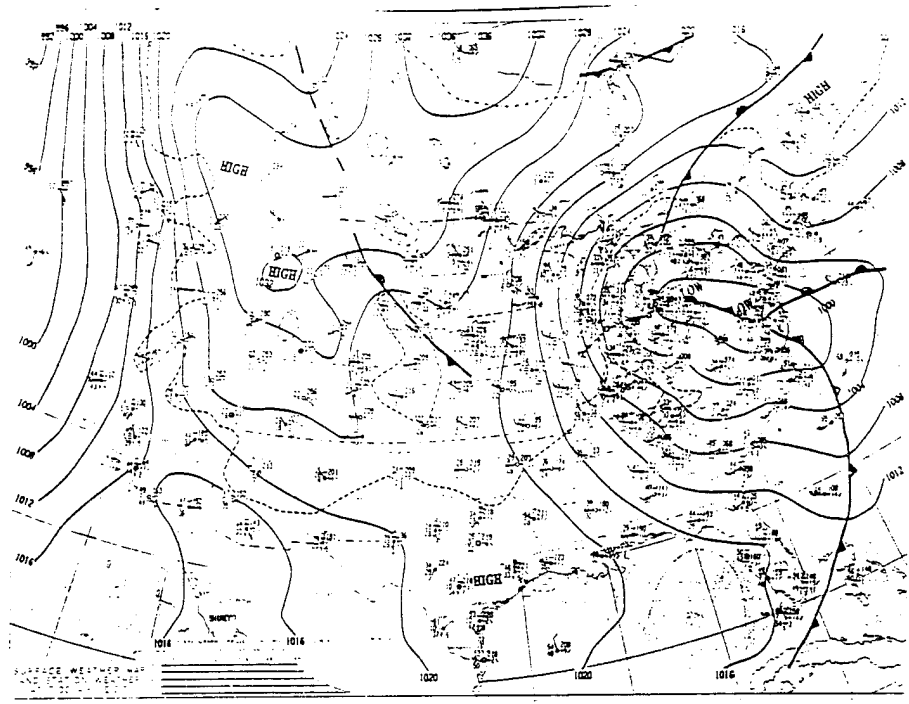
WEDNESDAY, JANUARY 18, 1995



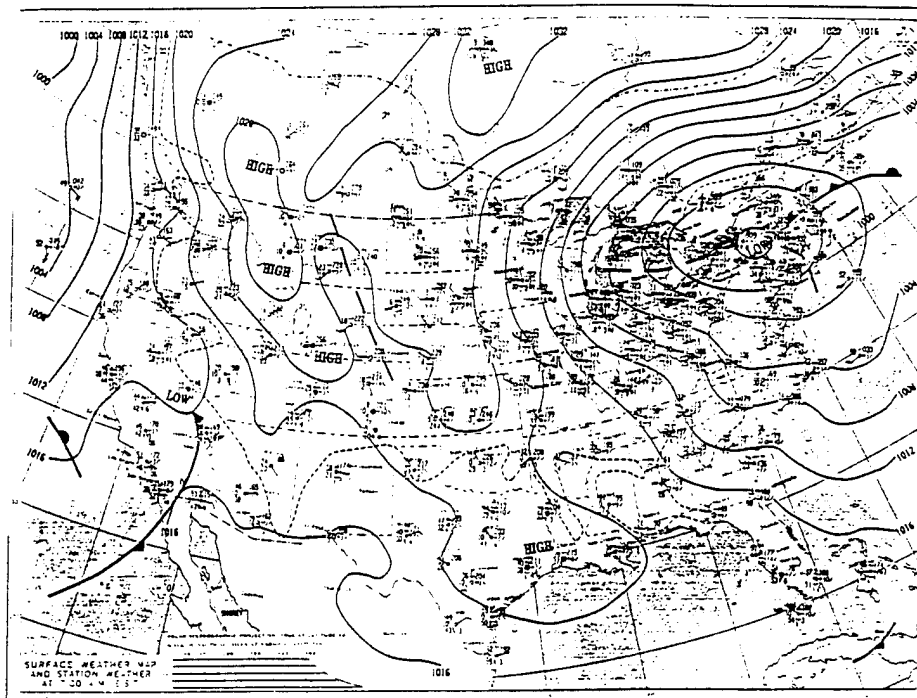
THURSDAY, JANUARY 19, 1995



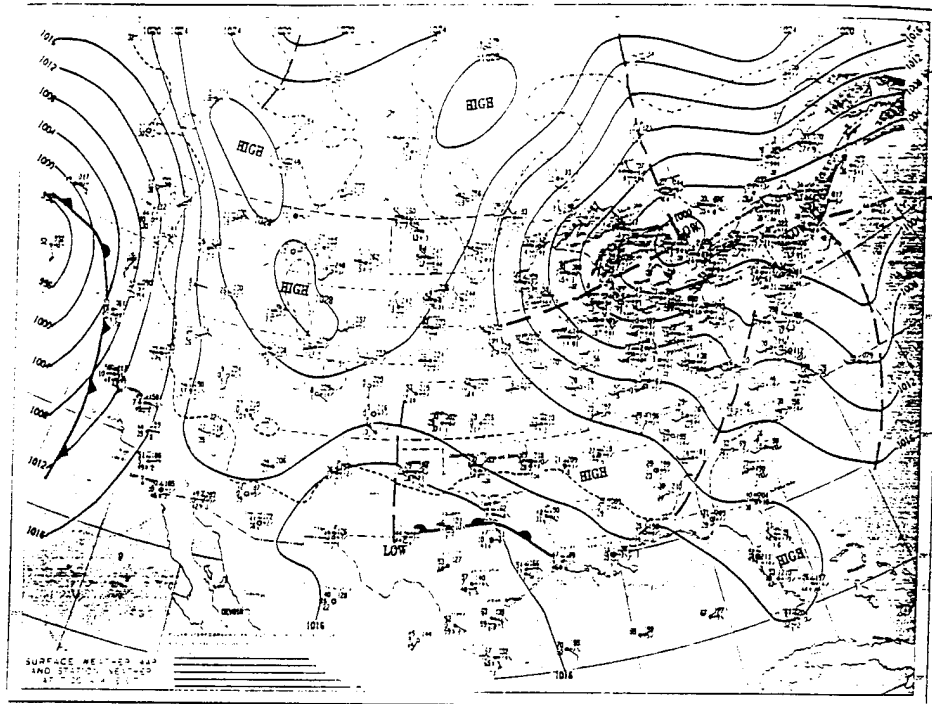
FRIDAY, JANUARY 20, 1995



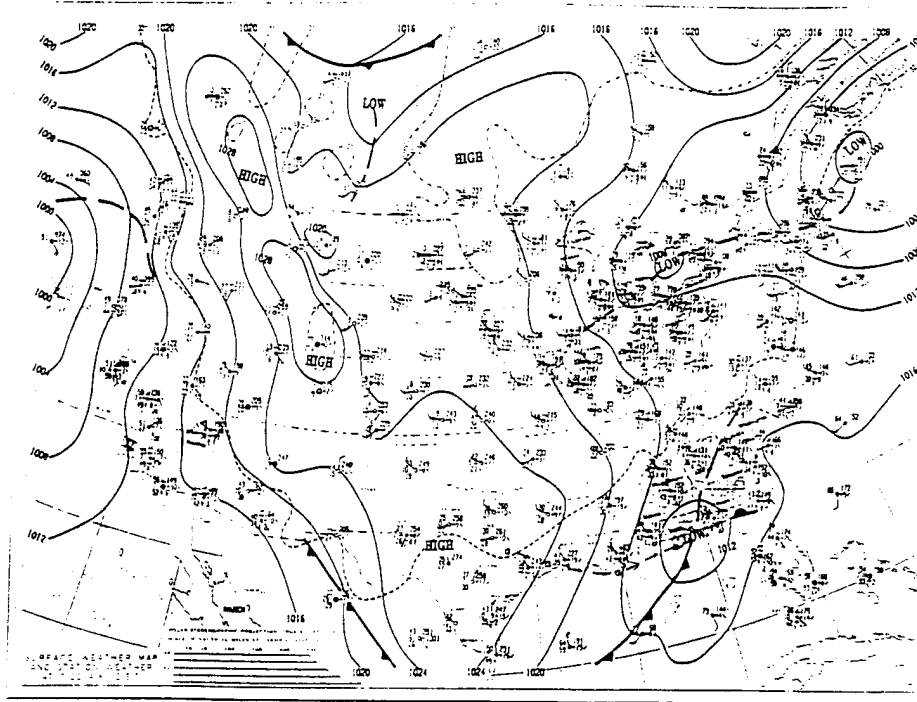
SATURDAY, JANUARY 21, 1995



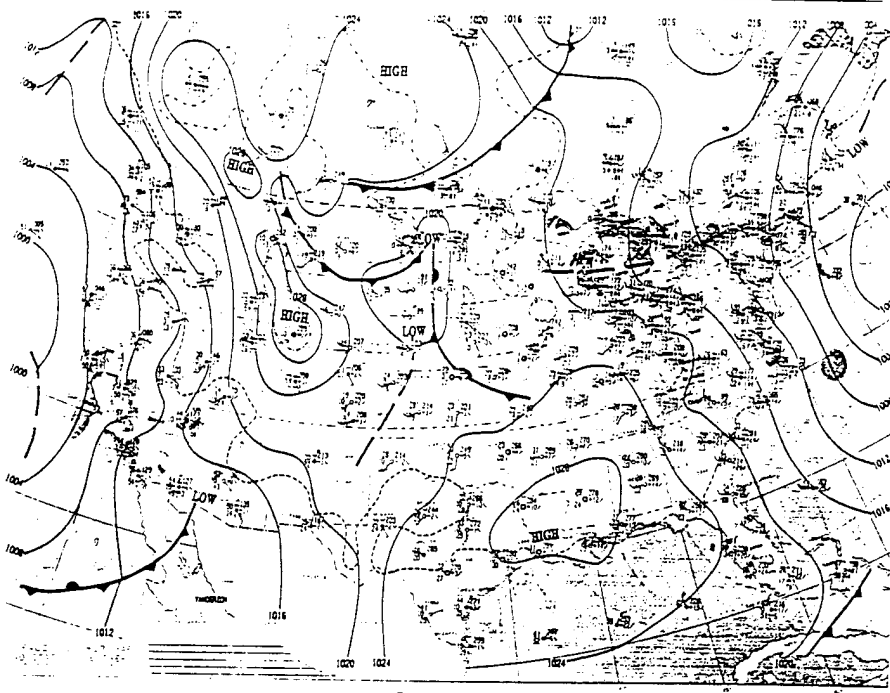
SUNDAY, JANUARY 22, 1995



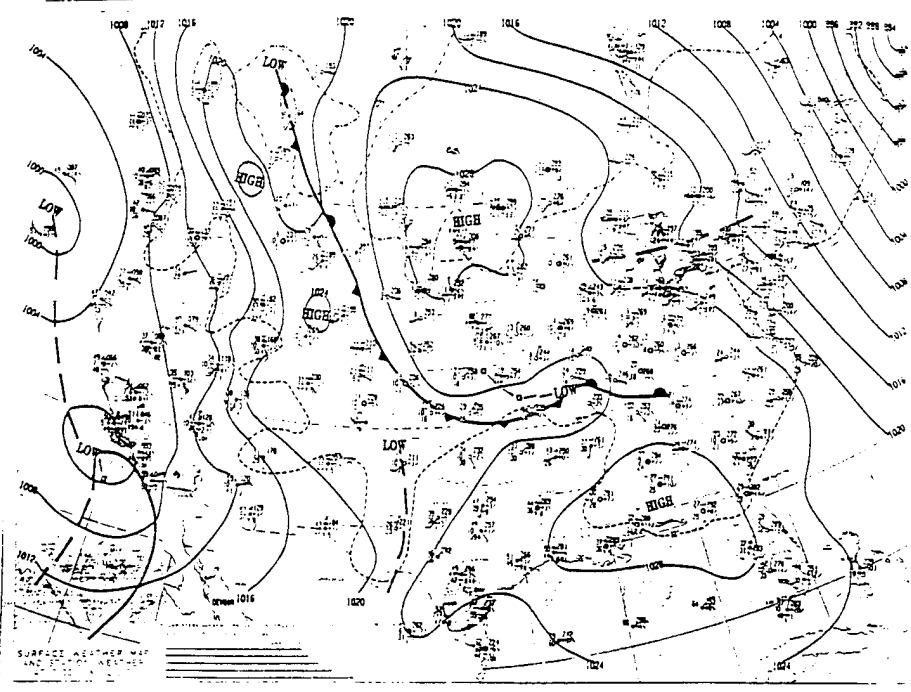
MONDAY, JANUARY 23, 1995



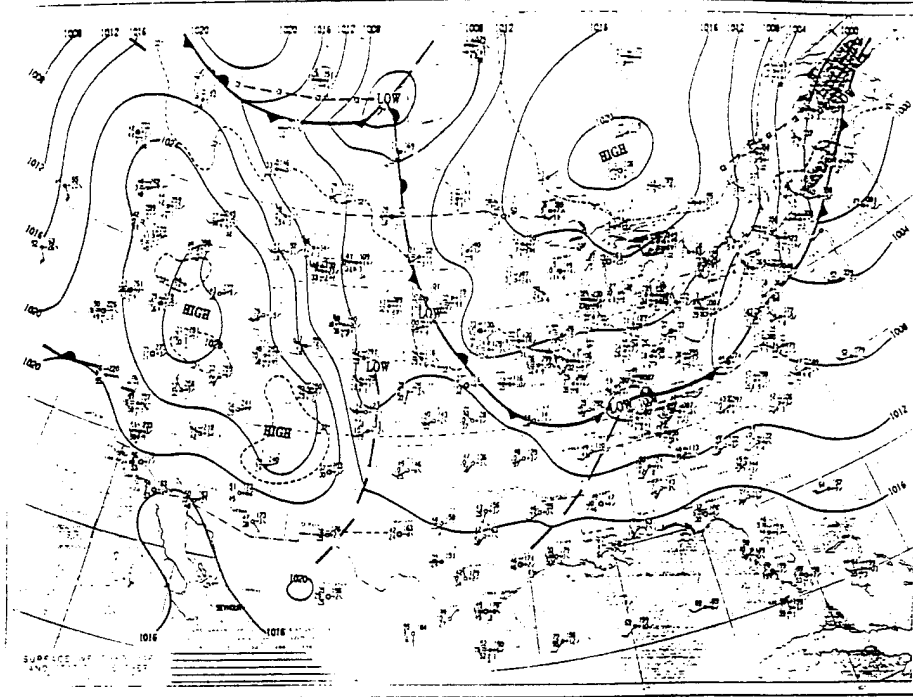
TUESDAY, JANUARY 24, 1995



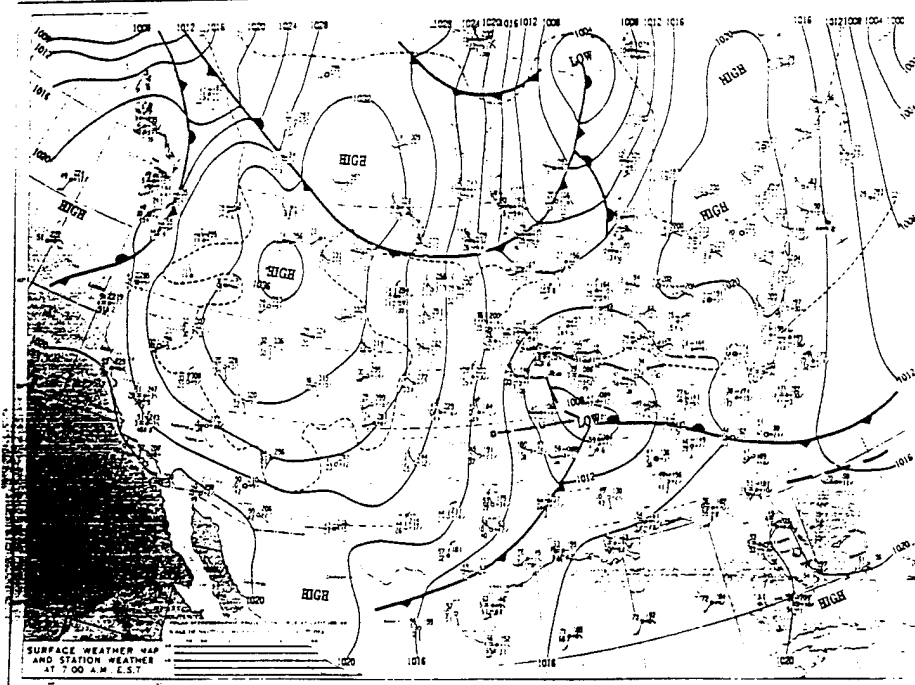
WEDNESDAY, JANUARY 25, 1995

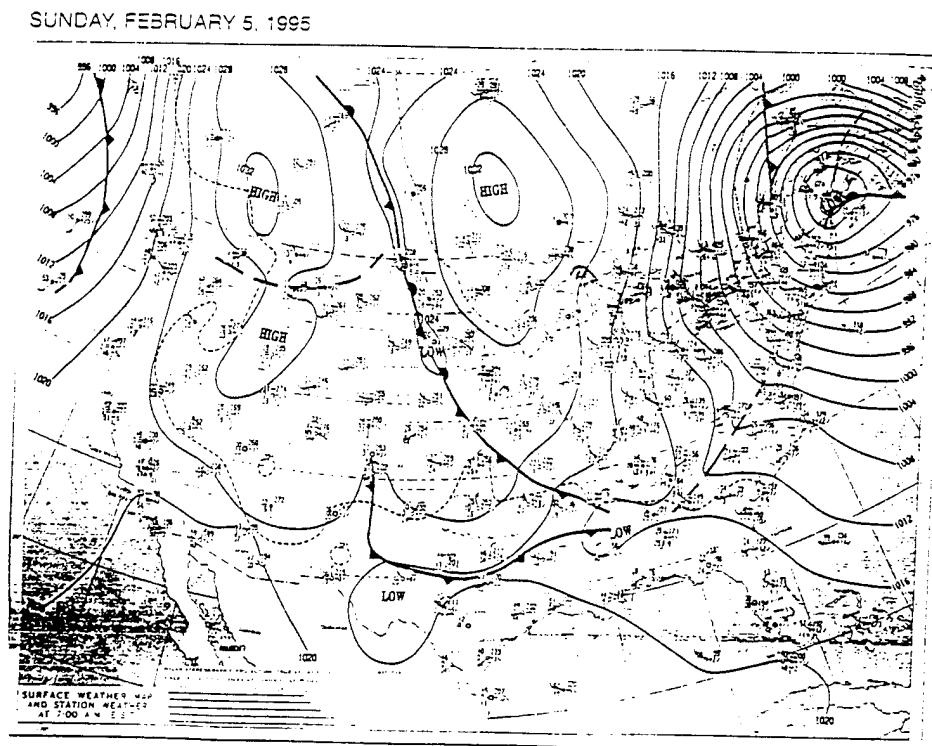
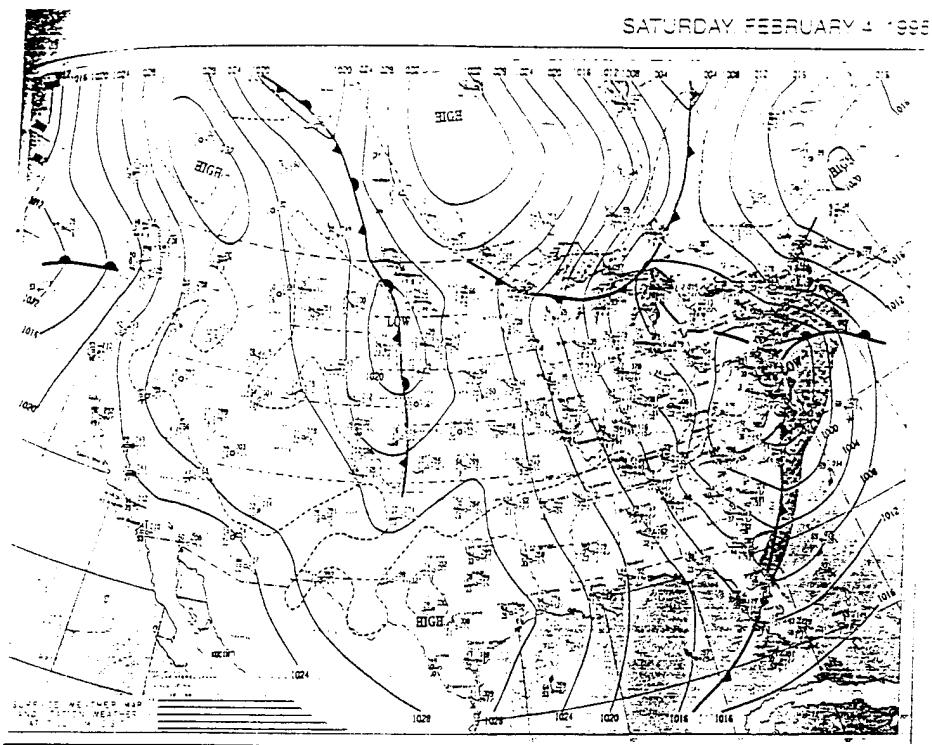


THURSDAY, FEBRUARY 2, 1995

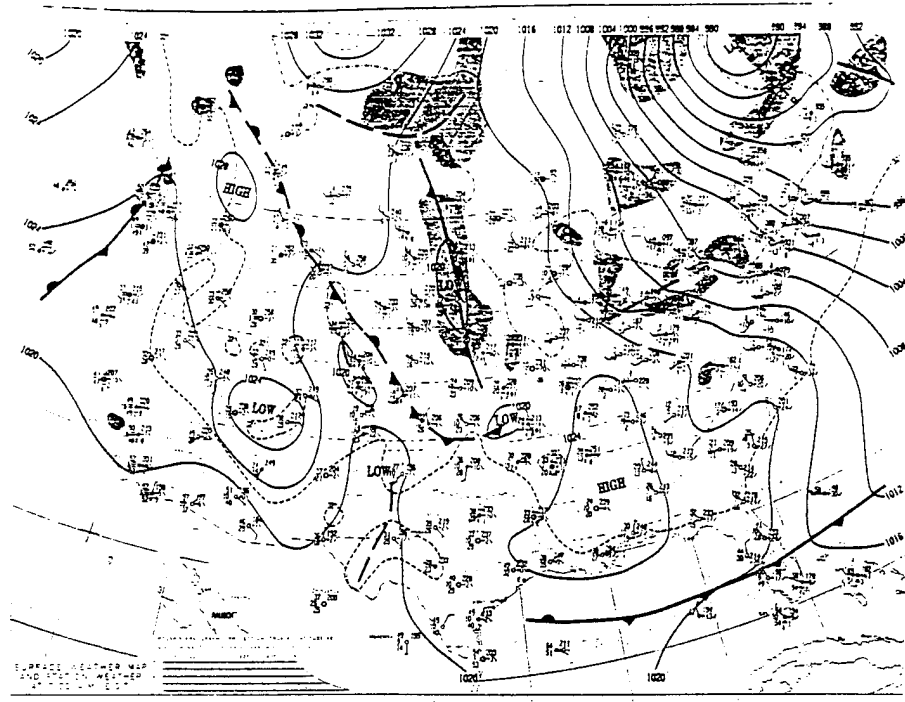


FRIDAY, FEBRUARY 3, 1995

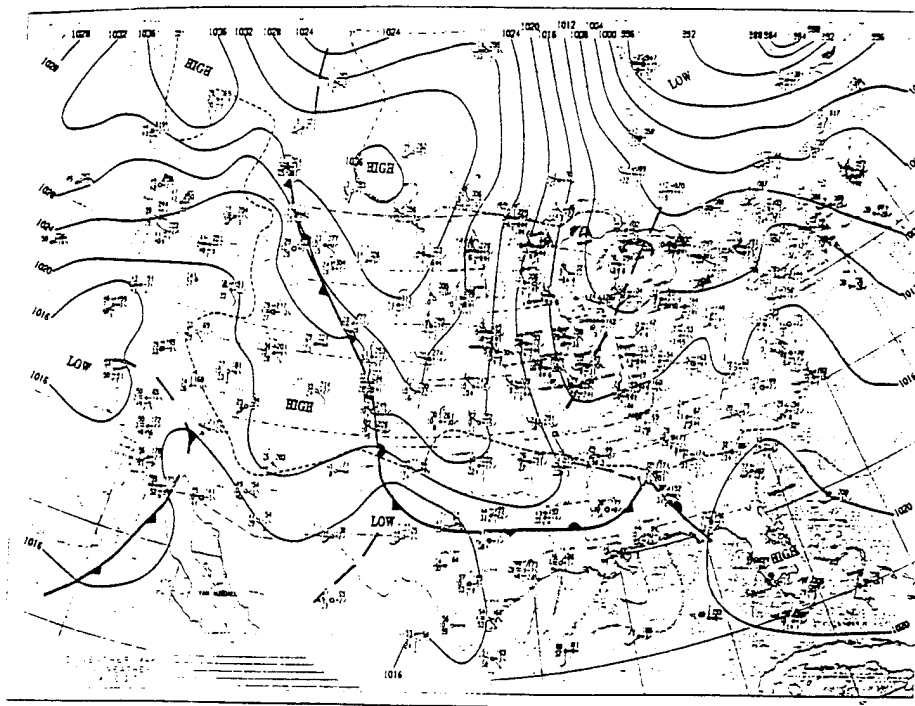




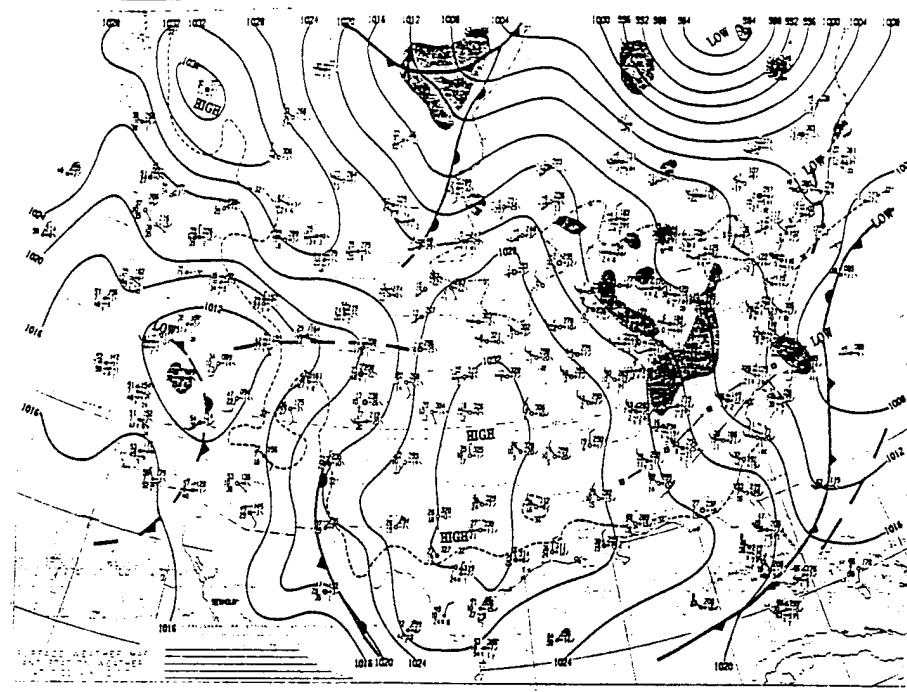
MONDAY, FEBRUARY 6, 1995



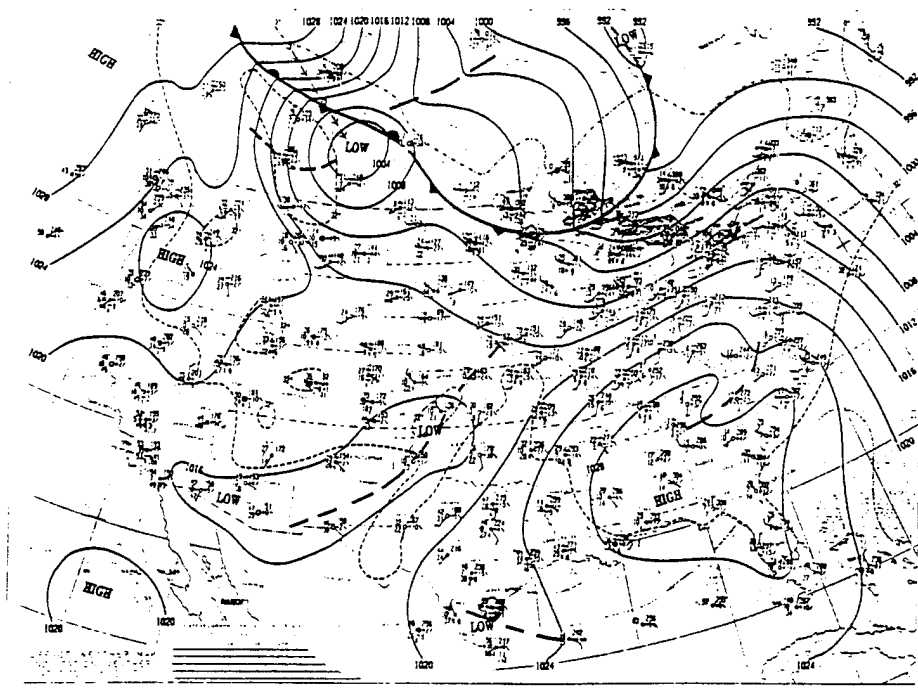
TUESDAY, FEBRUARY 7, 1995



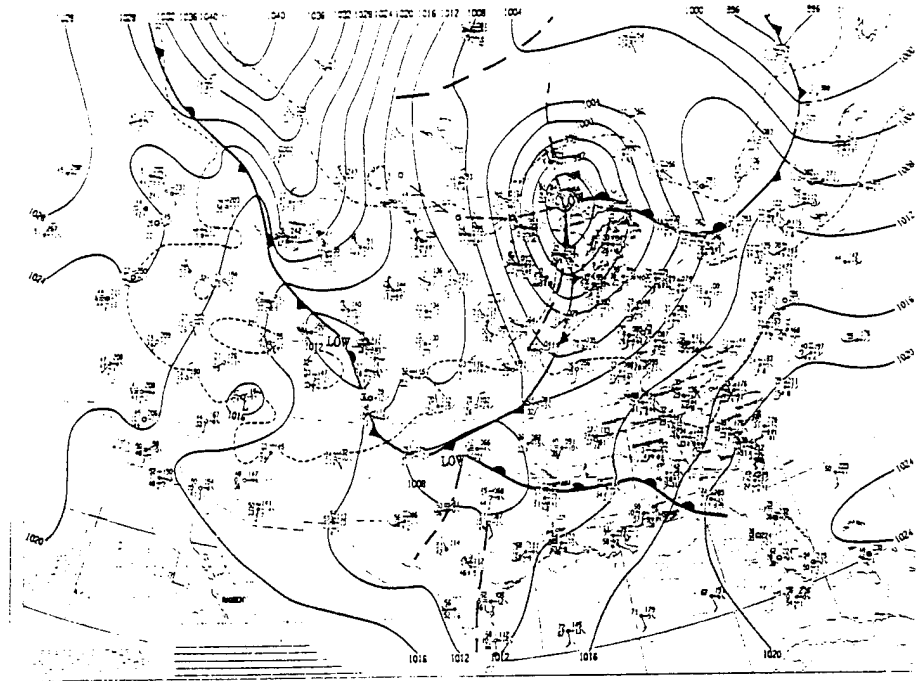
WEDNESDAY, FEBRUARY 8, 1995



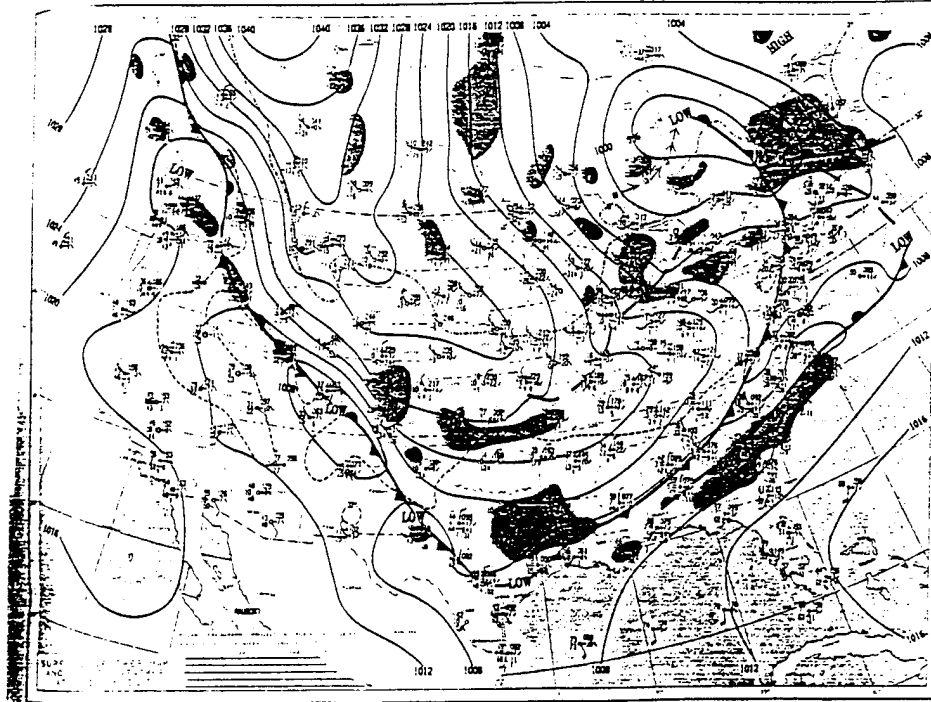
THURSDAY, FEBRUARY 9, 1995



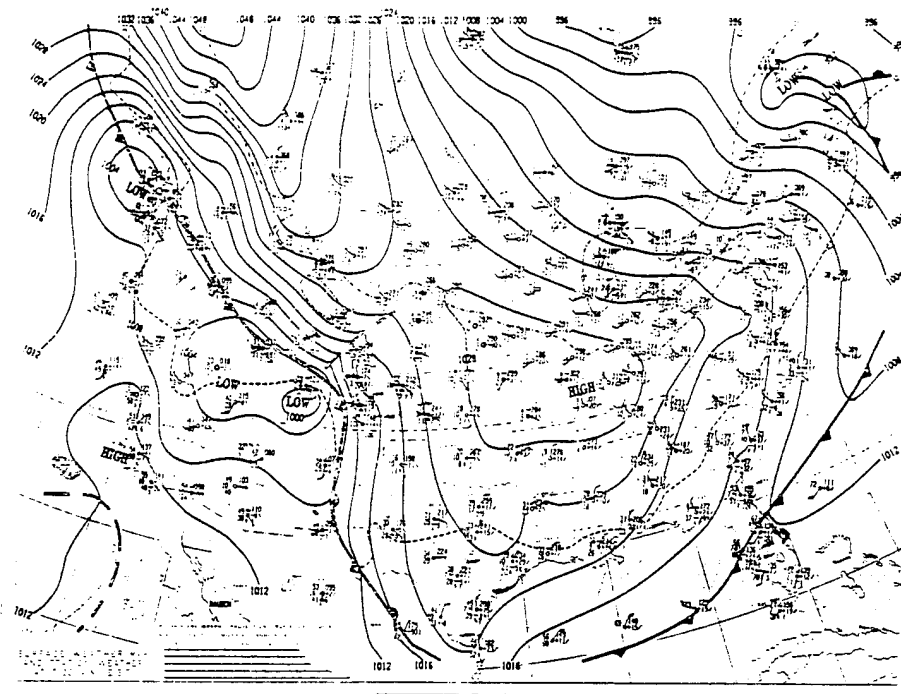
FRIDAY, FEBRUARY 10, 1995



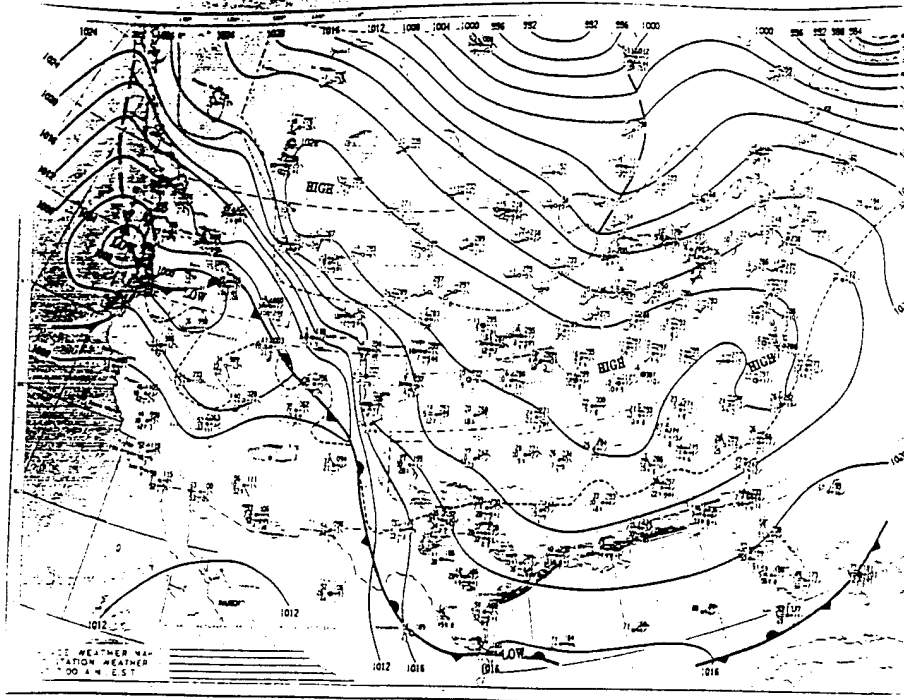
SATURDAY, FEBRUARY 11, 1995



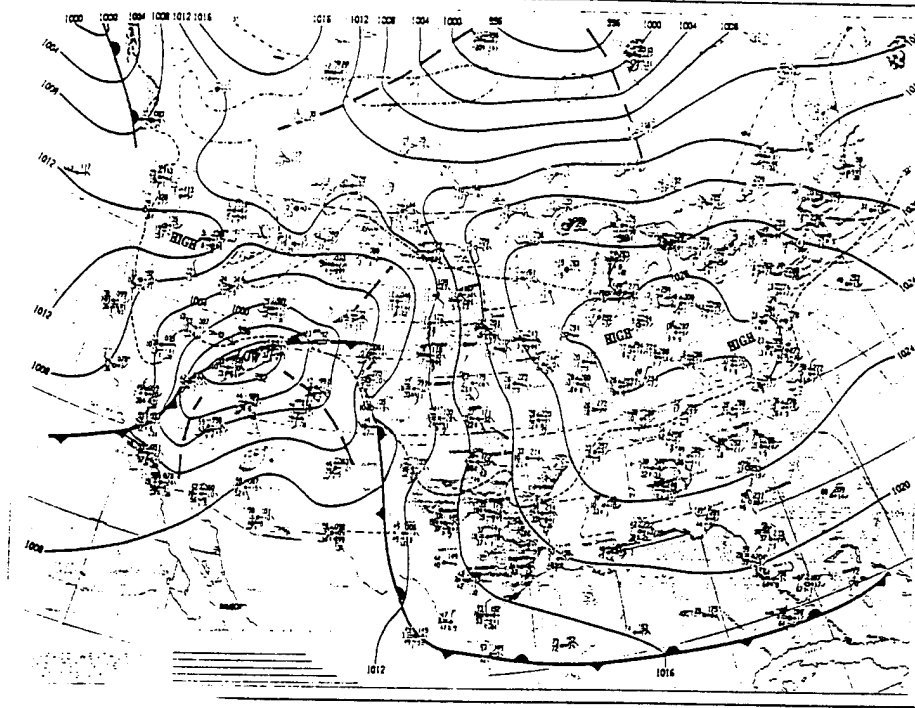
SUNDAY, FEBRUARY 12, 1995



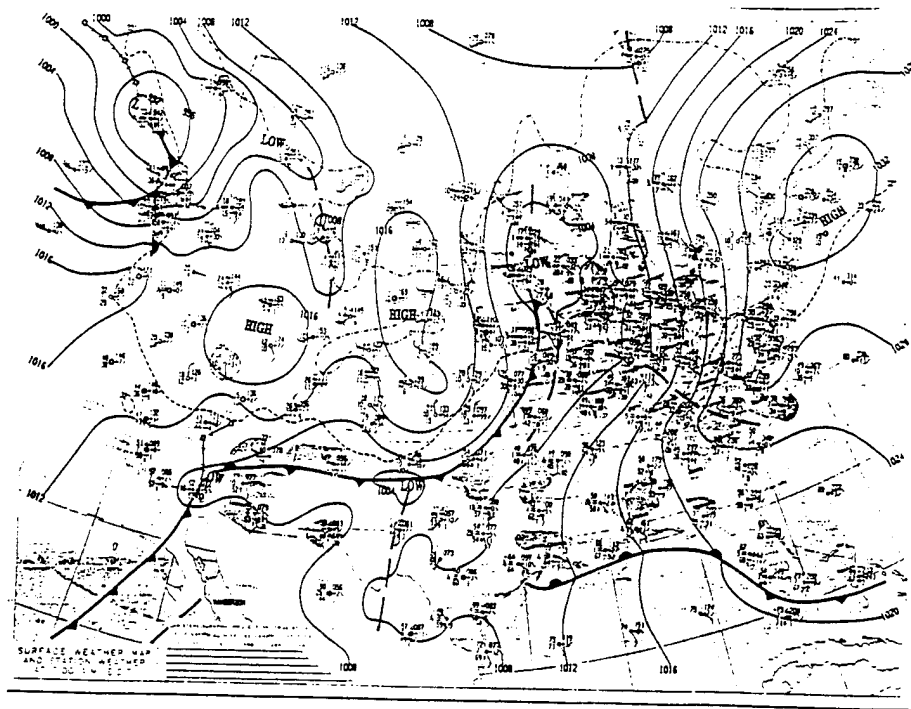
MONDAY, FEBRUARY 13, 1995



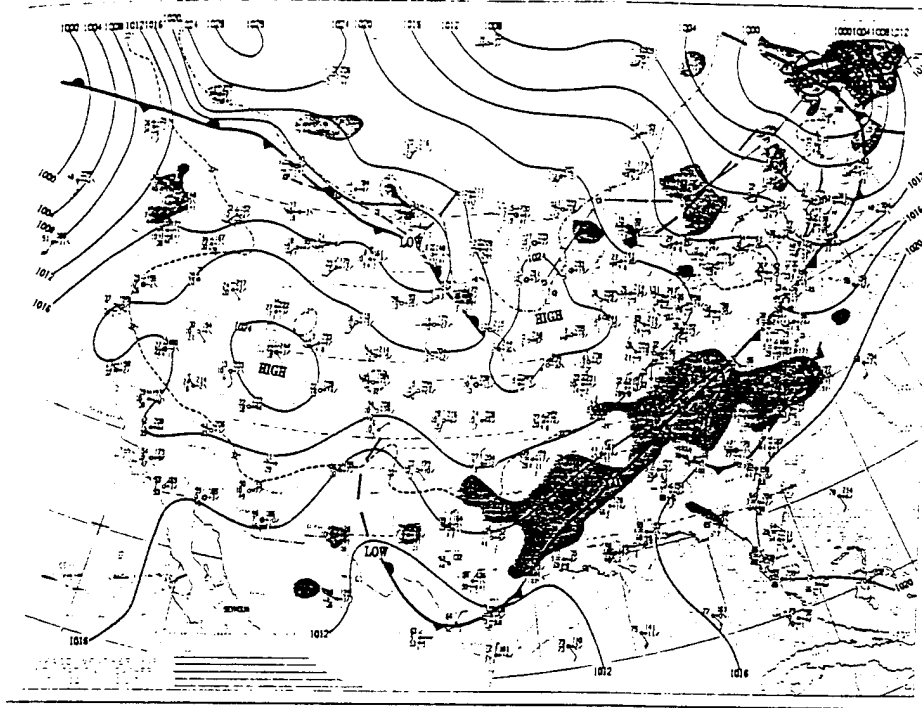
TUESDAY, FEBRUARY 14, 1995



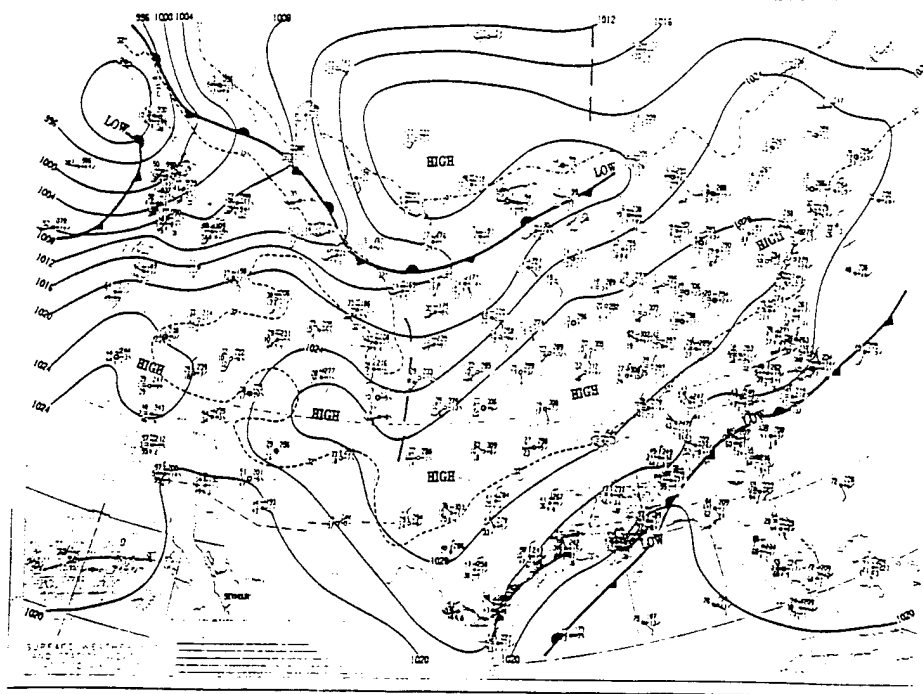
WEDNESDAY, FEBRUARY 15, 1995



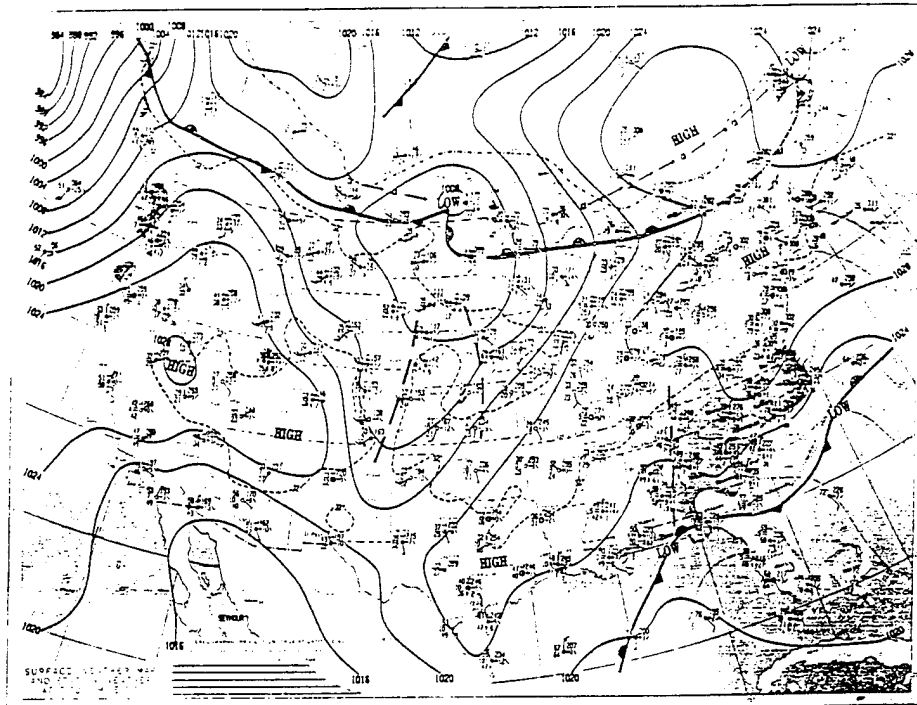
THURSDAY, FEBRUARY 16, 1995



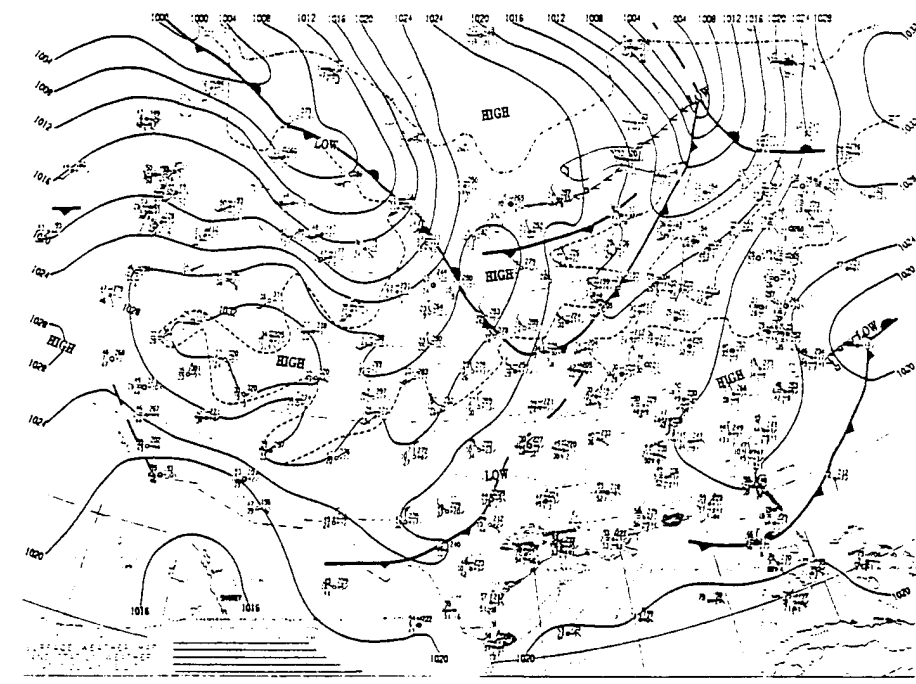
FRIDAY, FEBRUARY 17, 1995



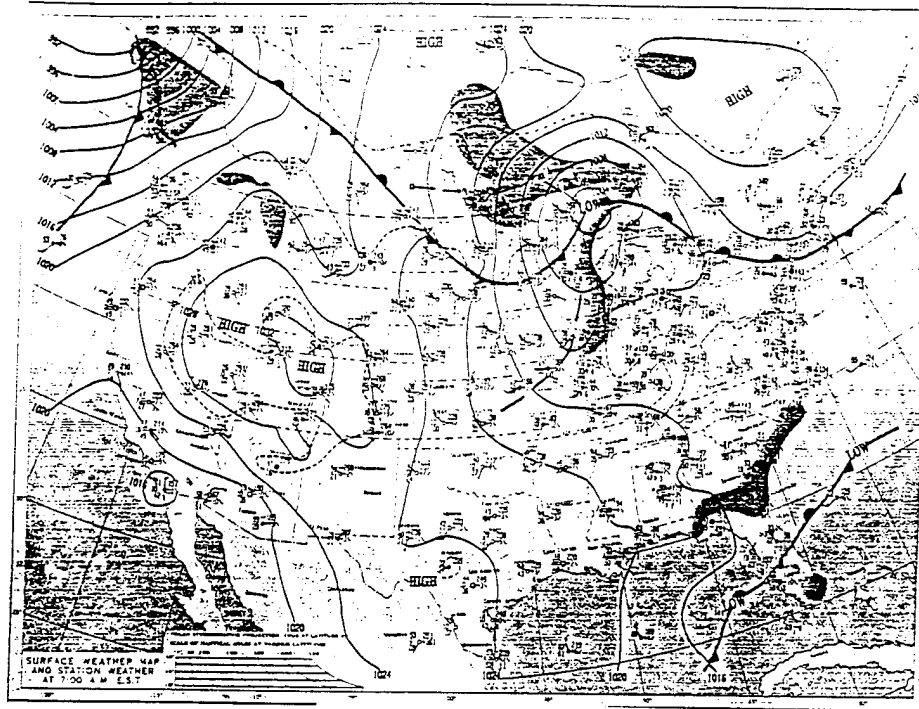
SATURDAY, FEBRUARY 18, 1995



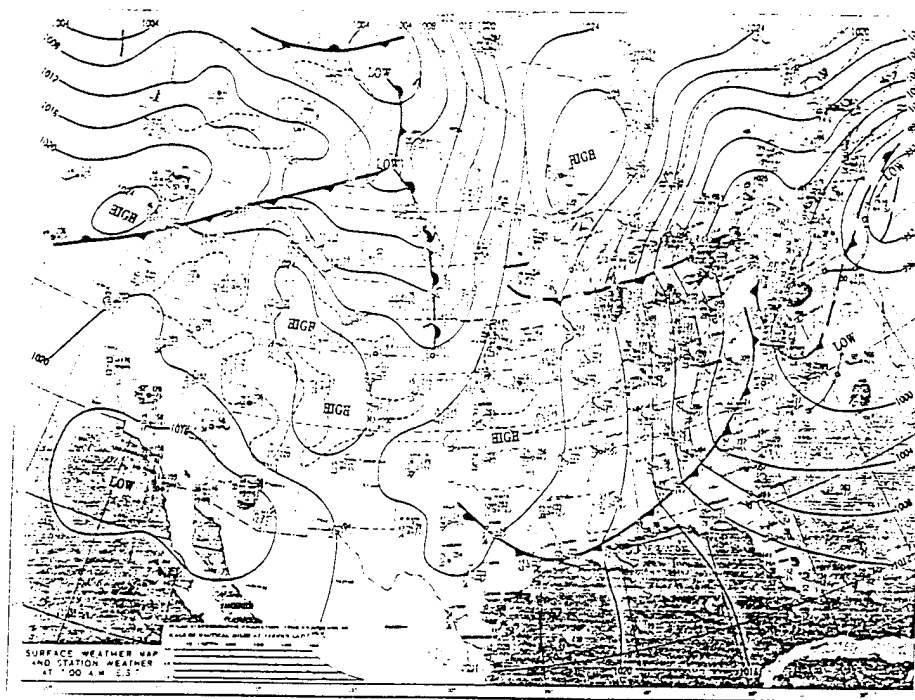
SUNDAY, FEBRUARY 19, 1994



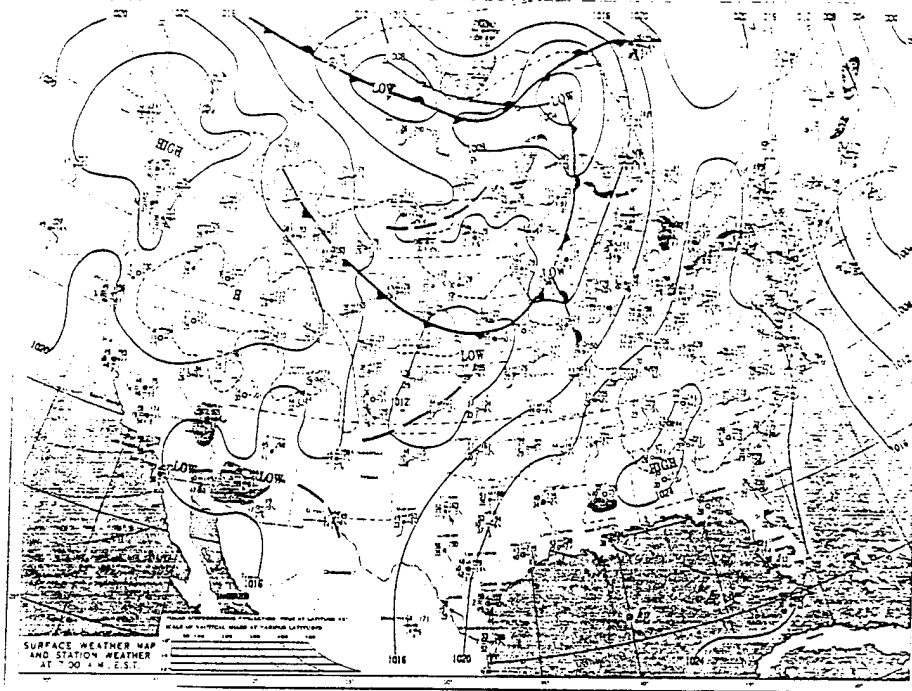
MONDAY, FEBRUARY 20, 1995



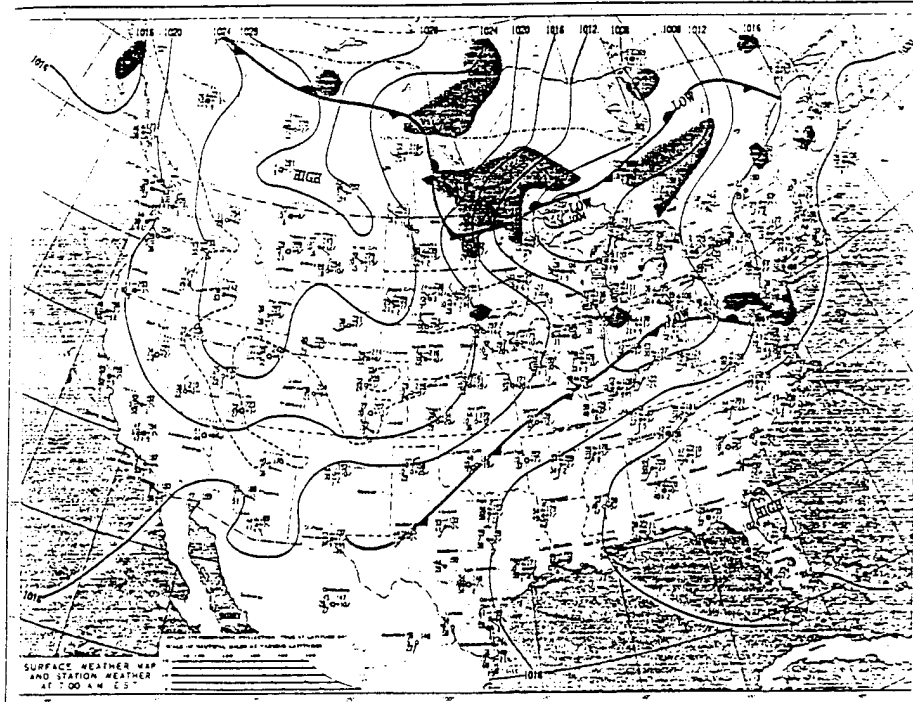
TUESDAY, FEBRUARY 21, 1995



WEDNESDAY, FEBRUARY 22, 1955



THURSDAY, FEBRUARY 23, 1955



7.2 Appendix 2. Raw Data

7.2.1 250 and 433 Meters

7.2.1.1 NO Mixing Ratios

	12/7/95	12/8/95	12/9/95	12/10/95	12/11/95	12/12/95	12/13/95	12/14/95	12/15/95	12/16/95
12:15 AM		0.00	0.00	0.00	0.00	0.00	0.00	0.00	0.00	0.00
12:30 AM		0.00	0.00	0.00	0.00	0.00	0.00	0.00	0.00	0.00
12:45 AM		0.30	0.00	0.36	0.00	0.00	0.00	0.00	0.00	0.00
1:00 AM		0.00	0.00	0.39	0.00	0.00	0.00	0.00	0.00	0.27
1:15 AM		0.00	0.00	0.70	0.00	0.00	0.00	0.00	0.00	0.48
1:30 AM		0.00	0.00	0.92	0.00	0.00	0.00	0.00	0.00	0.00
1:45 AM		0.00	0.00	0.31	0.00	0.00	0.00	0.00	0.00	0.25
2:00 AM		0.00	0.00	0.38	0.00	0.00	0.00	0.00	0.00	0.00
2:15 AM		0.93	0.00	0.40	0.00	0.00	0.00	0.00	0.00	0.74
2:30 AM		0.96	0.00	0.29	0.00	0.00	0.00	0.00	0.00	0.55
2:45 AM		0.76	0.00	0.47	0.00	0.00	0.00	0.00	0.00	0.58
3:00 AM		1.09	0.00	0.39	0.00	0.00	0.00	0.00	0.00	0.00
3:15 AM		1.02	0.00	0.32	0.00	0.00	0.00	0.00	0.00	0.00
3:30 AM		1.17	0.00	0.34	0.00	0.00	0.00	0.00	0.00	0.00
3:45 AM		1.24	0.00	0.87	0.00	0.00	0.00	0.00	0.00	0.41
4:00 AM		0.79	0.00	0.60	0.00	0.00	0.00	0.00	0.00	0.33
4:15 AM		0.88	0.00	0.26	0.00	0.00	0.00	0.25	0.00	0.00
4:30 AM		0.29	0.00	0.24	0.00	0.00	0.00	0.00	0.00	0.00
4:45 AM		1.06	0.00	0.60	0.30	0.00	0.00	0.00	0.00	0.00
5:00 AM		3.33	0.00	0.38	1.80	0.00	0.00	0.26	0.00	0.00
5:15 AM		1.66	0.00	0.00	0.26	0.00	0.00	0.00	0.00	0.00
5:30 AM		1.00	0.00	0.00	0.00	0.00	0.00	0.23	0.00	0.00
5:45 AM		1.27	0.00	0.00	0.00	0.00	0.00	0.66	0.00	0.00
6:00 AM		0.90	0.00	0.00	0.24	0.00	0.00	0.39	0.00	0.00
6:15 AM		0.51	0.00	0.00	0.37	0.00	0.00	0.24	0.00	0.00
6:30 AM		0.82	0.00	0.31	0.67	0.00	0.00	0.00	0.00	0.00
6:45 AM		1.08	0.00	0.25	3.91	0.00	0.00	0.00	0.00	0.00
7:00 AM		0.77	0.00	0.00	4.23	0.00	0.00	0.00	0.00	0.00
7:15 AM		1.11	0.00	0.00	6.32	0.00	0.00	0.46	0.00	0.00
7:30 AM		3.15	0.00	0.00	6.73	0.28	0.00	1.12	0.00	0.00
7:45 AM		8.52	0.00	0.55	6.13	0.61	0.00	1.41	0.00	0.00
8:00 AM		13.64	0.00	0.00	10.21	0.99	0.00	2.25	0.00	0.31
8:15 AM		7.82	0.00	0.00	13.60	0.92	0.00	3.28	0.25	0.54
8:30 AM		4.10	0.00	0.40	14.50	0.89	0.00	3.12	0.31	0.60
8:45 AM		4.14	0.00	0.00	8.77	0.91	0.00	4.14	0.42	
9:00 AM		3.96	0.00	0.25	5.77	0.93	0.00	4.51	0.44	
9:15 AM		3.54	0.00	0.00	3.71	0.92	0.00	5.26	0.61	
9:30 AM	0.00	2.54	0.00	0.39	3.00	1.12	0.00	5.75	0.69	
9:45 AM	0.00	2.32	0.00	0.54	2.54	1.30	0.00	5.96	0.95	
10:00 AM	0.00	1.80	0.00	0.57	2.50	1.50	0.00	6.81	1.19	
10:15 AM	0.44	1.70	0.00	0.67	2.34	1.70	0.00	5.39	1.25	
10:30 AM	1.37	1.59	0.00	0.65	2.52	2.09	0.00	6.43	1.24	
10:45 AM	2.11	1.71	0.00	0.43	2.25	1.74	0.00	7.29	1.55	
11:00 AM	9.02	1.69	0.00	0.32	2.31	1.72	0.00	6.30	1.54	
11:15 AM	10.88	1.51	0.00	0.95	2.63	1.78	0.00	7.19	1.73	
11:30 AM	12.63	1.57	0.00	0.28	2.50	1.92	0.00	6.32	1.96	
11:45 AM	9.83	1.52	0.00	1.29	2.14	1.83	0.00	4.19	1.77	
12:00 PM	7.32	1.46	0.00	1.16	2.24	1.91	0.00	5.36	1.85	

	12/7/95	12/8/95	12/9/95	12/10/95	12/11/95	12/12/95	12/13/95	12/14/95	12/15/95	12/16/95
12:15 PM	5.65	1.51	0.00	1.00	1.98	1.94	0.00	6.48	2.09	
12:30 PM	5.12	1.43	0.58	1.30	1.95	1.80	0.00	6.76	2.18	
12:45 PM	5.31	1.40	0.33	0.59	1.84	1.92	0.00	6.65	2.22	
1:00 PM	5.56	0.00	1.05	0.69	1.50	1.77	0.00	6.65	2.47	
1:15 PM	5.18	0.00	0.51	0.88	1.38	1.70	0.00	6.28	2.41	
1:30 PM	5.32	0.00	0.32	23.36	1.37	1.67	0.00	5.01	2.48	
1:45 PM	6.16	0.00	0.00	40.78	1.46	1.68	0.00	4.06	2.49	
2:00 PM	7.05	0.00	0.66	34.10	1.77	1.69	0.00	3.47	2.20	
2:15 PM	7.02	0.00	0.46	15.18	1.72	1.34	0.00	3.36	2.95	
2:30 PM	7.89	0.00	1.25	7.26	1.67	1.51	0.00	2.90	2.71	
2:45 PM	8.08	0.00	0.34	5.09	1.56	1.51	0.00	2.12	1.43	
3:00 PM	8.02	0.00	1.05	4.33	1.75	1.35	0.00	1.31	1.53	
3:15 PM	8.40	0.00	0.69	1.56	1.50	1.21	0.00	1.55	1.75	
3:30 PM	7.89	0.00	0.46	0.26	1.34	1.03	0.00	1.40	1.32	
3:45 PM	6.35	0.00	0.36	1.25	0.92	0.84	0.00	1.33	0.93	
4:00 PM	4.70	0.00	0.24	1.23	0.80	0.61	0.00	1.13	0.82	
4:15 PM	4.27	0.00	0.25	2.38	0.51	0.52	0.00	1.02	0.70	
4:30 PM	2.32	0.00	0.40	0.88	0.45	0.36	0.00	1.03	0.44	
4:45 PM	1.46	0.00	0.45	0.28	0.27	0.00	0.00	0.77	0.30	
5:00 PM	0.59	0.00	0.69	0.00	0.00	0.00	0.00	0.30	0.00	
5:15 PM	0.00	0.00	0.52	0.00	0.00	0.00	0.00	0.00	0.00	
5:30 PM	0.00	0.00	1.16	0.00	0.00	0.00	0.00	0.00	0.00	
5:45 PM	0.00	0.00	0.30	0.00	0.00	0.00	0.00	0.00	0.00	
6:00 PM	0.00	0.00	0.46	0.00	0.00	0.00	0.00	0.00	0.00	
6:15 PM	0.00	0.00	0.64	0.24	0.00	0.00	0.00	0.00	0.00	
6:30 PM	0.00	0.00	1.01	0.00	0.00	0.00	0.00	0.00	0.00	
6:45 PM	0.00	0.00	0.75	0.00	0.00	0.00	0.00	0.00	0.00	
7:00 PM	0.00	0.00	0.30	0.00	0.00	0.00	0.00	0.00	0.00	
7:15 PM	0.00	0.00	0.34	0.00	0.00	0.00	0.00	0.00	0.00	
7:30 PM	0.00	0.00	0.79	0.00	0.00	0.00	0.00	0.42	0.00	
7:45 PM	0.00	0.00	0.75	0.00	0.00	0.00	0.00	0.25	0.00	
8:00 PM	0.00	0.00	0.26	0.00	0.00	0.00	0.00	0.00	0.00	
8:15 PM	0.00	0.00	0.12	0.00	0.00	0.00	0.00	0.00	0.00	
8:30 PM	0.47	0.00	0.67	0.00	0.00	0.00	0.00	0.00	0.00	
8:45 PM	0.24	0.00	0.81	0.00	0.00	0.00	0.00	0.00	0.00	
9:00 PM	0.65	0.00	1.12	0.00	0.00	0.00	0.00	0.00	0.25	
9:15 PM	0.00	0.00	0.47	0.00	0.00	0.00	0.00	0.00	0.24	
9:30 PM	0.00	0.00	0.46	0.00	0.00	0.00	0.00	0.00	0.49	
9:45 PM	0.00	0.00	0.45	0.00	0.00	0.00	0.00	0.00	0.29	
10:00 PM	0.00	0.00	0.73	0.00	0.00	0.00	0.00	0.00	0.28	
10:15 PM	0.00	0.00	0.00	0.00	0.00	0.00	0.00	0.00	0.00	
10:30 PM	0.00	0.00	0.41	0.00	0.00	0.00	0.00	0.00	0.24	
10:45 PM	0.00	0.00	0.44	0.00	0.00	0.00	0.00	0.00	0.00	
11:00 PM	0.00	0.00	0.36	0.25	0.00	0.00	0.00	0.00	0.00	
11:15 PM	0.35	0.00	0.45	0.00	0.00	0.00	0.00	0.00	0.00	
11:30 PM	0.00	0.00	0.55	0.00	0.00	0.00	0.00	0.00	0.00	
11:45 PM	0.00	0.00	0.94	0.00	0.00	0.00	0.00	0.00	0.00	
12:00 AM	0.00	0.00	0.69	0.00	0.00	0.00	0.00	0.00	0.00	

	1/12/95	1/13/95	1/14/95	1/15/95	1/16/95	1/17/95	1/18/95	1/19/95	1/23/95
12:15 AM		0.00	0.00	0.00	0.00	0.00	0.00	0.00	
12:30 AM		0.00	0.00	0.00	0.00	0.00	0.00	0.00	
12:45 AM		0.00	0.00	0.00	0.00	0.00	0.00	0.00	
1:00 AM		0.00	0.00	0.00	0.00	0.00	0.00	0.00	
1:15 AM		0.00	0.00	0.00	0.00	0.00	0.00	0.00	
1:30 AM		0.00	0.00	0.00	0.00	0.00	0.00	0.00	
1:45 AM		0.00	0.00	0.00	0.00	0.00	0.00	0.00	
2:00 AM		0.00	0.00	0.00	0.00	0.00	0.00	0.00	
2:15 AM		0.00	0.00	0.00	0.00	0.00	0.00	0.00	
2:30 AM		0.00	0.00	0.00	0.00	0.00	0.00	0.00	
2:45 AM		0.00	0.00	0.00	0.00	0.00	0.00	0.00	
3:00 AM		0.00	0.00	0.00	0.00	0.00	0.00	0.00	
3:15 AM		0.00	0.00	0.00	0.00	0.00	0.00	0.00	
3:30 AM		0.00	0.00	0.00	0.00	0.00	0.00	0.00	
3:45 AM		0.00	0.00	0.00	0.00	0.00	0.00	0.00	
4:00 AM		0.00	0.00	0.00	0.00	0.00	0.00	0.00	
4:15 AM		0.00	0.00	0.00	0.00	0.00	0.00	0.00	
4:30 AM		0.00	0.00	0.00	0.00	0.00	0.00	0.00	
4:45 AM		0.00	0.00	0.00	0.00	0.00	0.00	0.00	
5:00 AM		0.00	0.00	0.00	0.00	0.00	0.00	0.00	
5:15 AM		0.00	0.00	0.00	0.00	0.00	0.00	0.00	
5:30 AM		0.00	0.00	0.00	0.00	0.00	0.00	0.00	
5:45 AM		0.00	0.00	0.00	0.00	0.00	0.00	0.00	
6:00 AM		0.00	0.00	0.00	0.00	0.00	0.00	0.00	
6:15 AM		0.00	0.00	0.00	0.00	0.00	0.00	0.00	
6:30 AM		0.00	0.00	0.00	0.00	0.00	0.00	0.00	
6:45 AM		0.00	0.00	0.00	0.00	0.00	0.00	0.00	
7:00 AM		0.00	0.00	0.00	0.00	0.00	0.00	0.00	
7:15 AM		0.00	0.00	0.00	0.00	0.00	0.00	0.00	
7:30 AM		0.00	0.00	0.00	0.00	0.00	0.00	0.00	
7:45 AM		0.00	0.00	0.00	0.00	0.00	0.00	0.06	
8:00 AM		0.00	0.00	0.00	0.00	0.00	0.00	0.05	
8:15 AM		0.00	0.00	0.00	0.00	0.00	0.00	0.08	
8:30 AM		0.00	0.00	0.00	0.00	0.00	0.00	0.10	
8:45 AM		0.00	0.00	0.00	0.00	0.00	0.00	0.17	
9:00 AM		0.00	0.00	0.00	0.00	0.00	0.00	0.24	
9:15 AM		0.00	0.00	0.00	0.00	0.00	0.00	0.30	
9:30 AM		0.00	0.00	0.00	0.00	0.00	0.00	0.41	
9:45 AM		0.00	0.00	0.00	0.00	0.00	0.00	0.51	
10:00 AM		0.00	0.00	0.00	0.00	0.00	0.00	0.58	
10:15 AM		0.00	0.00	0.00	0.00	0.00	0.00	0.00	
10:30 AM		0.00	0.00	0.00	0.00	0.00	0.00	0.00	
10:45 AM		0.00	0.00	0.00	0.00	0.00	0.00	0.00	
11:00 AM		0.00	0.00	0.00	0.00	0.00	0.00		
11:15 AM		0.00	0.00	0.00	0.00	0.00	0.00		
11:30 AM		0.00	0.00	0.00	0.00	0.00	0.00		
11:45 AM		0.00	0.00	0.00	0.00	0.00	0.00		
12:00 PM		0.00	0.00	0.00	0.00	0.05	0.31		

	1/12/95	1/13/95	1/14/95	1/15/95	1/16/95	1/17/95	1/18/95	1/19/95	1/23/95
12:15 PM		0.00	0.00	0.00	0.00	0.49	0.85		
12:30 PM		0.00	0.00	0.00	0.00	0.25	0.49		
12:45 PM		0.05	0.00	0.00	0.00	0.15	0.24		
1:00 PM		0.17	0.00	0.00	0.00	0.19	0.31		
1:15 PM		0.11	0.00	0.00	0.00	1.68	0.28		
1:30 PM		0.12	0.00	0.00	0.00	0.19	0.17		
1:45 PM		0.06	0.00	0.00	0.00	0.00	0.00		
2:00 PM		0.00	0.00	0.00	0.00	0.00	0.06		
2:15 PM		0.08	0.00	0.00	0.00	0.38	0.00		
2:30 PM		0.18	0.00	0.00	0.00	0.00	0.04		
2:45 PM		0.00	0.00	0.00	0.00	0.10	0.00		
3:00 PM		0.00	0.00	0.00	0.00	0.06	0.17		
3:15 PM		0.00	0.00	0.00	0.00	0.06	0.33		
3:30 PM	0.71	0.00	0.00	0.00	0.00	0.08	0.25		
3:45 PM	0.59	0.00	0.00	0.00	0.00	0.00	0.14		
4:00 PM	0.28	0.00	0.00	0.00	0.00	0.00	0.05		
4:15 PM	0.25	0.00	0.00	0.00	0.00	0.00	0.00		
4:30 PM	0.24	0.00	0.00	0.08	0.00	0.00	0.00		
4:45 PM	0.18	0.00	0.00	0.08	0.00	0.00	0.00		
5:00 PM	0.14	0.00	0.00	0.00	0.00	0.00	0.00		
5:15 PM	0.11	0.00	0.00	0.00	0.00	0.00	0.00		
5:30 PM	0.00	0.00	0.00	0.00	0.00	0.00	0.00		
5:45 PM	0.00	0.00	0.00	0.00	0.00	0.00	0.00		
6:00 PM	0.00	0.00	0.00	0.00	0.00	0.00	0.00		
6:15 PM	0.00	0.00	0.00	0.00	0.00	0.00	0.00		
6:30 PM	0.04	0.00	0.00	0.00	0.00	0.00	0.00		
6:45 PM	0.00	0.00	0.00	0.00	0.00	0.00	0.00		
7:00 PM	0.00	0.00	0.00	0.00	0.00	0.00	0.00		
7:15 PM	0.00	0.00	0.00	0.00	0.00	0.00	0.00		
7:30 PM	0.00	0.00	0.00	0.00	0.00	0.00	0.00		
7:45 PM	0.00	0.00	0.00	0.00	0.00	0.00	0.00		
8:00 PM	0.00	0.00	0.00	0.00	0.00	0.00	0.00		
8:15 PM	0.00	0.00	0.00	0.00	0.00	0.00	0.00		
8:30 PM	0.00	0.00	0.00	0.00	0.00	0.00	0.00		
8:45 PM	0.00	0.00	0.00	0.00	0.00	0.00	0.00		
9:00 PM	0.00	0.00	0.00	0.00	0.00	0.00	0.00		
9:15 PM	0.00	0.00	0.00	0.00	0.00	0.00	0.00		
9:30 PM	0.00	0.00	0.00	0.00	0.00	0.00	0.00		
9:45 PM	0.00	0.00	0.00	0.00	0.00	0.00	0.00		
10:00 PM	0.00	0.00	0.00	0.00	0.00	0.00	0.00		
10:15 PM	0.00	0.00	0.00	0.00	0.00	0.00	0.00		
10:30 PM	0.00	0.00	0.00	0.00	0.00	0.00	0.00		
10:45 PM	0.00	0.00	0.00	0.00	0.00	0.00	0.00		0.00
11:00 PM	0.00	0.00	0.00	0.00	0.00	0.00	0.00		0.00
11:15 PM	0.00	0.00	0.00	0.00	0.00	0.00	0.00		0.00
11:30 PM	0.00	0.00	0.00	0.00	0.00	0.00	0.00		0.00
11:45 PM	0.00	0.00	0.00	0.00	0.00	0.00	0.00		0.00
12:00 AM	0.00	0.00	0.00	0.00	0.00	0.00	0.00		0.99

	1/24/95	1/25/95	2/2/95	2/3/95	2/4/95	2/5/95	2/6/95	2/7/95	2/8/95
12:15 AM	0.00	0.00		0.00	0.00	0.00	0.00	0.00	0.00
12:30 AM	0.00	0.00		0.00	0.00	0.00	0.00	0.00	0.00
12:45 AM	0.00	0.00		0.00	0.00	0.00	0.00	0.00	0.00
1:00 AM	0.00	0.00		0.00	0.00	0.00	0.00	0.00	0.00
1:15 AM	0.05	0.00		0.00	0.00	0.00	0.00	0.00	0.00
1:30 AM	0.00	0.00		0.00	0.00	0.00	0.00	0.00	0.00
1:45 AM	0.00	0.00		0.04	0.00	0.00	0.00	0.00	0.00
2:00 AM	0.00	0.00		0.11	0.00	0.00	0.00	0.00	0.00
2:15 AM	0.00	0.00		0.14	0.00	0.00	0.00	0.00	0.00
2:30 AM	0.00	0.00		0.14	0.04	0.00	0.00	0.00	0.00
2:45 AM	0.00	0.00		0.12	0.11	0.00	0.00	0.00	0.00
3:00 AM	0.00	0.00		0.08	0.11	0.00	0.00	0.00	0.00
3:15 AM	0.00	0.00		0.05	0.15	0.00	0.00	0.00	0.00
3:30 AM	0.00	0.00		0.00	0.10	0.00	0.00	0.00	0.00
3:45 AM	0.00	0.00		0.00	0.10	0.00	0.00	0.00	0.00
4:00 AM	0.00	0.00		0.00	0.13	0.00	0.00	0.00	0.00
4:15 AM	0.00	0.00		0.00	0.12	0.00	0.00	0.00	0.00
4:30 AM	0.00	0.00		0.00	0.12	0.00	0.00	0.00	0.00
4:45 AM	0.00	0.00		0.00	0.12	0.00	0.00	0.00	0.00
5:00 AM	0.00	0.00		0.00	0.00	0.00	0.00	0.00	0.00
5:15 AM	0.00	0.00		0.00	0.00	0.00	0.00	0.00	0.00
5:30 AM	0.00	0.00		0.00	0.00	0.00	0.00	0.00	0.00
5:45 AM	0.00	0.00		0.00	0.00	0.00	0.00	0.00	0.00
6:00 AM	0.00	0.00		0.00	0.00	0.00	0.00	0.00	0.00
6:15 AM	0.00	0.00		0.00	0.00	0.00	0.00	0.00	0.00
6:30 AM	0.00	0.00		0.00	0.00	0.00	0.00	0.00	0.00
6:45 AM	0.00	0.00		0.00	0.00	0.00	0.00	0.00	0.00
7:00 AM	0.00	0.00		0.00	0.00	0.00	0.00	0.00	0.00
7:15 AM	0.06	0.00		0.00	0.00	0.00	0.00	0.00	0.00
7:30 AM	0.21	0.00		0.00	0.07	0.00	0.00	0.00	0.00
7:45 AM	0.64	0.00		0.12	0.43	0.09	0.09	0.00	0.00
8:00 AM	1.64	0.00		0.28	0.84	0.20	0.30	0.81	0.00
8:15 AM	2.87	0.00		0.75	1.69	0.36	0.81	2.02	0.00
8:30 AM	3.89	0.00		1.49	2.44	0.50	4.17	1.47	0.06
8:45 AM	4.50	0.00		3.50	3.61	0.51	3.74	3.12	0.15
9:00 AM	4.79	0.00		4.60	4.58	0.60	5.03	3.13	0.77
9:15 AM	4.81	0.00		3.35	4.35	0.57	3.65	2.24	0.37
9:30 AM	7.32	0.00		4.89	3.51	0.67	2.21	6.94	0.59
9:45 AM	8.02	0.12		6.33	3.04	1.07	1.78	5.32	0.38
10:00 AM	7.65	0.42		8.16	2.60	1.67	3.12	3.51	0.93
10:15 AM	7.67	0.00		7.65	3.19	1.61	3.57	2.29	1.20
10:30 AM	8.32	0.40		7.04	3.68	2.61	3.50	1.87	0.76
10:45 AM	9.49	0.23		5.49	3.99	4.40	2.60	1.83	0.21
11:00 AM	8.78	1.08		3.64	6.30	5.19	2.75	1.57	0.19
11:15 AM	7.74	1.23		3.76	7.92	4.68	4.36	1.55	0.11
11:30 AM	6.94	10.99		3.44	8.62	4.38	6.46	3.80	1.84
11:45 AM	6.61	9.80		2.74	7.29	3.94	4.05	2.90	1.02
12:00 PM	5.86	13.00		3.60	6.73	4.79	2.02	2.13	0.80

	1/24/95	1/25/95	2/2/95	2/3/95	2/4/95	2/5/95	2/6/95	2/7/95	2/8/95
12:15 PM	5.16	10.17		4.16	6.32	3.66	1.61	1.35	2.07
12:30 PM	4.97	9.28		3.14	3.86	2.98	1.49	2.08	3.29
12:45 PM	3.72	8.16		3.51	3.91	2.01	1.34	1.12	1.72
1:00 PM	3.40	6.07		2.29	5.05	1.55	0.91	1.00	2.44
1:15 PM	3.36	4.53		3.94	4.14	2.25	1.05	1.07	1.43
1:30 PM	2.93	3.62		2.15	3.89	3.20	0.94	1.52	0.27
1:45 PM	3.07	2.75		2.07	3.33	3.75	1.07	1.40	0.23
2:00 PM	3.20	1.81		1.24	2.49	4.62	0.91	1.01	0.14
2:15 PM	3.19	1.24		1.33	2.64	5.66	1.18	1.70	0.35
2:30 PM	3.27	0.81		0.66	2.46	3.72	0.85	1.32	1.63
2:45 PM	2.64			0.77	2.22	3.05	0.83	1.58	3.09
3:00 PM	2.54			0.36	2.04	2.97	0.78	1.30	1.94
3:15 PM	2.50			0.38	1.94	2.43	1.04	1.37	1.03
3:30 PM	2.03		1.94	0.31	2.12	1.92	1.31	1.45	1.55
3:45 PM	3.01		1.48	0.16	1.97	2.02	1.45	1.29	2.08
4:00 PM	5.29		0.64	0.19	2.65	1.84	1.62	1.37	1.72
4:15 PM	3.73		0.53	0.04	2.10	1.85	1.79	1.05	2.45
4:30 PM	3.29		0.39	0.00	1.81	1.45	1.29	0.68	1.19
4:45 PM	3.43		0.51	0.00	1.41	1.12	1.15	0.45	1.06
5:00 PM	2.18		0.38	0.00	1.01	0.65	0.71	0.40	0.68
5:15 PM	1.38		0.30	0.00	0.69	0.51	0.45	0.26	0.46
5:30 PM	0.37		0.32	0.00	0.39	0.27	0.28	0.19	0.24
5:45 PM	0.11		0.09	0.00	0.18	0.07	0.21	0.06	0.16
6:00 PM	0.00		0.00	0.00	0.00	0.00	0.07	0.00	0.00
6:15 PM	0.00		0.04	0.00	0.00	0.00	0.00	0.00	0.00
6:30 PM	0.00		0.08	0.00	0.00	0.00	0.00	0.00	0.00
6:45 PM	0.00		0.05	0.00	0.00	0.00	0.00	0.00	0.00
7:00 PM	0.00		0.00	0.00	0.00	0.00	0.00	0.00	0.00
7:15 PM	0.04		0.00	0.00	0.00	0.00	0.00	0.00	0.00
7:30 PM	0.00		0.00	0.00	0.00	0.00	0.00	0.00	0.00
7:45 PM	0.00		0.00	0.00	0.00	0.00	0.00	0.00	0.00
8:00 PM	0.00		0.00	0.00	0.00	0.00	0.00	0.00	0.00
8:15 PM	0.00		0.00	0.00	0.00	0.00	0.00	0.00	0.00
8:30 PM	0.00		0.00	0.00	0.00	0.00	0.00	0.00	0.00
8:45 PM	0.00		0.00	0.00	0.00	0.00	0.00	0.00	0.00
9:00 PM	0.00		0.00	0.00	0.00	0.00	0.00	0.00	0.00
9:15 PM	0.00		0.00	0.00	0.00	0.00	0.00	0.00	0.00
9:30 PM	0.00		0.00	0.00	0.00	0.00	0.00	0.00	0.00
9:45 PM	0.00		0.00	0.00	0.00	0.00	0.00	0.00	0.00
10:00 PM	0.00		0.00	0.00	0.00	0.00	0.00	0.00	0.00
10:15 PM	0.00		0.00	0.00	0.00	0.00	0.00	0.00	0.00
10:30 PM	0.00		0.00	0.00	0.00	0.00	0.00	0.00	0.00
10:45 PM	0.00		0.00	0.00	0.00	0.00	0.00	0.00	0.00
11:00 PM	0.00		0.00	0.00	0.00	0.00	0.00	0.00	0.00
11:15 PM	0.00		0.00	0.00	0.00	0.00	0.00	0.06	0.00
11:30 PM	0.00		0.00	0.00	0.00	0.00	0.00	0.06	0.00
11:45 PM	0.00		0.00	0.00	0.00	0.00	0.00	0.00	0.00
12:00 AM	0.00		0.00	0.00	0.00	0.00	0.00	0.00	0.00

	2/9/95	2/10/95	2/11/95	2/12/95	2/13/95	2/14/95	2/15/95	2/16/95	2/17/95
12:15 AM	0.00	0.00	0.25	0.00	0.00	0.00	0.00	0.68	5.89
12:30 AM	0.00	0.00	0.29	0.00	0.00	0.00	0.00	0.89	2.64
12:45 AM	0.00	0.00	0.36	0.00	0.00	0.00	0.00	0.94	0.22
1:00 AM	0.00	0.00	0.27	0.00	0.00	0.00	0.00	0.81	0.00
1:15 AM	0.00	0.00	0.21	0.00	0.00	0.00	0.00	0.72	0.00
1:30 AM	0.00	0.00	0.10	0.00	0.00	0.00	0.00	0.75	0.00
1:45 AM	0.00	0.00	0.10	0.00	0.00	0.00	0.00	1.04	0.04
2:00 AM	0.00	0.00	0.07	0.00	0.00	1.05	0.00	0.35	0.00
2:15 AM	0.00	0.00	0.07	0.00	0.00	8.21	0.00	0.21	0.00
2:30 AM	0.00	0.00	0.04	0.00	0.00	0.00	0.00	0.20	0.00
2:45 AM	0.00	0.00	0.00	0.00	0.00	0.00	0.00	0.20	0.00
3:00 AM	0.00	0.00	0.00	0.00	0.00	0.00	0.00	0.16	0.00
3:15 AM	0.00	0.00	0.00	0.00	0.00	0.00	0.00	0.16	0.00
3:30 AM	0.00	0.00	0.00	0.00	0.00	0.00	0.00	0.18	0.00
3:45 AM	0.00	0.00	0.09	0.00	0.00	0.00	0.00	0.28	0.00
4:00 AM	0.00	0.00	0.00	0.00	0.00	0.00	0.00	0.49	0.00
4:15 AM	0.00	0.00	0.00	0.00	0.00	0.00	0.00	0.64	0.00
4:30 AM	0.00	0.00	0.04	0.00	0.00	0.00	0.00	0.49	0.00
4:45 AM	0.00	0.00	0.00	0.00	0.00	0.00	0.00	0.27	0.00
5:00 AM	0.00	0.00	0.00	0.00	0.00	0.00	0.00	0.27	0.00
5:15 AM	0.00	0.00	0.00	0.00	0.00	0.00	0.00	0.32	0.00
5:30 AM	0.00	0.00	0.00	0.00	0.00	0.00	0.00	0.25	0.00
5:45 AM	0.00	0.00	0.00	0.00	0.00	0.00	0.00	0.18	0.00
6:00 AM	0.00	0.00	0.00	0.00	0.00	0.00	0.00	0.25	0.00
6:15 AM	0.00	0.00	0.00	0.00	0.00	0.00	0.00	0.26	0.00
6:30 AM	0.00	0.00	0.00	0.00	0.00	0.00	0.00	0.41	0.00
6:45 AM	0.00	0.00	0.00	0.00	0.00	0.00	0.00	0.51	0.00
7:00 AM	0.00	0.00	0.00	0.00	0.00	23.42	0.00	0.30	0.00
7:15 AM	0.00	0.00	0.00	0.00	0.00	49.92	0.00	0.33	0.00
7:30 AM	2.06	0.00	0.00	0.00	0.00	33.79	0.00	0.49	0.04
7:45 AM	36.36	0.08	0.00	0.00	0.00	0.23	0.00	0.57	0.13
8:00 AM	5.31	0.22	0.00	0.00	0.20	0.09	0.00	0.64	0.20
8:15 AM	7.64	0.34	0.00	0.00	0.10	6.36	0.00	0.82	0.27
8:30 AM	25.31	0.38	0.00	0.00	0.10	7.70	0.00	1.14	0.34
8:45 AM	21.40	0.39	0.00	0.00	0.21	3.53	0.00	0.84	0.43
9:00 AM	5.71	0.33	0.00	0.00	1.15	2.15	0.00	0.69	0.57
9:15 AM	3.81	0.42	0.00	0.00	2.03	2.47	0.00	1.08	0.49
9:30 AM	2.87	0.48	0.00	0.07	2.41	0.93	0.00	1.73	0.37
9:45 AM	2.73	0.57	0.07	0.16	2.21	1.94	0.00	1.43	0.73
10:00 AM	2.62	0.65	0.00	0.00	2.08	4.15	0.00	1.01	0.94
10:15 AM	2.37	0.62	0.04	0.00	2.07	10.60	0.00	1.41	1.07
10:30 AM	2.31	0.61	0.00	0.00	2.09	10.55	0.00	1.79	1.36
10:45 AM	2.90	0.79	0.00	0.09	1.59	9.15	0.10	2.52	2.05
11:00 AM	2.74	1.11	0.05	0.00	1.80	5.84	0.13	2.63	2.69
11:15 AM	1.75	1.36	0.00	0.06	1.76	3.67	0.37	2.81	2.96
11:30 AM	1.28	1.80	0.09	0.00	1.55	2.92	0.13	3.83	2.68
11:45 AM	1.48	1.95	0.11	0.04	1.48	2.02	0.40	3.27	3.25
12:00 PM	1.25	2.02	0.19	2.05	1.64	2.29	0.21	2.15	3.35

	2/9/95	2/10/95	2/11/95	2/12/95	2/13/95	2/14/95	2/15/95	2/16/95	2/17/95
12:15 PM	1.21	2.00	0.00	1.58	1.48	2.24	0.61	2.72	3.39
12:30 PM	1.47	2.37	0.07	0.00	1.56	2.63	0.46	2.41	2.90
12:45 PM	1.82	2.41	1.05	1.27	1.47	2.34	0.42	1.85	3.74
1:00 PM	1.56	2.38	1.29	0.63	1.20	1.87	0.21	2.41	6.26
1:15 PM	1.77	2.16	2.84	0.28	1.37	1.52	0.31	2.97	6.31
1:30 PM	1.51	2.15	2.99	0.56	1.01	1.45	0.39	2.52	6.00
1:45 PM	0.77	1.97	10.10	0.82	0.89	1.52	0.35	1.48	5.79
2:00 PM	0.74	1.70	5.76	0.00	0.72	1.73	0.21	2.42	4.76
2:15 PM	0.86	1.55	5.97	0.00	0.62	1.01	0.44	2.40	3.85
2:30 PM	1.09	1.33	7.86	0.00	0.72	1.46	0.38	2.01	2.38
2:45 PM	1.34	1.26	6.13	0.49	0.83	1.33	0.19	1.88	2.22
3:00 PM	0.88	1.15	6.43	0.00	0.67	1.45	0.11	1.64	3.76
3:15 PM	0.60	1.03	3.86	0.64	0.62	0.80	0.10	2.04	3.01
3:30 PM	0.42	0.80	3.83	0.00	0.23	1.42	0.07	2.52	2.06
3:45 PM	0.71	0.84	3.46	0.04	0.32	0.88	0.09	3.32	1.06
4:00 PM	0.50	0.73	2.18	0.00	0.38	0.75	0.07	2.81	0.92
4:15 PM	0.70	0.78	1.81	0.00	0.39	0.76	0.15	2.90	1.25
4:30 PM	0.38	0.63	1.16	0.00	0.27	0.66	0.23	4.33	0.94
4:45 PM	0.28	0.66	0.61	0.00	0.18	0.40	0.14	2.13	0.61
5:00 PM	0.22	0.58	0.32	0.00	0.06	0.47	0.00	1.78	0.51
5:15 PM	0.15	0.48	0.15	0.00	0.10	0.34	0.00	2.38	0.41
5:30 PM	0.16	0.39	0.05	0.00	0.00	0.21	0.00	1.59	0.30
5:45 PM	0.08	0.27	0.00	0.00	0.00	0.19	0.00	0.70	0.23
6:00 PM	0.00	0.22	0.00	0.00	0.00	0.15	0.00	0.51	0.08
6:15 PM	0.00	0.20	0.00	0.00	0.00	0.00	0.00	0.23	0.00
6:30 PM	0.00	0.15	0.00	0.00	0.00	0.00	0.00	0.28	0.00
6:45 PM	0.00	0.15	0.00	0.00	0.00	0.00	0.00	0.17	0.00
7:00 PM	0.00	0.18	0.00	0.00	0.00	0.00	0.00	0.30	0.00
7:15 PM	0.00	0.17	6.27	0.00	0.00	0.00	0.00	0.32	0.00
7:30 PM	0.00	0.15	0.00	0.00	0.00	0.00	0.00	0.17	0.00
7:45 PM	0.00	0.17	0.00	0.00	0.00	0.00	0.00	0.21	0.00
8:00 PM	0.00	0.18	0.00	0.00	0.00	0.00	0.13	0.14	0.00
8:15 PM	0.00	0.16	0.00	0.00	0.00	0.00	0.09	0.54	0.00
8:30 PM	0.00	0.16	0.00	0.00	0.00	0.00	0.00	1.93	0.00
8:45 PM	0.00	0.20	0.00	0.00	0.00	0.00	0.06	0.34	0.00
9:00 PM	0.00	0.21	0.00	0.00	0.00	0.00	0.20	0.24	0.00
9:15 PM	0.00	0.22	0.00	0.00	0.00	0.00	0.22	3.21	0.00
9:30 PM	0.00	0.21	0.00	0.00	0.00	0.00	0.23	11.33	0.00
9:45 PM	0.00	0.21	0.00	0.00	0.00	0.00	0.29	13.13	0.00
10:00 PM	0.00	0.22	0.00	0.00	0.00	0.00	0.38	14.88	0.00
10:15 PM	0.00	0.22	0.00	0.00	0.00	0.00	0.29	12.37	0.00
10:30 PM	0.00	0.22	0.00	0.00	0.00	0.00	0.25	11.89	0.00
10:45 PM	0.00	0.19	0.00	0.00	0.00	0.00	0.21	19.10	0.00
11:00 PM	0.00	0.19	0.00	0.00	0.00	0.00	0.42	13.72	0.00
11:15 PM	0.00	0.18	0.00	0.00	0.00	0.00	0.49	7.25	0.00
11:30 PM	0.00	0.18	0.00	0.00	0.00	0.00	0.56	8.20	0.00
11:45 PM	0.00	0.22	0.00	0.00	0.00	0.00	0.38	9.55	0.00
12:00 AM	0.00	0.20	0.00	0.00	0.00	0.00	0.74	8.78	0.00

	2/18/95	2/19/95	2/20/95	2/21/95	2/22/95		2/18/95	2/19/95	2/20/95	2/21/95	2/22/95
12:15 AM	0.00			0.00	0.00	12:15 PM		2.09	0.00		
12:30 AM	0.00			0.00	0.00	12:30 PM		3.24	0.00		
12:45 AM	0.00			0.00		12:45 PM		2.64	0.00		
1:00 AM	0.00			0.00		1:00 PM		1.92	0.00		
1:15 AM	0.00			0.00		1:15 PM		1.73	0.00		
1:30 AM	0.00			0.00		1:30 PM		2.50	0.00		
1:45 AM	0.00			0.00		1:45 PM		1.35	0.00		
2:00 AM	0.00			0.00		2:00 PM		0.80	0.00		
2:15 AM	0.00			0.00		2:15 PM		2.45	0.00		
2:30 AM	0.00			0.00		2:30 PM		0.88	0.00		
2:45 AM	0.00			0.00		2:45 PM		0.58	0.00		
3:00 AM	0.00			0.00		3:00 PM		1.43	0.00		
3:15 AM	0.00			0.00		3:15 PM		1.03	0.00		
3:30 AM	0.00			0.00		3:30 PM		0.29	0.00		
3:45 AM	0.00			0.00		3:45 PM		0.23	0.00		
4:00 AM	0.00			0.00		4:00 PM		0.59	0.00		
4:15 AM	0.00			0.00		4:15 PM		0.48	0.00		
4:30 AM	0.00			0.00		4:30 PM		0.69	0.14		
4:45 AM	0.00			0.00		4:45 PM		0.33	0.07		
5:00 AM	0.00			0.00		5:00 PM		0.17	0.36		
5:15 AM	0.00			0.00		5:15 PM		0.00	0.05		
5:30 AM	0.00			0.00		5:30 PM		0.00	0.00		
5:45 AM				0.00		5:45 PM		0.00	0.00		
6:00 AM				0.00		6:00 PM		0.00	0.00		
6:15 AM				0.00		6:15 PM		0.00	0.00		
6:30 AM				0.00		6:30 PM		0.00	0.00		
6:45 AM				0.00		6:45 PM		0.00	0.00		
7:00 AM				0.00		7:00 PM		0.00	0.00		
7:15 AM				0.00		7:15 PM		0.00	0.00		
7:30 AM				0.00		7:30 PM		0.00	0.00		
7:45 AM				0.00		7:45 PM		0.00	0.00		
8:00 AM				0.13		8:00 PM		0.00	0.00		
8:15 AM				0.21		8:15 PM		0.00	0.00		
8:30 AM				0.34		8:30 PM		0.00	0.00		
8:45 AM				1.04		8:45 PM		0.00	0.00		
9:00 AM				1.13		9:00 PM		0.00	0.00		
9:15 AM				0.20		9:15 PM		0.00	0.00		
9:30 AM				0.11		9:30 PM		0.00	0.00		
9:45 AM				0.17		9:45 PM		0.00	0.00		
10:00 AM				0.00		10:00 PM		0.00	0.00		
10:15 AM				0.00		10:15 PM		0.00	0.00		
10:30 AM				0.00		10:30 PM		0.00	0.00		
10:45 AM				0.00		10:45 PM		0.00	0.00		
11:00 AM				0.00		11:00 PM		0.00	0.00		
11:15 AM				0.00		11:15 PM		0.00	0.00		
11:30 AM				0.00		11:30 PM		0.00	0.00		
11:45 AM				0.00		11:45 PM		0.00	0.00		
12:00 PM			2.14	0.00		12:00 AM	0.00	0.00			

7.2.1.2 NO_y Mixing Ratios

	12/7/95	12/8/95	1/12/95	1/13/95	1/14/95	1/15/95	1/16/95	1/17/95	1/18/95	1/19/95	1/20/95
12:15 AM		4.61		4.92	4.42	2.92	2.54	11.42	5.09	12.35	4.24
12:30 AM		4.50		5.09	4.18	2.90	2.20	11.91	4.11	12.55	3.90
12:45 AM		4.74		4.91	3.92	3.01	2.01	10.69	3.53	12.40	3.80
1:00 AM		4.67		5.09	3.75	2.82	2.03	9.81	3.69	12.48	3.53
1:15 AM		4.12		4.94	3.75	2.82	1.98	10.05	5.14	11.82	3.83
1:30 AM		4.28		4.44	3.80	2.78	1.50	9.34	5.11	12.46	3.49
1:45 AM		4.05		4.46	3.77	2.74	1.67	8.32	4.85	11.59	2.58
2:00 AM		4.02		4.44	3.60	2.68	1.91	8.85	4.06	10.96	2.30
2:15 AM		4.18		4.48	3.50	2.52	2.03	8.55	3.12	10.81	3.24
2:30 AM		4.85		3.12	3.44	2.74	2.28	8.73	2.83	10.27	4.47
2:45 AM		5.60		2.99	3.52	2.78	2.34	8.33	2.87	9.53	4.82
3:00 AM		4.49		4.28	3.67	2.58	3.46	8.14	2.82	8.42	5.20
3:15 AM		4.37		4.84	3.70	2.38	3.21	7.61	2.74	8.03	5.22
3:30 AM		3.97		4.95	3.79	2.97	2.53	7.31	2.66	7.60	5.08
3:45 AM		4.42		5.23	3.76	3.85	2.32	7.63	2.75	7.56	4.98
4:00 AM		3.90		5.00	3.56	4.26	2.34	7.91	3.54	7.38	5.29
4:15 AM		3.92		4.65	3.58	4.04	2.66	7.85	4.43	7.14	5.29
4:30 AM		3.90		3.93	3.39	4.12	2.97	6.58	3.70	7.49	5.17
4:45 AM		4.15		3.98	3.28	3.32	2.22	6.26	2.75	7.85	4.98
5:00 AM		4.08		4.66	3.12	3.37	1.49	6.39	2.65	7.52	4.65
5:15 AM		4.45		4.23	3.11	3.55	1.91	6.79	2.59	7.85	4.51
5:30 AM		4.43		3.92	3.11	3.20	1.91	7.26	2.71	7.47	4.47
5:45 AM		4.36		3.76	3.12	2.71	2.07	6.92	2.63	6.99	4.52
6:00 AM		4.59		4.25	3.75	2.78	2.25	6.69	2.63	6.99	4.63
6:15 AM		5.35		3.86	3.36	3.01	2.29	7.26	2.64	6.61	4.74
6:30 AM		6.03		4.26	3.41	2.88	1.74	6.62	2.67	6.45	4.94
6:45 AM		7.46		3.45	3.25	2.85	2.22	6.90	2.90	6.11	5.11
7:00 AM		8.25		3.26	3.25	2.95	2.18	6.98	2.95	6.01	5.36
7:15 AM		8.87		3.28	3.31	2.89	2.03	7.60	3.21	5.56	5.53
7:30 AM		9.35		3.25	3.29	2.82	2.37	7.78	3.64	5.32	5.67
7:45 AM		9.65		2.81	3.34	2.91	3.12	9.75	3.89	5.39	6.08
8:00 AM		9.87		3.05	3.33	3.03	4.27	9.95	4.54	5.35	6.37
8:15 AM		10.20		2.84	3.29	2.87	7.97	10.32	4.30	5.51	6.83
8:30 AM		10.29		3.02	3.22	3.10	18.86	10.66	3.24	5.69	7.19
8:45 AM		10.05		2.85	3.28	3.18	20.69	10.09	3.36	5.86	7.02
9:00 AM				3.89	3.49	3.24	22.48	10.44	3.61	5.98	6.96
9:15 AM				4.81	3.65	3.23	16.68	10.59	3.87	5.79	7.09
9:30 AM	2.12			4.36	4.21	3.04	10.77	10.49	4.12	6.23	7.24
9:45 AM	1.45			5.92	4.01	3.12	13.01	13.12	4.36	6.62	7.44
10:00 AM	1.43			6.04	4.24	2.92	12.79	15.56	4.40	6.41	6.98
10:15 AM	1.31			6.09	4.68	2.85	13.17	13.74	4.64	6.80	6.61
10:30 AM	1.69			6.10	5.14	3.62	13.44	13.98	4.52	7.06	6.80
10:45 AM	3.39			5.96	5.56	2.63	15.54	14.08	4.53	11.10	6.97
11:00 AM	5.77			5.79	5.62	4.74	14.91	14.26	4.47	9.77	7.22
11:15 AM	7.51			5.89	5.61	4.22	16.19	14.46	4.90	8.74	7.56
11:30 AM	6.75			6.02	4.83	4.68	18.69	14.33	4.68	9.61	8.35
11:45 AM	6.48			7.24	5.02	4.64	19.53	14.03	6.15	10.48	8.54
12:00 PM	5.96			6.98	5.08	4.29	19.42	14.87	15.45	13.08	9.20

	12/7/95	12/8/95	1/12/95	1/13/95	1/14/95	1/15/95	1/16/95	1/17/95	1/18/95	1/19/95	1/20/95
12:15 PM	5.67			8.90	4.87	4.34	19.62	15.05	19.90	6.86	9.88
12:30 PM	5.88			10.57	5.21	4.35	19.08	15.34	21.79	4.49	10.27
12:45 PM	6.32			11.57	5.22	3.54	19.05	15.45	20.14	4.55	10.77
1:00 PM	6.52			15.56	4.82	3.76	19.19	15.63	19.96	5.01	11.41
1:15 PM	6.67			11.55	4.35	4.16	17.94	15.68	18.15	7.16	10.62
1:30 PM	7.31			11.13	4.93	4.62	18.54	15.03	17.15	6.98	9.27
1:45 PM	7.73			9.68	4.32	4.60	18.50	14.08	15.41	6.88	8.20
2:00 PM	8.52			10.51	4.92	5.37	17.70	14.29	15.43	7.09	8.26
2:15 PM	8.93			11.71	4.67	5.02	17.43	14.52	13.34	4.03	8.42
2:30 PM	9.60			13.88	4.37	5.20	16.45	13.97	11.80	5.10	8.81
2:45 PM	9.96			11.92	4.22	5.26	15.34	14.23	11.80	4.11	9.30
3:00 PM	10.49			11.26	4.66	5.20	14.60	14.00	11.25	3.02	9.57
3:15 PM	10.96			11.14	4.40	4.59	14.29	14.40	10.01	2.93	10.25
3:30 PM	11.13		13.66	10.61	4.62	4.30	14.10	12.13	8.18	3.00	10.70
3:45 PM	11.04		12.13	9.39	4.90	3.69	14.64	13.32	7.61	2.87	10.07
4:00 PM	11.12		11.62	8.97	4.78	2.36	14.56	13.18	7.64	3.18	9.74
4:15 PM	10.97		11.57	7.86	4.10	3.08	13.12	12.08	6.98	3.34	9.75
4:30 PM	11.16		12.62	8.32	3.94	4.50	12.05	12.32	6.32	3.73	10.11
4:45 PM	11.25		13.55	9.59	3.68	4.47	12.29	11.47	6.47	4.03	9.93
5:00 PM	11.37		13.66	9.66	3.59	3.60	13.64	11.45	5.85	4.14	10.40
5:15 PM	11.11		12.71	9.51	3.72	3.20	12.99	11.47	6.37	4.09	11.51
5:30 PM	10.94		12.01	10.12	3.89	3.69	10.66	11.39	5.99	3.96	12.43
5:45 PM	10.63		10.79	10.95	3.80	3.94	10.49	10.82	6.52	3.90	11.77
6:00 PM	10.63		10.19	7.60	3.62	4.11	10.79	10.05	7.42	3.65	11.71
6:15 PM	9.58		10.84	6.63	3.43	4.77	10.70	9.77	6.75	3.34	12.41
6:30 PM	10.25		10.84	6.52	3.07	4.70	9.71	9.79	6.78	3.58	12.71
6:45 PM	10.34		9.26	6.38	3.21	4.57	9.43	9.42	7.33	3.30	13.06
7:00 PM	9.68		8.90	5.93	3.55	4.56	9.57	10.24	8.13	2.68	13.33
7:15 PM	8.79		9.53	6.15	4.01	3.48	10.11	11.67	10.01	2.71	13.05
7:30 PM	9.22		7.34	6.29	3.88	2.70	10.47	11.90	12.46	2.47	12.29
7:45 PM	9.84		6.70	5.45	3.50	2.89	10.12	10.20	14.70	2.15	11.91
8:00 PM	9.73		5.74	5.00	3.43	3.20	9.44	10.40	14.40	2.05	11.21
8:15 PM	11.25		5.48	5.21	3.35	3.64	9.33	10.52	14.68	1.97	10.93
8:30 PM	10.35		6.96	5.11	3.16	3.64	9.45	10.40	16.56	1.93	10.97
8:45 PM	8.26		6.84	4.67	3.11	3.58	9.12	9.96	18.30	1.89	10.66
9:00 PM	7.07		5.93	4.27	3.01	3.58	11.95	8.74	21.67	1.80	10.46
9:15 PM	6.13		4.93	4.11	2.97	3.13	14.60	8.38	24.25	1.75	10.23
9:30 PM	6.60		4.74	4.13	2.93	2.52	13.11	7.69	20.99	1.75	10.22
9:45 PM	6.54		4.88	4.22	2.90	2.58	11.38	7.18	18.47	1.61	10.19
10:00 PM	5.36		5.26	4.08	2.93	2.35	10.79	7.27	17.80	1.44	10.05
10:15 PM	4.79		5.34	3.88	2.88	2.49	10.68	6.57	18.12	1.61	10.29
10:30 PM	4.46		5.13	3.98	2.87	2.53	10.61	6.04	18.66	2.19	10.44
10:45 PM	4.10		4.98	3.99	2.78	2.76	10.86	6.17	18.95	2.34	10.94
11:00 PM	3.88		5.44	4.21	2.73	2.68	10.70	6.13	19.15	2.75	10.71
11:15 PM	4.33		5.27	4.40	2.77	2.54	10.44	6.43	16.69	2.90	11.36
11:30 PM	3.71		5.01	4.62	2.71	2.60	10.34	6.78	14.27	4.11	13.65
11:45 PM	3.83		4.95	4.42	2.69	2.57	10.41	5.80	13.06	4.72	18.11

	1/21/95	1/22/95	1/23/95	1/24/95	1/25/95	2/2/95	2/3/95	2/4/95	2/5/95	2/6/95
12:15 AM	21.69	6.49	3.78	16.96	8.76		10.30	6.10	11.11	5.32
12:30 AM	17.48	6.32	4.34	18.00	8.71		15.15	6.84	9.78	5.01
12:45 AM	19.34	5.75	5.19	14.68	8.72		28.40	6.60	8.92	4.99
1:00 AM	17.63	5.40	6.86	12.69	8.61		27.09	6.42	10.25	5.39
1:15 AM	17.99	5.04	7.43	37.40	8.81		32.25	6.58	8.81	4.84
1:30 AM	17.27	5.30	10.71	31.39	8.80		31.92	6.77	8.24	4.61
1:45 AM	17.27	4.99	13.86	5.47	9.31		33.55	5.96	7.98	4.56
2:00 AM	16.47	4.49	13.04	4.95	9.68		33.68	5.85	8.1	4.45
2:15 AM	14.52	3.93	10.50	5.10	9.12		29.02	5.43	9.53	4.19
2:30 AM	13.31	3.61	6.24	5.14	8.80		18.91	4.71	9.07	4.19
2:45 AM	12.03	9.11	5.37	5.30	8.41		17.25	3.84	7.25	4.14
3:00 AM	12.23	12.60	14.51	6.86	8.34		18.38	3.75	5.664	4.04
3:15 AM	11.87	17.22	13.11	16.16	7.79		20.16	3.85	5.457	3.73
3:30 AM	10.83	9.21	4.93	13.48	7.07		21.25	3.75	4.98	3.58
3:45 AM	10.12	11.81	3.79	6.21	6.85		20.47	4.17	4.695	3.48
4:00 AM	10.02	6.74	3.60	9.52	8.81		18.22	4.69	4.119	3.42
4:15 AM	10.08	9.84	3.66	19.69	7.14		17.71	4.90	3.826	3.21
4:30 AM	9.06	11.23	4.99	8.14	7.29		18.30	5.16	3.832	3.26
4:45 AM	7.72	11.94	5.18	6.33	6.44		17.75	5.79	3.891	2.96
5:00 AM	8.64	31.47	5.23	20.53	6.27		21.11	5.98	3.715	3.04
5:15 AM	8.04	28.23	5.10	7.80	6.37		19.44	5.16	3.587	3.73
5:30 AM	8.00	15.94	4.90	6.50	5.70		19.61	5.18	3.491	3.73
5:45 AM	6.55	8.45	4.88	6.81	5.36		17.26	5.61	3.264	3.39
6:00 AM	6.94	8.47	4.91	6.67	5.54		18.08	5.21	3.359	3.46
6:15 AM	7.00	39.31	5.01	7.46	5.26		16.64	4.74	3.251	3.65
6:30 AM	5.36	28.35	5.41	12.13	5.19		11.81	3.98	3.054	3.71
6:45 AM	4.97	19.59	6.17	12.65	5.29		10.74	3.81	2.845	4.14
7:00 AM	5.10	5.68	10.66	13.25	5.30		9.41	5.04	2.797	5.16
7:15 AM	4.75	8.72	31.95	13.73	5.39		8.08	5.35	2.95	6.10
7:30 AM	4.33	10.20	25.33	14.18	5.49		7.28	5.03	3.04	7.71
7:45 AM	4.40	3.77	35.68	13.87	6.42		12.50	10.42	3.224	8.53
8:00 AM	4.74	4.07	39.27	16.10	5.59		14.05	10.13	3.282	9.48
8:15 AM	4.30	3.90	16.98	17.85	5.83		15.83	13.61	3.584	11.48
8:30 AM	4.24	4.00	21.78	17.72	6.07		17.64	14.55	4.003	22.51
8:45 AM	4.20	3.91	7.91	17.29	6.17		24.30	18.87	4.159	19.37
9:00 AM	4.42	3.62	30.97	16.78	13.46		27.70	19.99	4.377	21.04
9:15 AM	4.26	6.44	48.87	15.97	12.72		25.88	19.37	4.508	14.42
9:30 AM	4.66	8.81	12.83	19.54	21.33		21.71	17.39	4.908	9.23
9:45 AM	4.02	7.61	9.38	21.99	24.06		23.27	17.49	5.852	7.43
10:00 AM	3.95	8.31	9.11	21.84	22.18		27.14	18.71	5.88	11.34
10:15 AM	6.52	8.36	8.94	20.97	17.45		26.72	19.22	6.051	12.70
10:30 AM	6.99	6.67	8.59	22.32	18.88		25.59	20.91	8.62	11.91
10:45 AM	6.49	6.24	8.90	24.85	22.06		24.84	23.05	13.25	9.30
11:00 AM	5.78	6.09	13.35	23.49	27.84		22.83	22.89	14.78	9.59
11:15 AM	5.17	5.41	14.48	23.40	27.94		22.71	23.76	13.87	14.16
11:30 AM	4.83	5.10	12.59	22.08	36.48		20.19	23.48	13.29	19.67
11:45 AM	4.81	5.14	14.14	19.29	34.85		20.04	20.42	12.38	13.29
12:00 PM	6.26	5.20	15.05	16.77	37.79		22.74	20.31	14.66	7.88

	1/21/95	1/22/95	1/23/95	1/24/95	1/25/95	2/2/95	2/3/95	2/4/95	2/5/95	2/6/95
12:15 PM	6.93	4.85	13.56	15.10	32.39		22.98	21.48	12.05	6.69
12:30 PM	7.08	4.55	13.43	14.78	30.01		22.53	17.70	9.21	6.17
12:45 PM	6.64	5.02	13.33	11.72	26.80		22.00	16.53	6.684	5.80
1:00 PM	5.64	4.68	12.93	11.09	21.85		21.29	16.91	5.84	4.77
1:15 PM	4.55	5.19	11.57	11.23	17.38		20.84	16.23	7.73	4.93
1:30 PM	4.13	5.07	11.01	10.73	15.44		16.76	16.22	10.98	4.76
1:45 PM	3.79	4.90	10.61	11.59	12.48		16.54	16.37	11.98	5.08
2:00 PM	4.38	5.21	11.04	12.74	9.39		14.99	15.95	15.04	4.68
2:15 PM	5.41	6.32	10.60	12.35	7.24		14.56	15.97	18.04	5.62
2:30 PM	5.33	7.20	13.41	12.77	5.51		13.59	14.77	13.24	5.06
2:45 PM	5.13	7.75	19.83	11.16			13.45	11.46	11.55	4.81
3:00 PM	5.09	8.47	13.16	11.04			13.26	11.67	11.32	4.91
3:15 PM	5.04	8.19	11.43	11.28			13.03	12.35	9.76	5.62
3:30 PM	5.14	8.01	12.24	9.83		25.94	13.28	13.33	8.33	6.83
3:45 PM	5.00	7.67	11.36	13.95		27.88	13.18	14.10	9.31	8.08
4:00 PM	5.93	7.10	12.40	22.16		18.05	11.59	16.58	9.1	8.88
4:15 PM	5.65	6.58	11.73	19.06		18.08	10.29	15.33	9.41	10.05
4:30 PM	5.73	5.69	9.70	19.57		18.48	11.05	13.87	9.4	10.56
4:45 PM	5.71	6.01	10.05	23.91		22.17	11.98	14.18	9.01	9.42
5:00 PM	5.84	5.64	10.09	21.68		21.36	11.33	12.69	7.86	10.56
5:15 PM	6.23	4.91	9.07	21.83		21.94	10.84	12.55	8.58	11.20
5:30 PM	6.04	4.72	8.61	13.96		30.70	10.96	12.36	8.12	11.90
5:45 PM	5.91	4.48	8.06	12.68		28.55	10.46	11.74	6.944	13.73
6:00 PM	5.76	4.01	7.58	10.56		14.47	11.34	11.92	7.46	16.48
6:15 PM	6.17	3.66	7.75	17.31		16.42	9.60	13.06	7.57	17.14
6:30 PM	6.03	3.69	7.22	20.91		18.59	8.69	9.69	7.99	16.34
6:45 PM	6.14	3.81	8.72	20.24		16.29	8.19	9.44	8.76	16.45
7:00 PM	5.79	3.95	12.27	14.90		9.20	9.00	7.05	10.43	11.81
7:15 PM	5.82	3.96	12.77	13.85		8.42	11.87	5.79	9.68	9.41
7:30 PM	5.73	3.71	13.51	12.69		6.15	10.21	5.65	9.4	8.34
7:45 PM	6.28	3.98	12.06	11.01		6.60	8.72	5.06	8.86	8.10
8:00 PM	6.95	3.86	12.00	9.55		7.42	8.33	5.79	9.15	9.34
8:15 PM	7.74	3.04	13.43	8.77		7.89	6.95	5.61	8.49	8.53
8:30 PM	8.14	3.03	13.61	10.60		8.65	5.98	5.18	8.26	8.44
8:45 PM	8.42	3.34	11.41	9.81		7.46	6.00	5.63	8.66	8.20
9:00 PM	7.94	4.81	15.38	10.49		4.80	6.53	9.32	9.25	6.95
9:15 PM	8.53	4.79	16.58	9.70		4.30	6.68	10.43	8.19	4.90
9:30 PM	10.16	2.60	19.01	9.99		4.48	6.81	11.33	7.53	4.77
9:45 PM	14.65	2.48	18.79	9.87		3.88	6.66	12.25	7.75	4.68
10:00 PM	17.24	2.25	16.59	9.62		5.17	7.05	11.93	8.22	5.64
10:15 PM	20.69	2.24	29.57	9.27		6.92	6.54	12.65	7.84	5.86
10:30 PM	22.96	2.24	13.61	9.45		9.41	6.71	9.27	8.35	8.60
10:45 PM	18.87	2.22	6.86	9.60		11.37	6.88	11.86	7	7.70
11:00 PM	12.65	2.23	5.90	9.53		14.13	6.30	13.96	6.793	5.23
11:15 PM	10.61	2.05	6.86	9.46		10.15	5.96	13.45	6.797	6.14
11:30 PM	9.86	2.16	7.68	9.21		13.12	6.24	12.31	6.795	7.68
11:45 PM	13.05	2.81	9.44	8.80		16.53	6.36	11.25	6.596	8.21
12:00 AM	8.35	3.07	24.34	8.72		16.40	6.26	9.99	6.518	9.94

	2/7/95	2/8/95	2/9/95	2/10/95	2/11/95	2/12/95	2/13/95	2/14/95	2/15/95	2/16/95
12:15 AM	10.99	8.52	9.73	3.62	8.74	8.51	8.38	5.46	11.40	20.66
12:30 AM	7.79	11.96	9.37	3.72	9.42	6.96	3.54	5.32	14.86	25.29
12:45 AM	8.37	9.74	8.24	3.19	9.33	6.70	3.47	4.55	13.03	19.81
1:00 AM	14.02	10.29	8.23	3.94	8.21	6.69	3.07	6.62	12.56	14.66
1:15 AM	4.79	10.92	7.69	6.09	8.11	6.68	4.54	6.00	13.39	14.63
1:30 AM	4.30	12.89	7.57	8.97	7.77	5.76	5.91	4.59	13.22	12.72
1:45 AM	3.81	16.30	7.62	9.14	6.44	5.37	6.53	5.86	13.66	12.73
2:00 AM	3.79	16.59	6.98	10.22	6.65	4.82	8.77	11.28	11.55	7.40
2:15 AM	3.85	15.65	7.07	11.87	7.29	4.61	11.81	20.83	12.91	7.60
2:30 AM	4.65	13.03	6.87	10.66	8.37	4.39	5.63	5.19	11.34	6.76
2:45 AM	5.20	11.59	6.71	9.93	4.60	4.17	2.99	5.14	11.41	6.68
3:00 AM	5.99	11.48	6.68	11.04	3.52	4.14	3.01	3.58	13.75	9.82
3:15 AM	5.89	10.79	6.95	11.22	4.06	4.15	2.98	3.86	13.93	12.02
3:30 AM	3.26	10.71	6.59	11.54	3.77	4.32	2.88	3.83	11.69	10.94
3:45 AM	2.87	10.49	6.24	11.65	4.24	4.47	2.73	4.14	8.89	18.93
4:00 AM	2.92	12.40	5.90	11.23	4.04	6.06	4.24	4.02	8.52	21.08
4:15 AM	3.41	13.93	5.62	11.25	3.79	7.74	3.74	5.57	7.93	17.22
4:30 AM	3.15	15.16	5.44	11.41	3.81	9.25	3.04	19.39	8.72	11.63
4:45 AM	3.24	13.67	5.35	11.00	5.11	10.64	3.04	31.87	10.01	16.81
5:00 AM	3.28	11.45	5.12	11.22	7.16	11.29	2.94	41.49	10.63	14.90
5:15 AM	3.13	11.00	4.67	11.40	5.38	8.45	2.42	30.59	13.04	13.92
5:30 AM	3.09	10.27	5.01	11.69	7.88	8.10	2.42	29.54	15.30	14.26
5:45 AM	3.34	10.63	7.78	12.33	3.52	10.94	2.18	22.90	14.81	15.73
6:00 AM	3.33	17.62	7.84	12.91	6.24	7.90	2.18	20.70	15.32	18.23
6:15 AM	6.71	13.43	7.17	13.10	12.47	7.60	2.52	23.19	14.05	17.96
6:30 AM	4.13	14.34	7.30	13.51	7.84	3.99	2.81	25.00	11.73	22.57
6:45 AM	4.16	40.03	12.49	13.58	5.80	4.44	2.62	28.66	8.96	21.36
7:00 AM	2.86	36.48	8.78	13.49	6.26	4.97	2.48	41.41	7.64	14.58
7:15 AM	2.85	35.47	8.84	13.42	6.12	4.94	2.53	49.88	6.88	12.78
7:30 AM	3.51	33.96	24.93	13.29	6.21	5.51	2.77	49.88	6.07	13.49
7:45 AM	3.97	14.51	49.10	13.34	9.64	6.26	3.45	48.89	6.53	12.15
8:00 AM	15.50	15.44	28.97	14.07	6.35	6.20	4.46	43.28	5.51	11.54
8:15 AM	23.82	16.26	31.48	14.52	6.82	7.27	4.61	45.70	3.58	11.45
8:30 AM	17.72	16.52	46.40	14.46	7.50	6.13	4.99	49.88	6.38	10.60
8:45 AM	23.98	17.68	41.29	13.74	7.81	6.41	6.20	40.40	3.73	9.99
9:00 AM	22.51	20.07	20.46	11.91	7.24	6.44	10.71	33.95	3.61	9.36
9:15 AM	17.75	21.88	15.25	12.17	5.74	7.15	13.99	33.11	3.78	10.06
9:30 AM	31.05	18.77	11.25	12.58	5.09	6.89	14.71	28.21	4.00	12.09
9:45 AM	29.92	18.66	10.62	13.21	5.30	6.00	16.02	29.03	3.78	11.65
10:00 AM	25.24	21.01	10.10	13.87	5.61	6.07	16.67	34.99	4.78	10.78
10:15 AM	20.30	29.86	9.15	12.30	5.47	7.03	15.41	43.70	4.76	11.52
10:30 AM	16.78	33.87	8.98	11.01	5.65	8.23	15.03	46.74	5.63	12.65
10:45 AM	14.59	18.75	11.06	10.45	5.67	6.69	13.96	42.70	5.42	13.06
11:00 AM	14.27	11.47	10.69	11.51	5.81	7.37	14.63	32.93	7.26	13.43
11:15 AM	15.34	11.61	7.62	12.40	4.56	6.04	14.51	25.64	8.11	14.82
11:30 AM	19.41	11.98	7.25	14.08	4.68	8.46	13.06	20.72	8.49	18.35
11:45 AM	18.69	10.35	6.63	13.91	5.12	16.93	14.28	17.26	8.48	18.97
12:00 PM	14.53	11.84	6.72	13.46	6.47	22.60	15.34	17.69	8.85	15.22

	2/7/95	2/8/95	2/9/95	2/10/95	2/11/95	2/12/95	2/13/95	2/14/95	2/15/95	2/16/95
12:15 PM	10.06	12.92	6.85	12.65	6.30	14.55	13.60	19.56	8.61	14.21
12:30 PM	10.92	14.48	7.99	13.17	11.91	11.96	12.97	18.68	8.65	11.79
12:45 PM	8.24	12.06	8.99	13.24	21.95	6.87	12.35	17.63	8.81	9.58
1:00 PM	8.02	12.23	10.70	13.25	28.69	7.40	12.16	15.29	7.91	10.94
1:15 PM	9.20	12.22	12.21	12.22	31.47	7.19	12.26	16.01	9.49	15.24
1:30 PM	10.28	11.84	9.93	11.82	29.87	7.79	11.12	16.07	8.06	17.94
1:45 PM	9.78	12.07	6.52	10.96	40.55	5.97	10.95	16.15	8.28	15.85
2:00 PM	9.08	11.77	5.89	10.09	32.23	5.80	10.65	16.92	6.80	15.56
2:15 PM	10.09	12.41	6.74	10.03	33.00	7.46	10.74	15.92	7.77	12.50
2:30 PM	9.68	14.55	7.80	9.22	37.08	7.11	10.67	17.05	6.21	11.31
2:45 PM	11.22	15.02	8.58	9.48	33.96	5.16	10.90	17.11	5.26	12.06
3:00 PM	12.07	14.20	7.44	9.59	33.09	7.23	10.29	16.38	4.41	11.92
3:15 PM	12.21	13.09	6.22	9.50	25.79	5.55	10.41	15.85	4.17	14.52
3:30 PM	12.66	13.11	5.68	9.19	28.57	4.80	10.30	16.81	4.94	17.39
3:45 PM	12.17	13.70	5.73	9.08	30.35	5.51	12.17	17.06	4.78	21.51
4:00 PM	11.32	14.07	5.60	8.88	27.93	5.88	12.83	15.35	4.88	20.61
4:15 PM	9.99	13.27	6.70	8.43	25.84	6.65	12.35	15.86	5.46	22.41
4:30 PM	9.84	14.06	6.50	8.24	19.44	8.11	12.65	16.61	5.44	31.83
4:45 PM	9.03	13.88	7.31	11.31	15.59	7.63	12.84	18.36	6.16	27.16
5:00 PM	9.88	11.01	7.92	10.54	11.72	7.80	11.57	18.33	6.37	27.12
5:15 PM	10.45	10.11	8.52	9.75	10.84	7.57	11.40	18.11	6.94	25.92
5:30 PM	10.87	10.94	8.29	9.23	9.78	6.90	11.07	18.14	6.20	23.02
5:45 PM	8.28	10.10	8.42	8.76	9.14	5.90	11.01	21.38	6.72	19.78
6:00 PM	7.50	10.12	8.58	8.33	8.32	5.85	10.69	24.57	8.73	20.01
6:15 PM	8.51	10.62	7.71	8.19	7.96	7.67	11.27	23.73	7.72	19.12
6:30 PM	9.90	9.83	6.69	7.92	7.50	8.93	14.08	23.92	7.69	19.83
6:45 PM	9.89	12.20	5.15	7.53	7.10	11.66	16.60	23.22	7.13	19.00
7:00 PM	8.34	10.24	4.60	7.67	8.19	12.93	13.04	23.99	8.34	17.53
7:15 PM	8.32	11.06	4.73	7.77	19.16	12.61	9.25	24.07	11.05	16.74
7:30 PM	8.30	12.15	6.15	8.63	7.59	12.00	9.40	21.72	8.11	19.92
7:45 PM	8.39	10.07	5.89	8.71	6.29	10.99	8.74	21.24	7.82	17.69
8:00 PM	8.27	9.10	7.59	8.40	5.54	7.92	9.95	17.65	8.36	16.23
8:15 PM	8.55	10.48	8.15	7.81	5.73	6.08	9.82	16.46	8.64	21.64
8:30 PM	8.58	10.22	8.60	8.07	6.62	6.40	9.24	12.24	8.86	33.80
8:45 PM	7.73	9.18	8.45	8.83	5.91	4.47	9.23	11.30	9.76	29.43
9:00 PM	8.02	9.83	8.21	8.99	9.19	4.08	8.46	10.55	13.46	23.41
9:15 PM	10.03	9.56	8.27	9.25	9.85	4.50	6.70	9.87	14.99	37.98
9:30 PM	12.01	8.62	10.26	9.03	10.63	3.91	5.97	9.76	17.84	49.82
9:45 PM	10.76	9.10	11.66	8.97	13.56	4.31	5.83	8.46	13.42	49.87
10:00 PM	11.81	9.28	8.93	9.35	14.78	4.52	7.16	9.47	11.82	49.88
10:15 PM	10.23	10.17	6.77	9.19	15.21	4.72	7.04	8.37	8.11	49.88
10:30 PM	10.60	10.11	5.90	9.07	17.19	5.33	8.28	8.28	8.04	49.89
10:45 PM	10.44	10.74	5.48	8.51	25.69	4.02	8.09	8.81	8.97	49.89
11:00 PM	10.07	11.19	4.32	8.65	16.82	2.45	7.98	9.02	9.96	49.89
11:15 PM	13.46	11.24	5.95	8.18	18.86	3.81	7.82	11.45	10.90	48.89
11:30 PM	14.16	10.80	5.58	8.07	21.03	5.41	7.86	10.41	14.91	49.25
11:45 PM	21.12	10.69	4.07	8.22	20.02	5.15	7.15	9.82	13.18	49.88
12:00 AM	11.97	9.98	3.53	8.09	19.66	3.81	6.28	11.78	14.06	49.88

	2/17/95	2/18/95	2/19/95	2/20/95	2/21/95	2/22/95	2/23/95
12:15 AM	48.83	9.59	10.70	2.00	5.09	6.24	2.45
12:30 AM	43.27	8.24	10.51	1.63	7.13	5.97	4.11
12:45 AM	34.39	6.93	10.15	2.03	5.35	5.67	4.17
1:00 AM	28.51	5.37	10.29	1.51	5.10	5.81	3.02
1:15 AM	25.26	4.85	10.06	1.45	9.72	5.61	2.70
1:30 AM	23.39	7.18	9.33	1.46	8.24	5.53	3.15
1:45 AM	22.54	8.05	9.67	1.55	7.18	5.06	3.13
2:00 AM	21.95	8.86	9.76	1.64	6.54	4.62	3.90
2:15 AM	21.05	9.20	8.62	1.83	6.10	4.42	4.56
2:30 AM	20.10	10.34	7.54	1.71	5.80	4.27	5.90
2:45 AM	18.60	10.64	8.25	2.07	6.40	4.29	10.42
3:00 AM	17.79	10.79	7.79	3.07	6.41	4.29	6.51
3:15 AM	17.51	11.20	6.78	8.56	5.72	4.25	5.44
3:30 AM	17.69	12.05	6.02	10.36	4.55	4.27	3.17
3:45 AM	18.47	11.90	5.49	6.69	3.83	4.08	4.98
4:00 AM	18.50	11.51	5.61	4.60	3.60	4.10	4.64
4:15 AM	18.66	11.60	6.21	6.41	2.99	4.16	4.61
4:30 AM	20.53	12.95	7.27	4.69	2.39	4.32	3.46
4:45 AM	19.70	12.07	7.23	2.97	2.17	4.32	3.53
5:00 AM	18.37	9.96	7.11	6.24	2.85	4.27	3.42
5:15 AM	17.35	8.91	6.84	5.18	3.23	4.28	3.74
5:30 AM	14.67	8.75	7.34	4.93	2.76	4.02	4.34
5:45 AM	11.96	8.09	8.00	3.79	2.66	3.89	4.39
6:00 AM	9.41	7.52	8.49	3.82	2.16	3.41	3.29
6:15 AM	8.08	7.82	8.00	6.06	2.68	3.28	2.76
6:30 AM	7.58	8.39	7.69	8.90	2.50	3.53	2.57
6:45 AM	7.14	8.98	7.99	7.89	2.60	4.28	2.67
7:00 AM	7.53	9.46	7.76	7.46	2.79	4.00	2.93
7:15 AM	7.80	9.00	4.95	8.83	2.97	5.50	3.50
7:30 AM	8.46	8.15	3.24	8.36	3.24	7.00	4.34
7:45 AM	9.76	7.51	1.22	9.36	3.23	9.26	5.51
8:00 AM	10.89	6.93	1.21	19.44	3.66	10.76	6.29
8:15 AM	11.73	7.28	2.19	14.02	3.94	12.57	7.40
8:30 AM	10.56	6.89	4.40	9.60	5.27	15.28	7.71
8:45 AM	10.80	6.49	5.95	10.25	11.77	16.22	7.63
9:00 AM	11.11	6.21	4.03	10.46	14.46	15.57	9.33
9:15 AM	10.74	6.27	3.07	12.02	15.51	16.45	9.78
9:30 AM	7.84	6.28	3.56	12.46	15.83	16.86	9.88
9:45 AM	9.38	6.00	5.81	11.09	17.45	13.88	10.56
10:00 AM	10.85	5.87	7.84	9.35	15.93	11.47	10.59
10:15 AM	11.71	6.17	7.73	9.64	13.44	11.48	11.74
10:30 AM	13.20	5.51	6.81	10.33	12.37	10.91	11.21
10:45 AM	15.11	5.20	6.80	12.26	8.74	11.05	11.25
11:00 AM	16.37	5.13	8.33	15.12	7.30	12.77	11.86
11:15 AM	18.15	5.07	9.26	15.63	7.80	12.39	10.40
11:30 AM	19.22	4.98	7.70	16.72	7.22	12.33	12.02
11:45 AM	20.37	4.76	6.54	17.03	5.73	12.17	10.81
12:00 PM	22.07	5.06	6.60	18.40	4.97	13.08	10.09

	2/17/95	2/18/95	2/19/95	2/20/95	2/21/95	2/22/95	2/23/95
12:15 PM	22.97	5.36	8.62	16.24	4.66	12.17	8.88
12:30 PM	23.99	5.73	6.53	17.75	4.77	12.91	8.54
12:45 PM	25.63	5.06	8.10	15.90	4.99	10.70	8.21
1:00 PM	26.90	5.35	6.97	14.45	5.54	8.50	6.50
1:15 PM	26.74	5.45	7.72	13.46	5.87	10.62	6.09
1:30 PM	25.79	5.90	6.01	15.59	6.65	8.40	7.71
1:45 PM	24.58	6.24	7.73	15.35	8.13	8.85	6.15
2:00 PM	23.00	6.32	10.03	14.17	11.11	6.30	6.90
2:15 PM	22.98	5.62	10.73	15.81	10.20	6.07	5.72
2:30 PM	22.36	5.53	9.21	12.67	8.18	6.65	6.03
2:45 PM	22.48	5.71	8.34	12.10	9.44	5.46	5.27
3:00 PM	21.94	5.98	8.18	13.58	12.40	5.34	5.11
3:15 PM	21.54	6.60	8.29	10.85	10.99	4.29	5.70
3:30 PM	20.40	6.88	8.82	8.18	11.93	4.54	
3:45 PM	19.58	6.11	7.60	7.88	10.56	5.89	
4:00 PM	18.92	6.26	8.93	9.38	9.51	9.61	
4:15 PM	18.75	5.85	8.83	8.62	10.11	8.25	
4:30 PM	18.38	6.00	8.60	9.36	10.13	8.97	
4:45 PM	18.97	6.15	7.87	9.12	10.70	9.76	
5:00 PM	18.98	6.71	6.80	8.37	11.38	9.49	
5:15 PM	18.92	6.16	6.48	5.81	8.87	9.08	
5:30 PM	19.01	6.01	5.59	5.16	7.50	7.64	
5:45 PM	19.03	5.74	5.16	4.46	7.23	6.84	
6:00 PM	18.56	5.68	5.10	4.41	7.35	5.38	
6:15 PM	18.51	5.71	4.41	4.02	7.60	4.60	
6:30 PM	18.43	5.96	3.89	3.75	7.54	4.18	
6:45 PM	18.03	6.26	3.52	3.98	6.94	3.67	
7:00 PM	18.46	7.27	2.85	4.82	6.75	3.27	
7:15 PM	18.92	7.96	2.26	6.25	6.69	2.66	
7:30 PM	18.38	8.54	3.22	4.54	6.05	2.44	
7:45 PM	18.97	8.35	6.71	4.16	5.24	2.39	
8:00 PM	21.09	8.33	5.72	4.54	5.69	2.33	
8:15 PM	22.02	8.12	4.60	3.79	6.38	2.38	
8:30 PM	19.41	7.69	3.50	2.51	6.14	2.43	
8:45 PM	19.17	9.23	3.51	2.38	6.42	3.05	
9:00 PM	17.22	10.46	2.83	2.64	6.72	5.42	
9:15 PM	18.25	11.48	2.96	3.61	7.28	5.12	
9:30 PM	18.31	12.26	3.18	3.86	7.63	5.48	
9:45 PM	18.66	12.86	2.99	4.95	7.93	7.39	
10:00 PM	20.69	13.33	2.08	5.30	8.23	6.51	
10:15 PM	21.41	13.38	2.20	3.90	6.71	4.35	
10:30 PM	17.02	13.29	2.43	4.34	6.60	3.19	
10:45 PM	13.46	13.25	2.62	6.35	6.43	13.40	
11:00 PM	9.85	13.67	2.63	8.01	6.69	3.11	
11:15 PM	8.03	13.53	2.41	7.83	6.67	3.15	
11:30 PM	8.33	12.36	1.87	5.06	6.51	2.74	
11:45 PM	10.14	11.44	2.23	4.43	6.31	3.01	
12:00 AM	10.07	11.72	2.47	4.65	6.07	5.67	

7.2.2 Surface (10 Meters), NO Mixing Ratios Only

	1/18/95	1/20/95	1/24/95	1/25/95	2/3/95	2/4/95
12:15 AM					0.00	0.00
12:30 AM					0.00	0.00
12:45 AM					0.00	0.00
1:00 AM					0.00	0.00
1:15 AM					0.00	0.00
1:30 AM					0.00	0.00
1:45 AM					0.00	0.00
2:00 AM					0.00	0.00
2:15 AM					0.00	0.00
2:30 AM					0.00	0.00
2:45 AM					0.00	0.00
3:00 AM					0.11	0.00
3:15 AM					0.00	0.00
3:30 AM					0.00	0.00
3:45 AM					0.00	0.00
4:00 AM					0.00	0.00
4:15 AM					0.13	0.00
4:30 AM					0.00	0.00
4:45 AM					0.00	0.00
5:00 AM					0.15	0.00
5:15 AM					0.11	0.00
5:30 AM					0.00	0.00
5:45 AM					0.15	0.00
6:00 AM			0.24			0.11
6:15 AM		0.84	0.10	7.01	36.40	0.23
6:30 AM		0.43	0.23	6.58	21.01	0.16
6:45 AM		0.27	0.12	11.97	48.16	0.00
7:00 AM		0.43	0.40	12.35	85.72	0.30
7:15 AM	16.33	0.26	1.21	14.19	52.05	0.16
7:30 AM	14.30	0.27	2.82	21.23	51.31	0.39
7:45 AM	17.37	0.72	4.12	11.76	39.43	0.61
8:00 AM	11.33	0.48	5.09	24.07	21.47	1.03
8:15 AM	20.16	0.76	5.88	19.84	26.03	1.26
8:30 AM	19.01	0.85	8.61	17.83	17.49	1.50
8:45 AM	21.96	0.81	14.75	21.37		1.89
9:00 AM	18.82	1.20	14.21	30.34		2.33
9:15 AM	21.59	1.40	12.42	26.47	13.86	3.55
9:30 AM	29.89	1.43	11.77	23.32	14.15	4.72
9:45 AM	31.80	1.09	11.90	18.90	12.10	3.60
10:00 AM	29.83	0.82	12.50	11.44	12.38	2.22
10:15 AM	32.30	0.60	13.12	11.84	12.63	2.82
10:30 AM	30.85	0.90	11.66	13.96	14.05	4.41
10:45 AM	13.85	0.74	11.79	15.00	11.36	4.39
11:00 AM	23.29	0.84	10.98	12.65	11.25	6.28
11:15 AM	21.40	1.16	8.60	13.31	11.07	8.43
11:30 AM	18.41	1.03	8.17	11.99	10.56	10.86
11:45 AM	14.87	1.72	6.51	12.89	9.21	11.53
12:00 PM	18.18	2.30	5.66	14.80	9.49	9.71

	1/18/95	1/20/95	1/24/95	1/25/95	2/3/95	2/4/95
12:15 PM	12.16	3.36	4.79	15.08	8.42	7.51
12:30 PM	8.48	3.08	4.80	11.71	9.58	6.79
12:45 PM	8.17	2.60	3.11	11.14	8.70	4.31
1:00 PM	7.70	1.61	2.94	6.68	8.77	6.49
1:15 PM	5.19	2.32	3.00	5.69	6.70	6.16
1:30 PM	4.26	2.52	3.38	4.55	5.72	5.67
1:45 PM	4.88	2.58	3.45	3.45	5.45	4.37
2:00 PM	4.96	2.25	3.37	3.19	4.95	3.96
2:15 PM	5.94	2.92	2.77	2.09	4.31	3.00
2:30 PM	3.86	3.16	3.07	0.97	4.05	3.26
2:45 PM	4.19	3.16	2.32	1.00	3.50	3.31
3:00 PM	3.44	3.24	2.18	1.05	2.75	2.84
3:15 PM	2.56	3.18	2.13	0.87	2.48	3.04
3:30 PM	2.24	2.82	1.74	1.07	2.59	2.94
3:45 PM	2.36	1.76	2.32	1.46	2.05	2.93
4:00 PM	2.05	1.23	3.33	1.83	1.65	3.14
4:15 PM	2.42	1.14	2.42	3.00	1.52	3.15
4:30 PM	2.15	1.53	2.27	4.19	1.03	2.54
4:45 PM	2.17	1.15	2.53	3.51	0.79	2.14
5:00 PM	2.26	0.90	1.90	1.66	0.73	2.11
5:15 PM	1.88	0.67	1.26	0.55	0.59	1.45
5:30 PM	2.12	0.58	0.68		0.41	1.22
5:45 PM	2.16	0.44	0.33		0.28	0.63
6:00 PM	2.51	0.41	0.23		0.12	0.52
6:15 PM					0.00	0.14
6:30 PM					0.00	0.00
6:45 PM					0.00	0.00
7:00 PM					0.00	0.00
7:15 PM					0.75	0.00
7:30 PM					0.26	0.00
7:45 PM					0.00	0.00
8:00 PM					0.00	0.00
8:15 PM					0.00	0.00
8:30 PM					0.00	0.00
8:45 PM					0.00	0.00
9:00 PM					0.00	0.00
9:15 PM					0.00	0.00
9:30 PM					0.00	0.00
9:45 PM					0.00	0.00
10:00 PM					0.00	0.00
10:15 PM					0.00	0.00
10:30 PM					0.00	0.00
10:45 PM					0.00	0.00
11:00 PM					0.00	0.00
11:15 PM					0.00	0.00
11:30 PM					0.00	0.00
11:45 PM					0.00	0.00
12:00 AM					0.00	0.00

	2/6/95	2/7/95	2/10/95	2/11/95	2/13/95	2/14/95	2/16/95
12:15 AM			0.00				
12:30 AM			5.84				
12:45 AM			2.40				
1:00 AM			1.61				
1:15 AM			1.30				
1:30 AM			1.89				
1:45 AM			1.59				
2:00 AM			1.13				
2:15 AM			0.25				
2:30 AM			0.51				
2:45 AM			0.00				
3:00 AM			0.12				
3:15 AM			0.00				
3:30 AM			0.26				
3:45 AM			0.00				
4:00 AM			1.91				
4:15 AM			0.46				
4:30 AM			3.12				
4:45 AM			5.43				
5:00 AM			1.90				
5:15 AM			2.43				
5:30 AM			3.60				
5:45 AM			1.34				
6:00 AM		0.65	0.00	2.13		12.09	0.14
6:15 AM		0.32	0.00	3.66		18.99	19.74
6:30 AM		0.23	0.00	2.16	2.70	15.87	0.76
6:45 AM		0.13	0.00	0.99	8.03	14.98	0.32
7:00 AM	1.19	0.38	0.00	2.81	35.23	48.63	0.34
7:15 AM	2.88	0.57	0.20	5.03	18.41	20.25	1.60
7:30 AM	1.67	1.88	0.32	1.66	13.80	22.69	7.34
7:45 AM	2.68	4.79	0.50	1.39	13.56	18.96	5.36
8:00 AM	3.45	17.98	0.89	1.67	8.94	57.12	1.53
8:15 AM	5.81	31.09	0.96	1.75	8.69	94.98	8.89
8:30 AM	6.89	33.27	0.90	7.56	8.63	92.38	7.05
8:45 AM	6.58	17.47	0.74	12.75	8.73	98.23	12.57
9:00 AM	5.80	9.94	0.67	8.39	9.30	90.17	11.94
9:15 AM	4.90	11.45	0.69	11.51	10.01	61.39	12.61
9:30 AM	2.54	7.61	0.84	9.27	8.03	34.42	11.92
9:45 AM	1.79	6.92	1.01	9.76	6.58	33.01	8.84
10:00 AM	0.00	6.38	1.20		6.34	22.44	4.61
10:15 AM	3.52	7.41	1.44		5.94	25.30	4.00
10:30 AM	3.71	7.23	1.81		5.31	32.36	4.50
10:45 AM	2.93	5.20	2.24		7.24	24.33	5.14
11:00 AM	2.82	5.00	2.06		3.83	18.99	6.45
11:15 AM	3.68	5.06	2.18		3.45	15.00	7.16
11:30 AM	6.07	4.58	2.26		3.28	12.48	7.62
11:45 AM	7.04	3.61	2.58		2.76	9.19	6.99
12:00 PM	2.57	2.98	2.63		3.25	8.20	6.37

	2/6/95	2/7/95	2/10/95	2/11/95	2/13/95	2/14/95	2/16/95
12:15 PM	1.66	2.92	2.39		2.76	6.94	7.25
12:30 PM	1.47	2.64	2.18		2.40	6.43	10.12
12:45 PM	1.17	2.00	2.10		2.18	7.81	10.78
1:00 PM	0.99	2.15	1.96		2.18	7.06	9.34
1:15 PM	0.92	2.15	2.29		1.83	6.08	9.58
1:30 PM	0.90	2.08	1.99		2.04	6.43	9.38
1:45 PM	0.94	1.91	1.63		2.65	7.61	11.08
2:00 PM	0.97	1.71	1.34		2.16	6.67	8.32
2:15 PM	1.13	1.61	1.14		2.10	5.71	13.42
2:30 PM	0.89	1.79	0.97		2.34	5.92	15.60
2:45 PM	0.77	1.89	0.97		1.82	5.88	17.23
3:00 PM	0.67	1.89	0.75		1.41	5.78	14.88
3:15 PM	0.79	2.02	0.60		1.27	4.76	13.43
3:30 PM	0.88	2.76	0.61		1.04	4.98	13.31
3:45 PM	1.07	2.27	0.60		0.91	5.56	13.67
4:00 PM	1.28	1.69	0.52		0.83	5.62	14.15
4:15 PM	1.41	1.53	0.50		0.92	4.42	14.99
4:30 PM	1.18	1.16	0.37		0.86	3.62	27.77
4:45 PM	0.87	0.78	0.34		0.68	4.51	51.12
5:00 PM	0.75	0.59	0.31		0.61	5.67	54.98
5:15 PM	0.52	0.41	0.19		0.45	7.10	62.92
5:30 PM	0.39	0.30	0.14		0.36	5.37	129.23
5:45 PM	0.24	0.22	0.00		0.30	10.44	91.25
6:00 PM	0.14	0.13	0.00			16.53	55.22
6:15 PM			0.00				
6:30 PM			0.00				
6:45 PM			0.00				
7:00 PM			0.00				
7:15 PM			0.00				
7:30 PM			0.00				
7:45 PM			0.00				
8:00 PM			0.00				
8:15 PM			0.00				
8:30 PM			0.00				
8:45 PM			0.00				
9:00 PM			0.00				
9:15 PM			0.00				
9:30 PM			0.00				
9:45 PM			0.00				
10:00 PM			0.00				
10:15 PM			0.00				
10:30 PM			0.00				
10:45 PM			0.00				
11:00 PM			0.00				
11:15 PM			0.00				
11:30 PM			0.22				
11:45 PM			0.00				
12:00 AM			0.00				